2019

Regulation of Acetyl Phosphate-Dependent Acetylation and Identification of Novel Lysine Acetyltransferases in Escherichia Coli

David George Christensen

LOYOLA UNIVERSITY CHICAGO

REGULATION OF ACETYL PHOSPHATE-DEPENDENT ACETYLATION AND IDENTIFICATION OF NOVEL LYSINE ACETYLTRANSFERASES IN *ESCHERICHIA COLI*

A DISSERTATION SUBMITTED TO

THE FACULTY OF THE GRADUATE SCHOOL

IN CANDIDACY FOR THE DEGREE OF

DOCTOR OF PHILOSOPHY

PROGRAM IN MICROBIOLOGY AND IMMUNOLOGY

BY

DAVID GEORGE CHRISTENSEN

CHICAGO, ILLINOIS

MARCH 2019

ACKNOWLEDGMENTS

I must first thank my parents for their unending love and encouragement throughout my education that has brought me to this point. I would also like to express my thanks to my Aunt Heidi who has greatly supported my education and ensured that I had many opportunities. I would also like to thank my future spouse, Carolyn, for constant love, support, and understanding.

I would like to thank my mentor, Dr. Alan Wolfe, who has given me guidance and support that has greatly fostered my growth as a scientist. I would like to thank the Wolfe lab members past and present who have shaped a wonderful community for scientific and non-scientific discussions, especially Drs. Robert Davis, Linda Hu, and Bruno Lima upon whose work my studies stand. I am thankful for each of the students that I mentored and who taught me as much as I taught them. I would like to thank the Microbiology and Immunology Department for being a brilliant group who have provided diverse perspectives on my work. I would also like to thank my committee for giving me constructive feedback on my work at the bench, in my writing, and in my thinking. I would like to thank my collaborators who have provided me with valuable expertise and ideas that were essential to drive my studies. I'd like to especially thank Dr. Christopher Rao and James Orr for their assistance in measuring metabolites, Dr. Birgit Schilling for her assistance in performing mass spectrometry, and Dr. Misty Kuhn for her assistance with enzymology.

For my parents who have provided me with every opportunity
and Carolyn who provides me with love, encouragement, and joy.

You are an aperture through which the universe is looking at and exploring itself.

Alan W. Watts

TABLE OF CONTENTS

LIST OF TABLES

LIST OF FIGURES

LIST OF ABBREVIATIONS

AcCoA	acetyl-CoA
AcP	acetyl phosphate
Acs	acetyl-CoA synthetase
cAMP	cyclic AMP
CoA	coenzyme A
CRP	cAMP receptor protein
ED	Entner-Doudoroff
EMP	Embden-Meyerhof-Parnas
GNAT	GCN5-related N-acetyltransferase
KAT	lysine acetyltransferase
KDAC	lysine deacetylase
OD600	optical density at 600 nm
PP	pentose phosphate
PTM	Post-translation modification
PTS	phosphotransferase system
SDS-PAGE	sodium dodecyl sulfate-polyacrylamide gel electrophoresis
TB7	tryptone broth buffered to pH 7
TCA	tricarboxylic acid
WT	wild-type

ABSTRACT

Over billions of years, organisms have organized chemical reactions into metabolic pathways to sustain life. However, metabolic substrates can undergo many uncatalyzed, extra-metabolic reactions. Acetyl phosphate (AcP), an intermediate of the acetate fermentation pathway in *E. coli*, is one such metabolite that has been shown to non-enzymatically acetylate hundreds of proteins. This diverse set of targets suggests that acetylation could be a way for the cell to sense its nutritional status and regulate protein activity accordingly. However, how *E. coli* regulates acetylation, if at all, is unknown.

Previous work showed that acetylation becomes pronounced in stationary phase cells. I determined that acetylation only increases once the culture enters stationary phase and continues to accumulate until carbon source depletion. Mass spectrometry indicated that the accumulation results from both additional lysine residues becoming acetylated and an increased ratio of acetylated to unacetylated isoforms. I performed anti-acetyllysine western blot analysis and metabolite measurements that suggested acetylation does not accumulate during exponential phase because 1) acetylated isoforms are diluted into nascent proteins and 2) glucose is not consumed until stationary phase. Additionally, I found that acetylation required rapid flux of carbon into the cell and through glycolysis. These data suggest that AcP-dependent acetylation is an unavoidable consequence of fermentation. I hypothesized that there is a physiological relevance to AcP-dependent acetylation such as utilization of acetylation as a carbon source or as protection against non-enzymatic protein damage, but I was unsuccessful in showing any effect.

In addition to non-enzymatic acetylation, one lysine acetyltransferase (KAT), YfiQ, had been described in *E. coli*. I recognized that acetylation could occur without AcP or YfiQ. Indeed, I identified four proteins that produced acetylated bands in a strain lacking both mechanisms of acetylation. Variants of these proteins with conserved catalytic residues changed to alanine did not produce these acetylated bands, consistent with these proteins having KAT activity. One of these KATs, YiaC, inhibited migration in soft agar dependent on its KAT activity. To determine targets of these KATs, we determined proteins whose acetylation increased upon overexpresson of each of these proteins. Thus, this work opens new avenues of study to determine the regulatory potential of acetylation by these KATs.

CHAPTER ONE

LITERATURE REVIEW

Introduction

The two competing theories for the origin of life (metabolism-first and gene-first) assert that abiotic chemical reactions were the progenitors of biotic life. These chemical reactions formed the basis for metabolism and provided building blocks for both RNA and protein synthesis. Over millions of years, cells formed and then evolved and, in doing so, generated the diversity of life we observe today. Across phylogeny, the core metabolic pathways necessary for life have been well conserved (1). In these pathways, anabolism and catabolism generate a multitude of different metabolites. The potential chemical reactions in which these metabolites can participate greatly exceed the metabolic requirements. Indeed, these "extra-metabolic" non-enzymatic reactions can and do occur, which results in the production of toxic compounds and causes damage to macromolecular structures within cells (2). While cells have evolved means of controlling the damage incurred by these deleterious chemistries, it is thought that accumulation of this damage may be a prototypic driver of aging (3).

Despite the constant possibility for damage to occur because of their own metabolism, bacteria have survived and evolved to adapt to various niches. However, these environments are rarely constant outside of a laboratory setting, and bacteria will often face adverse conditions. In these niches, one of the major challenges is acquisition of nutrients necessary to grow and divide.

While some nutrients like carbon may be readily abundant, other nutrients can be scarce, like iron sequestered by a host (4). These conditions may come on suddenly, so the bacteria must respond accordingly or perish. While transcription and translation are time- and energy-intensive processes, post-translational control of protein function can rapidly alter cellular physiology and permit fitness or survival in otherwise suboptimal or lethal conditions. While small ligands may allosterically regulate proteins in a reversible manner, covalent chemical modification of the existing proteome also occurs, a process that may or may not be reversible. These chemical modifications of the proteome are called post-translational modifications (PTMs). With hundreds of PTMs known and more being discovered, understanding how these modifications interact with one another and affect protein function are critical to generating a complete picture of the cell.

Of these hundreds of PTMs, many occur on lysines, including propionylation (5), butyrylation (5), crotonylation (6, 7), succinylation (8), malonylation (9, 10), glutarylation (11), 2-hydroxyisobutyrylation (12), β-hydroxybutyrylation (13) and Nε-lysine acetylation, which is becoming recognized as a prominent modification that is conserved across phylogeny (14, 15). While lysine acetylation is best understood as an activating modification of eukaryotic histones (16), extensive study into the role of lysine acetylation in bacteria only began about a decade ago. While acetylation of certain lysines may have a clear consequence, such as inhibition of enzyme activity due to modification of an active site, the functional importance of many acetyllysine modifications are more difficult to discern. To uncover the role of lysine acetylation in these unclear cases, it is helpful to use a model bacterium (e.g., *Escherichia coli*) with a vast knowledgebase of pathways, protein structure-function relationships, and physiology.

This first chapter will detail what is known about lysine acetylation in bacteria with some attention paid to eukaryotic acetylation for context. I will begin by describing the different types of acetylation, the mechanisms of lysine acetylation, and some of the known effects of acetylation on protein function. Then, I will describe metabolism in *E. coli*, as it is required to generate both acetyl coenzyme A and the predominant acetyl donor, acetyl phosphate. Finally, I will describe the behavior of *E. coli* in stationary phase, as this is the phase of growth when we observe the most elevated levels of acetylation.

Acetylation

Acetylation – From Small Molecules to Proteins

Acetylation is simply the transfer of an acetyl group (CH_3CO) onto a molecule. These acetylation reactions can occur on small molecules and metabolites, or they can occur on proteins. The acetyl group can be added to a variety of atoms on the target molecule. The atom to which the acetyl group is attached is usually denoted in the name of either the final molecule or the enzyme that performs the acetylation. These atoms can be sulfur, oxygen, carbon, and often nitrogen.

Multiple metabolic pathways require the transfer of acetyl groups from one metabolite to the next. For example, N-acetylglutamate synthase catalyzes acetylation of L-glutamate, the first step in arginine biosynthesis (17). Acetylation of multiple aminoglycoside antibiotics has been reported to inactivate their bactericidal or bacteriostatic activity (18-20). For example, the gene commonly used to confer resistance to chloramphenicol encodes a protein called chloramphenicol acetyltransferase (19). This protein adds two acetyl groups onto chloramphenicol to generate 1,3-diacetyl chloramphenicol. The acetylated antibiotic is unable to inhibit translation because it no longer can bind to the 23S ribosomal RNA of the 50S ribosomal

subunit (21). The chitin of insects, plants, and fungi and the peptidoglycan of the bacterial cell wall are composed of complex polysaccharides (22). These polysaccharides often contain monomers such as N-acetylglucosamine (GlcNAc) and N-acetylmuramic acid (MurNAc), which are monosaccharide derivatives acetylated on the primary amine (N) group, as their names suggest. However, these can be further acetylated on hydroxyl groups to increase resistance to degradative enzymes, such as lysozyme and autolysins (22).

The most widely studied protein acetylations occur on amino groups, although acetylations on serine, threonine, and histidine residues of proteins have recently been detected (23-26). The two varieties of amino group acetylations that occur on proteins are lysine acetylation (Nε-acetylation) and N-terminal acetylation (Nα-acetylation). Lysine acetylation will be discussed in more detail below. Nα-acetylation is very common in eukaryotes, but rare in bacteria with only 47 proteins N-terminally acetylated in *E. coli* and 117 in *Pseudomonas aeruginosa* (27, 28). It occurs either on the free amino group of methionine or on the exposed amino acid after cleavage of the N-terminal methionine. The modification is usually co-translational in eukaryotes but post-translational in bacteria, mitochondria, and chloroplasts, as the methionine first must be deformylated (29). Nα-acetylation has been shown to alter protein stability in eukaryotes and is typically irreversible (30, 31). *E. coli* encodes three proteins that have demonstrated Nα-acetyltransferase activity: RimI, RimJ, and RimL. The only known targets of RimI, RimJ, and RimL are the ribosomal proteins S5, L12, and S18, respectively (32, 33). The exact physiological effects of Nα-acetylation in *E. coli* are not known. There is evidence that RimJ plays a role in ribosome assembly, but it is not known whether this phenotype requires the Nα-acetyltransferase activity of RimJ (32, 34). RimJ also plays a role in transcriptional regulation of the P pilus of uropathogenic *E. coli*, but the specific target and

whether Nα-acetyltransferase activity is required remain unknown (35, 36). One defined role for Nα-acetylation comes from the ESAT-6 virulence factor of *Mycobacterium tuberculosis*. Cleavage of the N-terminal methionine of ESAT-6 reveals a threonine, which is then acetylated on the amino terminus. This acetylation alters protein-protein interactions with the binding partner CFP-10, which attenuates virulence (37-39).

Until recently, the only known internal residue that could be acetylated was lysine. However, recent work of a few groups found that a family of bacterial effector molecules from certain pathogenic species can acetylate serine, threonine, and histidine in addition to lysine residues. In some *Yersinia* species, YopJ can act as an acetyltransferase to modify serine and threonine residues of kinases in mammalian host cells to subvert host immunity (24-26, 40). Similarly, HopZ3, a YopJ family member from the plant pathogen *Pseudomonas syringae*, can acetylate plant proteins on lysine, serine, threonine, and histidine residues, as well as bacterial effector proteins AvrB and AvrB3 (23). In both cases, the acetylation by YopJ or HopZ3 prevents effective immune signaling, which results in successful bacterial infection. This does not appear to be an exclusively inter-kingdom modification, because O-acetylation of serine and threonine was found to occur on a proteome-wide scale in *M. tuberculosis* (41). Finally, O-acetylation of a single serine (S608) in acetyl-CoA synthetase (Acs) regulates the ability of a neighboring lysine (K610) to be acetylated in *Streptomyces lividans* (42). The discovery of these unusual acetylated residues opens new questions concerning the prevalence of these modifications and their potential interaction with other PTMs.

Nε-Lysine Acetylation

Nε-lysine acetylation (hereafter acetylation) is the donation of an acetyl group onto the epsilon amino group of the lysine sidechain (**Fig. 1**). Acetylation increases the size of the side

chain and neutralizes the positive charge (+1 to 0). Losing the positive charge and increasing the size of lysine disrupts salt bridges and introduces steric bulk that can alter protein-protein interactions, protein-DNA interactions, stability, and enzymatic activity (43-45). This was first and extensively studied in the context of the histone code (46), where acetylation of the lysine rich C-terminal tail reduces protein-DNA binding. This remodels chromatin to activate gene transcription (16, 47-49). However, recent mass spectrometric studies of acetylation have detected acetylation in all three domains of life (50-53). The first acetylome in a bacterium was reported in 2008 (54); since then >50 bacterial acetylomes have been reported (**Table 1**). As mass spectrometric techniques and software have improved, the breadth of targets modified by acetylation has expanded. It is now clear that the extent of acetylation, the mechanisms by which acetylation occurs, the identities of acetylated proteins, and the locations of acetylation on those proteins can vary between organisms; yet, in most cases, there is great conservation among the identities of the lysines being acetylated (55).

It is well known that acetylation can be catalyzed by a **lysine acetyltransferase** (KAT) that transfers the acetyl group from acetyl-CoA (AcCoA) onto the target lysine residue. However, evidence has accumulated showing that non-enzymatic acetylation is also possible. *In vitro*, AcCoA and the bacterial metabolite acetyl phosphate (AcP) can non-enzymatically acetylate lysine residues. *In vivo,* the impact that AcP has on the consortium of acetylated proteins, the acetylome, has been assessed in multiple bacteria. In the cases of *E. coli* (56, 57), *Bacillus subtilis* (58), and *Neisseria gonorrhoeae* (59), it is the predominant acetyl donor.

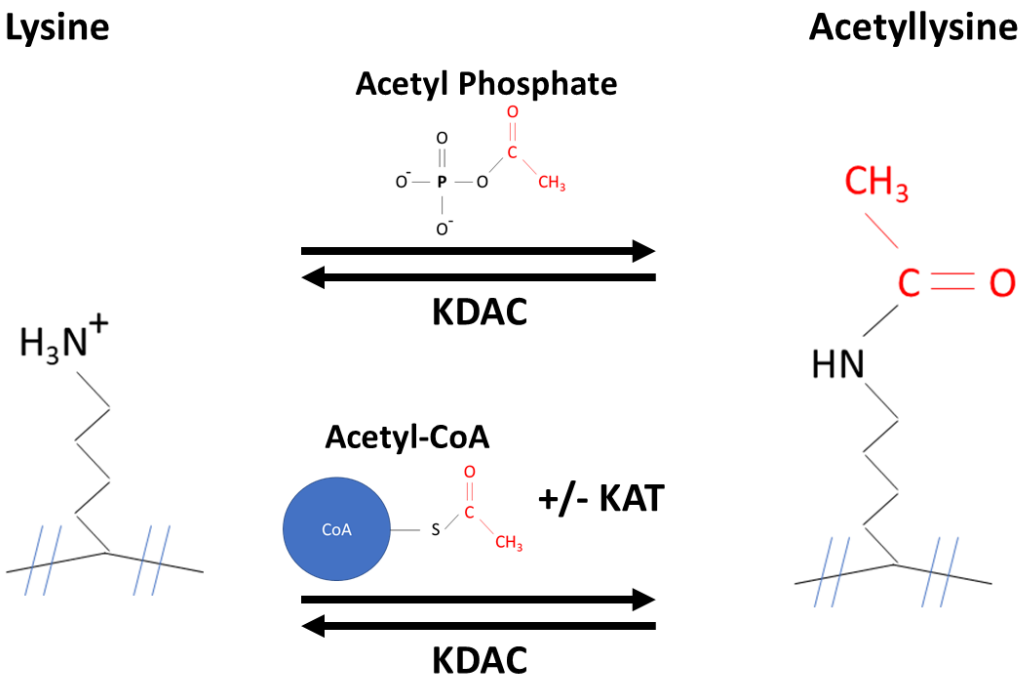

Figure 1. Two Mechanisms of Lysine Acetylation in *E. coli*. Acetyl phosphate can non-enzymatically acetylate lysine, while Acetyl-CoA can acetylate a lysine with or without a lysine acetyltransferase (KAT). Some acetylations are reversed by a lysine deacetylase (KDAC).

While multiple families of acetyltransferases have been described, all bacterial acetyltransferases discovered thus far are part of the **G**cn5-related **N**-**a**cetyl**t**ransferase (GNAT) family (60-62). Thus, the subset of acetyltransferases that have KAT activity are also GNAT family members. In *E. coli*, there is only one known KAT, YfiQ (also called Pat, PatZ or Pka) (63). Homologs of YfiQ exist in many bacterial species, but as described below, additional KATs with distinctly different structures have been identified.

Table 1. List of archaeal, bacterial, and some simple eukaryotic acetylomes

Ref.	Organism(s)[a]	Mutants assessed	Conditions assessed		# of lysines	# of proteins
			Time/Growth phase[b]	Media		
(55)	48 bacteria from *Proteobacteria, Firmicutes, Bacteroidetes, Actinobacteria, Cyanobacteria,* and *Fibrobacteres*	None	See (55) Table S1		24397	9107
(64)	*Acinetobacter baumannii* ATCC 17978	None	SP	MHB	551	411
(65)	*Aspergillus flavus* CA43	None	48 hours	PDA-cellophane	1383	652
(66)	*Bacillus amyloliquefaciens DSM7*	None	EP	LB	3268	1254
(67)	*Bacillus nematocida* B16	None	12 hours	Solid LB with or without nematode incubation	529	349
(68)	*Bacillus subtilis* 168	None	SP	LB	332	185
(58)	*Bacillus subtilis* 168	None	0.5 OD (EP)	Minimal medium with glucose	1355	629
(69)	*Bacillus subtilis* 168	None	Multiple conditions from previous mass spectrometry runs		4893	1277
(70)	*Bacillus subtilis* 3610	*pta, acuA*	SP	LB with 1% glycerol and 100 μM manganese	1172	826
(71)	*Bacillus subtilis* BD630	None	EP and SP	Minimal glucose medium	2372	841
(72)	*Borrelia burgdorferi* B31-A3	*pta, ackA*	EP and SP	BSK-II medium	199	68
(73)	*Clostridium acetobutylicum*	None	EP, transition, and SP	Defined medium	458	254
(74)	*Corynebacterium glutamicum* ATCC13869	None	9 hours	Glutamate-producing medium +/- Tween 40	1328	288
(75)	*Cyanobacterium Synechococcus* sp. PCC 7002	None	EP (under various stresses)	A+ medium	1653	802
(76)	Erwinia amylovora	None	SP	MBMA minimal	141	96

	Ea1189, Ea273			medium		
(77)	*Escherichia coli* BL21	*cobB*	SP	2XYT	2206	899
(78)	*Escherichia coli* BW25113	None	EP and SP SP	TB7/glucose TB7	2813	780
(56)	*Escherichia coli* BW25113, BL21, MG1655	*yfiQ, cobB, ackA, pta*	EP and SP Growth arrested	M9/glucose Nitrogen limited M9/glucose	8284	1000
(79)	*Escherichia coli* DH10	None	EP	LB	1070	349
(80)	*Escherichia coli DH10B*	None	EP	M9/glucose/lysine/ arginine	2803	782
(50)	*Escherichia coli* DH5α	None	EP	LB	138	91
(57)	*Escherichia coli* MG1655	*ackA, pta ackA, cobB, yfiQ*	1 OD (EP-SP transition)	TB7 and TB7/glucose	2730	806
(81)	*Escherichia coli* MG1655 and BW25113	MG1655: *cobB* BW25113: *ackA, pta*	EP and SP EP	M9/glucose/lysine/ arginine	3669	Not stated
(54)	*Escherichia coli* W3110	None	EP and SP	LB	125	85
(82)	*Escherichia coli* BW25113	*yfiQ, cobB*	EP and SP EP Steady state	Minimal glucose batch Minimal acetate batch Glucose chemostat	2502	809
(83)	*Geobacillus kaustophilus* 7263	None	SP	Difco nutrient broth	253	114
(84)	*Haloferax mediterranei*	None	EP	MG medium	1017	643
(85)	*Mycobacterium abscessus* GZ002	None	EP	Middlebrook 7H9 medium	459	289
(86)	*Mycobacterium smegmatis* MC2 155	None	EP, early SP, and middle SP	Middlebrook H79 liquid with 10 mM glucose	146	121
(87)	*Mycobacterium tuberculosis* H37Ra	None	EP and SP	Middlebrook 7H9 liquid culture medium	226	137
(88)	*Mycobacterium tuberculosis* H37Ra	None	EP 3 weeks	Middlebrook 7H9 aerobically Middlebrook 7H9	441 111	286 83

				anaerobically		
(89)	*Mycobacterium tuberculosis* H37Rv	None	EP	Middlebrook 7H9 medium	1128	658
(90)	*Mycobacterium tuberculosis* H37Rv	None	12 days (EP)	7H9 broth aerobically and anaerobically	1215	679
(41)	*Mycobacterium tuberculosis* L7-35, L7-28, and H37Rv	None	32 days	Middlebrook 7H10 plates	141	109
(91)	*Mycoplasma pneumoniae* M129	*pnkB, hprK, prpC* Mpn027, Mpn114	EP	Hayflick medium	719	221
(59)	*Neisseria gonorrhoeae* 1291	*ackA*	Overnight	IsoVitaleX-supplemented GC broth	2686	656
(92)	*Porphyromonas gingivalis* W50	None	SP	BHI	130	92
(27)	*Pseudomonas aeruginosa* PA14	None	24 hours	Minimal glucose medium	430	320
(93)	*Pseudomonas aeruginosa* PA14	None	SP (24 hours)	Minimal medium with citrate, glucose, glutamate, or succinate	1102	522
(94)	*Rhodopseudomonas palustris* CGA009	*ldaA srtN, ldaA srtN pat, ldaA srtN pat katA*	0.5 OD	Photosynthetic medium with benzoate	32	24
(95)	*Saccharomyces cerevisiae* BY4742	*rpd3*	EP	Synthetic complete medium	2878	1059
(96)	*Saccharopolyspora erythraea* NRRL233338	None	EP	TSBY	664	363
(97)	*Salmonella enterica* Typhimurium ATCC 13311	Ciprofloxacin resistant vs WT	EP	LB	1259	631
(63)	*Salmonella enterica* serovar typhimurium LT2 (G2466)	*pat, cobB*	EP	M9/glucose and M9/citrate	235	191
(98)	*Spiroplasma eriocheiris* TDA-040725-5T	None	EP	R2 medium	2567	555
(99)	*Staphylococcus aureus* 209P	None	24 hours	Cell medium	1361	412
(100)	*Streptococcus pneumoniae* D39	None	EP	THY medium	653	392

(101)	*Streptomyces griseus* IFO13350	None	SP Sporulation	Liquid TMPD medium Solid YMPD medium	162	134
(102)	*Streptomyces roseosporus* NRRL15998	None	EP (3 days)	F10A medium	1143	667
(103)	*Sulfurospirillum halorespirans* DSM 13726	None	Early and late EP	Defined mineral medium	Not stated	640
(104)	*Synechocystis sp* PCC 6803	None	EP	BG11 medium	776	513
(105)	*Thermus thermophilus* HB8	None	SP	TT broth	197	128
(106)	*Toxoplasma gondii* RH strain	None	64-128 parasites/vacuole	Infected hTERT+HFF cells in DMEM	411	274
(107)	*Toxoplasma gondii* RH strain	None	95% host lysis	Infected hTERT+HFF cells in DMEM	571	386
(108)	*Trichophyton rubrum*	None	Conidia Mycelia	PDA Sabouraud liquid medium	386 5414	285 2335
(109)	*Vibrio cholerae* V52	None	EP and SP	LB	3402	1240
(110)	*Vibrio parahemolyticus* O3:K6	None	8 hours	High salt LB	1413	656

[a]Organism species and strains [b]Exponential phase (EP) and Stationary phase (SP)

Acetyltransferases in Bacteria

Multiple families of acetyltransferases have been discovered since the initial finding that an acetyltransferase can inactivate aminoglycoside antibiotics (111). Most of these families have been discovered in relation to histone acetylation in eukaryotes. The two major families of acetyltransferases are the GNAT and MYST families (112, 113). Two smaller groups of acetyltransferases known as p300/CBP family and SRC family also exist, as well as the unique acetyltransferases $TAF_{II}250$, TFIIIC, Rtt109, and CLOCK (114-117). The mechanisms of these acetyltransferases vary. While GNATs form a ternary complex allowing a direct transfer of the acetyl group, the MYST family can either use this ternary complex mechanism or utilize a ping-pong mechanism that generates an acetylated KAT intermediate (118). In contrast to these larger families, the p300/CBP family has been shown to use a sequential mechanism called a Theorell-Chance mechanism (119). Since only GNATs are present in bacteria, we will focus on them.

In bacteria, GNATs were first characterized as aminoglycoside N-acetyltransferases (120, 121) and, to date, every acetyltransferase discovered in bacteria belongs to the GNAT family. These GNATs are present across bacterial phylogeny (122) and modify a wide range of substrates, including proteins and small molecules/metabolites (113, 123, 124). They are generally small, AcCoA-binding proteins that share low sequence identity, but share a characteristic fold by which they are identified (125). The number of GNATs contained in a given genome can vary wildly with *Listeria monocytogenes* containing ~14 GNATs and *Streptomyces lividans* containing ~72 GNATs (126).

The lysine acetylation reaction commonly occurs in a ternary complex between the substrate, AcCoA, and the GNAT, or more specifically KAT. There are three key steps to this acetylation reaction: 1) deprotonation of the target lysine, 2) nucleophilic attack of the lysine on

the carbonyl carbon of the acetyl group of AcCoA, and 3) protonation and dissociation of CoA (113). Within the catalytic pocket of the KAT, there is often a catalytic glutamate that acts as a general base to deprotonate the target lysine. In the namesake Gcn5 enzyme of yeast, this glutamate is E173, which can be found conserved in many of the bacterial GNATs (127-129) and some MYST family members in eukaryotes (118, 130). However, in the absence of this conserved glutamate, it is hypothesized that a series of residues form a water channel instead to create a "proton wire" whereby protons are carried away from active site to other residues or to the solvent (131). Once the lysine is deprotonated, it can perform a nucleophilic attack on the carbonyl carbon of AcCoA, which is bound to the KAT via a positively charged patch that coordinates the CoA moiety via pyrophosphate and pantothenate moieties (116, 119, 128, 132, 133). The newly acetylated substrate dissociates from the KAT, but for the CoA to dissociate, it must first be protonated. Often, a tyrosine in the active site donates a proton to the thiolate of CoA.

The GNATs can be categorized into three main classes based on sequence length and number of GNAT domains present that are subdivided into five types based on domain identities and arrangements. Class I GNATs (Types I-III) are large, multi-domain enzymes with a single GNAT domain. Class II GNATs (Type IV) are smaller enzymes composed of a single GNAT domain. Class III GNATs (Type IV) have multiple GNAT domains (Christensen *et al* 2019, accepted).

Within Class I, there are two families: Class Iα (NDP-forming acyl-CoA synthetase domain and a GNAT catalytic domain) and Class Iβ (effector/regulatory domain and a GNAT catalytic domain). If a Class Iα GNAT encodes the GNAT domain at the C-terminus, this enzyme is considered Type I, but if it the GNAT domain is at the N-terminus, it is considered

Type II (134). YfiQ of *E. coli* and its homologs are members of Type I (135), while PatA of *Streptomyces lividans* and its homologs in other actinomycetes are members of Type II (136). The NDP-forming acyl-CoA synthetase domain of both Type I and Type II is a major target of regulation via acetylation, as will be discussed below. These large NDP-forming acyl-CoA synthetase domains lack catalytic activity because a catalytic histidine is mutated (137, 138), but they can still bind AcCoA, which may have regulatory implications.

In Class Iβ (Type III), three different types of regulatory domains have been found fused to the classical GNAT catalytic domain: an amino acid binding domain (ACT), a cAMP binding domain, and an $NADP^+$ binding domain (139-142). In mycobacterial species, Type III GNATs have an N-terminal cyclic AMP (cAMP) binding domain fused to the small C-terminal GNAT domain. Binding of cAMP to the N-terminal domain has been shown to enhance KAT activity of these Type III GNATs (140, 141, 143, 144). In the case of Pat from *Mycobacterium tuberculosis*, the active site is blocked via auto-inhibition until cAMP is bound (145). Type III GNATs found in Actinobacteria have been shown to be regulated by amino acid binding. First described in *Micromonospora aurantiaca*, these GNATs have an N-terminal ACT domain attached to the C-terminal GNAT domain (146). ACT domains are regulatory domains that respond to amino acids and are often found attached to metabolic enzymes. There appear to be two main subclasses of these ACT-GNAT enzymes: those that have enhanced activity in the presence of cysteine or those that have enhanced activity in the presence of asparagine (139). Addition of cysteine to PatA was shown to cause a conformational change with a subsequent decrease in the K_m for a substrate protein, Acs. Another Type III GNAT that appears unique is the Pat enzyme of *Myxococcus xanthus* which contains a Rossmann fold that binds and responds to $NADP^+$ (142).

Whether this domain structure exists outside of *M. xanthus* or is truly unique remains to be determined.

Class II GNATs (Type IV) are minimal enzymes that consist solely of the GNAT domain. While these enzymes are smaller than members of the other types (150-200 amino acids long), they appear able to perform the same functions. *Bacillus subtilus* AcuA (147), *Saccharopolyspora erythraea* SacAcuA (148), *Rhodopseudomonas palustris* RpKatA (94), *Sulfolobus solfataricus* Pat (51, 149), *S. enterica* TacT (150), and *M. tuberculosis* Rv2170 (151) are each members of this class. The *M. tuberculosis* Rv2170 KAT protein was found to acetylate key lysine residues on isocitrate dehydrogenase (ICDH), which results in a reduction of ICDH activity (151). TacT (STM3651) from *S. enterica* is the toxin protein of the TacAT toxin/antitoxin system, which acetylates amino acyl tRNAs (152) and Lys44 of its own TacA antitoxin pair (150). Recently, four new Class II GNATs from *E. coli* have been identified (YiaC, YjaB, RimI, and PhnO), and they appear to acetylate a wide range of protein substrates (153).

Finally, the only Class III (Type V) GNAT is the enhanced intracellular survival (Eis) from *M. tuberculosis* (154-156). This Class III KAT was initially discovered as an aminoglycoside acetyltransferase (157, 158), but it also has protein acetylation activity, acetylating over thirty lysine residues on an *M. tuberculosis* nucleoid-associated protein (MtHU or HupB) (154) and acetylating Lys55 of host macrophage dual-specificity protein phosphatase 16/mitogen-activated protein kinase phosphatase-7 (DUSP16/MKP-7) (156).

While KATs and GNATs are typically associated with and studied in the context of acetyl groups, the capabilities of these proteins may extend beyond acetylation. Pat from *Salmonella enterica* could catalyze the propionylation of propionyl-CoA synthetase (PrpE) using

propionyl-CoA instead of AcCoA (159). In *E. coli*, overexpression of YfiQ results in increased propionylation (160). Though these results are not direct evidence for YfiQ-dependent propionylation in *E. coli*, based on the *S. enterica* data, it follows that *E. coli* YfiQ could catalyze some of these propionylations. Utilization of an additional acyl-CoA substrate may not be entirely surprising because binding of AcCoA occurs via interactions with the pyrophosphate and pantothenate moieties of CoA with no discernable contribution of the acetyl group. It is due to this binding that these acyl-CoA thioesters are bound with high affinity but low specificity (131, 161). Thus, it is worth considering the possibility that these acetyltransferases are acyltransferases. This makes even more sense in the context of sirtuins (NAD^+-dependent deacylases) that appear to have broader specificity than originally determined, as discussed below.

YfiQ, the Only Known Acetyltransferase in *E. coli* and *S. enterica*

There are 26 genes encoding GNATs or putative GNATs in *E. coli* and *S. enterica*, and of these, only half have known functions (113, 126, 162). Three of these, RimI, RimJ, and RimL, acetylate the α-amine group at the N-terminus of the ribosomal proteins S18, S5, and L12, respectively (32, 33). However, the only Nε-lysine acetyltransferase in *E. coli* prior to this work was YfiQ (also known as PatZ or Pka) (63). This protein was first characterized via its homolog, Pat, in *S. enterica*, which is 96% similar and 92% identical (163), and homologs exist in *Rhodopseudomonas palustris, Vibrio* species, cyanobacteria, and more (126, 164). YfiQ is a Type I GNAT and, as such, contains a large (~700 amino acid) N-terminal domain attached to a smaller (~200 amino acid) GNAT domain at the C-terminus. While the exact role of the large N-terminal domain is not clear, there is evidence it plays a regulatory role. Indeed, YfiQ can be regulated both post-translationally and transcriptionally.

Mutations within the N-terminal domain of the YfiQ homolog of *S. enterica* reduce activity (165), while deletion of the N-terminal domain completely inactivates the enzyme (166, 167). As mentioned above, this large domain looks like an NDP-forming acyl-CoA synthetase (Pfam 13380), but is unable to catalyze the synthetase reaction due to the lack of a catalytic histidine (166). As the normal enzymatic activity of an acyl-CoA synthetase is reversible interconversion of acyl-CoA and free acid, YfiQ/Pat is still capable of binding AcCoA. Thus, there are two sites of AcCoA binding per YfiQ enzyme, one in the N-terminal domain and one in the GNAT domain (166-168). Pat was found to oligomerize and form tetramers in response to AcCoA (166). YfiQ can also form tetramers *in vitro*; however, it favors formation of octamers in the presence of high concentrations of AcCoA (167). It is at these high AcCoA concentrations that YfiQ can undergo autoacetylation on six lysines that, via structural modeling, is suggested to alter shape and charge of a surface patch that allows multimerization (167).

YfiQ expression is transcriptionally regulated. One known mechanism of transcriptional activation is through the cyclic AMP – catabolite activator protein (cAMP-CRP) complex. CRP is a transcription factor that binds cAMP and activates or represses transcription via interaction with RNA polymerase (169). The *yfiQ* promoter contains a CRP binding site -41.5 bp upstream of the +1, which designates this as a Class II site (170). However, *yfiQ* is also in an operon with the upstream gene, *yfiP*. The *yfiP* promoter has a CRP binding site -61.5 bp upstream of the +1, which designates this as a Class I site (170). Thus, *yfiQ* has the potential to be regulated via two different promoters, but both in a CRP-dependent manner. In the presence of glucose, cAMP levels are low; thus, YfiQ expression is minimal due to weakly active CRP. Indeed, exponential growth of *E. coli* in minimal glucose medium results in low *yfiQ* expression, but once the cells deplete the glucose and enter stationary phase, *yfiQ* expression greatly increases. Conversely,

expression of *yfiQ* is high regardless of growth phase when *E. coli* is grown in the presence of a non-catabolite repressing carbon source (e.g., acetate) instead of glucose (135). This regulation may be conserved in the human pathogen, *Yersinia pestis* (171).

Comparisons are often made between YfiQ of *E. coli* and Pat of *S. enterica* because of the evolutionary relatedness of both the organisms and the genes themselves; however, one major difference comes in the regulation of these genes. In *S. enterica*, expression of *pat* depends on IolR, a repressor of myo-inositol catabolism, in addition to CRP (168). The reason for this additional layer of regulation, however, is not clear. The regulation of *yfiQ/pat* expression appears to be linked to at least one target, Acs. Acs is required for assimilation of and growth on low concentrations of acetate (<10 mM) when cells have exhausted a preferred catabolite-repressing carbon source, such as glucose. Acetylation of a conserved lysine by YfiQ/Pat inactivates Acs (172). In *E. coli* and *S. enterica*, the transcription of *yfiQ*/*pat* and *acs* are linked, as they are both activated by CRP. In *S. enterica*, IolR can activate *acs* expression as it does *pat*.

Mass spectrometry of the proteome and *in vitro* acetylation with YfiQ have revealed dozens of YfiQ-dependent acetylated lysines (56, 57, 173). However, when inspecting a *yfiQ* mutant via anti-acetyllysine western blot, the deletion casuses little effect on the acetylome compared to WT cells. Indeed, in *E. coli*, our group and others have shown that most of the observed acetylation is YfiQ-independent and instead depends on AcP, which will be discussed below (56, 57). The determinants that direct YfiQ to a given protein substrate are not fully defined and a linear motif is generally insufficient to predict whether a protein will be a target of YfiQ or not (57). However, specificity clearly exists, as certain lysines on the same protein can be acetylated by YfiQ, while others cannot. Specificity of YfiQ therefore is predicted to be based on a 3D interface formed between the KAT and the substrate protein. One example of this was

shown for *Rp*Pat, the YfiQ homolog in *R. palustris*. *Rp*Pat was found to be unable to acetylate MatB, but chimeric proteins that fused parts of the *Rp*Pat substrate PimA with the unacetylatable MatB yielded certain MatB variants that could then be acetylated. This "chimeric loop" was around 20 Å away from the acetylated lysine, suggesting *Rp*Pat recognizes additional structural components beyond those adjacent to the lysine (94, 174). Furthermore, slight differences in KAT sequence from nearly identical homologs yield very different substrate specificity (42).

Deacetylases in Bacteria

To make a PTM versatile and energetically efficient, the ability to add and remove the PTM is essential. Lysine acetylation can be reversed via the action of a lysine deacetylase (KDAC). Two types of deacetylases are known: NAD^+-dependent sirtuins (175) and Zn^{2+}-dependent deacetylases, which can be broken further into three other classes (I, II, and IV with sirtuins being III) (176-179). Putative homologs of both families are encoded by bacteria, but only a few have been shown to function as true deacetylases (126, 180).

The Zn^{2+}-dependent deacetylases are simple hydrolases that cleave the acetyl group from the lysine to release acetate. To do this, a conserved histidine residue acts as a general base to activate a metal-bound water to attack the carbonyl of the acetyl group. This class of deacetylase has yet to be found in *E. coli*, but AcuC of *B. subtilis* (147) and LdaA of *R. palustris* (164) are family members. Enzymes of the hydrolase family can be inhibited by the addition of butyrate (181).

Sirtuins bind NAD^+ through a Rossmann fold domain (182) and use the NAD^+ as a co-substrate to remove acetyl groups from proteins and produce nicotinamide (NAM) and 2'-O-acetyl-ADP-ribose as a result. Since NAD^+ levels are linked to nutritional status of the cell, it is thought that sirtuins allow the cell to recognize these changes and adjust acetylation accordingly

(183). Furthermore, sirtuins may regulate their own activity by producing NAM. NAM inhibits noncompetitively by condensing with an ADP-ribose-like intermediate formed during the deacetylation reaction; this condensation blocks the progression of the reaction (184) at physiological levels (185-190). NADH also competitively inhibits the reaction at physiological levels (191-193).

While sirtuins are classically thought of as deacetylases, it appears that they may have a broader specificity than originally thought. Sirtuins in the mitochondria have been reported to desuccinylate (10, 80), demalonylate (9, 10, 194), depropionylate (195), deglutarylate (11), decrotonylate (196), and debutyrylate (195) lysines in addition to their role as deacetylases. Bacterial sirtuins have similar abilities to desuccinylate (80), depropionylate (159, 160), and possibly debutyrylate (197) lysines. Many of these PTMs occur on the same lysine, possibly implicating sirtuins with a role as a general cleanup enzyme for certain lysines. Further complicating the possible role of sirtuins, there is evidence that a sirtuins can ADP ribosylate proteins using the NAD^+ substrate (198).

CobB, the Only Known Deacetylase in *E. coli*

CobB is a member of the sirtuin family. Like YfiQ, its activity was first described in *S. enterica* (199, 200), and later in *E. coli* (63, 201). As described above, CobB is a deacetylase, but it can also desuccinylate, depropionylate, and debutyrylate lysines in *E. coli* (80, 159, 160, 197), *M. tuberculosis* (202), and *Lactobacillus acidophilus* (203). It also has been implicated as a lipoamidase (204). CobB is the only gene product annotated as a deacetylase in the *E. coli* genome and, under at least one condition, it was determined to be the sole deacetylase of *E. coli*, as all deacetylase activity was absent from a Δ*cobB* mutant (205). While YcgC was suggested to

be a novel class of deacetylase (206), this was found to be an erroneous result due to preparations of the YcgC protein contaminated with proteases (207).

Depending on the study, the number of acetylated proteins that are deacetylated by CobB fall between 3% and 17% (56, 57, 82, 205). However, the effect of CobB is small when assessed via anti-acetyllysine western blot (50, 57, 201). Like lysines acetylated by YfiQ, there is no obvious linear motif that defines a CobB-sensitive lysine. However, CobB shows a preference for deacetylating lysines contained in disordered regions, loops, α-helices and termini (82, 205). The propensity for CobB to recognize disordered regions appears to be a shared trait among sirtuins (208). To determine whether there was a motif that CobB recognized in linear space, self-assembled monolayers and matrix assisted laser desorption-ionization (SAMDI) mass spectrometry was used to monitor peptide modification of a peptide library immobilized onto a gold surface (209-211). Analysis of acetylated linear peptide motifs did show that CobB prefers lysines with adjacent hydrophobic/non-polar amino acids, while CobB was not able to deacetylate lysine with a proline in the +1 position. *In vivo*, negatively charged amino acids can more commonly be found in the +1 and -1 positions, while CobB-insensitive acetyllysines tend to not have negatively charged amino acids in an adjacent position (205).

The counteracting activities of YfiQ and CobB have been referred to as the "reversible lysine acetylation" or RLA system of *E. coli*. Specific lysines susceptible to these enzymes permit the bacterium to rapidly add or remove acetyl groups from proteins. This process was first established in *S. enterica* on Acs, where initially CobB was found to deacetylate Acs (199) and later it was found that K609 could be acetylated by YfiQ (163). Acetylation and deacetylation of Acs was then confirmed to behave in the exact same manner in *E. coli* (63, 135). The number of lysines and proteins known to be regulated by RLA has been greatly expanded through mass

spectrometric studies, as well as more directed biochemical studies (**Table 2**). However, not all lysines that are acetylated by YfiQ are deacetylated by CobB and vice versa (153, 205). Thus, these enzymes do not act together on each lysine, and therefore the designation of these enzymes as a system should be tempered.

Table 2. Acetylated Proteins in Bacteria

Organism	Acetylated protein	Acetylated lysine(s)	Acetylation mechanism	KDAC(s)	Effect	Refs
Actinosynnema mirium	Acs	620	*Ami*PatA and 23 homologs	Not determined	Inhibits activity	(139)
Bacillus subtilis	Acs	549	AcuA	AcuC, SrtN	Abolishes activity	(147, 212, 213)
	Eno	339, 390	*in vitro* AcP	Not determined	Abolishes activity	(55)
	TufA	42	Unknown	AcuC, SrtN	No effect	(214)
	MreB	240	Not determined	Not determined	Reduces cell length, width, and peptidoglycan thickness	(71)
	CshA	244, 296	Unknown	Not determined	Enhances induction of SigX and SigM-dependent genes	(215, 216)
Borrelia burgdorferi	GapA	Not determined	AcP	Not determined	Inhibits activity	(72)
	LDH	Not determined	AcP	Not determined	Mixed results	
Escherichia coli	ArgRS	126, 408	AcP	CobB	Impairs tRNA charging	(217)
	CRP	100	AcP	Not determined	Reduces interaction with RNAP, enhances protein stability	(218)
	LeuRS	619, 624, 809	AcP	CobB	Impairs tRNA charging	(217)
	Mdh	99 140	AcP	None CobB	Cooperatively increases activity	(219, 220)
	RpoA	291	AcP	Not determined	Reduces *cpxP* transcription	(221)
	TyrRS	85, 235, 238	AcP	CobB	Impairs tRNA charging	(222)
	RcsB	154	AcP	CobB	Enhances migration, impairs acid survival	(82, 223)
	TopA	13, 45, 346, 488	AcP	CobB	Reduces relaxation activity by inhibiting	(224, 225)

					DNA binding and cleavage activity	
	DnaA	178	AcP, YfiQ	CobB	Inhibits ATP binding	(226)
	DnaA	243	AcP, YfiQ	CobB	Inhibits *oriC* binding at low affinity sites	(227)
	CheY	92, 109	Acs, AcCoA	Acs, Pta, CobB	Inhibits interaction with CheA, FliM, and CheZ Activates CheY, promotes clockwise rotation	(228-230)
	YfiQ	146, 149, 391, 446, 635, 819	AcCoA	CobB	Favors formation of octamers	(167)
	Eno	342, 393	*in vitro* AcP	Not determined	Abolishes activity	(55)
	AceA	308	Not determined	CobB	Inhibits activity	(82)
	AlaRS	73	Not determined	CobB	Inhibits activity	(231)
	Mat	12 lysines	Not determined	CobB (9 lysines susceptible)	Inhibits activity, may affect dimerization	(232)
	NhoA	214, 281	Not determined	CobB	Inhibits activity	(233)
	RcsB	180	*Se*Pat, YfiQ	*Se*CobB, *Ec*CobB	Inhibits DNA binding	(173)
	Acs	609	YfiQ	CobB	Inhibits activity by preventing first half reaction	(82, 135, 185)
	RNase II	501	YfiQ	CobB	Inhibits RNase II activity due to reduced substrate binding	(234)
	RNase R	544	YfiQ	None	Destabilizes protein	(235, 236)
	RpoA	298	YfiQ	Not determined	Enhances *cpxP* transcription	(201)
Micromonospora aurantiaca	Acs	619	MaKat	Not determined	Inhibits activity	(146)
Mycobacterium	Acs	616	KATbcg	Not determined	Abolishes activity	(144)

bovis BCG	FadD13	487	KATbcg	Not determined	Inhibits activity	(144)
Mycobacterium smegmatis	FadD33	511	*MsPat*	MSMEG_5175	Abolishes activity	(237)
	MbtA	546	*Ms*Pat	Rv1151c	Inhibits activity	(238)
	PrpE	586	*MsPat*	Not determined	Abolishes activity	(86)
	USP	104	*Mt*PatA, *Ms*PatA	Not determined	Unknown	(141)
	Ku	29, 40	Not determined	Not determined	Correlates with impaired NHEJ activity	(239)
	HupB	86	Not determined	Not determined	Prevents small colony variant formation	(240)
	Acs	589	PatA	SrtN	Impairs growth on acetate	(241)
Mycobacterium tuberculosis	DUSP16 (eukaryotic)	55	Eis	Not determined	Inhibits activation of JNK pathway	(156)
	Histone H3 (eukaryotic)	Not determined	Eis	Not determined	Enhances binding to the IL-10 promoter	(242)
	HupB	32 lysines	Eis	Rv1151c	Inhibits DNA binding	(154, 155)
	Acs	617	*Ms*Pat	Rv1151c, MSMEG_5175	Abolishes activity	(140, 144, 243)
	MbtA	542	*Ms*Pat	Rv1151c	Inhibits activity	(238)
	DosR	182	*Mt*Pat	Rv1151c	Inhibits DNA binding	(90, 244)
	FadD2 FadD4 FadD5 FadD10 FadD12 FadD13 FadD22 FadD35	551 525 519 519 523 487 480 529	*Mt*Pat	MSMEG_5175	Impairs palmitoyl-AMP synthesis activity for FadD2, FadD5, and FadD15	(144)
	PtpB	224	*Mt*Pat	Rv1151c	Decreases reaction rate due to reduced Vmax	(245)

	HspX	64, 78, 85	Not determined	Not determined	Reduced immunogenicity	(87)
	ICL1 (Rv0467)	322 331 392	Not determined	Not determined	Inhibits activity (K322) Enhances activity (K331) Enhances activity (K392)	(88, 89)
	Histone H3 (eukaryotic)	9, 14	Rv3423.1	Not determined	Inhibits DNA binding by histone H3	(246)
Myxococcus xanthus	Acs	622	*Mx*Kat	Not determined	Inhibits activity	(142)
Neisseria gonorrhoeae	PilT	117	AcP	Not determined	May contribute to membrane association, alters microcolony formation	(247)
Porphyromonas gingivalis	RprY	Not determined	*Pg*Pat	CobB	Inhibits DNA binding	(248)
	pro-RgpB	247, 248	VimA, PG1842	Not determined	Permits proper processing of pro-RgpB	(249)
Rhodobacter sphaeroides	FnrL	175, 213, 223	AcP	*Rs*CobB	Impairs transcriptional activation	(250)
Rhodopseudomonas palustris	FadD	546	*Rp*Pat	Not determined	Inhibits activity	(94)
	HcsA	524	*Rp*Pat	LdaA	Inhibits activity	(94)
	LcsA	499	*Rp*Pat	LdaA	Inhibits activity	(94)
	PimA	534	*Rp*Pat	Not determined	Inhibits activity	(251)
	Acs	606	*Rp*Pat, KatA	SrtN and LdaA	Inhibits activity	(94, 164)
	AliA	532	*Rp*Pat, KatA	SrtN and LdaA	Inhibits activity	(94, 164)
	BadA	512	*Rp*Pat, KatA	SrtN and LdaA	Inhibits activity	(94, 164)
	FcsA	496	*Rp*Pat, KatA	LdaA	Inhibits activity	(94)
	HbaA	503	*Rp*Pat, KatA	SrtN and LdaA	Inhibits activity	(94, 164)
	IbuA	539	*Rp*Pat, KatA	LdaA	Inhibits activity	(94)
	PrpE	598	*Rp*Pat, KatA	LdaA	Inhibits activity	(94)

Saccharopolyspora erythraea	AcsA2	611	AcP	Not determined	Inhibits activity by reducing affinity for acetate	(148)
	AcsA1 AcsA2 AcsA3	620 628 615	AcuA	SrtN	Inhibits activity	(148, 252)
	GlnA1	179, 357	AcuA	SrtN	Enhances GlnA1 interaction with GlnR, which enhances DNA binding affinity	(253)
	GlnA4	319	AcuA	SrtN	Inhibits activity	(253)
	AceA	308	Pat	CobB	Inhibits activity	(63, 94)
Salmonella enterica	AceK	72, 83, 553	Pat	CobB	Enhances activation of ICDH	(63, 94)
	GapA	331	Pat	CobB	Enhances glycolytic activity, decreases gluconeogenesis activity	(63, 94)
	HilD	297	Pat	None	Enhances stability, inhibits DNA binding	(254, 255)
	PhoP	201	Pat	CobB	Inhibits DNA binding	(256)
	PrpE	592	Pat	CobB	Abolishes activity	(159)
	Lrp	36	Pat	CobB	Inhibits DNA binding	(257)
	Acs	609	Pat	CobB	Inhibits activity by preventing first half reaction	(163, 199, 258)
	charged aminoacyl tRNAs	N-terminus	TacT	N/A	Inhibits translation	(152, 259)
	TacA	44	TacT	CobB	Enhances TacT activity	(259)
Streptomyces coelicolor	Acs	610	Not determined	CobB1	Inhibits activity	(260)
	GlnR	142, 153, 159, 200	Not determined	CobB2	Alters DNA binding	(261)

Streptomyces griseus	StrM	70	SGR1683, *Ec*YfiQ	Not determined	Inhibits activity	(101)
Streptomyces lividans	Aacs	617	*Sl*Pat	*Se*CobB	Inhibits activity	(134)
	Acs	610	*Sl*PatA, *Sl*PatB	*Sl*SrtA	Inhibits activity	(42, 134)
Streptomyces venezuelae	Acs	665	*Sve*PatA	Not determined	Inhibits activity	(139)
Sulfolobus solfataricus	Alba	16	Pat	Sir2	Inhibits DNA binding	(51)
Vibrio cholerae	Acs	609	YfiQ	CobB	Inhibits activity	(262)
Yersinia pestis	PhoP	Not determined	YfiQ	CobB	Not determined	(171)

In *S. enterica*, the regulation of *cobB* follows *yfiQ* in that it can be activated by IolR (168). In *E. coli*, *cobB* is constitutively transcribed (135), but protein levels have been observed to be higher in glucose-containing medium when compared to acetate-containing medium (204). Whether this discrepancy results from post-transcriptional regulation of CobB or from differences in media or strains used remains an open question. Both *E. coli* and *S. enterica* produce two forms of CobB, a long form ($CobB_L$) and a short form ($CobB_S$) that lacks the 37 N-terminal amino acid extension found in the long form (263, 264). These two isoforms are generated from two monocistronic *cobB* mRNAs from two transcriptional start sites. $cobB_L$ is expressed from a promoter within the upstream gene, *nagK*, while $cobB_S$ is expressed from a promoter within $cobB_L$ itself. The $CobB_S$ isoform is made at 10-fold higher levels than $CobB_L$. Current data suggests they are functionally equivalent at deacetylating two targets, Acs (263) and AlaRS (264). Thus, the reason that two isoforms exist is currently unknown, but one could hypothesize that the existence of the additional 37 amino acids may be a signal sequence to localize $CobB_L$ or to achieve specificity (263, 264).

Effects of Enzymatic Acetylation and Deacetylation on Physiology and Pathogenesis

Many studies have explored the role of enzymatic acetylation on bacterial physiology, often through reverse genetics approaches where the deacetylase, acetyltransferase, or both are deleted or overexpressed. In this section, I will focus on CobB and YfiQ and their homologs in *S. enterica*, as they have been studied the most extensively.

As stated in the above sections, YfiQ and CobB perform opposing roles on the acetylation status of Acs, an enzyme that can irreversibly convert acetate into Acs via two half reactions. Acs requires lysine 609 (K609) for the first half-reaction that forms an acetyl-AMP intermediate (199). Thus, mutation or modification of this residue leads to a catalytically inactive

enzyme (160, 163, 199, 265). Indeed, an epistasis analysis of Δ*acs*, Δ*cobB*, and Δ*yfiQ* mutants showed that regulation of Acs is essential for growth on acetate. *E. coli* Δ*acs* mutants are unable to grow in the presence of <10 mM acetate as the sole carbon source since the alternative pathway, the Pta-AckA pathway, is insufficient due to its low affinity for acetate. A Δ*cobB* mutant phenocopies a Δ*acs* mutant, while a double Δ*yfiQ cobB* mutant can grow on <10 mM acetate (135). This result confirmed that YfiQ-dependent acetylation of Acs shuts down acetate utilization through Acs; but, by deacetylating Acs with CobB, Acs activity is restored (135). Acs was found to be regulated in the exact same fashion in >15 organisms tested, ranging from bacteria to humans (**Table 2**) (266). Beyond Acs, RLA was found to extend to other AMP-forming acyl-CoA synthetases, which are proteins that share a similar structure and the same conserved acetylated lysine found in Acs. *Rhodopseudomonas palustris* possesses 40 of these Acs-like proteins; 10 of them are reversibly acetylated on this conserved lysine (94, 164). As in Acs, acetylation inactivates these enzymes.

In addition to Acs, the Regulator of Capsule Synthesis B (RcsB) protein can be reversibly acetylated through YfiQ and CobB *in vitro*. RcsB is a major transcriptional regulator of *E. coli* and *S. enterica* that regulates approximately 5% and 20% of their respective genomes (267, 268). RcsB promotes capsule biosynthesis and biofilm formation, while impairing transcription of genes required for motility. In *E. coli* and *S. enterica*, RcsB is acetylated on multiple residues. K180 is acetylated in a YfiQ- or Pat-dependent manner and deacetylated by CobB from either bacterium (173). K180 is found in the RcsB DNA binding motif, and acetylation of this residue reduces DNA binding, which can then be reversed by CobB. In two independent studies, CobB was found to be an inhibitor of migration in *E. coli* (82, 269). A Δ*cobB* mutant has more numerous and longer flagella than the parent strain, which could partially be explained by the

ability of CobB to deacetylate RcsB (269). RNase II of *E. coli* was also shown to be a target of these enzymes (234). Acetylation of K501 by YfiQ inhibits substrate binding, which results in reduced exoribonuclease activity. Treatment of RNase II with CobB restores this activity. In *S. enterica*, there have been many more enzymes shown to be regulated by reversible lysine acetylation. PhoP is a member of a two-component regulatory system that responds to low Mg^{2+} and acid stress. It is acetylated by Pat on K201; a modification that decreases DNA binding and thus reduces expression of PhoP-regulated genes (256, 270). CobB could restore DNA binding to acetylated PhoP. Expression of a K201Q variant of PhoP that mimics a constitutively acetylated isoform impaired *S. enterica* virulence in mice. Lrp, an important global transcriptional regulator across bacteria and archaea (271, 272), was shown to be acetylated on K36 in *S. enterica*, which prevented DNA binding (257). CobB treatment permitted DNA binding of Lrp.

While the mechanistic role of RLA on Acs and other enzymes described above has been well established, multiple phenotypes have been found for Δ*pat* and Δ*cobB* mutants in *S. enterica* that are not directly attributed to acetylation of a specific enzyme but are consistent with the opposing effects of these enzymes. Compared to wild-type cells, a Δ*pat* mutant grows slower on minimal glucose but faster on minimal citrate, suggesting Pat plays a role in regulating glycolysis (63). CobB had the exact opposite effect on growth. Furthermore, a Δ*pat* mutant had reduced flux through glycolysis and the TCA cycle, while a Δ*cobB* mutant again had the opposite phenotype and promoted gluconeogenesis (63). For this phenotype, a Δ*cobB* Δ*pat* double mutant behaved like a Δ*pat* mutant, which suggests that CobB is dispensable in the absence of acetylation via Pat. Acetylation by Pat was reported on isocitrate lyase (AceA), isocitrate dehydrogenase (Icd), and Isocitrate dehydrogenase kinase/phosphatase (AceK), and this acetylation was shown to reduce activity for each protein, which could partially explain this

phenotype (63). However, these results were called into question when another group could not confirm these findings (94). Thus, the exact role of Pat- or YfiQ-dependent acetylation in central metabolism is still unclear, but these data suggest they may play a role.

A conserved role for YfiQ and CobB, as well as their homologs, could be as responders to stress, though the acetylated targets that exert these effects are still uncertain. Contrary to the above examples, the effects of YfiQ and CobB or their homologs in certain instances described below may be through independent pathways because deletion of either enzyme results in the same phenotype. For example, *E. coli* and *Y. pestis* both have reduced survival in acid stress when *yfiQ* or *cobB* are deleted, while *S. enterica* survives better when *pat* is deleted and more poorly when *cobB* is deleted (82, 171, 270). When exposed to heat stress, survival of *E. coli* is diminished in Δ*yfiQ* mutants but is increased in Δ*cobB* mutants (273). In contrast, *Y. pestis* survival is diminished in both Δ*cobB* and Δ*yfiQ* mutants when exposed to heat, cold, or high salt stress (171). Additionally, *E. coli* Δ*cobB* mutants have enhanced survival against reactive oxygen species, while YfiQ has no effect. In a more distantly related organism, *Mycobacterium tuberculosis*, loss of its sirtuin (Rv1151c) instead promotes growth in acidic pH (88). Furthermore in *Mycobacterium smegmatis*, the acetyltransferase PatA acetylates Universal Stress Protein (MSMEG_4207) (141). While the effect of this acetylation is untested, it may suggest a common role for acetylation in stress response. The stresses that *pat*/*yfiQ* mutants become sensitized to indicates that acetylation is a general regulator of stress pathways that result in these sensitivities.

Pat has been strongly implicated in *S. enterica* survival and infection. Pat enhances invasion of the bacteria into HeLa cells and enhances survival of the bacteria within macrophages (254). Pat also helps promote survival under acid stress, which may be partially

responsible for the macrophage survival phenotype (270). Importantly, expression of the *Salmonella pathogenicity island* (SPI-1) that is required for virulence is enhanced by Pat (254). SPI-1 is controlled by transcription factor HilD, and acetylation of HilD on K297 by Pat was suggested to stabilize the protein, which could enhance SPI-1 transcription. The role of Pat in virulence was further established by infecting mice with Δ*pat* and Δ*cobB* mutants. The Δ*pat* mutants were hypovirulent and caused reduced mortality, implicating Pat and therefore acetylation as necessary for infection (254). However, Δ*cobB* mutants had little effect. Like *S. enterica*, a Δ*yfiQ* mutant of *Yersinia pestis*, the causative agent of plague, is attenuated in mice (171), but unlike *S. enterica*, a Δ*cobB* mutant is equally attenuated.

The above examples demonstrate how mechanistically similar machinery has evolved in different organisms to suit their specific niches. In many cases, Pat/YfiQ and CobB act antagonistically to reversibly acetylate a specific lysine. However, in response to certain stresses, loss of either the KAT or KDAC can be detrimental to the survival of the bacterium, which suggests that these enzymes are regulating independent pathways. Thus, dysregulation of acetylation in either direction can become detrimental under certain stresses. The pathogenicity data from *S. enterica* and *Y. pestis* suggest that, while there may be some commonalities between the requirements for acetylation in certain scenarios, there are cases where KATs and KDACs do not always act in opposition.

Glucose-Induced Acetylation in *E. coli* Is Acetyl Phosphate-Dependent

Addition of glucose to *E. coli* grown in buffered tryptone broth was found to potently enhance acetylation compared to cells grown without glucose addition (56, 63, 201, 221). However, this glucose-induced acetylation was found to be independent of YfiQ, as a Δ*yfiQ* mutant retained this strong acetylation. Instead, glucose-induced acetylation depended on the

small high-energy central metabolite AcP, as the acetylation was abolished in a Δ*pta* mutant, which cannot synthesize AcP. Taken together, these results showed that AcP-dependent acetylation does not depend on YfiQ. However, glucose-induced, AcP-dependent acetylation did depend on CRP, which was striking because CRP is usually poorly active in the presence of glucose due to low levels of its ligand, cAMP (274, 275). Furthermore, glucose-induced acetylation was most prominent in stationary phase and nitrogen-limited cultures (54, 57, 63, 276). AcP also was found to be responsible for glucose-induced acetylation in *B. subtilis*, rather than the only known acetyltransferase, AcuA (70). Furthermore, acetylation in the spirochete *Borrelia burgdorferi* and in the actinomycete *Corynebacterium glutamicum* also appears to depend on AcP (72, 74). Below, the ability of AcP to acetylate proteins will be discussed.

Non-Enzymatic Acetylation via AcP and AcCoA

Chemical reactions are the basis of all life. While enzymatic catalysis is a primary driver in the kinds of substrates used and products formed, the possible chemical reactions of those substrates and products greatly exceeds those that are catalyzed (3). Many of these uncatalyzed reactions are thought of as deleterious to the cell, causing macromolecular damage such as oxidation of DNA or proteins. Often, the damage can be caused by products of the cell's own metabolism, such as reactive oxygen species (277). Indeed, non-enzymatic modification has been implicated in multiple human diseases (278). As cells have evolved alongside this damaging potential of their own metabolism, it is not surprising that repair pathways exist to mitigate this damage. Perhaps cells have evolved ways to utilize these extra-metabolic occurrences as means of regulation. Specifically, in this context, we will consider acetylation via two acetyl donors, AcCoA and AcP.

The ability of AcCoA and AcP to non-enzymatically modify proteins is not a new idea. AcP has been shown to chemically acetylate amine, thiol, and hydroxyl groups (279, 280). It was first discovered in the 1970s that AcP could non-enzymatically acetylate histones, albumin, and polylysine (281). Due to its high energy nature (ΔG° of -43.1 kJ/mol), which is even greater than that of AcCoA (ΔG° of -31.4 kJ/mol), AcP readily hydrolyzes in water and can acetylate without the need for an enzyme (282, 283). The concentrations needed to achieve non-enzymatic acetylation *in vitro* are comparable to or below physiological levels, which in *E. coli* are around 300 - 500 μM for AcCoA and for AcP between 200 μM in exponential phase to 3 mM in stationary phase (284-286). *In vitro* acetylation reactions are often carried out at basic pH. While basic pH promotes deacetylation of lysine, which may prime the lysine for acetylation, this also increases the rate at which AcP and AcCoA dissociate (279, 283). The non-enzymatic acetylation differs for each lysine and each acetyl donor used. Using bovine serum albumin as an example, it was shown that non-enzymatic acetylation on each lysine is not equal. *In vitro* acetylation reactions with AcP and AcCoA showed that acetylation rates can vary by three orders of magnitude, suggesting that regulation of acetylation depends on the environment surrounding the lysine (287). However, the rate and regulation of acetylation *in vivo* prior to this manuscript was unknown.

Assessment of non-enzymatic acetylation *in vivo* for AcCoA is difficult. In most cases, it is an essential molecule that if depleted would result in lack of viability. However, attempts to recreate the mitochondrial environment have shown that AcCoA could acetylate proteins at physiological levels *in vivo* (288). Furthermore, attempts to reduce the levels of AcCoA, such as by draining acetyl groups into an acetyl group polymer like PHB, do not preclude the effects of KATs. Work in an organism where AcCoA can be non-essential, like the reduced genome

bacterium *Borrelia burgdorferi* that solely synthesizes AcCoA to generate mevalonate, a precursor of cell wall lipid I, might be a useful reductionist system to determine whether this truly occurs *in vivo* (72). Without knowing all possible KATs and eliminating them, it is hard to say whether the reaction is truly non-enzymatic *in vivo*.

Fortunately for most bacteria, modulation or complete elimination of AcP levels is much simpler and less detrimental than elimination of AcCoA, which greatly facilitates studying AcP-dependent acetylation. In *E. coli* and many other bacteria, AcP is generated as an intermediate of the acetate fermentation pathway catalyzed by the reversible enzymes acetate kinase (AckA) and phosphotransacetylase (Pta) (289). Pta catalyzes the conversion of AcCoA and inorganic phosphate to AcP and free CoA. AckA then converts AcP into acetate by transferring the phosphoryl group to ADP to generate one molecule of ATP. In the presence of high acetate concentrations (>10 mM), the pathway can run in reverse, synthesizing AcCoA from acetate, ATP, and CoA (172, 290). By genetically manipulating this pathway, the levels of AcP and thus acetylation can be altered. For example, if cells are grown on glucose, the cells ferment acetate and generate AcP as an intermediate. If one prevents the conversion of AcCoA to AcP by deleting Pta or the entire Pta AckA pathway, AcP cannot be generated. When these mutants are analyzed by western blot, the intensity of the acetylated proteins is greatly reduced to background levels (56, 57). It is worth noting that acetylation can still be detected by mass spectrometry in Δ*pta* and Δ*pta ackA* mutants, but the relative amount of acetylation and number of acetylated lysines is greatly reduced. On the other hand, by deleting *ackA*, AcP accumulates to 10–20 mM (56, 284, 291), which can be seen via western blot as a greatly intensified acetylation profile relative to wild-type cells (56, 57). Mass spectrometry confirms that many more unique lysines on many more unique proteins become acetylated in this mutant, and the population of

those lysines that are detected as acetylated in wild-type become further acetylated as the proportion of the total pool of each unique peptide shifts towards acetylated.

While non-enzymatic acetylation does not require a KAT, it appears that the mechanism by which this occurs has many parallels with enzymatic acetylation. While the KAT serves as an AcCoA binding protein to properly position the acetyl group near the target lysine, non-enzymatic acetylation requires that the protein being acetylated coordinates the CoA group for AcCoA or the phosphate moiety for AcP. Often, the coordinating amino acids are positively charged amino acids (R and K) that make ionic bonds or polar amino acids that can make or hydrogen bonds via hydroxyl groups (S, T, Y) or side chain amides (Q and N) (57). In contrast to KAT-dependent acetylation, where a glutamate from the KAT typically extracts a proton from the lysine to be acetylated, during non-enzymatic acetylation, this process requires an internal glutamate or a water molecule (57, 105). It may be expected that lysines acetylated non-enzymatically may have a reduced pK_a, and thus more propensity to lose a proton. However, the pK_a has not been found to correlate with reactivity (287). Like KATs and KDACs, there is no clear motif that is predictive of whether a lysine is susceptible to chemical acetylation. *In vitro* acetylation of peptides with AcP on a SAMDI chip showed almost every peptide could be acetylated, but by adding magnesium and salt, selectivity and specificity was achieved (57). The SAMDI results indicated adjacent arginines and lysines favored acetylation; *in vivo*, however, there is a propensity for glutamates and aspartates to be adjacent to the lysines acetylated by AcP. Similar results were found for AcCoA, where glutamates were found near lysines *in vivo* (287). For both AcP and AcCoA, there is a tendency for susceptible lysines to be surface-exposed (57, 287). However, due to their relatively small size, AcP and AcCoA can access buried lysines that a KAT could not. Thus, protein structures could have evolved to utilize non-

enzymatic acetylation to regulate protein functions in locations that are impossible for enzymatic acetylation to access.

A Simplified Overview of Central Metabolism and Overflow Metabolism

Acetylation is intimately linked to central metabolism. The two acetyl donors, AcCoA and AcP, are produced as a result of these metabolic pathways, while sirtuins depend on NAD^+, a reporter of cellular carbon and energy status that acts as a cofactor in redox reactions of glycolysis and the TCA cycle (190). Thus, acetylation levels may be a way for cells to sense the nutritional status of the cell. In this section, I will focus primarily on how *E. coli* metabolizes glucose into AcCoA, whether the fate of that AcCoA is fermentation or the TCA cycle, and then review how other organisms can form AcP without fermentation.

Glucose is the preferred carbon source of *E. coli*. This preference is achieved through three mechanisms: catabolite repression (292), transient repression (293), and inducer exclusion (294). Catabolite repression inhibits the transcription of the enzymes necessary to catabolize a carbon source other than the preferred carbon source. Although glucose-dependent repression of lactose is the most common association, catabolite repression (CR) is not a glucose-specific phenomenon, but rather is related to the flux of carbon into the cell. To understand CR and inducer exclusion, we first must discuss the phosphotransferase system (PTS), the phosphorylation cascade that mediates uptake of glucose (**Fig. 2**). In this pathway, glucose enters the cytoplasm through the inner membrane transporter $EIICB^{glc}$ (*ptsG*), where it becomes phosphorylated to become glucose-6-phosphate, the molecule that can enter glycolysis. The carbon from glucose eventually goes on to form 2 molecules of phosphoenolpyruvate. One of these molecules is converted to pyruvate and can be used to make AcCoA, while the other can act as a phosphodonor to EI (*ptsI*), a sugar non-specific phosphotransferase system enzyme.

Another sugar non-specific protein, HPr (*ptsH*), accepts the phosphoryl group from E1, which can then phosphorylate the glucose-specific $EIIA^{glc}$ (*crr*). Phospho-$EIIA^{glc}$ can phosphorylate $EIICB^{glc}$ to permit continued glucose uptake, resulting in most of the $EIICB^{glc}$ being in the dephosphorylated form. Furthermore, this dephosphorylated form of $EIIA^{glc}$ can interact with permeases of the non-preferred carbon sources, preventing transport of those carbon sources into the cell and thus subsequent induction of the operons that permit their metabolism (295). When glucose is fully consumed, phosphorylated PTS proteins become the dominant forms as there is no sugar to phosphorylate. Under these conditions, when glucose is absent, the phospho-$EIIA^{glc}$ interacts with and activates adenylate cyclase, while dissociating from the permeases for alternate carbon sources. This scenario results in production of cAMP, formation of cAMP-CRP transcription factor complex, activation of cAMP-CRP-dependent transcription, and transport of alternate carbon sources.

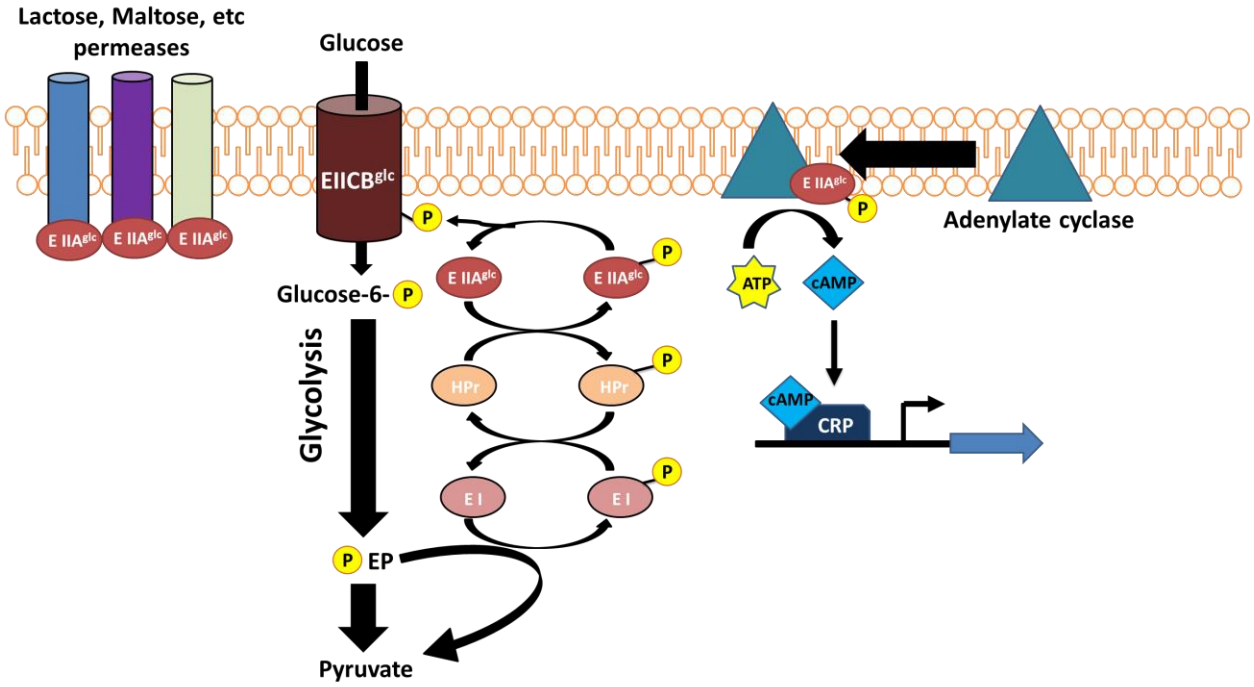

Figure 2. The PTS System of *E. coli*. Glucose is transported and phosphorylated by EIICB^{glc} (encoded by the *ptsG* gene). The carbon from glucose passes through glycolysis to make phosphoenolpyruvate (PEP), which can either donate its phosphoryl group to EI or be converted into pyruvate by Pyk. The phosphoryl group passes from EI to HPr to EIIA and back to EIICB^{glc}. When glucose is abundant, the PTS enzymes remain in a most unphosphorylated form. Unphosphorylated EIIA^{glc} binds to permeases for other carbon sources and prevents import of these carbon sources. When glucose is depleted, the PTS enzymes are mostly phosphorylated. Phosphorylated EIIA^{glc} binds to and activates adenylate cyclase. Adenylate cyclase synthesizes cAMP, which can bind CRP to activate transcription.

Once glucose has entered the cytoplasm and become phosphorylated, glucose-6-phosphate passes through one of three glycolytic pathways: the Embden-Meyerhof-Parnas (EMP) pathway, the Entner-Doudoroff (ED) pathway, or the pentose phosphate (PP) pathway (**Fig. 3**). The EMP pathway is that which is commonly thought of as glycolysis. Relative to the ED and PP pathways, it has high carbon flux. The common result of each of these pathways is the formation of energy and AcCoA. When cells are growing and dividing, the AcCoA is used to make fatty acids and enters the TCA cycle to form amino acid precursors and energy. However,

the flux of carbon into the AcCoA node can be greater than the outward flux. To permit continued consumption of carbon from glycolysis, the cells regenerate CoA by fermenting acetate.

Fermentation is often thought of as a metabolic program during anaerobic growth; however, *E. coli* cells grown aerobically in the presence of excess extracellular glucose will ferment acetic acid (acetate) (296, 297). This phenomenon, called aerobic fermentation or the Crabtree Effect, was first described in cancer cells. When exposed to excess glucose, these tumor cells perform lactic acid fermentation rather than aerobic respiration even when oxygen is present (298, 299). The phenomenon also occurs in yeast; instead of acetic acid or lactic acid, *Saccharomyces cerevisiae* ferments ethanol during growth in the presence of high glucose concentrations. In all three cases, the cells excrete the excess carbon as partially oxidized metabolites (e.g., acetate, lactate, ethanol) rather than putting the excess carbon into biomass via the tricarboxylic acid (TCA) cycle (300, 301). The phenomenon described for yeast appears to be close to the one described for *E. coli* and other bacteria (302). In yeast, a short-term and a long-term form of the Crabtree Effect have been described, but only a phenomenon like the short-term effect has been described in bacteria. The short-term effect is described as the appearance of fermentative products upon addition of excess sugar (303). The short-term mechanism is thought to be overflow in sugar metabolism based on physiological constraints such as maximum velocity of respiration-associated enzymes in yeast (303-305), as well as *E. coli* (306). Essentially, rapid glucose consumption by glycolysis overwhelms the capacity of the TCA cycle, thereby forcing the cells to ferment. In *E. coli*, this is also suspected to be a means of maintaining proper NAD/NADH redox balance as fermentation of acetate produces no NADH, while the TCA cycle will produce 8 NAD(P)H and 2 $FADH_2$ (307, 308). Additionally, the apparent

wasting of resources by fermenting may be due to energy costs. The proteomic demands for respiration are high compared to fermentation and, thus in fast growing cells, the efficiency of respiration is less cost effective than the less efficient fermentation (309).

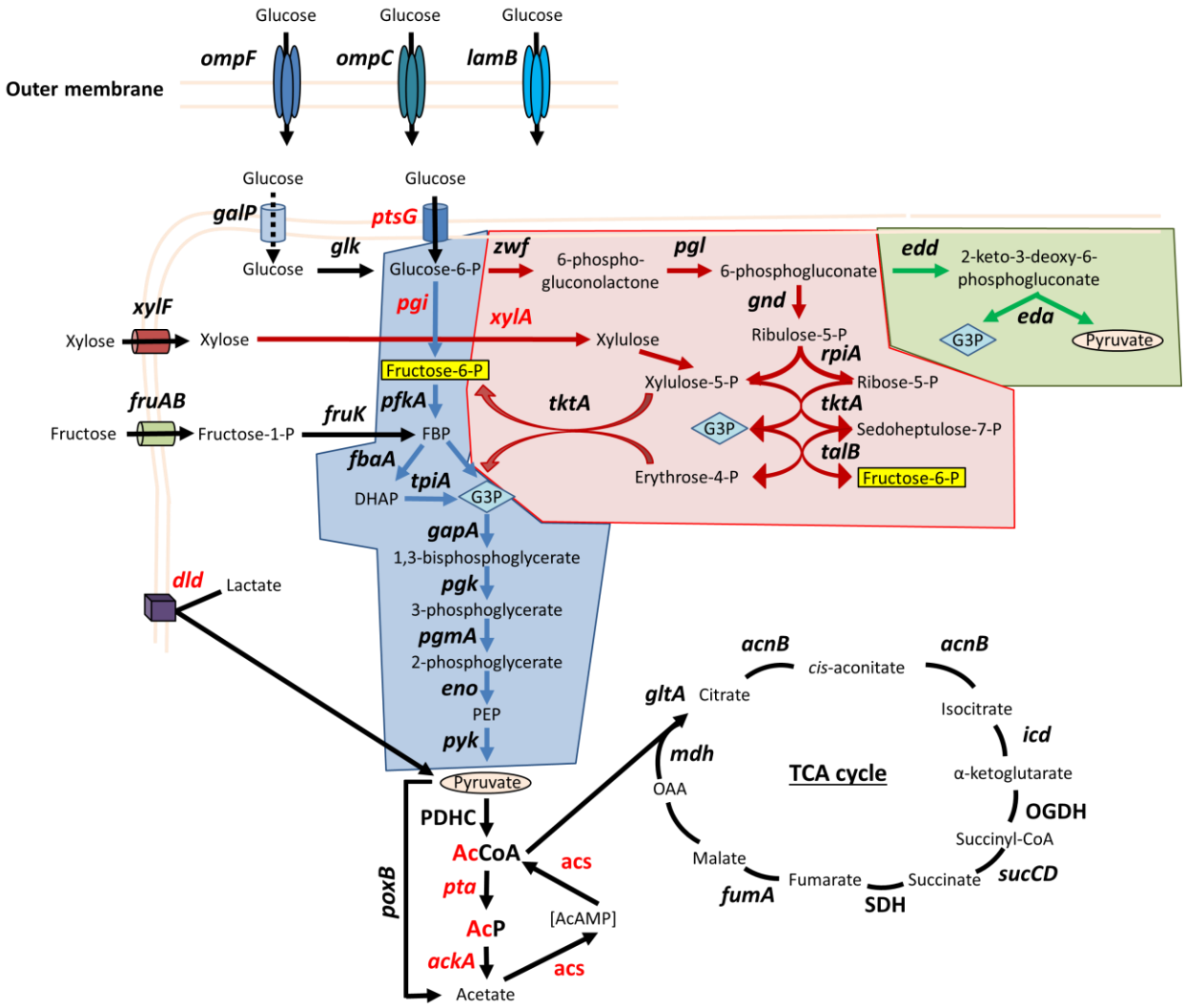

Figure 3. Central Metabolic Pathways of *Escherichia coli*. Three glycolytic pathways exist in *E. coli*: Embden-Meyerhof-Parnas (EMP) pathway (blue), Pentose Phosphate pathway (red), and Entner-Doudoroff pathway (green). Enzyme gene names are shown with the exception of multi-protein enzymes complexes: pyruvate dehydrogenase complex (PDHC), oxoglutarate dehydrogenase complex (OGDH), and succinate dehydrogenase (SDH). Enzymes described in more detail in the text are shown in red. Entry points of glucose, xylose, fructose, and lactate are shown.

Stationary Phase Cultures of *E. coli* – Physiological Shifts

Glucose-induced acetylation increases and accumulates during stationary phase, a time when nutrients are insufficient to maintain steady growth. Under laboratory conditions, bacterial growth occurs in five main stages, of which stationary phase is one (310). A culture begins in *lag phase*, during which the cells must adjust to their new environment; this adjustment requires metabolic reprogramming and nascent protein biosynthesis. The amount of time in lag phase depends on the bacteria, the extent of difference between the old and new environments, and the length of time in starvation (311). Once the cells have adjusted to the new environment, they enter *exponential phase* (sometimes erroneously called *logarithmic phase* or *log phase*). The cells grow at a constant rate that is dictated by the richness of the available (312). Once nutrient sources become exhausted, growth is no longer exponential, and the cells transition into *stationary phase*, where no increase in cell number is observed. The depleted nutrient that sets off this phase could be any that, in its absence, would cause growth cessation; these depleted nutrients could be carbon, nitrogen, or trace elements such as magnesium or iron. As waste products accumulate during this *stationary phase*, the cells will enter a *death phase* during which viable cell counts dramatically decrease. However, not all the cells die, and the remaining survivors enter *long-term stationary phase*. In this final phase, subpopulations die or grow from scavenged nutrients in a balance that results in stable viability of the culture. It should be noted that 60% of earth's biomass is hypothesized to consist of microbes in a stationary phase state (313).

In terms of morphology and transcription, a great change takes place between those cells that grow exponentially from those that are in stationary phase (reviewed in (312).) The cells in stationary phase become smaller and more spherical as they undergo reductive division due to

insufficient resources to generate full sized daughter cells (314). In *E. coli*, the spherical shape is achieved via regulation of penicillin-binding proteins by the transcriptional regulator BolA, whose expression depends on RpoS (also known as σ^S) (314). The stationary phase cells also experience dwarfing, where endogenous resources, cell wall, and inner membrane are degraded (314). Interestingly, in *E. coli*, the size of the outer membrane remains unchanged, resulting in an increase in periplasmic space (315). Extensive structural changes do occur in the outer membrane, inner membrane, and peptidoglycan (316). These changes make the cell wall become more rigid and resistant to stress. Inside the cell, the nucleoid becomes condensed via the Dps protein, which acts during starvation (317, 318).

The starved cells reduce growth rate drastically, reduce transcription, and reduce protein synthesis to 20% that of cells growing exponentially (315). This is done via multiple mechanisms. The levels of ribosomal RNA and transfer RNA both decrease in stationary phase cells, resulting in less capacity for translation (315). The alarmone ppGpp is produced by the proteins RelA and SpoT. RelA binds to the ribosome and becomes activated once an uncharged tRNA binds to the ribosomal A site (319). ppGpp can then bind to the beta subunit of RNA polymerase, affecting promoter specificity and thus gene transcription (320, 321).

During this phase of culture, the alternative sigma factor, σ^S becomes dominant to the housekeeping sigma factor, σ^{70}, partially due to the association with ppGpp (322). σ^S controls up to 10% of the genes in *E. coli* (323, 324), including many genes that respond to osmotic stress (325) and temperature stress (326). In addition to σ^S, the extracytoplasmic sigma factor σ^{32} becomes activated and induces the expression of chaperones and proteases to mitigate oxidative damage occurring on proteins, such as carbonylation (327-329). The activities of IHF and Lrp, two other transcriptional regulators, are also increased when cells experience nutrient limitation

(330, 331). Lrp appears to prepare the cell to direct internal nutrient reserves and metabolize fermentation products (330). IHF induces expression of chaperones and DNA damage response proteins (332, 333).

While chaperones and proteases are utilized for protein maintenance in response to damage, they also generally have increased activity. During growth, the ClpP protease associates with the subunit ClpX to recognize and degrade σ^S (334). During stationary phase, ClpXP and ClpAP complexes facilitate protein turnover, which is increased fivefold in starved cells (335). By turning over proteins, the cells can utilize the freed amino acids and peptides to perform *de novo* biosynthesis in the absence of carbon (336). As mentioned above, protein biosynthesis is reduced on top of this increased proteolysis. In part, this is due to reductions in tRNA and rRNA. There is also a phenomenon that occurs, known as the hibernation stage, wherein ribosomes form inactive, 100S dimers (337), which could be a way to store ribosomes until nutrients become available again. This hibernation is mediated by the Rmf protein, whose expression is induced by ppGpp during stationary phase (338). The combination of reduced biosynthesis and increased proteolysis results in a significantly reduced proteome relative to its exponential phase counterpart, which means any modifications that occur on these proteins have the propensity to have greater effect when there are fewer copies.

Metabolically, these stationary phase cells switch from a respiratory metabolism to more of a fermentative metabolism. The response regulator complex ArcAB/RssB mediates increased synthesis of glycolytic enzymes, while decreasing TCA cycle enzyme synthesis (314). The exact rationale for this change is not clear, but it is hypothesized that this may serve to either prevent uncontrolled use of endogenous nutrient reserves or as a defense mechanism against damaging reactive oxygen species that are produced during respiration (314). Thus, it would be expected

that cells limited by a non-carbon resource but with access to glucose would strongly ferment acetate and acetylate their proteins with AcP.

Summary

When bacteria deplete a nutrient, they will enter stationary phase, during which cell division ceases, but metabolism remains active. If carbon remains during stationary phase, the cells undergo overflow metabolism and ferment acetate. Production of acetate yields AcP, which can acetylate proteins. Since the bacteria cannot help but make AcP when they ferment acetate, one must ask whether the cells have evolved to cope with and/or utilize this non-enzymatic acetylation.

Bacterial protein acetylation has become a field with rapidly growing interest. Since the first determination that a bacterial protein can be regulated by acetylation, CheY of *E. coli* (339), the number of acetylated bacterial proteins detected has grown to the thousands. While acetylation of certain lysines may have a clear output, such as inhibition of enzyme activity due to active site Nε-lysine acetylation, the functional importance of many acetyllysine modifications are more difficult to discern. To uncover the role of acetylation in these unclear cases, it is helpful to use a model bacterium (e.g., *E. coli*) with a vast knowledgebase of pathways, protein structure-function relationships, and physiology. Understanding how AcP-dependent acetylation is regulated can give clues as to how this global modification affects cellular physiology.

In Chapter Three, I investigate the regulation of acetylation by AcP. First, I characterize AcP-dependent acetylation and determine how to modulate acetylation through genetic and non-genetic means. To test the hypothesis that acetylation may serve to differentially regulate metabolism, I then asked whether exposure to different carbon sources, the six-carbon compound glucose and five-carbon compound xylose, yield different acetylated targets. Next, I test the

hypothesis that acetylation could be a means to protect proteins against oxidative damage during stationary phase. Finally, I test the hypothesis that AcP-dependent acetylation could be used as a carbon source during prolonged survival.

Furthermore, although we now know two mechanisms by which acetylation can occur, additional mechanisms might exist. In Chapter Four, I ask whether these two known mechanisms are the only means of acetylation. There are 26 GNATs in *E. coli*, and only YfiQ has been shown to have KAT activity. With the knowledge gained in Chapter Three, I find that four of these GNATs have KAT activity. Finally, I assess mutants and overexpression constructs of these novel KATs to determine when they are physiologically relevant.

CHAPTER TWO

MATERIALS AND METHODS

Bacterial Strains, Plasmids, and Primers

All bacterial strains, plasmids, and primers used in this dissertation are listed in **Table 3**, **Table 4**, and **Table 5**, respectively. Mutant strains were constructed by generalized transduction using P1kc (for details, see "Generalized P1 Transduction"). Transformants were generated via two different methods (for details, see "Transformation").

Culture Conditions

For strain construction, cells were grown in Luria Broth (LB), which contains 10 g/liter tryptone, 5 g/liter yeast extract, and 5 g/liter sodium chloride; LB plates also contained 15 g/liter agar. Where stated, *E. coli* strains were aerated at 225 rpm with a flask-to-medium ratio of 10:1 at 37°C in TB7 (10 g/liter tryptone buffered at pH 7.0 with 100 mM potassium phosphate [61.5 mM potassium phosphate dibasic, and 38.5 mM potassium phosphate monobasic]) or M9 minimal medium (11.3 g/liter M9 salts [5×], 0.1 mM $CaCl_2$, 1 mM $MgSO_4$, 2.45 μM ferric citrate, and 0.03 mM thiamine). In many instances, TB7 was supplemented with 0.4% glucose, 0.4% lactate, 0.4% fructose, or 33 mM succinate. M9 was supplemented with 0.4% glucose, 0.4% xylose, 4% glucose, or 4% xylose. Cell growth was monitored by determining the optical density at 600 nm (OD_{600}) via spectrophotometer (DU640; Beckman Instruments, Fullerton, CA).

Table 3. Bacterial Strains Used in This Study

Strain	Genotype	Refs
AJW2198	AJW678 λ*42*(*acs'-lacZ*) Δ*crp*::frt kn	(340)
AJW2573	BW25113 Δ*pta ackA*	(341)
AJW2922	BW25113 Δ*pta*	(342)
AJW4883	BW25113 λ*rprA142* Δ*rcsB*::frt kn	(78)
AJW5070	AJW678 Δ(*ackA pta hisJ hisP dhu*) *zej223*-Tn*10* Δ*yfiQ*::frt kn	(153)
AJW5231	BW25113 Δ*crp*::frt kn	(78)
AJW5384	BW25113 Δ*ptsG*::frt kn	(78)
AJW5389	BW25113 Δ*cra*::frt kn (aka Δ*fruR*::frt kn)	(78)
AJW5416	BW25113 Δ*csrA*::frt kn	(78)
AJW5426	BW25113 Δ*pta*::frt Δ*yfiQ*::frt Δ*acs*::frt Δ*cobB*::frt kn	(153)
AJW5433	BW25113 Δ*cya*::frt kn	(78)
AJW5441	BW25113 Δ*pgi*::frt kn	(341)
AJW5493	BW25113 Δ*pta*::frt Δ*yfiQ*::frt Δ*acsA*::frt Δ*cobB*::frt kn + pCA24n-*yiiD*	(153)
AJW5494	BW25113 Δ*pta*::frt Δ*yfiQ*::frt Δ*acsA*::frt Δ*cobB*::frt kn + pCA24n-*yhbS*	(153)
AJW5495	BW25113 Δ*pta*::frt Δ*yfiQ*::frt Δ*acsA*::frt Δ*cobB*::frt kn + pCA24n-*speG*	(153)
AJW5496	BW25113 Δ*pta*::frt Δ*yfiQ*::frt Δ*acsA*::frt Δ*cobB*::frt kn + pCA24n-*yjgM*	(153)
AJW5497	BW25113 Δ*pta*::frt Δ*yfiQ*::frt Δ*acsA*::frt Δ*cobB*::frt kn + pCA24n-*yfiQ*	(153)
AJW5498	BW25113 Δ*pta*::frt Δ*yfiQ*::frt Δ*acsA*::frt Δ*cobB*::frt kn + pCA24n-*rimJ*	(153)
AJW5499	BW25113 Δ*pta*::frt Δ*yfiQ*::frt Δ*acsA*::frt Δ*cobB*::frt kn + pCA24n-*rimI*	(153)
AJW5500	BW25113 Δ*pta*::frt Δ*yfiQ*::frt Δ*acsA*::frt Δ*cobB*::frt kn + pCA24n-*argA*	(153)
AJW5501	BW25113 Δ*pta*::frt Δ*yfiQ*::frt Δ*acsA*::frt Δ*cobB*::frt kn + pCA24n-*yiaC*	(153)
AJW5502	BW25113 Δ*pta*::frt Δ*yfiQ*::frt Δ*acsA*::frt Δ*cobB*::frt kn + pCA24n-*yhhY*	(153)
AJW5503	BW25113 Δ*pta*::frt Δ*yfiQ*::frt Δ*acsA*::frt Δ*cobB*::frt kn + pCA24n-*yncA*	(153)
AJW5504	BW25113 Δ*pta*::frt Δ*yfiQ*::frt Δ*acsA*::frt Δ*cobB*::frt kn + pCA24n-*yjaB*	(153)
AJW5505	BW25113 Δ*pta*::frt Δ*yfiQ*::frt Δ*acsA*::frt Δ*cobB*::frt kn + pCA24n-*yedL*	(153)
AJW5506	BW25113 Δ*pta*::frt Δ*yfiQ*::frt Δ*acsA*::frt Δ*cobB*::frt kn + pCA24n-*aat*	(153)
AJW5507	BW25113 Δ*pta*::frt Δ*yfiQ*::frt Δ*acsA*::frt Δ*cobB*::frt kn + pCA24n-	(153)

	elaA	
AJW5508	BW25113 Δ*pta*::frt Δ*yfiQ*::frt Δ*acsA*::frt Δ*cobB*::frt kn + pCA24n-*yjdJ*	(153)
AJW5509	BW25113 Δ*pta*::frt Δ*yfiQ*::frt Δ*acsA*::frt Δ*cobB*::frt kn + pCA24n-*atoB*	(153)
AJW5510	BW25113 Δ*pta*::frt Δ*yfiQ*::frt Δ*acsA*::frt Δ*cobB*::frt kn + pCA24n-*yafP*	(153)
AJW5511	BW25113 Δ*pta*::frt Δ*yfiQ*::frt Δ*acsA*::frt Δ*cobB*::frt kn + pCA24n-*ypeA*	(153)
AJW5512	BW25113 Δ*pta*::frt Δ*yfiQ*::frt Δ*acsA*::frt Δ*cobB*::frt kn + pCA24n-*yjhQ*	(153)
AJW5513	BW25113 Δ*pta*::frt Δ*yfiQ*::frt Δ*acsA*::frt Δ*cobB*::frt kn + pCA24n-*phnO*	(153)
AJW5533	BW25113 Δ*glnA*::frt kn	(341)
AJW5537	BW25113 Δ*pta*::frt Δ*yfiQ*::frt Δ*cobB*::frt kn + pCA24n	(153)
AJW5538	BW25113 Δ*pta*::frt Δ*yfiQ*::frt Δ*cobB*::frt kn + pCA24n-*yfiQ*	(153)
AJW5539	BW25113 Δ*pta*::frt Δ*yfiQ*::frt Δ*acsA*::frt Δ*cobB*::frt kn + pCA24n	(153)
AJW5566	BW25113 Δ*gltA*::frt kn	(341)
AJW5567	BW25113 Δ*glnD*::frt kn	(341)
AJW5568	BW25113 Δ*glnE*::frt kn	(341)
AJW5569	BW25113 Δ*phnP*::frt kn	(341)
AJW5570	BW25113 Δ*phoQ*::frt kn	(341)
AJW5614	BW25113 Δ*ptsG*::frt kn + pCA24n	This study
AJW5615	BW25113 Δ*ptsG*::frt kn + pCA24n-*crp*	This study
AJW5616	BW25113 Δ*crp*::frt kn + pCA24n	This study
AJW5617	BW25113 Δ*crp*::frt kn + pPtsG	This study
AJW5852	BW25113 Δ*thyA*+ pKD46	This study
AJW5864	BW25113 Δ*rimI*::frt kn	This study
AJW5865	BW25113 Δ*phnO*::frt kn	This study
AJW5866	BW25113 Δ*yjgM*::frt kn	This study
AJW5867	BW25113 Δ*yjaB*::frt kn	This study
AJW5868	BW25113 Δ*yiaC*::frt kn	(153)
AJW5874	BW25113 + pCA24n-*rimI*	(153)
AJW5875	BW25113 + pCA24n-*phnO*	(153)
AJW5876	BW25113 + pCA24n-*yjgM*	This study
AJW5877	BW25113 + pCA24n-*yjaB*	(153)
AJW5878	BW25113 + pCA24n-*yiaC*	(153)
AJW5882	BW25113 Δ*yfiQ*::frt kn	(153)
AJW5895	BW25113 Δ*pta*::frt Δ*yfiQ*::frt Δ*acsA*::frt Δ*cobB*::frt kn + pCA24n-locus 31 (FA-2)	This study
AJW5896	BW25113 Δ*pta*::frt Δ*yfiQ*::frt Δ*acsA*::frt Δ*cobB*::frt kn + pCA24n-locus 876 (FA-3)	This study

AJW5897	BW25113 Δ*pta*::frt Δ*yfiQ*::frt Δ*acsA*::frt Δ*cobB*::frt kn + pCA24n-locus 1878 (FA-4)	This study
AJW5901	BW25113 Δ*pta*::frt Δ*yfiQ*::frt Δ*acsA*::frt Δ*cobB*::frt kn + pCA24n-locus 241 (1291-2)	This study
AJW5902	BW25113 Δ*pta*::frt Δ*yfiQ*::frt Δ*acsA*::frt Δ*cobB*::frt kn + pCA24n-locus 1685 (1291-4)	This study
AJW5925	BW25113 Δ*thyA*::*thyA*	This study
AJW5927	BW25113 Δ*xylA*::*xylA* K17Q	This study
AJW5928	BW25113 Δ*xylA*::*xylA* K17R	This study
AJW5930	BW25113 Δ*xylA*::*xylA* K381R	This study
AJW5942	BW25113 *cysK*::*cysK* K42R + pCA24n-*cysK*	This study
AJW5967	BW25113 Δ*pta*::frt lac+	This study
AJW5968	BW25113 Δ*ackA*::frt lac+	This study
AJW5970	BW25113 Δ*pta*::frt ara+	This study
AJW5971	BW25113 Δ*ackA*::frt ara+	This study
AJW5994	BW25113 + pCA24n	(153)
AJW6000	BW25113 Δ*pta*::frt Δ*yfiQ*::frt Δ*acsA*::frt Δ*cobB*::frt kn + pCA24n-locus 27 (FA-1)	This study
AJW6001	BW25113 Δ*pta*::frt Δ*yfiQ*::frt Δ*acsA*::frt Δ*cobB*::frt kn + pCA24n-locus 237 (1291-1)	This study
AJW6005	BW25113 Δ*xylA*::*xylA* K381Q	This study
AJW6030	BW25113 Δ*alkA*::frt kn	This study
AJW6033	BW25113 Δ*yiaC*::frt	This study
AJW6034	BW25113 Δ*yiaC*::frt Δ*alkA*::frt kn	This study
AJW6049	BW25113 Δ*alkA*::frt	This study
AJW6052	BW25113 Δ*tag*::frt kn	This study
AJW6053	BW25113 Δ*alkA*::frt Δ*tag*::frt kn	This study
AJW6055	BW25113 Δ*tag-yiaC*::frt kn	This study
AJW6056	BW25113 *alkA*::frt *tag-yiaC*::frt kn	This study
AJW6067	BW25113 + pCA24n-yfiQ	(153)
AJW6068	BW25113 Δ*tag*::frt	This study
AJW6069	BW25113 Δ*yiaC*::frt Δ*alkA*::frt	This study
AJW6070	BW25113 Δ*alkA*::frt Δ*tag*::frt	This study
AJW6126	BW25113 Δ*pta*::frt Δ*yfiQ*::frt Δ*acsA*::frt Δ*cobB*::frt kn + pCA24n-*yjaB* Y117F	(153)
AJW6130	BW25113 Δ*pta*::frt Δ*yfiQ*::frt Δ*acsA*::frt Δ*cobB*::frt kn + pCA24n-*phnO* E78A	(153)
AJW6131	BW25113 Δ*pta*::frt Δ*yfiQ*::frt Δ*acsA*::frt Δ*cobB*::frt kn + pCA24n-*phnO* Y128A	(153)
AJW6132	BW25113 Δ*pta*::frt Δ*yfiQ*::frt Δ*acsA*::frt Δ*cobB*::frt kn + pCA24n-*rimI* Y115A	(153)

AJW6136	BW25113 Δ*pta*::frt Δ*yfiQ*::frt Δ*acsA*::frt Δ*cobB*::frt kn + pCA24n-*yiaC* F70A	(153)
AJW6137	BW25113 Δ*pta*::frt Δ*yfiQ*::frt Δ*acsA*::frt Δ*cobB*::frt kn + pCA24n-*yjaB* Y117A	(153)
AJW6138	BW25113 Δ*pta*::frt Δ*yfiQ*::frt Δ*acsA*::frt Δ*cobB*::frt kn + pCA24n-*yiaC* Y115A	(153)
AJW6145	BW25113 + pCA24n-*yiaC* F70A	(153)
AJW6146	BW25113 + pCA24n-*yiaC* Y115A	(153)
AJW6163	BW25113 Δ*pta*::frt Δ*yfiQ*::frt Δ*acsA*::frt Δ*cobB*::frt kn + pCA24n-*ypfI*	(153)
AJW6164	BW25113 Δ*pta*::frt Δ*yfiQ*::frt Δ*acsA*::frt Δ*cobB*::frt kn + pCA24n-*astA*	(153)
AJW6165	BW25113 Δ*pta*::frt Δ*yfiQ*::frt Δ*acsA*::frt Δ*cobB*::frt kn + pCA24n-*rffC*	(153)
AJW6166	BW25113 Δ*pta*::frt Δ*yfiQ*::frt Δ*acsA*::frt Δ*cobB*::frt kn + pCA24n-*yhhK*	(153)
AJW6167	BW25113 Δ*pta*::frt Δ*yfiQ*::frt Δ*acsA*::frt Δ*cobB*::frt kn + pCA24n-*yghO*	(153)
AJW6168	BW25113 Δ*pta*::frt Δ*yfiQ*::frt Δ*acsA*::frt Δ*cobB*::frt kn + pCA24n-*citC*	(153)
AJW678	*thi-1 thr-1(Am) leuB6 metF159(Am) rpsL136 lacX74*	(343)
BW25113	F- λ- Δ(*araD-araB*)*567* Δ(*rhaD-rhaB*)*568* Δ*lacZ4787 rrnB3 rph-1 hsdR514*	(344)
BW27422	BW25113 Δ*arcA*43	(345)
ES114	Wild type isolate from *E. scolopes*	(346)
JW0030	Keio Δ*carA*::*kan*	(342)
JW0031	Keio Δ*carB*::*kan*	(342)
JW0162	Keio Δ*glnD*::*kan*	(342)
JW0389	Keio Δ*phoB*::*kan*	(342)
JW0440	Keio Δ*glnK*::*kan*	(342)
JW0474	Keio Δ*ybaS*::*kan*	(342)
JW0660	Keio Δ*asnB*::*kan*	(342)
JW0710	Keio Δ*gltA*::*kan*	(342)
JW0715	Keio Δ*sucA*::*kan*	(342)
JW0911	Keio Δ*aspC*::*kan*	(342)
JW1115	Keio Δ*phoQ*::*kan*	(342)
JW1116	Keio Δ*phoP*::*kan*	(342)
JW1256	Keio Δ*trpE*::*kan*	(342)
JW1328	Keio Δ*fnr*::*kan*	(342)
JW1517	Keio Δ*yneH*::*kan*	(342)
JW1750	Keio Δ*gdhA*::*kan*	(342)
JW2005	Keio Δ*hisH*::*kan*	(342)
JW2309	Keio Δ*purF*::*kan*	(342)
JW2408	Keio Δ*ptsH*::*kan*	(342)

JW2409	Keio Δ*ptsI*::*kan*	(342)
JW2410	Keio Δ*crr*::*kan*	(342)
JW2491	Keio Δ*guaA*::*kan*	(342)
JW2537	Keio Δ*glnB*::*kan*	(342)
JW2541	Keio Δ*purL*::*kan*	(342)
JW3025	Keio Δ*glnE*::*kan*	(342)
JW3179	Keio Δ*gltB*::*kan*	(342)
JW3180	Keio Δ*gltD*::*kan*	(342)
JW3789	Keio Δ*corA*::*kan*	(342)
JW3839	Keio Δ*glnG*::*kan*	(342)
JW3840	Keio Δ*glnL*::*kan*	(342)
JW3841	Keio Δ*glnA*::*kan*	(342)
JW3985	Keio Δ*pgi*::*kan*	(342)
JW4099	Keio Δ*aspA*::*kan*	(342)
JW4201	Keio Δ*mgtA*::*kan*	(342)
MC4100	F-, [*araD139*]*B/r*, Δ(*argF-lac)169*, lambda-, e14-, *flhD5301*, Δ(*fruK-yeiR*)*725*(*fruA25*), *relA1*, *rpsL150*(strR), *rbsR22*, Δ(*fimB-fimE*)*632*(::IS1), *deoC1*	(347)
MG1655	F^-, $lambda^-$, *rph-1*	(348)
PY79	*Bacillus subtilis* PY79	(349)

Table 4. Plasmids Used in This Study

Plasmid	**Resistance**	**Description**	**Refs**
pBR322	Amp	Empty vector	(350)
pCA24n	Cm	Empty vector	(351)
pCA24n-*aat*	Cm	ASKA collection	(351)
pCA24n-*argA*	Cm	ASKA collection	(351)
pCA24n-*astA*	Cm	ASKA collection	(351)
pCA24n-*atoB*	Cm	ASKA collection	(351)
pCA24n-*citC*	Cm	ASKA collection	(351)
pCA24n-*crp*	Cm	ASKA collection	(351)
pCA24n-*cysK*	Cm	ASKA collection	(351)
pCA24n-*elaA*	Cm	ASKA collection	(351)
pCA24n-locus 1685 (1291-4)	Cm	pCA24n carrying *phnO* homolog from GC strain 1291	This study
pCA24n-locus 1878 (FA-4)	Cm	pCA24n carrying *phnO* homolog from GC strain FA1090	This study
pCA24n-locus 241 (1291-2)	Cm	pCA24n carrying *rimI* homolog from GC strain 1291	This study

pCA24n-locus 31 (FA-2)	Cm	pCA24n carrying *rimI* homolog from GC strain FA1090	This study
pCA24n-locus 876 (FA-3)	Cm	pCA24n carrying locus 876 from GC strain FA1090	This study
pCA24n-*phnO*	Cm	ASKA collection	(351)
pCA24n-*phnO* E78A	Cm	SDM of pCA24n-*phnO*	(351)
pCA24n-*phnO* Y128A	Cm	SDM of pCA24n-*phnO*	(351)
pCA24n-*ptsG*	Cm	ASKA collection	(351)
pCA24n-*rffC*	Cm	ASKA collection	(351)
pCA24n-*rimI*	Cm	ASKA collection	(351)
pCA24n-*rimI* Y115A	Cm	SDM of pCA24n-*rimI*	(153)
pCA24n-*rimJ*	Cm	ASKA collection	(351)
pCA24n-*speG*	Cm	ASKA collection	(351)
pCA24n-*yafP*	Cm	ASKA collection	(351)
pCA24n-*yedL*	Cm	ASKA collection	(351)
pCA24n-*yfiQ*	Cm	ASKA collection	(351)
pCA24n-*yghO*	Cm	ASKA collection	(351)
pCA24n-*yhbS*	Cm	ASKA collection	(351)
pCA24n-*yhhK*	Cm	ASKA collection	(351)
pCA24n-*yhhY*	Cm	ASKA collection	(351)
pCA24n-*yiaC*	Cm	ASKA collection	(351)
pCA24n-*yiaC* F70A	Cm	SDM of pCA24n-*yiaC*	(153)
pCA24n-*yiaC* Y115A	Cm	SDM of pCA24n-*yiaC*	(153)
pCA24n-*yiiD*	Cm	ASKA collection	(351)
pCA24n-*yjaB*	Cm	ASKA collection	(351)
pCA24n-*yjaB* Y117A	Cm	SDM of pCA24n-*yjaB*	(153)
pCA24n-*yjaB* Y117F	Cm	SDM of pCA24n-*yjaB*	(153)
pCA24n-*yjdJ*	Cm	ASKA collection	(351)
pCA24n-*yjgM*	Cm	ASKA collection	(351)
pCA24n-*yjhQ*	Cm	ASKA collection	(351)
pCA24n-*yncA*	Cm	ASKA collection	(351)
pCA24n-*ypeA*	Cm	ASKA collection	(351)
pCA24n-*ypfI*	Cm	ASKA collection	(351)
pCP20	Cm, Amp	Temperature sensitive plasmid carrying FLP gene	(352)
pDCRP	Amp	pBR322 carrying wild-type *crp* cloned under the control of the *crp* promoter	(350)
pDCRP-H159L	Amp	pBR322 carrying *crp* H159L cloned under the control of the *crp* promoter	(350)
pDCRP-	Amp	pBR322 carrying *crp* H159L,K101E cloned	(78)

H159L,K101E		under the control of the *crp* promoter	
pDCRP-K101E	Amp	pBR322 carrying *crp* K101E cloned under the control of the *crp* promoter	(350)
pKD46	Amp	Carries lambda Red genes under an arabinose-inducible promoter	(344)

Table 5. Primers Used in This Study

Primer	**Sequence**
PhnO E78A F	5’-gtcaactggatcggcgcaattcaggagttggtg-3’
PhnO E78A R	5’-caccaactcctgaattgcgccgatccagttgac-3’
PhnO Y128A F	5’-gacgcgcaccgtttcgctctgcgcgaaggcta-3’
PhnO Y128A R	5’-tagccttcgcgcagagcgaaacggtgcgcgtc-3’
RimI Y115A F	5’-gctgccgccattgccctggccgaaagtttaggctttaa-3’
RimI Y115A R	5’-ttaaagcctaaactttcggccagggcaatggcggcagc-3’
YiaC F70A F	5’-cagcattatggaaggccgagctctggcagcgatgtttg-3’
YiaC F70A R	5’-caaacatcgctgccagagctcggccttccataatgctg-3’
YiaC Y115A F	5’-gtttatcaaaaaaatcaaccggcgataaattttgcccaggcacagggttttc-3’
YiaC Y115A R	5’-gaaaaccctgtgcctgggcaaaatttatcgccggttgatttttttgataaac-3’
YjaB Y117A F	5’-tgagcaggcggttgggttcgctaagaaggtgggttttaag-3’
YjaB Y117A R	5’-cttaaaacccaccttcttagcgaacccaaccgcctgctca-3’
YjaB Y117F F	5’-gcaggcggttgggttctttaagaaggtgggtttta-3’
YjaB Y117F R	5’-taaaacccaccttcttaaagaacccaaccgcctgc-3’
thyA up	5'-ccgacgcgcagttta-3'
thyA dn	5'-cacgttgtgttttcatgc-3'
xylA K17 TU	5'-ctattttgaccagctcgatcgcgttcgttatgaaggctcaaaatagacagctgcatgcat-3’
xylA K17 TD	5'-gttcgtcgggattgtagtgacggaatgctaacgggtttgaggagtgtaggctggagctg-3’
xylA MU 17A	5'-cgttcgttatgaaggctcagcatcctcaaacccgttagca-3’
xylA MD 17A	5’-tgctaacgggtttgaggatgctgagccttcataacgaacg-3’
xylA MU 17Q	5’-cgatcgcgttcgttatgaaggctcacagtcctcaaacccgt-3’
xylA MD 17Q	5’-acgggtttgaggactgtgagccttcataacgaacgcgatcg-3’
xylA MU 17R	5’-cgcgttcgttatgaaggctcaagatcctcaaaccc-3’
xylA MD 17R	5’-gggtttgaggatcttgagccttcataacgaacgcg-3’
xylA K17 F1U	5’-gcgagcgagcgcacacttgt-3’
xylA K17 F1D	5’-gttccagcagaaggtgtgccagta-3’
xylA K17 F2U	5’-tcttacttttgttgcgcaat-3’
xylA K17 F2D	5’-gtggaaaaactcaaatgcgac-3’
xylA K381 TU	5’-gaaaattgcagcgcgcatgattgaagatggcgagctggataaatagacagctgcatgcat-3’
xylA K381 TD	5’-tggcccaattcgctattccagccggaataacgctgcgcgatgcggtgtaggctggagctg-3’
xylA MU 381A	5’-gaagatggcgagctggatgcacgcatcgcgcag-3’
xylA MD 381A	5’-ctgcgcgatgcgtgcatccagctcgccatcttc-3’
xylA MU 381Q	5’-aagatggcgagctggatcagcgcatcgcgcagc-3’

xylA MD 381Q	5’-gctgcgcgatgcgctgatccagctcgccatctt-3’
xylA MU 381R	5’-gaagatggcgagctggatagacgcatcgcg-3’
xylA MD 381R	5’-cgcgatgcgtctatccagctcgccatcttc-3’
xylA K381 F1U	5’-gtggtctgaacttcgatgcc-3’
xylA K381 F1D	5’-tcctggcgaccactctgatg-3’
xylA K381 F2U	5’-gtgtggaagagaatgcgctg-3’
xylA K381 F2D	5’-tgcccggtatcgctaccgat-3’
CRP AR1 H159L - F	5'-caaaacaaccagacgctatgactctgccggacggtatg-3'
CRP AR1 H159L - R	5'-cataccgtccggcagagtcatagcgtctggttgttttg-3'
CRP AR2 K101E - F	5'-gtgaagtggctgaaatttcgtacaaagaatttcgccaattgattca-3'
CRP AR2 K101E - R	5'-tgaatcaattggcgaaattctttgtacgaaatttcagccacttcac-3'
pCA24n Up	5’-gccctttcgtcttcacctc-3’
pCA24n Dn	5’-ggcagatcgtcagtcagtca-3’
ackA fwd	5’-gcgctacgctctatggct-3’
ackA rev 2	5’-cgttccattgcacggatcac-3’
pta fwd 2	5’-gcggtggttatcccaacc-3’
pta rev 2	5’-gcaaagtgggatggcgc-3’
acsA fwd 2	5’-gttgctgaccttcaaaaattaccc-3’
acsA rev 2	5’-cccgctcccttatgggag-3’
yfiQ fwd	5’-aacgcaacatctgggtagc-3’
yfiQ rev	5’-cctctgtgcaatgcagacg-3’
tag::frtkn deletion F	5’-cgatcgggtacatagcgagggaaagtatgattccggggatccgtcgacc-3’
yiaC::frtkn deletion R	5’-gaactgacacttacagcgtttgaaccaccggtgtaggctggagctgcttcg-3’

To determine the effect of magnesium on growth, a volume of $MgSO_4$ stock (1 M) was added to cells grown in TB7 or TB7 supplemented with 0.4% glucose to achieve the final concentrations indicated in the text.

Antibiotics were prepared as a stock solution 1000 times the working concentration. Working concentrations were as follows: ampicillin, 100 μg/mL; kanamycin, 40 μg/mL; tetracycline, 15 μg/mL; and chloramphenicol, 25 μg/mL. Stock solutions of ampicillin and kanamycin were dissolved in water and filter sterilized. Stock solutions of tetracycline and chloramphenicol were dissolved in 50% and 100% ethanol, respectively, and filter sterilized. All antibiotic stocks were stored at -20°C. To induce expression from the pCA24n plasmid, IPTG

(Isopropyl β-D-1-thiogalactopyranoside) was added to a final concentration of 50 μM or 100 μM.

Generalized P1 Transduction

To generate lysates, a donor strain (often from the KEIO collection (342)) was aerated until 0.3 OD600 in 5 mL TBT (TB with 0.2% [w/v] glucose, 10 mM calcium chloride, 10 mM magnesium sulfate, 0.04 mM ferric chloride) with antibiotic, if appropriate. Upon reaching this density, 100 μL of a P1kc phage lysate was added and aeration resumed for another three to five hours until complete lysis. This lysate was treated with 100 μL chloroform, vortexed, and centrifuged at 3000 rpm for 15 minutes. The supernatant was transferred to a new tube, treated with 100 μL chloramphenicol and stored at +4°C in the dark.

To transduce a recipient strain, the recipient was grown overnight in LB and diluted into 5 mL TBT to an OD600 of 0.02-0.04. The recipient was aerated until 0.5-1.0 OD500, and 1 mL of culture was transferred into 1.5 mL tubes. 100 μL of donor phage lysate was added to the recipient and the mixture was incubated statically for 30 minutes at 37°C. 200 μL of 1 M sodium citrate, pH 5.5 was added to the infected cells to prevent further infection. The infected cells were pelleted and suspended in 500 μL LB, then 200 μL of 1 M sodium citrate, pH 5.5 was added to the suspension. The cells were incubated statically at 37°C for 70 minutes. The cells were pelleted and suspended in 100 μL sodium citrate, pH 5.5. The entire 100 μL of transduced cells was plated onto LB plates containing the appropriate antibiotics and incubated at 37°C for 24 hours, or until colonies appeared. Note that, if the marker was chloramphenicol, half the normal working concentration was used, while if the marker was kanamycin, double the normal working concentration was used.

Elimination of Kanamycin Cassettes Flanked by FRT Sites

The KEIO collection replaces each non-essential gene of *E. coli* with a kanamycin cassette flanked by FRT sites that can permit elimination of the cassette upon expression of Flp recombinase. To achieve this, a mutant carrying an FRT-kanamycin-FRT cassette was transformed via the TBF protocol (see "Transformation") with the pCP20 plasmid carrying the *flp* gene. Cells were plated on LB/ampicillin, and recovery of the strain was carried out at 30°C or below due to the temperature-sensitive origin of replication of pCP20. To ensure loss of the kanamycin cassette, individual colonies that arose were struck on LB and LB/kanamycin and were grown at 30°C. To eliminate pCP20, kanamycin sensitive colonies were struck on LB and grown at 42°C. Loss of pCP20 was confirmed by replica streaking on LB and LB/ampicillin. The resultant kanamycin-sensitive, ampicillin-sensitive strains were checked for kanamycin cassette elimination by PCR.

Site-Directed Mutagenesis

Site-directed mutagenesis of *crp* in pDCRP and of *phnO, rimI, yiaC,* and *yjaB* in pCA24n was performed using the QuikChange II Site-Directed Mutagenesis Kit (Agilent Technologies, Santa Clara, CA) per the manufacturer's instructions. Primers used for site-directed mutagenesis can be found in **Table 5**. Mutations were confirmed by sequence analysis of the purified mutagenized plasmid (ACGT, inc, Wheeling, IL).

FRUIT: Flexible Recombineering Using Integration of *thyA*

To introduce mutant alleles of *xylA* into the chromosome, lambda Red-based technique, FRUIT, was employed (353). Briefly, a Δ*thyA* strain carrying the temperature sensitive plasmid pKD46 that encodes the lambda Red recombination genes was grown to 0.6 OD600 in 50 mL LB supplemented with 100 μg/mL thymine, 100 μg/mL ampicillin, and 0.15% arabinose. Cells

were pelleted at 4000 rpm for 7 minutes. The pellet was washed with 50 mL ice cold water three times. After the last wash, the water was decanted, and the pellet was resuspended in any remaining water. Cells were transformed with a PCR product containing a *thyA* cassette flanked by homology to the gene to be mutated. Cells that successfully recombined the *thyA* cassette into the chromosome were grown in LB supplemented with 100 μg/mL ampicillin and 0.15% arabinose. These cells were pelleted and transformed as described above. However, the PCR product contains the replacement allele of interest with regions of homology around the *thyA* cassette. Transformants were plated on M9 minimal medium supplemented with 0.4% glucose, 0.2% casamino acids, 100 μg/mL ampicillin, 100 μg/mL thymine, and 20 μg/mL trimethoprim, such that only cells that successfully replace the *thyA* cassette can grow. Finally, the *thyA* cassette was restored to the native site in the chromosome via the steps described above.

Transformation

Two transformation methods were used: transformation buffers (TBF) and electroporation.

TBF

To generate chemically competent cells, overnight cultures grown in LB (with antibiotic, if appropriate) were subcultured into 100 mL LB (with antibiotic, if appropriate) and aerated at 225 rpm at 37°C until the OD600 reached 0.4-0.6. The culture was cooled on ice for 5 minutes and then pelleted. The supernatant was removed, and the pellet was suspended with 7.5 mL cold TBF1 (30 mM potassium acetate, 100 mM potassium chloride, 10 mM calcium chloride, 50 mM manganese chloride, 15% glycerol, pH to 5.8 with acetic acid) and incubated for one hour on ice. The cells were pelleted, supernatant removed, then the pellet suspended with 2 mL cold TBF2 (10 mM MOPS, 75 mM calcium chloride, 10 mM potassium chloride, 15% glycerol, pH to 6.5 with potassium hydroxide). The cells were chilled on ice for 30 minutes before use.

1 μL plasmid DNA was added to 50 μL chemically competent cells and chilled on ice for 10 minutes. The cell-DNA mixture was heat shocked in a water bath for 45 seconds at 42°C, then chilled on ice for 2 minutes. 1 mL LB was added to the transformed cells, and the cells were shaken at 225 rpm at 37°C for one hour. 100 μL of the transformed cells were plated onto LB plates containing the appropriate antibiotics and incubated at 37°C overnight, or until colonies appeared.

Electroporation

Overnight cultures grown in LB (plus antibiotic if appropriate) were subcultured into 50 mL LB (plus antibiotic if appropriate) and shaken at 225 rpm at 37°C until the OD600 reached 0.4-0.6. The culture was transferred into a 50 mL conical tube and incubated on ice for 30 minutes. The tube was centrifuged at 4000 rpm for 7 minutes at +4°C. The supernatant was removed, and each pellet was suspended in 1 mL cold water. An additional 49 mL cold water was added to each cell suspension, bringing the volume to 50 mL. These washes were repeated three more times; after the last wash, the pellet was suspended in the liquid remaining after decanting. 1 μL plasmid DNA was added to 50 μL electrocompetent cells, which were then transferred to a chilled electroporation cuvette with a 0.2 cm gap and electroporated at 25 μF, 200 Ω, and 2.5 kV. 1 mL LB was added to the transformed cells, and the cells were shaken at 225 rpm at 37°C for one hour. 150 μL of the transformed cells were plated onto LB plates containing the appropriate antibiotics and incubated at 37°C overnight, or until colonies appeared.

Measurement of Glucose and Acetate in Media

At the indicated time points, culture supernatants were harvested. Supernatants were diluted 1:150 in 50 mM sodium acetate buffer. 50 μL of the diluted samples and standards were

added to a 96-well plate. To each well, 50 μL of reaction mix (48 mM sodium acetate [Sigma 241245], 320 μM o-Dianisidine [Sigma D3252], 4U/mL horseradish peroxidase [Sigma P8250], 0.8U/mL glucose oxidase [Sigma G2133]) was added. Reactions were incubated for 30 minutes and were stopped with 12N H_2SO_4. Color change was measured spectrophotometrically at OD540. Concentration of glucose in samples was determined using the standards.

Acetate measurements were performed using Acetate Colorimetric Assay Kit (Biovision, Milpitas, CA) per the manufacturer's instructions. Briefly, culture supernatants were harvested as above. 5 μL sample was added to 45 μL assay buffer. Diluted samples and standards were added to a 96-well plate. 50 μL of reaction mix was added to each well and allowed to proceed for 40 minutes at room temperature. OD450 was determined spectrophotometrically and standards were used to calculate acetate concentrations in the samples.

Western Immunoblot Analysis

E. coli cells were grown in TB7 overnight at 225 rpm at 37°C. The cultures were diluted to 0.05 OD600 in either TB7 or TB7 supplemented with 0.4% glucose. Cells were harvested and pelleted at the indicated times. Per 1 mL culture, pelleted cells were lysed with agitation for 30 minutes using 46 μL BugBuster protein extraction reagent (Novagen, Merck Millipore, Billerica, MA, USA) with 4 μL DNase/RNase mix (1 mg/mL DNase, 0.3 mg/mL RNase). The lysate was centrifuged, and the cleared lysate was separated from cell debris. The amount of cell lysate to be loaded on the gel was normalized to the total protein concentration (15 μg), as determined by the bicinchoninic acid (BCA) assay (Thermo Scientific Pierce, Waltham, MA, USA). After normalization, the lysates were boiled in a 1:5 mixture with NuPage LDS sample buffer supplemented with 10% beta-mercaptoethanol. Proteins were separated by sodium dodecyl sulfate-polyacrylamide gel electrophoresis (SDS-PAGE) at 125V until the dye front left the gel.

Normalization was verified by Coomassie staining. Transfer to nitrocellulose membrane was carried out for 1.5 hours at 100V at +4°C. The membrane was blocked with 5% milk. Protein acetylation was determined using a rabbit polyclonal anti-acetyllysine antibody (Cell Signaling #9441) at a dilution of 1:1,000 in 5% BSA with a secondary goat-anti-rabbit IgG HRP-linked antibody (Cell Signaling #7074) at a dilution of 1:2,000 in 5% milk. His-tagged proteins were detected using mouse anti-His tag (27E8) antibody at a dilution of 1:1,000 (Cell Signaling, Danvers, MA) and an anti-mouse IgG HRP-linked antibody at a dilution of 1:2,000 (Cell Signaling, Danvers, MA). To detect CRP, monoclonal mouse primary antibodies against CRP (BioLegend 664304) were used at a dilution of 1:2,000 and HRP-conjugated goat anti-mouse secondary antibody (Millipore AP503P) were used at a dilution of 1:2,500.

Detection of His-tagged KATs was carried out as above with slight modifications. His-tagged KATs were detected with crude lysates. One milliliter of 1 OD_{600} culture was harvested, pelleted, and suspended in 200 μL sample loading buffer. The samples were boiled for 10 minutes and 15 μL were loaded directly onto SDS-PAGE gels. His-tagged proteins were detected with mouse anti-His tag (27E8) antibody at a dilution of 1:1,000 (Cell Signaling, Danvers, MA) and an anti-mouse IgG HRP-linked antibody at a dilution of 1:2,000 (Cell Signaling, Danvers, MA).

Isolation and Qualitative Assessment of Protein Aggregates

E. coli cells were aerated overnight in TB7 at 225 rpm at 37°C. The cultures were diluted to 0.05 OD600 in TB7 supplemented with 0.4% glucose and aerated for 10 hours or 24 hours. After 10 or 24 hours, a 10 mL sample of the culture with lowest OD600 value and the equivalent cell number of the other cultures were harvested and pelleted. Cell pellets were suspended in 1 mL PBS and pelleted again. Cell pellets were suspended in 300 μL Lysis Buffer (10 mM Tris-

HCl pH 8.0, 1 mM EDTA pH 8.0, 1.4 mM PMSF) and were incubated on ice for 10 minutes. From here on, cells or cell components were kept on ice or at 4°C for centrifugation steps. Pellets were disrupted by sonication (10 bursts of 10 seconds each with 30 seconds rest in between). Cell suspensions were centrifuged at 2000 × g for 15 minutes to remove intact cells. Supernatant was removed and centrifuged at 15,000 × g for 20 minutes to collect the insoluble fraction. The insoluble pellet was suspended in 400 μL of Lysis Buffer with 2% NP40 to separate proteins from membranes. Aggregated proteins were centrifuged at 15,000 × g for 30 minutes, and the resultant pellets were suspended in Lysis Buffer with 2% NP40 twice. Pelleted proteins were suspended in 40 μL Gel Loading Buffer (62.5 mM Tris-HCl pH 6.8, 10% glycerol, 179 mM beta-mercaptoethanol, 0.2% SDS, 0.002% Bromophenol blue). Proteins were separated by SDS-PAGE at 125V until the dye front left the gel. Proteins were visualized by Coomassie staining.

Carbonylation Analysis

Carbonylated proteins were assessed via the OxyBlot™ Protein Oxidation Detection Kit (MilliporeSigma, Darmstadt, Germany) per the manufacturer's instructions. Cells were grown and harvested as described in the text. Cell lysis was performed with either sonication (10 bursts of 10 seconds each with 30 seconds rest in between) or with BugBuster protein extraction reagent. During cell lysis, 1% beta mercaptoethanol and 50 mM DTT were added to inhibit oxidation after lysis and 1 mM PMSF was added to inhibit proteolysis. 15 μg of isolated proteins were denatured by adding an equivalent volume of 12% SDS and derivatized by treatment with a 1× 2,4-dinitrophenylhydrazine (DNPH) solution or a control solution for 15 minutes. 3 μL of LDS sample buffer was added and volumes were normalized to 30 μL with water. Proteins were separated via SDS-PAGE and were transferred to a nitrocellulose membrane as described in

"**Western Immunoblot Analysis**". Derivatized proteins were detected via anti-DNP primary antibody with an HRP-linked secondary antibody.

Purification of His-Tagged Proteins

QIA*express*® Ni-NTA Fast Start kit (Qiagen, Hilden, Germany) was used to purify His-tagged proteins per the manufacturer's instructions. Briefly, cells carrying a plasmid encoding a His-tagged protein were aerated in 250 mL LB supplemented with chloramphenicol. Upon achieving an OD600 of 0.6, IPTG was added to a final concentration of 500 μM. After 5 hours, cells were pelleted, resuspended in 10 mL Native Lysis Buffer supplemented with 1 mL DNase/RNase mix and 40 μL lysozyme (25 mg/mL), and agitated for 30 minutes on ice. Cell debris was removed by centrifugation at 14,000 × g at 4°C. His-tagged proteins were purified using the supplied Ni-NTA column. Flow through, wash fractions, and elutions were collected at each step to monitor the His-tagged protein purity and loss.

In Vitro Acetylation Assays

Enzymatic

Acetylation reactions of CysK (20 μM) were carried out with YiaC (2 μM) in reaction buffer (50 mM Tris pH 8.0 or 50 mM Tris pH 7.0, 250 mM NaCl, 10% glycerol, 1 mM DTT, 10 mM sodium butyrate, 10 mM $MgCl_2$) with concentrations of AcCoA varying from 10 μM to 5 mM. Control reactions were carried out in the absence of YiaC or AcCoA. The reactions were allowed to proceed for 1 hour at 37°C. To stop the reactions, loading dye was added, and either samples were boiled for 5 minutes at 100°C or they were immediately loaded into the SDS-PAGE gel. Anti-acetyllysine western blots were performed as described above.

Non-Enzymatic

Acetylation reactions were carried out in reaction buffer (150 mM Tris pH 7.3, 150 mM NaCl, 10% glycerol, 10 mM $MgCl_2$) with varying concentrations of AcP or AcCoA. Reactions were incubated at 37°C for 2 hours. Reactions were stopped by adding an equivalent volume of LDS sample buffer. Samples were loaded on an SDS-PAGE gel, and anti-acetyllysine western blots were performed as described above.

Starvation Survival Assay

From a parent strain (BW25113) that could not grow on arabinose or lactose, two sets of Δ*pta* and Δ*ackA* strains were generated such that they could grow on either arabinose or lactose by performing three backcrosses initially using a lysate of strain MG1655 (lac+, ara+). All strains were aerated overnight in M9 minimal medium with 0.4% glucose (M9/gl) as the sole carbon source. The cultures were diluted into fresh M9/gl and aerated until stationary phase (~9 hours). Equivalent cell numbers were harvested from each flask. Cell pellets were resuspended in M9 without a carbon source and either maintained as a monoculture or combined with the cell suspension containing the opposing deletion and marker. These M9 cultures were aerated for 9-16 days. At the indicated days, serial dilutions were performed, and cells were plated on M9 agar supplemented with 0.4% arabinose or 0.4% lactose to enumerate colony forming units.

DNA Alkylation Survival Assay

Cells were aerated in LB until an OD600 of 0.4 – 0.6, whereupon they were harvested and pelleted. Cell pellets were resuspended in an equivalent volume of M9 without a carbon source. A volume of MNNG (1 mg/mL) was added to each cell suspension to achieve the desired concentration, and treatment was allowed to proceed for 20 minutes. After 20 minutes, two equivalents of PBS were added to stop the treatment. Then, cells were pelleted and resuspended

in fresh PBS. 10-fold dilutions were made in PBS, and dilutions were spotted on LB plates to determine cell survival.

Mucoidy Assay

Cells were grown overnight in LB with appropriate antibiotic. Equivalent cell numbers were spotted onto M9 minimal glucose plates. Plates were incubated at 28°C overnight. Colonies were assessed for visual mucoid phenotype.

Motility Assay

Cells were grown in tryptone broth medium (10 g/liter tryptone, 5 g/liter NaCl) overnight supplemented with antibiotics or 50 μM IPTG when appropriate. 5 μL spots containing equivalent cell numbers were spotted onto semisolid agar plates (10 g/liter tryptone, 5 g/liter, 2 g/liter agar) supplemented with antibiotics or 50 μM IPTG when appropriate. Alternatively, overnight cultures were diluted to 0.05 OD600 and aerated until exponential phase (~0.5 OD600). Then, equivalent cell numbers were spotted onto semisolid agar plates. Plates were incubated at 30°C. Diameters of the colonies were measured hourly.

Mass Spectrometry

Preparing Samples

In all experiments described, each sample described was obtained in triplicate biological samples. To determine how acetylation changed over time in response to glucose, wild-type *E. coli* was grown overnight in TB7 and then diluted into TB7 alone or into TB7 supplemented with 0.4% glucose. At the time points mentioned in the text, cultures were harvested. To identify proteins acetylated by YiaC, YjaB, PhnO, RimI, and YfiQ, the Δ*pta yfiQ acsA cobB* (gutted) strains overexpressing each putative KAT were aerated in TB7 supplemented with 0.4% glucose, 50 μM IPTG, and chloramphenicol for 10 hours. To identify acetylated proteins in response to

glucose or xylose, wild-type *E. coli* were grown overnight in M9 minimal medium with either 0.4% glucose (M9/glucose) or 0.4% xylose (M9/xylose) as the sole carbon source. The cells in M9/glucose were diluted into M9 minimal medium supplemented with 0.4% or 4% glucose, while the cells in M9/xylose were diluted into M9 minimal medium supplemented with 0.4% or 4% xylose. These cultures were aerated for 12 hours and harvested. In each experiment, the cells were pelleted, rinsed in 6 mL PBS, pelleted again, and frozen at -80°C until shipment to Dr. Birgit Schilling (Buck Institute for Research on Aging).

Proteolytic Digestion of Protein Lysates and Enrichment of Acetylated Peptides

The firm cell pellet was suspended and denatured in a final solution of 6 M urea, 100 mM Tris, 75 mM NaCl, and the deacetylase inhibitors tricostatin A (1 mM) and nicotinamide (3 mM). Samples were sonicated on ice (5× each for 15 sec), cellular debris was removed by centrifugation, and the supernatants were processed for proteolytic digestion. Lysates containing 1.5 mg of protein were reduced with 20 mM DTT (37°C for 1 h), and subsequently alkylated with 40 mM iodoacetamide (30 min at RT in the dark). Samples were diluted 10-fold with 100 mM Tris (pH 8.0) and incubated overnight at 37°C with sequencing grade trypsin (Promega) added at a 1:50 enzyme:substrate ratio (wt/wt). In parallel, separate 1.5 mg protein aliquots were digested using endoproteinase Glu-C (Roche, Indianapolis, IN) by adding Glu-C at a 1:50 protease to substrate protein ratio (wt:wt), and incubating overnight at 37 °C. Subsequently, samples were acidified with formic acid and desalted using HLB Oasis SPE cartridges (Waters) (354). Proteolytic peptides were eluted, concentrated to near dryness by vacuum centrifugation, and suspended in NET buffer (50 mM Tris-HCl, pH 8.0, 100 mM NaCl, 1 mM EDTA). A small aliquot of each protein digestion (~ 10 μg) was saved for protein-level identification and

quantification. The remaining proteolytic peptide samples were used for affinity purification of acetylated peptides (K^{ac}).

Acetylated peptides were enriched using 1/4 tube of anti-acetyl lysine antibody-bead conjugated 'PTMScan Acetyl-Lysine Motif [Ac-K]' Kit (Cell Signaling Technologies) for each of the 1 mg protein lysate samples according to the manufacturer's instructions. Prior to mass spectrometric analysis, the acetylated peptide enrichment samples were concentrated and desalted using C-18 zip-tips (Millipore, Billerica, MA).

Mass Spectrometric Analysis

Samples were analyzed by reverse-phase HPLC-ESI-MS/MS using the Eksigent Ultra Plus nano-LC 2D HPLC system (Dublin, CA) combined with a cHiPLC System, which was directly connected to a quadrupole time-of-flight SCIEX TripleTOF 6600 mass spectrometer (SCIEX, Redwood City, CA) (78). After injection, peptide mixtures were transferred onto a C18 pre-column chip (200 µm x 6 mm ChromXP C18-CL chip, 3 µm, 300 Å, SCIEX) and washed at 2 µl/min for 10 min with the loading solvent (H_2O/0.1% formic acid) for desalting. Subsequently, peptides were transferred to the 75 µm x 15 cm ChromXP C18-CL chip, 3 µm, 300 Å, (SCIEX), and eluted at a flow rate of 300 nL/min with a 3 h gradient using aqueous and acetonitrile solvent buffers (78).

Data-dependent acquisitions: To build a spectral library for protein-level quantification, the mass spectrometer was operated in data-dependent acquisition (DDA) mode where the 30 most abundant precursor ions from the survey MS1 scan (250 msec) were isolated at 1 m/z resolution for collision induced dissociation tandem mass spectrometry (CID-MS/MS, 100 msec per MS/MS, 'high sensitivity' product ion scan mode) using the Analyst 1.7 (build 96) software with a total cycle time of 3.3 sec as previously described (57, 78, 355).

Data-independent acquisitions: For quantification, all peptide samples were analyzed by data-independent acquisition (DIA, e.g. SWATH) (356), using 64 variable-width isolation windows (57, 357, 358). The SWATH cycle time of 3.2 sec included a 250 msec precursor ion scan followed by 45 msec accumulation time for each of the 64 variable SWATH segments.

CHAPTER THREE

EXPERIMENTAL RESULTS

Characterizing the Timing and Dynamics of Glucose-Dependent Acetylation

Introduction

Our group and others have determined that acetylation can globally modify proteins in *E. coli*. Acetylation in *E. coli* depends on two mechanisms. First, the only known lysine acetyltransferase (KAT) in *E. coli*, YfiQ, can enzymatically acetylate proteins using the metabolite Acetyl-CoA (AcCoA) (126, 166, 359, 360). Second, acetyl phosphate (AcP), an intermediate of the acetate fermentation pathway, can acetylate lysines in the absence of an enzyme (56, 57). Western blot analysis with confirmation by mass spectrometry showed that the majority of acetylation in wild-type (WT) *E. coli* cells depends on the synthesis of AcP, while YfiQ plays a relatively small role (56, 57). Structural analyses of the lysines sensitive to AcP revealed that the molecular determinants of an AcP-sensitive lysine must be able to bind the phosphoryl group, properly position the acetyl group, and deprotonate the target lysine (57). The proteins modified in an AcP-dependent manner are predominantly central metabolic enzymes, often on lysines known to be metabolically active. Thus, we hypothesize that AcP may be a signal used to control central metabolism through acetylation. While this hypothesis remains to be tested, the physiological effects of AcP-dependent acetylation are unknown.

Furthermore, the only known mechanism of deacetylation in *E. coli* is via CobB, a lysine deacetylase (KDAC) of the NAD^+-dependent sirtuin family. However, our determination of CobB-sensitive lysines by mass spectrometry only found 24 lysines were susceptible to both CobB and AcP (205). The disparity between these regulatory mechanisms raises the question: how do cells regulate AcP-dependent acetylation? Understanding this regulation may provide necessary insights into how cells have evolved to utilize this global PTM.

Thus, I sought to better characterize how AcP-dependent acetylation was regulated. I hypothesized that since AcP is an intermediate of acetate fermentation, AcP-dependent acetylation could be a mechanism to sense the metabolic status of the cell. Therefore, AcP-dependent acetylation may be regulated in a manner similar to fermentation, or it may be further regulated based on which lysines are acetylated at a given time. To address any of these questions, first we needed to describe the phenomenon more fully. I set out to better establish the timing of acetylation and to determine whether I could modulate acetylation by modulating exposure to carbon.

Carbon-Induced, AcP-Dependent Acetylation Accumulates during Stationary Phase

Previous work demonstrated that addition of 0.4% glucose (4 g/L or 22.2 mM) to tryptone broth buffered to pH 7 (TB7/gl) induced global acetylation in WT *E. coli* in an AcP-dependent manner (57). Broad time points indicated that this induction occurred between exponential growth and stationary phase, as assessed by anti-acetyllysine western blot. This phenomenon depended on glucose because the intensity of the acetylation profile was consistently low throughout exponential phase and stationary phase for cells grown in TB7 alone. In our efforts to determine how AcP-dependent acetylation is regulated, I sought to more fully characterize the timing of this phenomenon.

To more precisely determine when induction occurs, I repeated this experiment while taking more time points across the growth curve. Thus, I monitored the growth of WT cells in TB7/gl and harvested cells every hour for ten hours and again at 24 hours (**Fig. 4A**). Lysates were normalized for protein concentration (**Fig. 4B**) and analyzed by anti-acetyllysine western blot (**Fig. 4C**). The signal intensity of the global acetylation profile increased steadily, but the vast majority of that increase occurred after the cells had entered stationary phase (after 4 hours post-inoculation) and continued until a point between 10 and 24 hours.

Furthermore, a single band appeared at 24 hours that was also present in cells grown in TB7 alone. As described in **Appendix A**, this band corresponds to the YfiQ-dependent acetylation target, AcCoA synthetase (Acs). Since Acs expression depends on CRP, it is only produced when glucose is depleted, and thus it serves as a diagnostic marker for whether the cells are no longer experiencing catabolite repression.

I then asked whether this was a phenomenon exclusive to glucose or whether other carbon sources could induce acetylation. I grew cells in TB7 supplemented with 0.4% lactate and found the same trend, indicating that this is not a glucose-specific phenomenon but rather that acetylation is carbon-induced (**Fig. 5**).

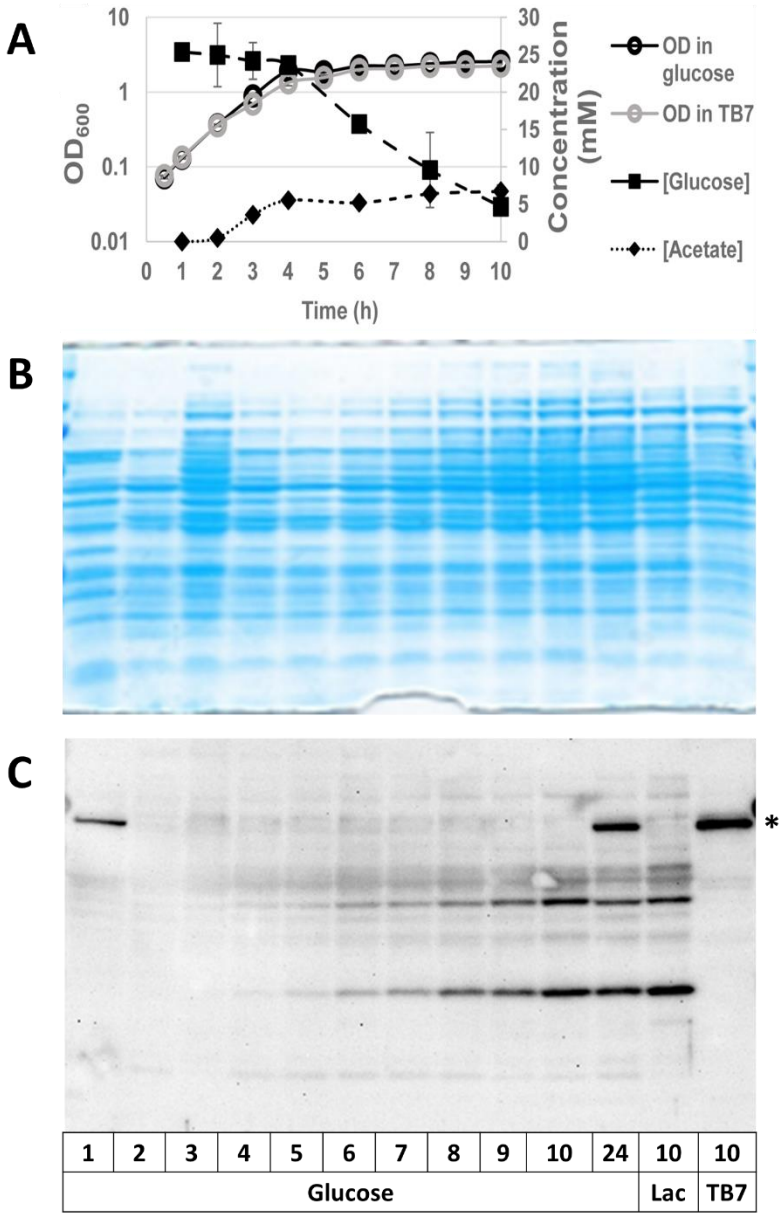

Figure 4. Glucose-Induced Acetylation. Wild-type cells of *E. coli* (strain BW25113) were aerated at 37°C in TB7 (gray circles) or in TB7 supplemented with 0.4% (w/v) glucose (black circles), harvested every hour up to 10 h, growth measured at OD600 and the filtered culture medium assessed for glucose (black squares) and acetate (black diamonds) concentrations (A). The whole cell protein lysate was normalized to protein concentration, separated by 1D-SDS PAGE and stained with Coomassie blue stain (B) and assessed for protein acetylation by anti-acetyllysine (α-acK) Western immunoblot analysis. This blot is representative of three experiments (C). In panels B and C, cells grown in TB7 and TB7 plus glucose were also harvested at 24 hours. Also, cells were grown in TB7 supplemented with 0.4% (w/v) lactate for 24 hours before harvesting. The band at the asterisk (*) corresponds to acetylated Acs.

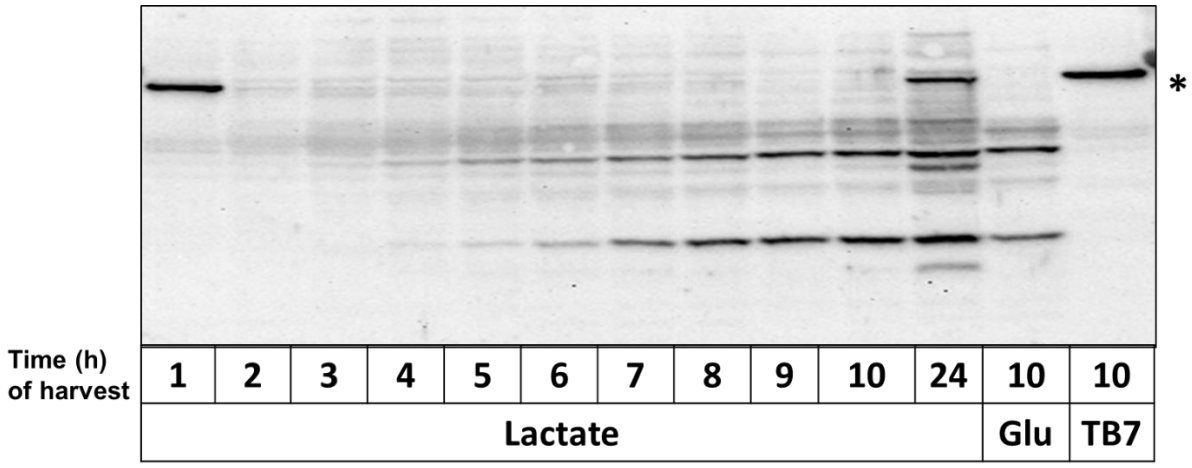

Figure 5. Lactate Induces Acetylation. Wild-type cells of *E. coli* (strain BW25113) were aerated at 37°C in TB7 supplemented with 0.4% (w/v) lactate. Samples were harvested every hour up to 10 h and again at 24 h. The whole cell protein lysate was normalized to protein concentration, separated by 1D-SDS PAGE and assessed for protein acetylation by anti-acetyllysine (α-acK) western immunoblot analysis. Two additional lanes with the 10 h glucose (Glu) and TB7 sample from 3.1C were included for reference. The band at the asterisk (*) corresponds to acetylated Acs.

Glucose Is Not Consumed until Stationary Phase in TB7

The finding that glucose-induced, AcP-dependent acetylation could occur in stationary phase was perplexing. In M9 minimal medium with glucose as the sole carbon source, glucose is consumed during exponential growth, and only once glucose is depleted does the culture enter stationary phase (361). Because AcP is generated as a consequence of glucose metabolism and acetate fermentation, this would mean one of two possibilities. First, glucose is metabolized during exponential phase, and AcP is stored/sequestered until stationary phase when it can acetylate proteins. Alternatively, glucose is not consumed until stationary phase in the rich, amino acid-based TB7 medium. To determine when glucose was consumed, I repeated the above experiment and measured the glucose in the medium via a colorimetric assay. This assay utilizes glucose oxidase to oxidize glucose to D-glucono-δ-lactone and hydrogen peroxide that can be a substrate for peroxidase, resulting in a color change of o-Dianisidine. Using this assay, I found

that cells grown in TB7/gl only appreciably depleted glucose once the cells had entered stationary phase (>4 hours) (**Fig. 4A**), in contrast to those grown in M9 minimal medium with glucose as the sole carbon source; in the latter condition, glucose depletion and entry into stationary phase co-occurred (**Fig. 6**). These data were independently confirmed by our collaborator James Orr (University of Illinois Urbana-Champaign), who used liquid chromatography to monitor glucose concentrations (341). These data further solidified the connection between consumption of glucose and induction of acetylation.

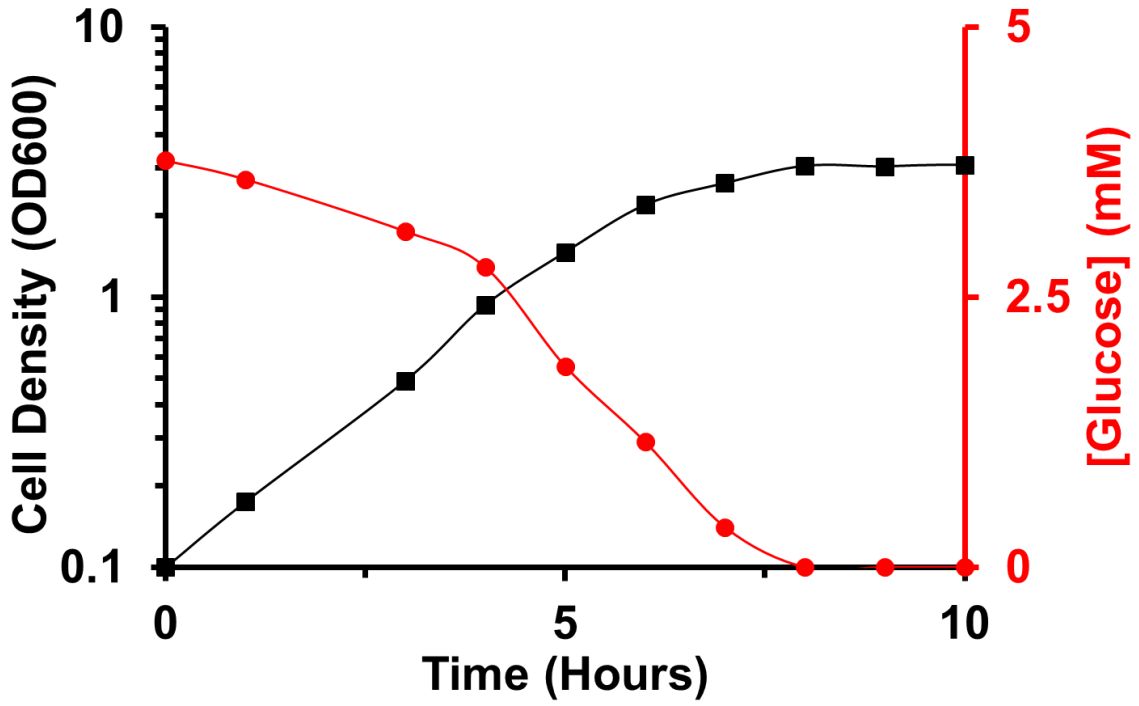

Figure 6. Glucose Is Consumed Prior to Stationary Phase in Minimal Medium. Wild-type cells of *E. coli* (strain BW25113) were aerated at 37°C in M9 minimal medium supplemented with 0.4% glucose, harvested hourly for 10 h, growth measured at OD600 (black line) and the filtered culture medium assessed for glucose (red line) concentration.

Continuous Carbon Exposure Is Required for Induction of Acetylation

To confirm that continuous metabolism of glucose in stationary phase is required for accumulation of acetylation, I asked whether removal of the excess carbon source could abrogate the accumulation of acetylation. Because glucose cannot be removed from the medium directly, I performed media swaps between parallel cultures of WT cells grown in TB7 or TB7/gl. I aerated cultures for three hours until just before the cells began to rapidly consume glucose. Then, every hour from three to eight hours, I swapped the media by pelleting cultures from TB7 and TB7/gl, filtering the supernatants, and then resuspending the pellets in the opposite medium from which they had begun growth. The swapped cultures were continually aerated until ten hours after initial inoculation and analyzed by anti-acetyllysine western blot. With this experimental design, cells that had been exposed to glucose from the beginning (0 hours) were further incubated in the media that had never contained glucose and vice versa. Consistent with the hypothesis that metabolism of glucose in stationary phase is required to achieve strong acetylation, cells that were exposed to glucose longer before the media swap had stronger acetylation intensity than those that had been swapped sooner (**Fig. 7**). Strangely, the cultures that received glucose after the swap at 3 hours never looked like cells exposed to glucose from the beginning of growth, though there should be plenty of glucose (**Fig. 7, compare lane 9 to lane 8**). Thus, exposure to glucose in exponential phase may induce a regulatory program that causes *E. coli* to accumulate acetylation in stationary phase.

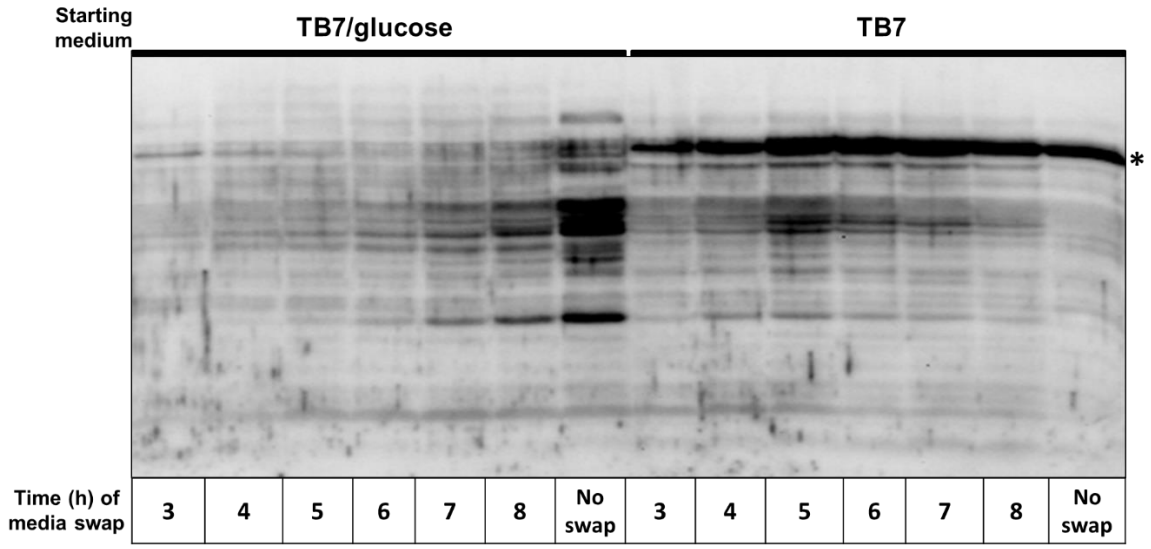

Figure 7. Continuous Glucose Exposure Is Required for Accumulation of Acetylation in Stationary Phase. Wild-type cells of *E. coli* (strain BW25113) were aerated at 37°C in TB7 or TB7 supplemented with 0.4% glucose (Starting medium). At the indicated hours (h), the cells were pelleted and resuspended in the opposite medium. Ten hours after inoculation, cells were harvested. Protein lysates were normalized to protein concentration, separated by 1D-SDS PAGE, and assessed for protein acetylation by anti-acetyllysine (α-acK) western immunoblot analysis. The band at the asterisk (*) corresponds to acetylated Acs.

Carbon Must be Added during Exponential Growth to Induce Acetylation

Since acetylation occurs in stationary phase and depends on glucose, I wondered whether timing of glucose addition could alter timing of acetylation or whether addition of glucose to cultures during stationary phase is sufficient to induce acetylation. To determine this, I grew WT cells in TB7. At each hour, I added 0.4% glucose. Ten hours after inoculation, I harvested the cells and performed anti-acetyllysine western blot analysis (**Fig. 8A**). Acetylation was strongest if I added glucose prior to the transition to stationary phase (prior to three hours after inoculation), and the signal intensity was further reduced with longer delays before glucose addition. Using 0.8% lactate, I was able to achieve the same results, which confirmed that this is not exclusively a glucose phenomenon (**Fig. 8B**).

Because the cells with later glucose addition had been exposed to glucose for less time, I ensured this weak acetylation was not due to insufficient exposure to glucose by growing the cells for an additional ten hours after the addition of glucose. Indeed, the acetylation intensity was strong when glucose was added during exponential phase (prior to three hours after inoculation), but weak when glucose was added after three hours (**Fig. 8C**).

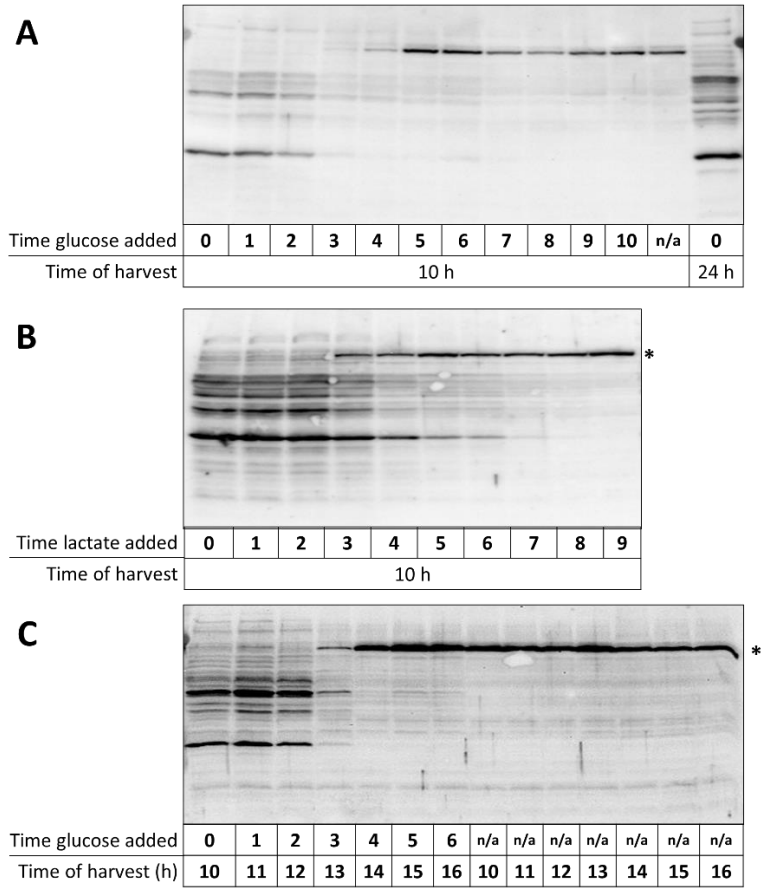

Figure 8. Acetylation in Stationary Phase Requires Carbon to Be Added During Exponential Phase. (A) Wild-type cells of *E. coli* (strain BW25113) were aerated at 37°C in TB7, and at the hour indicated, glucose was added to a final concentration of 0.4%. 10 or 24 hours after inoculation, cells were harvested. Protein lysates were normalized to protein concentration, separated by 1D-SDS PAGE, and assessed for protein acetylation by anti-acetyllysine (α-acK) western immunoblot analysis. (B) Instead of glucose, cells were supplemented with 0.8% lactate. (C) Glucose was added at the indicated hours. 10 hours after addition of glucose, cells were harvested and subjected to α-acK western immunoblot analysis. The band at the asterisk (*) corresponds to acetylated Acs.

A simple explanation for the lack of acetylation could be that cells do not consume glucose in cultures that received glucose after three hours. However, using the colorimetric assay described above, I found that all cultures rapidly consumed glucose at a rate comparable to the cells exposed to glucose from the start of the experiment (**Fig. 9A**). Western blot analysis of the cells from this experiment were consistent with the findings above (**Fig. 9B**).

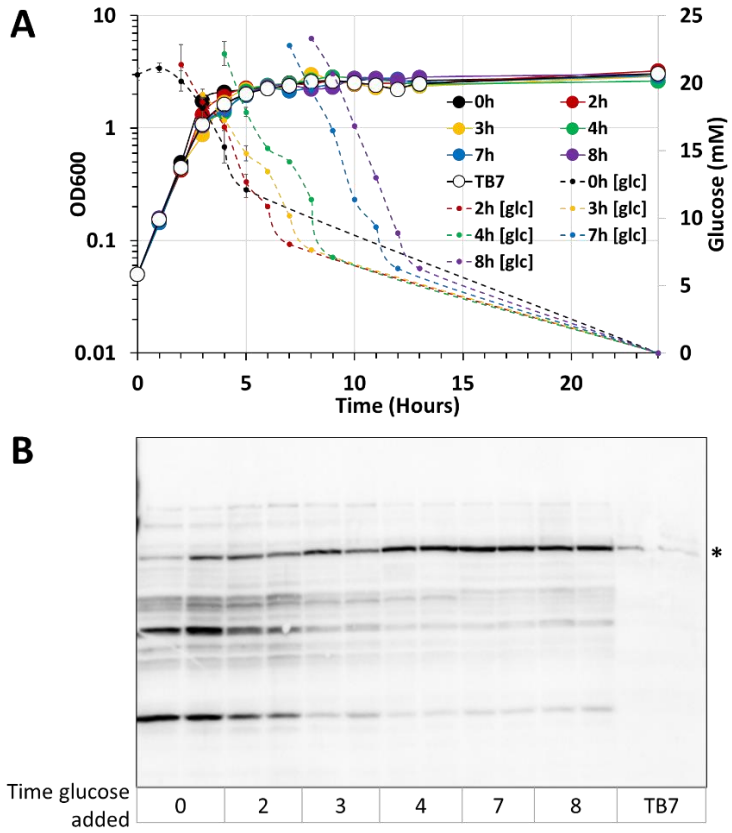

Figure 9. Glucose Is Readily Consumed by Stationary Phase Cells. (A) Wild-type cells of *E. coli* (strain BW25113) were aerated at 37°C in TB7, and at the hour indicated in the legend, glucose was added to a final concentration of 0.4%. Growth was measured at OD600 (solid lines), and filtered culture medium was assessed for glucose concentration (dashed lines). (B) Samples from (A) were harvested at 24 hours after inoculation. Protein lysates were normalized to protein concentration, separated by 1D-SDS PAGE, and assessed for protein acetylation by anti-acetyllysine (α-acK) western immunoblot analysis. The band at the asterisk (*) corresponds to acetylated Acs.

The most obvious explanation for the consumption of glucose but lack of acetylation is the enzyme pyruvate oxidase (PoxB), an enzyme expressed in stationary phase. PoxB catalyzes the oxidative decarboxylation of pyruvate to form acetate and CO_2; thus, PoxB consumes glucose without producing AcP. Furthermore, PoxB is known to be the main acetate production pathway during stationary phase (362). Preferential consumption of glucose via PoxB could easily explain why exposure to glucose only during stationary phase (after the first three hours incubation) does not lead to accumulation of acetylation. It does not, however, explain why exposure to glucose during exponential phase (following the first three hours incubation) results in acetylation during stationary phase. One possibility is that exposure to glucose during the first three hours of growth might somehow favor glucose metabolism via the Pta-AckA pathway over that of PoxB during stationary phase. Thoughts on this an unanswered question will be covered in the **Discussion** section.

Mass Spectrometric Analysis of Acetylated Targets over Time

Western blot analysis gives general information as to how acetylation changes over time, but to get a more detailed understanding of acetylation dynamics on specific lysines, as well as identify modified proteins, we sent samples to our collaborators at the Buck Institute for Aging for tandem mass spectrometry (MS/MS) analysis. The samples came from triplicate biological samples of cultures grown in TB7 for 12 hours or TB7/gl for 2, 5, 8, and 12 hours. Thus, we could determine how acetylation changes over time in TB7/gl and how glucose induces acetylation by comparing TB7/gl to TB7 alone. Please note that all of these data can be found in Schilling *et al.* (78).

From the MS spectra of all samples, we identified a total of 2813 unique acetylated lysines on 780 unique acetylated proteins. Most acetylated proteins were acetylated on one, two

or three lysines; however, 30% of proteins were acetylated on more than 3 lysines. There was only a slight correlation between the number of lysines on a protein and number of acetyllysines detected and no correlation with size of the protein. Growth for 12 h in TB7/gl resulted in substantially more protein acetylation (2338 acetylated lysines on 705 proteins) than growth for 12 h in TB7 without glucose (451 acetylated lysines on 216 proteins), which is consistent with the western blot data. During growth in TB7/gl, the number of unique acetylated lysines (1068, 1658, 2226 and 2338 at 2, 5, 8 and 12 hours, respectively) and proteins (395, 540, 671, and 705 at 2, 5, 8, and 12 hours, respectively) increased over time. Interestingly, most of the lysines detected as acetylated at 12 hours were already detected at 2 hours. This implies that acetylation occurs at a basal level and the accumulation of acetylation observed by western blot is a result of new sites being acetylated and increased occupancy on already acetylated lysines.

Next, quantification was performed by our collaborators on these acetylated lysines to determine relative fold-increases of acetylation over time. These changes were normalized to the protein levels detected to ensure we determined changes in acetylation and not protein abundance. Approximately half of all sites met the criteria as significantly increased (>2-fold, *P*-value ≤ 0.05). Comparing the two extremes, 1081 lysines on 406 lysines were significantly increased (median increase of 7.5-fold) in the 12-hour culture in TB7/gl compared to the 12-hour culture in TB7 alone. Over the glucose time course, acetylation of 1091 lysines on 420 proteins increased significantly with a median relative acetylation change of 2.7-fold (5 h/2 h), 5.7-fold (8 h/2 h) and 6.6-fold (12 h/2 h). The vast majority ($\sim$ 90%) of these regulated acetyllysine sites were both time- and glucose-dependent, which suggests that the increase in acetylation over time is a response to glucose. Supporting the hypothesis that glucose-regulated sites are AcP-sensitive sites, in the linear motif surrounding the glucose-regulated acetyllysines, the lysine is often

flanked by negatively charged amino acids at the +1 and -1 positions, which is similar to that of acetyllysines regulated by AcP (57).

We next determined whether the dynamics on glucose-regulated lysines are consistent between lysines by asking how the fold changes vary over time. This was performed on >400 proteins on >1000 lysines. For example, we assessed 10 lysines on malate dehydrogenase and found that while some lysines experienced gradual increases in acetylation over time, other lysines increased rapidly (**Fig. 10**). In most cases, acetylation peaked after 8 hours and changed very little by 12 hours, which was consistent with the western blot data. In some cases, the relative acetylation level decreased between 8 and 12 hours. This may suggest that specific lysines are susceptible to deacetylation, while others are not. Alternatively, acetylation of certain lysines may be a signal for degradation, which could result in the apparent reduction of acetylation.

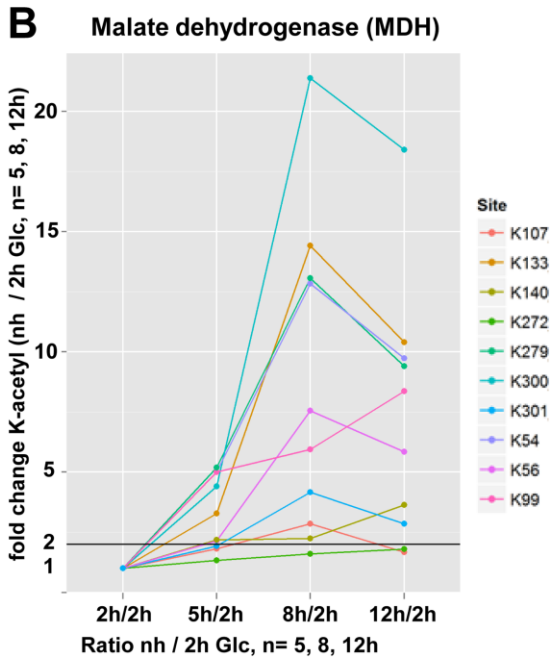

Figure 10. Differential Acetylation Rates. Wild-type cells of *E. coli* were grown in TB7/glucose for 12 hours with samples harvested at 2, 5, 8, and 12 hours. Mass spectrometry to detect acetylated lysines across the proteome was performed on pooled bacteria with 3× biological and 3× technical (MS injection) replicates. Fold changes were determined relative to the 2 hour time point. All Kac fold changes were normalized for protein level changes. Significance of the Kac site fold changes was assessed using two-tailed Student's t-test and requiring P-values < 0.05. Dynamic change of acetylation is displayed for MDH with 10 significantly changing Kac sites shown (K54, K56, K99, K107, K133, K140, K272, K279, K300 and K301).

As we are seeking to understand whether cells can use global, glucose-induced acetylation as a means of sensing their own metabolism, identification of acetylated enzymes is critical. The proteins with acetylated lysines are primarily involved in central metabolism including pathways responsible for glycolysis, gluconeogenesis, and fatty acid biosynthesis, as well as the TCA cycle and glyoxylate bypass. Comparing the sites that we detected as acetylated by AcP (57) to those we consider regulated by glucose, we observed a great overlap (**Fig. 11**), especially in central metabolism (**Fig. 12**). The overlap was not 100%, however. An explanation of this discrepancy most likely results from these experiments being carried out in two different

strain backgrounds; MG1655 was used in Kuhn *et al.* (57) but BW25113 was used in my work. Additionally, genetic manipulation of the AcP levels (i.e., deletion of *ackA*) could lead to aberrant metabolic flux, which could result in changes to gene expression that would either directly or indirectly affect acetylation targets. Furthermore, by not forcing AcP to accumulate, the lysines that reach the threshold for regulation in a Δ*ackA* mutant may not be acetylated at a sufficiently high level in wild-type cells.

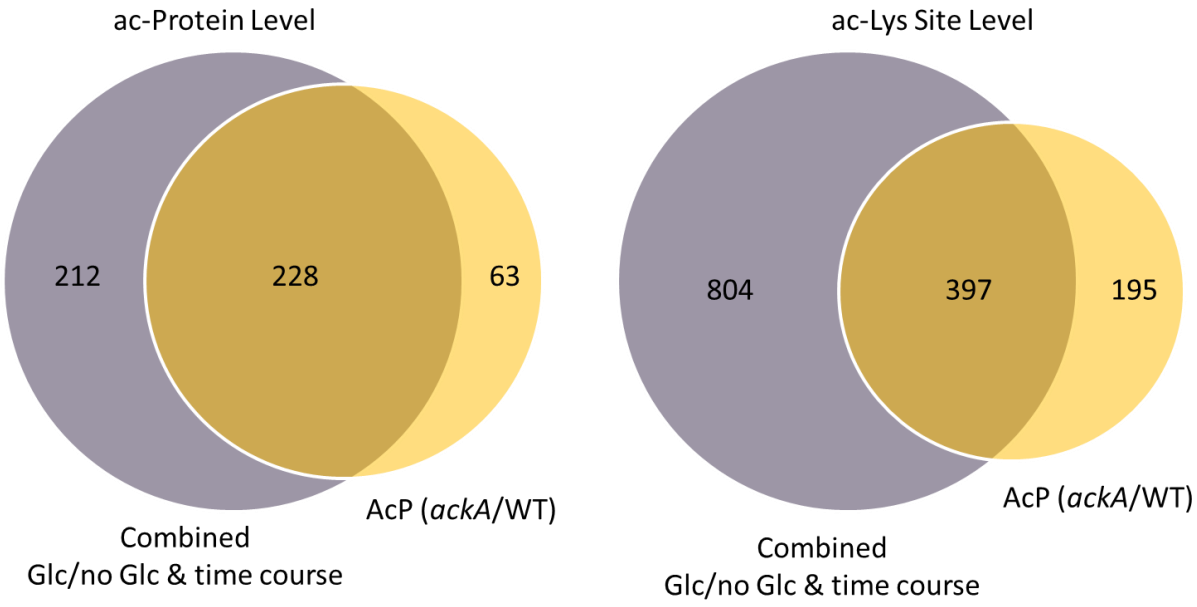

Figure 11. Overlap in Sites and Proteins Regulated by Glucose and AcP. After mass spectrometry analysis was performed as described in Figure 10, lysines were considered regulated by glucose if they were upregulated at least 2-fold in TB7/gl compared to TB7. A protein was considered regulated if it contained a lysine that met this criteria. This dataset was compared to the previously generated dataset from Kuhn *et al.* 2014 that used the same criteria when comparing a Δ*ackA* mutant to WT.

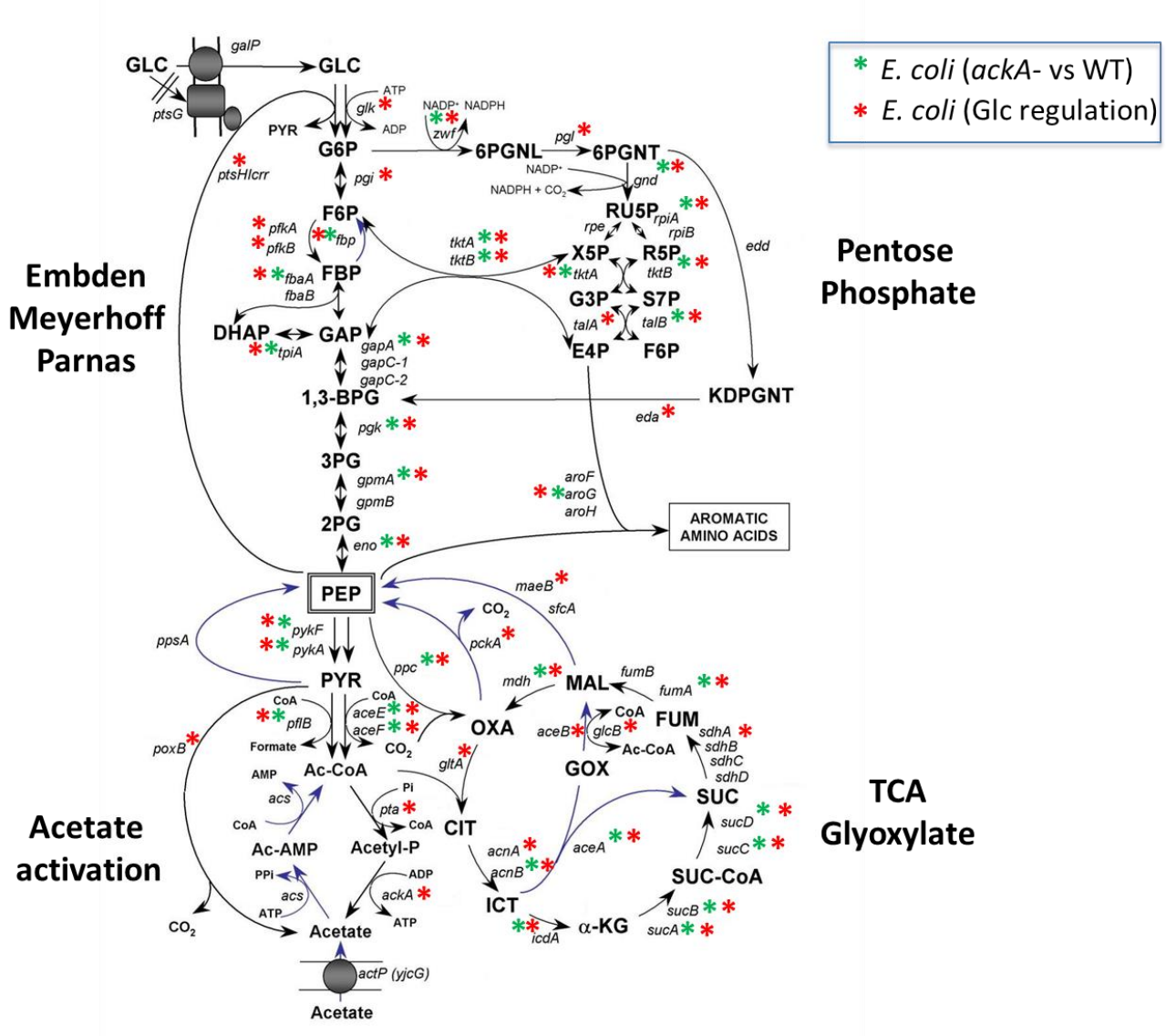

Figure 12. Proteins of Central Metabolism Regulated by AcP and/or Glucose. Proteins containing lysines that were regulated by either AcP (green) or glucose (red) are marked by asterisks.

Summary

Our group had previously established that AcP-dependent acetylation begins to accumulate somewhere between exponential phase and stationary phase. My initial contribution was to obtain a more granular view of acetylation dynamics over time. In doing so, I found that acetylation accumulates primarily after the culture transitions from exponential phase into

stationary phase. Surprisingly, this delay of acetylation appears to be due to a delay in glucose consumption in TB7 that is not observed when glucose is the sole carbon source in a minimal medium. The importance of glucose consumption was confirmed because by removing the glucose, acetylation failed to accumulate. This phenomenon is not exclusive to glucose as these findings were extended to lactate. Taken together, these data support a hypothesis in which acetylation is tightly linked to carbon metabolism, specifically through excess carbon flux via acetate fermentation. As such, acetylation by AcP may serve as a feedback to monitor the flux of carbon through central metabolism.

Consistent with that hypothesis, glucose-induced acetylation was found to be predominantly detected on central metabolic proteins and, as predicted, many of the lysines that were acetylated in a glucose-dependent manner were previously found to be AcP-dependent (57). With continued exposure to glucose, proteins became more acetylated, which matched the pattern seen via western blot. Interestingly, many of the proteins detected as acetylated over this time course were detected as acetylated as early as 2 hours after growth in glucose, which by western blot, looks comparable to cells grown in TB7 alone. Thus, we propose a model where acetylation accumulates due to i) new lysines becoming acetylated and ii) greater occupancy (stoichiometry) of previously acetylated lysines, i.e., an increasing fraction of a given lysine becomes acetylated over time.

Rate of Carbon Flux Dictates Glucose-Induced, AcP-Dependent Acetylation

Introduction

Overflow metabolism (also called aerobic fermentation) is a phenomenon whereby cells growing aerobically ferment acetate. This occurs because the flux of carbon into the AcCoA node of central metabolism is too rapid (**Fig. 3).** At this node, carbon from glycolysis is added

onto CoA to generate AcCoA, which can be used for fatty acid biosynthesis or biomass formation and/or energy production via the TCA cycle. However, the flux through glycolysis can exceed the metabolic capacities of the TCA cycle and fatty acid biosynthesis, resulting in an accumulation of AcCoA. Since CoA is a limiting factor, glycolysis would experience a backup that could cause toxic buildup of sugar phosphates (363). To regenerate CoA and keep glycolysis running, the cell removes the acetyl group from AcCoA and ferments acetate.

Because there is an intimate link between AcP-dependent acetylation and glucose metabolism, I hypothesized that AcP-dependent acetylation could simply be a consequence of fermentation. If this hypothesis were correct, I could modulate global acetylation by reducing flux into the AcCoA node to prevent overflow metabolism. To test this hypothesis, I used both genetic and non-genetic means to reduce fermentation and assessed the effect on AcP-dependent acetylation.

Rapid Carbon Flux through the Major Glucose Transporter, EIICB^{glc}, Is Required for Glucose-Induced Acetylation

For glucose to be consumed by *E. coli*, it must first pass through the porins OmpF, OmpC, and LamB in the outer membrane to enter the periplasm (364-367) (**Fig. 3**). In the periplasm, glucose preferentially is transported in the cytoplasm by the phosphotransferase system (PTS), specifically though the EIICB^{glc} transporter (also called PtsG), where it becomes phosphorylated and directly enters glycolysis. In the absence of EIICB^{glc}, glucose can still enter the cytoplasm through alternative transporters, such as the galactose permease, GalP (368, 369). However, the glucose is not phosphorylated and must become phosphorylated through glucokinase. This alternative process is relatively slow and inefficient (370, 371). To determine

whether acetylation required rapid flux through glycolysis, I started by slowing glucose consumption into the cytoplasm.

I grew WT *E. coli* alongside a mutant lacking EIICB^{glc} (Δ*ptsG*) in TB7/gl and TB7/lactate for ten hours, harvested proteins, verified normalization via Coomassie-stained SDS-PAGE gel, and performed an anti-acetyllysine western blot. With the knowledge that the Δ*ptsG* mutant would have reduced flux of glucose into the cytoplasm and thus into glycolysis (372), I hypothesized that this mutant should have reduced overflow metabolism and thereby reduced glucose-induced acetylation compared to WT. While the WT experienced glucose-induced acetylation, the Δ*ptsG* mutant appeared as though it was grown in the absence of glucose and only showed one acetylated band, Acs (**Fig. 13, compare lanes 1 and 5**). However, lactate bypasses the need for EIICB^{glc}, and thus I expected that the acetylation intensity of the Δ*ptsG* mutant would be comparable to WT in TB7/lactate. Indeed, the acetylation pattern in both strains looked comparable (**Fig. 13, compare lanes 6 and 10**). These data show that the Δ*ptsG* mutant is not generally defective for carbon-induced acetylation; instead, as I hypothesized, glucose-induced acetylation requires rapid flux of carbon via EIICB^{glc}.

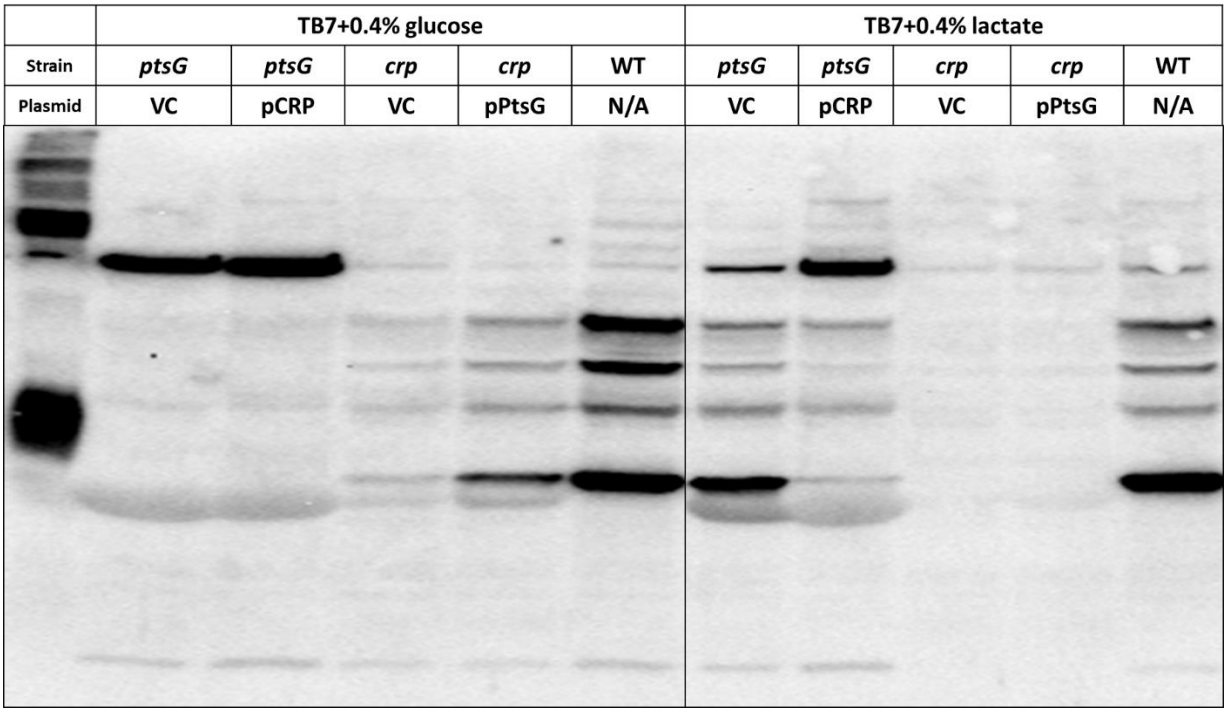

Figure 13. CRP Is Required for Glucose-Induced Acetylation and Lactate-Induced Acetylation. Wild-type and isogenic mutants of *E. coli* (strain BW25113) were aerated at 37°C in TB7 supplemented with 0.4% glucose or 0.4% lactate. Those strains carrying pCA24n-CRP, pCA24n-PtsG, or pCA24n vector control (VC) were also supplemented with 25 μg/mL chloramphenicol and 50 μM IPTG. After 10 hours, cells were harvested. Protein lysates were normalized to protein concentration, separated by 1D-SDS PAGE, and assessed for protein acetylation by anti-acetyllysine (α-acK) western immunoblot analysis.

Rapid Carbon Flux through the Embden-Meyerhof-Parnas Pathway Is Required for Glucose-Induced Acetylation

Glycolysis is traditionally thought of as the passage of glucose-derived carbon through what is known as the Embden-Meyerhof-Parnas (EMP) pathway. However, this carbon can enter two other pathways, the pentose phosphate (PP) pathway or the Entner-Doudoroff (ED) pathway. The flux through these pathways is slower than the flux through the EMP pathway. By deleting certain enzymes of the EMP pathway, the cell can be forced to metabolize glucose using these slower pathways. Slowing flux of carbon through glycolysis should reduce overflow metabolism,

and I hypothesized that a mutant of the EMP pathway would have reduced acetylation relative to WT. I chose phosphoglucose isomerase (Pgi) as this enzyme converts the first committed step of the EMP pathway, the conversion of glucose-6-phosphate into fructose-6-phosphate (**Fig. 3**). Furthermore, I can bypass the need for Pgi by supplementing the Δ*pgi* mutant with fructose, which can directly enter the EMP pathway.

I performed an endpoint analysis of WT and Δ*pgi* mutant cells after ten hours of growth in TB7/gl and TB7 supplemented with 0.4% fructose (**Fig. 14A**). Consistent with my hypothesis, deletion of *pgi* reduced acetylation relative to WT cells in the presence of glucose (**Fig. 14B**). The Δ*pgi* mutant did not produce an acetylated Acs band, as opposed to a Δ*ptsG* mutant, which indicates that these cells were still important and sensing glucose. Supplementing Δ*pgi* mutant with fructose restored global acetylation; indeed, the acetylation profile of the Δ*pgi* mutant was more intense than that of the WT cells exposed to either glucose or fructose. Since the Pgi reaction is reversible, these results may suggest that conversion of fructose-6-phosphate into glucose-6-phosphate occurs in WT cells, causing less carbon overflow and thus less AcP-dependent acetylation.

To ensure that the Δ*pgi* mutant was truly defective in glucose-induced acetylation and that the time point chosen did not mislead our interpretation, I performed a time course and monitored acetylation over time in TB7/gl. While the WT cells experienced carbon-induced acetylation, there was little change in acetylation intensity of the Δ*pgi* mutant over the entire 24-hour period (**Fig. 15**).

Together, these data support the model carbon-induced acetylation requires that carbon must rapidly enter the AcCoA node to promote overflow metabolism and generate the acetyl

donor, AcP. These data further confirm that glucose-induced acetylation is actually carbon-induced acetylation, as shown by induction with glucose, lactate, and now fructose.

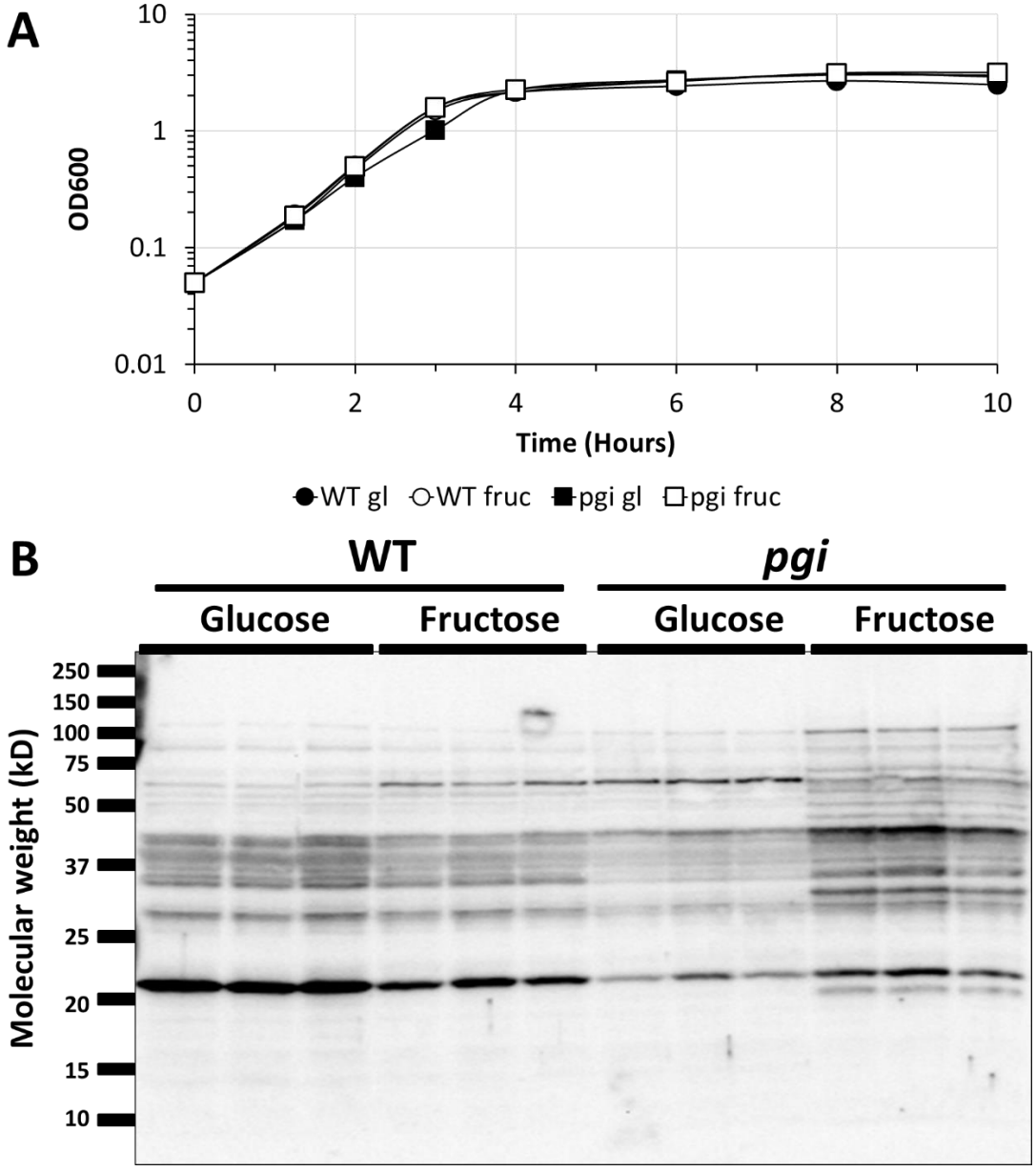

Figure 14. Acetylation Is Enhanced When Carbon Flux Is Rapid. Wild-type cells and an isogenic Δ*pgi* mutant of *E. coli* (strain BW25113) were aerated at 37°C in TB7 supplemented with 0.4% glucose or 0.4% fructose. (A) Growth measured at OD600. (B) Cells were harvested after 10 hours of aeration. Protein lysates were normalized to protein concentration, separated by 1D-SDS PAGE, and assessed for protein acetylation by anti-acetyllysine (α-acK) western immunoblot analysis.

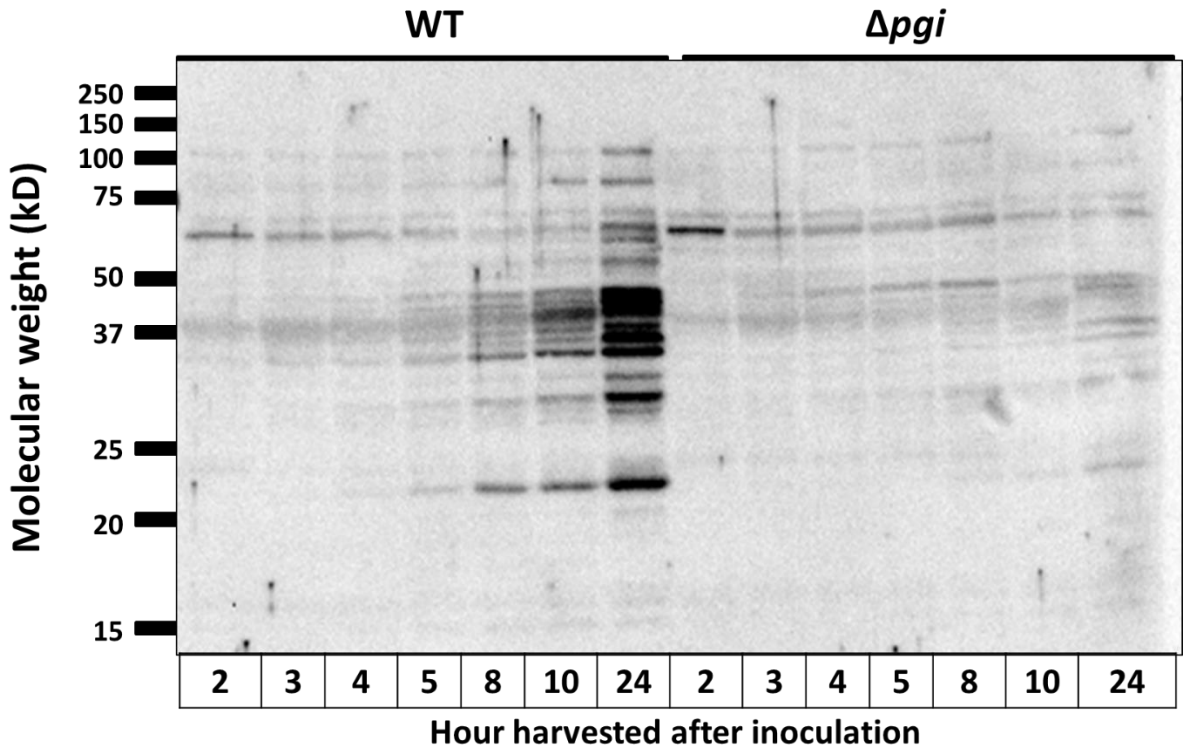

Figure 15. Acetylation Does Not Significantly Change Over Time in a Δ*pgi* Mutant. Wild-type cells and an isogenic Δ*pgi* mutant of *E. coli* (strain BW25113) were aerated at 37°C in TB7 supplemented with 0.4% glucose. Cells were harvested at the indicated time points. Protein lysates were normalized to protein concentration, separated by 1D-SDS PAGE, and assessed for protein acetylation by anti-acetyllysine (α-acK) western immunoblot analysis.

Major Transcription Factors Can Regulate Acetylation

If glucose- and, by extension, carbon-induced acetylation was a response to carbon flux, then this acetylation should be influenced by regulators of carbon flux. Therefore, I constructed an isogenic set of mutants defective for the carbon regulators ArcA, Cra, CsrA, and CRP. I also used a Δ*ptsG* mutant as a negative control and a Δ*rcsB* mutant as a control for a mutant that should not affect central metabolism. ArcA primarily represses operons involved in respiratory metabolism under anaerobic conditions, and I hypothesized that deletion of *arcA* may decrease acetylation by causing a loss of repression of these genes, driving carbon flux away from

fermentation. Cra is reported to be an activator of gluconeogenic enzymes and a repressor of glycolytic enzymes. I expected a Δ*cra* mutant to lose repression of glycolytic enzymes and perhaps increase the amount of fermentation and therefore acetylation. CsrA negatively influences transcription of gluconeogenic and glycogen synthesis enzymes while activating glycolytic enzymes. Thus, a Δ*csrA* mutant should lower acetylation as it would no longer be able to activate glycolytic enzymes and would decrease carbon flux to fermentation. CRP, or the catabolite activator protein, is important for activating gene transcription in the absence of glucose, and thus I would expect CRP to have little effect on glucose-induced acetylation.

Endpoint western blot analysis was performed on the Δ*arcA*, Δ*cra*, Δ*csrA*, Δ*crp*, Δ*ptsG*, and Δ*rcsB* mutant strains grown in TB7/gl for ten hours (**Fig. 16A**). Acetylation in the Δ*ptsG* mutant was significantly reduced compared to WT, consistent with what I had observed previously. The Δ*arcA* and Δ*csrA* mutants behaved like WT and the Δ*rcsB* control. Consistent with my hypothesis, the Δ*cra* mutant had a small reproducible increase in acetylation relative to WT. Strikingly, the Δ*crp* mutant looked comparable to a Δ*ptsG* mutant, indicating that CRP plays a major role in carbon-induced acetylation. This corroborated data found by former members of the lab Robert Davis, PhD (373) and Arti Walker (170), and will be discussed below. From these data, I conclude that carbon regulators can regulate acetylation, and I hypothesize that this would be due to control of carbon flux through central metabolism.

CRP-Dependent Transcriptional Activation Is Required for Carbon-Induced Acetylation

Arti Walker and Robert Davis found that a Δ*crp* mutant lost glucose-induced acetylation in the presence of exogenous cAMP, a small molecule produced in the absence of glucose that, with transcription factor CRP, forms a cAMP-CRP complex that activates transcription. CRP increases the rates at which glucose is consumed and acetate is produced, which should increase

the rate at which AcP is produced (374). Through epistasis analysis, Robert Davis showed that AcP was required for CRP-dependent, glucose-induced acetylation, and the loss of *crp* could be bypassed by overproducing AcP (in a Δ*ackA* mutant) (78). As described above, I was able to find that CRP played a role even in the presence of glucose, which should significantly reduce CRP-dependent transcription. Thus, I sought to determine the mechanism by which CRP controls acetylation.

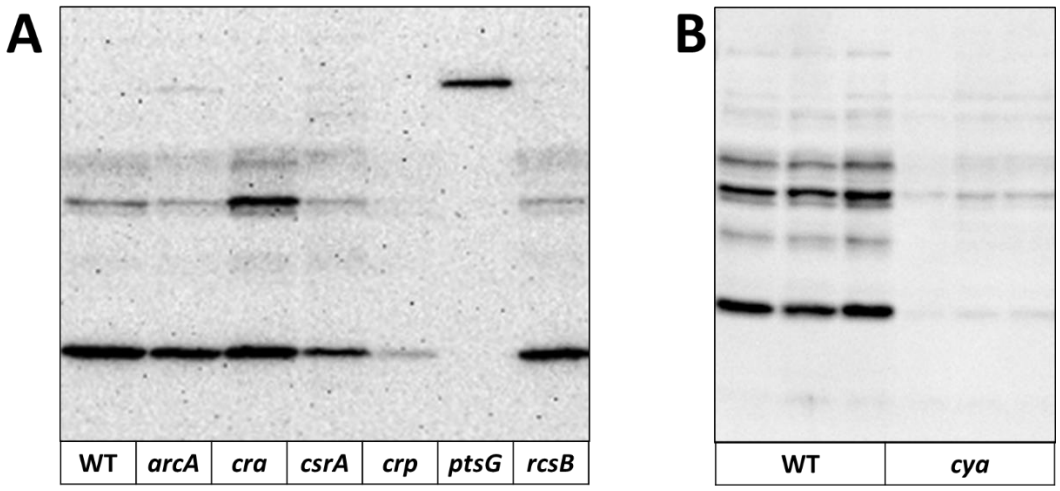

Figure 16. Effect of CRP and Other Carbon Regulators on Acetylation. (A) Wild-type cells and isogenic Δ*arcA*, Δ*cra*, Δ*csrA*, Δ*crp*, Δ*ptsG*, and Δ*rcsB* mutants of *E. coli* (strain BW25113) were aerated at 37°C in TB7 supplemented with 0.4% glucose. Cells were harvested after 10 hours. Protein lysates were normalized to protein concentration, separated by 1D-SDS PAGE, and assessed for protein acetylation by anti-acetyllysine (α-acK) western immunoblot analysis. (B) Triplicate cultures of Wild-type cells and an isogenic Δ*cya* mutant were aerated in TB7 supplemented with 0.4% glucose. Cells were harvested after 10 hours and analyzed by anti-acetyllysine western blot as in (A).

To determine the mechanism by which CRP regulates glucose-induced, AcP-dependent acetylation, I began by asking whether CRP required formation of the cAMP-CRP complex to regulate acetylation. I made a Δ*cya* mutant that lacks adenylate cyclase, the enzyme necessary to form cAMP. I performed an anti-acetyllysine western blot of this mutant grown in TB7/gl for ten

hours and found that it behaved like the Δ*crp* mutant (**Fig. 16B**). This indicated to me that CRP was probably exerting its effect through its canonical function, activating transcription.

CRP can bind to two sites on DNA, called Class I and Class II sites. A Class I site is characterized by being positioned at -60.5, -70.5, -81.5, or -91.5 relative to the transcription start site (TSS), while Class II sites are centered at -41.5 relative to the TSS. Activation of transcription from a Class I site depends on the interaction between a surface region called Activating Region 1 (AR1) on CRP with the C-terminal domain of the α-subunit (α-CTD) of RNA polymerase. In contrast, Class II sites depend on an interaction between both AR1 with the α-CTD and Activating Region 2 (AR2) of CRP with the α-subunit N-terminal domain. Thus, by disrupting AR1 and/or AR2, one can lose activation of Class I-dependent promoters, Class II-dependent promoters, or both.

To determine whether either or both activating regions are required for CRP-dependent acetylation, I complemented the Δ*crp* mutant strain in the AJW678 background with pDCRP carrying the wild-type CRP isoform, CRP variants lacking AR1 (H159L), AR2 (K101E), both AR1 and AR2 (H159L/K101E), or the vector control (pBR322). Each strain was grown in TB7/gl or TB7 alone for ten hours, harvested, and analyzed by anti-acetyllysine western blot (**Fig. 17A**). Complementation with the WT *crp* allele on the pDCRP plasmid restored glucose-induced acetylation to the Δ*crp* mutant, while the strain carrying the vector control did not. Complementation with mutant alleles carrying intact AR1 or AR2 alone was sufficient to promote glucose-induced acetylation. However, complementation with the AR1/2 double mutant allele produced a result similar to the Δ*crp* mutant. To generalize this effect, I recapitulated these data in another background of *E. coli*, BW25113 (Data not shown).

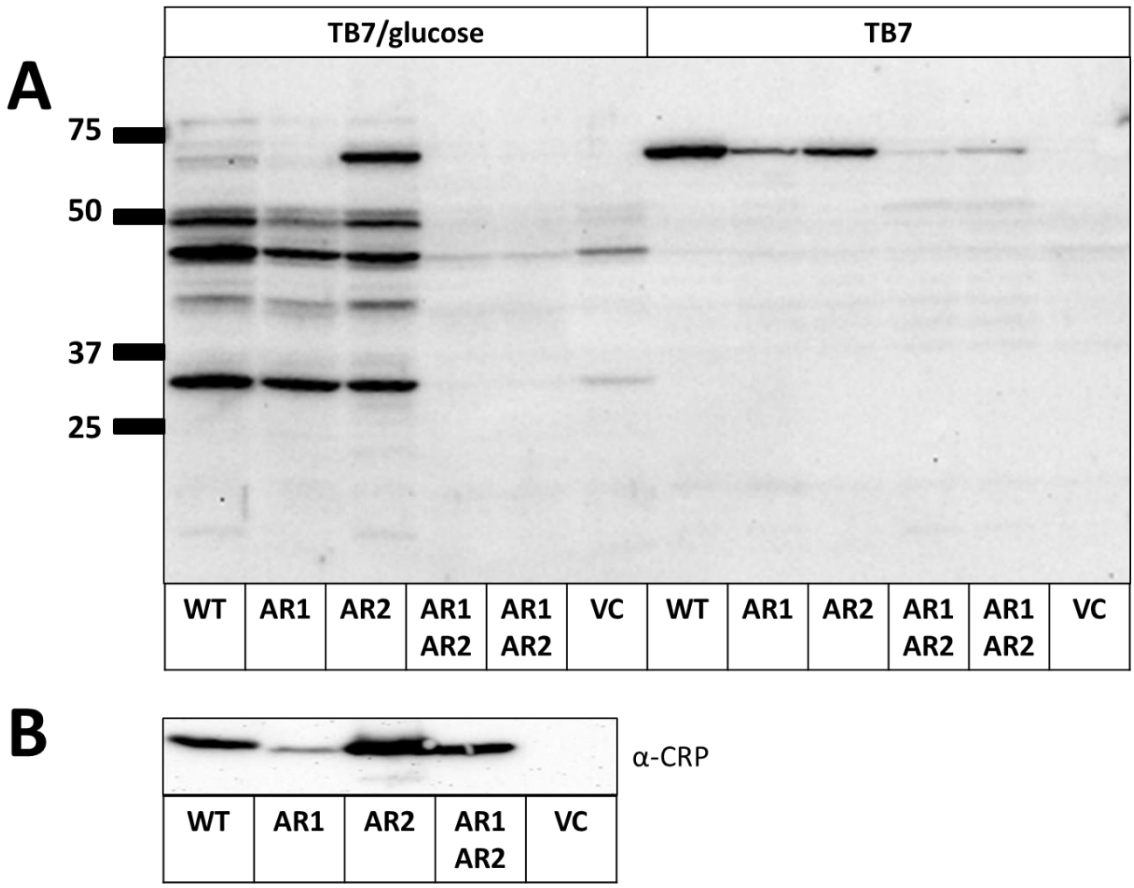

Figure 17. CRP Requires Both Activating Regions for Acetylation. (A) Δ*crp* mutants of *E. coli* (strain AJW678) carrying pDCRP (WT), vector control pBR322 (VC), or variants defective for AR1 (H159L), AR2 (K101E), both AR1 and AR2 (in duplicate) were aerated in TB7 alone or supplemented with 0.4% glucose (TB7/glucose). Cells were harvested after 10 hours. Protein lysates were normalized to protein concentration, separated by 1D-SDS PAGE, and assessed for protein acetylation by anti-acetyllysine (α-acK) western immunoblot analysis. (B) Lysates from cells grown in TB7/glucose in (A) were probed by anti-CRP western immunoblot analysis.

In TB7, each strain only varied in acetylation of one band, Acs. The acetylated Acs band was strong in WT and AR2, weak in AR1, and absent in AR1/2 and the vector control. In TB7/gl, the Acs band could be visualized in the AR2 defective variant. The reason for the variation in acetylation of Acs is most likely the expression levels of Acs. The Acs promoter is AR1-dependent, and thus inactivation of AR1 would reduce expression of Acs (375). Additionally, the Acs promoter is repressed in an AR2-dependent manner (340); thus, it makes

logical sense that mutating AR2 could relieve some of this repression even in the presence of glucose. Finally, since Acs depends on CRP, mutation of both activating regions and deletion of *crp* results in poor and no expression of Acs, respectively.

To ensure these constructs were properly expressed, I determined the protein levels of these CRP variants from the same lysates using an anti-CRP antibody (**Fig. 17B**). This confirmed the Δ*crp* mutant did not express CRP. While the AR2 and AR1/2 variants had similar protein levels to WT, AR1 protein levels were significantly reduced. However, since the AR1 CRP variant was still capable of promoting glucose-induced acetylation, while the AR1/2 mutant was not, this implies that the CRP protein levels do not correlate with acetylation. I conclude that CRP utilizes both AR1 and AR2 to promote acetylation by activating transcription.

CRP-Dependent Activation of EIICB^{glc} Is Required for Acetylation

One of the promoters that CRP regulates is that of *ptsG*, the gene that encodes the major glucose transporter EIICB^{glc}. The *ptsG* promoter is regulated in a Class I- and Class II-dependent manner (376, 377). I hypothesized that the reason a Δ*crp* mutant lacked acetylation was due to low EIICB^{glc} expression. To test this, I performed an epistasis experiment to determine whether CRP and EIICB^{glc} acted in the same pathway to promote glucose-induced acetylation. I first transformed a Δ*ptsG* mutant with a plasmid carrying CRP or vector control. In a WT strain, overexpression of CRP enhanced acetylation (78). However, overexpression of CRP in the Δ*ptsG* mutant had no effect, and the only visible acetylated band was Acs, which indicates that any effect of CRP must require EIICB^{glc} (**Fig. 13, compares lanes 1 and 2**). Next, I transformed a Δ*crp* mutant with a plasmid carrying *ptsG* or vector control with the expectation that if a Δ*crp* mutant poorly expresses EIICB^{glc}, overexpressing EIICB^{glc} would restore proper glucose utilization and acetylation. My hypothesis was partially correct. While the Δ*crp* mutant with

vector control had no induction of acetylation, overexpression of EIICB^{glc} was able to partially suppress the defect (**Fig. 13, compare lanes 3 and 4**). Thus, the reduced acetylation of a Δ*crp* mutant is, in part, due to poor EIICB^{glc} expression, which supports the previous findings that Δ*crp* mutants poorly consume glucose at a third of the rate of WT cells (374).

However, overexpression of EIICB^{glc} in the *crp* mutant does not completely restore the acetylation to WT levels. Why not? While the exact mechanism is not known, the paper from Perrenoud and Sauer provides further insights (374). In addition to the reduced rate of glucose consumption of a Δ*crp* mutant, they also found that CRP enhances flux through the EMP glycolytic pathway while diminishing flux through the PP pathway. However, the exact EMP and PP enzymes that CRP regulates to direct flux remain unclear. Fitting the findings of Perrenoud with my data from the Δ*pgi* mutant indicates that CRP may have a dual role in managing carbon flux both into the cell and through glycolysis and thus to promote acetylation.

Directing Carbon to Biomass Reduces Protein Acetylation

Overflow metabolism is a consequence of flux through the TCA cycle being too slow to meet demand from the AcCoA node. Further compounding this problem for the cells, in our conditions, glucose is mostly consumed after entry into stationary phase due to exhaustion of some other nutrient, which reduces the need for new biomass (see **Glucose Is Not Consumed until Stationary Phase in TB7**). Thus, TCA cycle intermediates are not being used as precursors for biomass, which further reduces the capacity of the TCA cycle to receive carbon from AcCoA. Instead, most of this carbon is fermented as acetate. In the **Appendix**, I describe my finding that cell growth is limited by magnesium in the standard medium we used to study acetylation, TB7/gl. I hypothesize that the accumulation of protein acetylation induced by excess carbon is a result of overflow metabolism (as described in **Rate of Carbon Flux Dictates**

Glucose-Induced, AcP-Dependent Acetylation) in combination with an "aging" proteome, due to reduced nascent protein synthesis in stationary phase.

Since addition of magnesium to cultures of *E. coli* extends exponential phase growth and can triple their final biomass (341), if my hypothesis is correct, this would mean that there would be a resultant reduction in acetylation due to more carbon being used to generate biomass and greater dilution of acetylated isoforms into nascent proteins. I added varying concentrations of magnesium (from 10 μM to 1 mM) to cultures of WT *E. coli* grown in TB7/gl, which resulted in a dose-dependent increase in biomass as measured by final OD_{600} measurements at 10 and 24 hours (**Fig. 18**). Anti-acetyllysine western blot showed that cells supplemented with up to 25 μM magnesium experienced carbon-induced acetylation comparable to unsupplemented TB7/gl (**Fig, 19A**). Cells exposed to 50 to 100 μM magnesium saw the expected decrease in acetylation. Unexpectedly, between 100 μM and 500 μM up to 1 mM, the acetylation increased but remained slightly below unsupplemented TB7/gl culture. Finally, if I restored carbon to excess over magnesium by increasing the concentration of glucose from 0.4% to 4%, addition of magnesium no longer reduced acetylation (**Fig. 19B**).

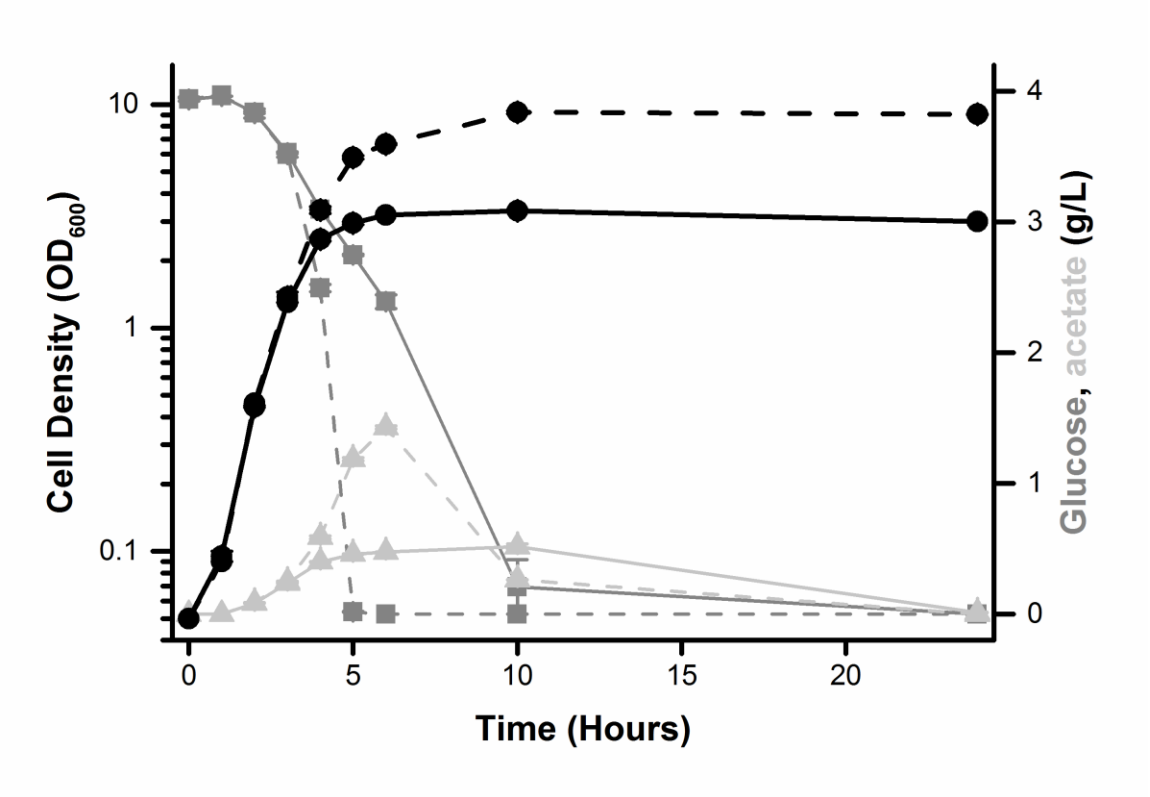

Figure 18. Magnesium Extends Exponential Phase and Increases Final Optical Density. Wild-type cells of *E. coli* (strain BW25113) were aerated at 37°C in TB7 supplemented with 0.4% glucose alone (Solid lines) or with 1 mM $MgSO_4$ (Dashed lines). Growth was measured at OD600 (Black lines) and the filtered culture medium was assessed for glucose (Dark gray lines) and acetate (Light gray lines) concentrations.

While my hypothesis that shifting carbon to biomass would reduce acetylation held true during supplementation with certain concentrations of magnesium, clearly something else was happening at the higher concentrations of magnesium. The reason remains unknown. However, metal ions like Ca^{2+} and Mg^{2+} promote AcP hydrolysis *in vitro* because they make the phosphate a better leaving group (283, 378). Also, addition of magnesium promotes selectivity and specificity of *in vitro* acetylation with AcP (57). Perhaps these characteristics of AcP explain how the high concentrations of magnesium promote acetylation when lower concentrations reduce acetylation.

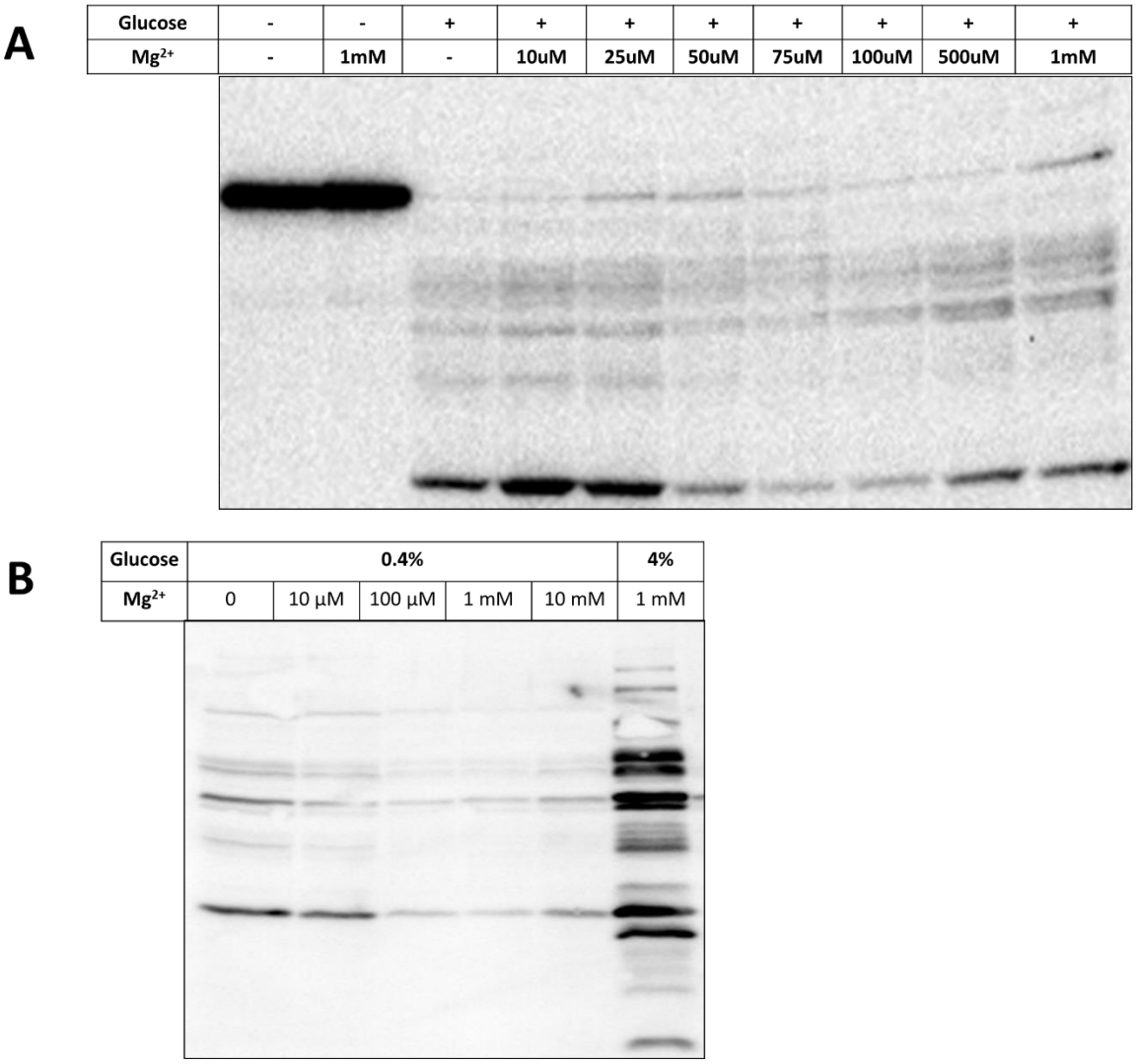

Figure 19. Magnesium Reduces Acetylation in TB7/glucose. (A) Wild-type cells of *E. coli* (strain BW25113) were aerated at 37°C in TB7 or TB7 supplemented with 0.4% glucose. To each culture, magnesium sulfate was added to the indicated final concentrations. (B) Wild-type cells of *E. coli* (strain BW25113) were aerated in 37°C in TB7 supplemented with 0.4% glucose or 4% glucose. To each culture, magnesium sulfate was added to the indicated final concentrations. Cells were harvested after 10 hours. Protein lysates were normalized to protein concentration, separated by 1D-SDS PAGE, and assessed for protein acetylation by anti-acetyllysine (α-acK) western immunoblot analysis.

Summary

Prior to this work, we knew that glucose could induce global acetylation in an AcP-dependent manner. The physiological consequences of widespread acetylation are unknown but

understanding how the cell regulates acetylation could direct our studies. Since AcP is produced as a result of fermentation, which is caused by overflow metabolism under our growth conditions, I hypothesized that by modulating overflow metabolism I could reduce or enhance acetylation.

Overflow metabolism is characterized by excessive carbon flux through glycolysis with a bottleneck at the AcCoA node that is relieved by fermentation of acetate. I therefore asked whether reducing flux into the cell or into the AcCoA node could reduce acetylation. Using a carbon source like glucose whose utilization by *E. coli* has been studied in great depth allowed me to make predictions about how certain mutants should influence acetylation. As I predicted, acetylation was reduced by slowing entry of glucose into the cell by deleting the major glucose transporter or by forcing cells to use the slower glycolytic pathways by deleting Pgi. Under the conditions used in our experiments, I found that CRP was required for AcP-dependent acetylation. The requirement for CRP depended on its ability to form a cAMP-CRP complex and activate transcription via either AR1 or AR2. At least one mechanism by which CRP controls acetylation is through expression of $EIICB^{glc}$, thus increasing flux of carbon into the cell. However, the literature suggests CRP is also required for driving flux into the EMP pathway and away from the PP pathway. Therefore, glucose-induced acetylation is caused by overflow metabolism, but this phenomenon is not exclusive to glucose and should be more correctly described as carbon-induced acetylation.

In addition to reducing flux through glycolysis, I also found that acetylation could be reduced by preventing carbon from becoming excessive by adding the limiting nutrient magnesium. I hypothesize that this attempt to balance carbon and magnesium results in more carbon entering biomass and any proteins that become acetylated are rapidly diluted into nascent

proteins. Thus, when magnesium is limiting and thus depleted before full consumption of glucose or some other fermentable carbon source, the cells cease exponential phase growth ferment the excess carbon as acetate. Any proteins with a lysine in the proper molecular environment (57) will be able to bind AcP and become acetylated. Together, these data support a model in which acetylation cannot help but occur on permissive lysines when AcP is produced via fermentation.

Global Acetylation Occurs in a Carbon Source Agnostic Manner

Introduction

Our current model suggests that acetylation occurs as a result of fermentation and that the only factors that dictate acetylation are production of the acetyl donor AcP and the proper 3D structure/molecular environment to facilitate acetylation. Therefore, regardless of carbon source, we should observe the same targets acetylated as long as the cells ferment. To further test our model, I chose the hexose sugar, glucose, and the pentose sugar, xylose, as the sole carbon sources. These two sugars are relevant because *(i) E. coli* grows faster on glucose than on xylose and thus may have different lysine acetylation patterns and *(ii)* their metabolism requires different enzymes, which may also be differentially acetylated. Furthermore, by making these sugars the sole carbon sources, I avoid any complications with other carbon sources coming from the tryptone broth of TB7. In addition to the usual 0.4% carbon source, I also grew the cells in 4% carbon to ensure that the cells experience carbon excess and thus ferment via overflow metabolism.

Neither Carbon Source nor Amount Cause Major Changes to Protein Abundance

I grew cells in M9 minimal medium supplemented with xylose or glucose at a final concentration of 0.4% or 4%. After 12 hours, I harvested samples and submitted them to our

collaborators for mass spectrometric analysis. Comparing the protein expression levels between conditions, only 61 proteins exhibited significant differences in expression. The abundance of many of these proteins was reduced, especially during growth at 4% sugar, presumably through catabolite repression, as many of these are CRP-regulated. Four of the proteins that were increased in 4% carbon are members of the NtrC regulon that controls genes in response to high carbon-to-nitrogen ratio (379), suggesting these cells are experiencing nitrogen limitation. During growth on xylose, members of the XylR regulon were induced; this regulon includes genes that encode proteins required for the uptake and metabolism of xylose and arabinose (380).

Acetylation Modifies the Same Targets Independent of Carbon Source

To determine whether glucose and xylose induce acetylation of the same proteins, we identified lysines acetylated under all four conditions. Through this analysis, we identified 3840 unique acetylated lysines that corresponded to 978 proteins. Using the above protein abundances, we were able to calculate the relative fold-change between conditions. Comparing 4% to 0.4% glucose, 278 lysines on 157 proteins increased acetylation by at least 2-fold in 4% glucose. Similarly, 256 sites on 147 proteins had at least a 2-fold increase in acetylation comparing 4% xylose to 0.4% xylose. In neither case was acetylation observed to decrease between 4% and 0.4% carbon. Anti-acetyllysine western blot confirmed these findings, where more carbon resulted in a stronger acetylation pattern, although not as strikingly as expected (**Fig. 20**).

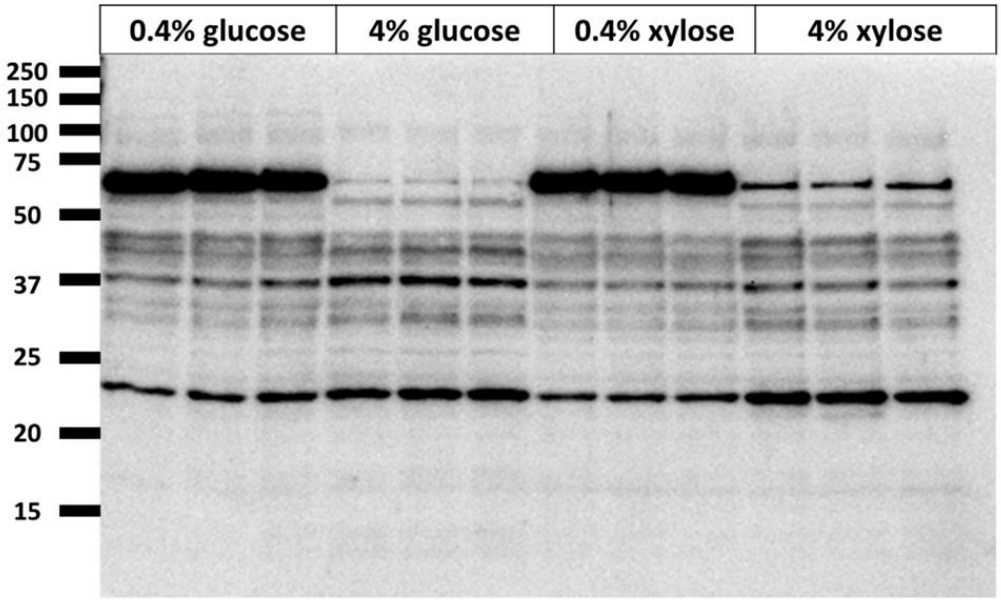

Figure 20. Xylose and Glucose Induce Acetylation. Triplicate cultures of wild-type cells of *E. coli* (strain BW25113) were aerated at 37°C in M9 minimal medium supplemented with glucose or xylose at a final concentration of 0.4% or 4%. Cells were harvested after 10 hours. Protein lysates were normalized to protein concentration, separated by 1D-SDS PAGE, and assessed for protein acetylation by anti-acetyllysine (α-acK) western immunoblot analysis.

When comparing both carbon sources of the same concentration to one another, most of the acetylations were regulated independent of the identity of the carbon source. In other words, the proteins that were acetylated in the presence of glucose were the same proteins acetylated in the presence of xylose. In one interesting case, xylose isomerase (XylA) was found to be differentially acetylated on two lysines. Specifically, the relative abundance of acetylation for one lysine, K17, increased, while the other, K381, decreased during growth on 4% glucose versus 4% xylose. The acetylation of K17 also increased during growth on 4% versus 0.4% xylose, suggesting that it is sensitive to the energy state of the cells. I hypothesized that the differential acetylation in response to the different carbon sources could be a regulatory modification to adjust metabolism of xylose.

Lysines 17 and 381 Acetylation Mimics of XylA Do Not Affect Growth on Xylose

To determine whether acetylation of either lysine affects XylA activity, I asked whether *E. coli* strains carrying *xylA* alleles mimicking acetylated lysines would hinder growth in medium with xylose as the sole carbon source. Into the native *xylA* gene in the chromosome, I recombined *xylA* alleles that encoded variants of XylA with lysine to glutamine substitutions that mimic and acetylated lysine (K17Q and K381Q) or variants of XylA with lysine to arginine substitutions that mimic an unacetylatable lysine (K17R and K381Q). To ensure that the cells would grow initially, I aerated cultures overnight in M9 minimal medium supplemented with 0.4% glucose. Normalized cell numbers were harvested, washed three times in PBS, and resuspended in 0.4% xylose or 4% xylose with 0.4% glucose and 4% glucose serving as controls where XylA should not have an effect on growth (**Fig. 21**). As a further control, a Δ*xylA* mutant was unable to grow in xylose, and thus confirmed that XylA is required for growth on xylose (381). The rate of growth was reduced in the xylose cultures compared to their glucose counterparts, while the final densities achieved were comparable between the two sugars. However, there was no significant difference in growth between WT cells or the cells carrying the XylA variants. Thus, these lysine residues do not appear to be required for growth of *E. coli* on xylose.

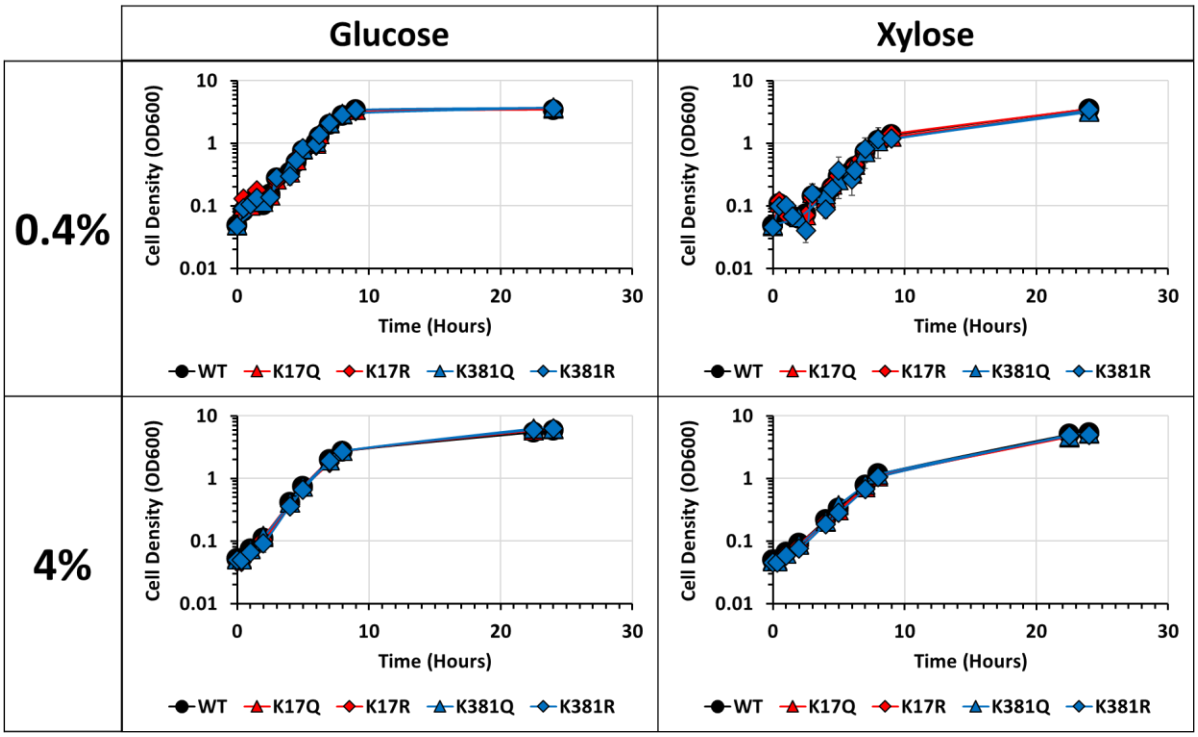

Figure 21. Comparison of Growth for Different XylA Mutants During Growth in 0.4% Xylose or 4% Xylose. Wild-type *E. coli* (strain BW25113) or strains carrying the indicated mutant variants of XylA K17 or K381 were aerated in M9 minimal medium supplemented with 0.4% or 4% of glucose or xylose as the sole carbon source.

Summary

To conclude this section, we found that independent of the carbon source, the identities of acetylated proteins did not change. This finding is consistent with the hypothesis that the major factors that regulate acetylation are the synthesis of AcP and a molecular environment that facilitates acetyl transfer. Indeed, the only factor that meaningfully altered acetylation was the concentration of carbon. Increased carbon caused an increase in acetylation, which is not surprising since this should cause more AcP to be generated and be available for protein modification. One of the targets that was differentially acetylated in the two carbon sources was XylA. However, neither lysine appears to regulate XylA activity.

Assessing Phenotypes for Global AcP-Dependent Acetylation

Introduction

The evidence thus far suggests that acetylation by AcP is simply a consequence of fermentation. This raises the question: has *E. coli* evolved to cope with or utilize this unavoidable modification? AcP accumulates when cells are exposed to excess carbon and increases greatly during stationary phase. AcP may serve one or many functions for the cell. As many of the proteins acetylated by AcP are in central metabolism, acetylation could be a regulator of carbon flux.

Stationary phase is a time when individual cells in a culture adjust their physiology, shifting from a program of growth and division to one in which the cell prepares defenses against stresses that may cause macromolecular damage. Many amino acids are subject to damage via reactive oxygen species or products of oxidation. Lysine can be oxidized by at least 8 different chemical oxidations (277), one of which, carbonylation, has been found to readily occur in stationary phase cultures of *E. coli* (327, 382). Carbonylation results in protein misfolding and aggregation, which can be lethal to the cell if not mitigated by proteolytic degradation. Thus, I hypothesized that AcP is a preventative non-enzymatic modification of lysines against more deleterious non-enzymatic modifications like carbonylation. In the first part of this section, I will test the hypothesis that cells containing high acetylation will have reduced carbonylation and/or reduced protein aggregates.

Another hypothesis that is independent of the previous two is that acetylation may serve as carbon storage. Across the phylogenetic tree, cells store excess carbon in glycogen, a glucose polymer, as a carbon source for use during starvation. Perhaps acetylation could similarly be a way for cells to stockpile two-carbon subunits on proteins. When grown in 2XYT medium, a rich

medium but without glucose, Baeza *et al.* estimated there may be approximately 1.7 – 2.8 mM acetate stored on proteins as acetylation (77). Thus, cells that accumulate AcP, such as a Δ*ackA* mutant or cells grown in glucose may have even higher amounts of acetate stored on proteins. In the second part of this section, I will test the hypothesis that acetylation can serve as a carbon source to permit survival in starvation conditions.

Carbonylation and Acetylation Are Not Inversely Related

To test the hypothesis that acetylation protects proteins against carbonylation, I began by comparing aggregated proteins of cells with low acetylation (e.g. Δ*pta* or Δ*pta ackA* mutants that cannot generate AcP) to those with higher acetylation (WT). To obtain the aggregated proteins, I grew the WT cells, Δ*pta*, and Δ*pta ackA* mutants in TB7/gl for 10 hours, harvested samples, and isolated the insoluble fractions to obtain protein aggregates as described in the **Methods** section. These insoluble proteins were visualized by Coomassie-stained SDS-PAGE. Contrary to the hypothesis, the aggregation observed in wild-type cells and AcP-deficient mutants was not visually different in three independent replicates of three biological replicates each (a representative image is found in **Fig. 22**).

To directly determine whether acetylation of a lysine could protect proteins against carbonylation, I utilized a carbonylation detection assay. Δ*pta*, Δ*pta ackA*, and WT cells were grown in TB7/gl for 10 hours, and lysates were generated. Carbonylation could be measured by reaction of protein lysates with DNPH reagent, which reacts with carbonyl groups and labels them for subsequent detection with an anti-DNPH antibody. Again, in data that contradicted my hypothesis, the carbonylation was indistinguishable between the low acetylation strains and the WT cells (**Fig. 23**). While both of these experiments yielded negative data under these

conditions, it may yet be possible that acetylation may have an effect under more stressful conditions like hydrogen peroxide stress.

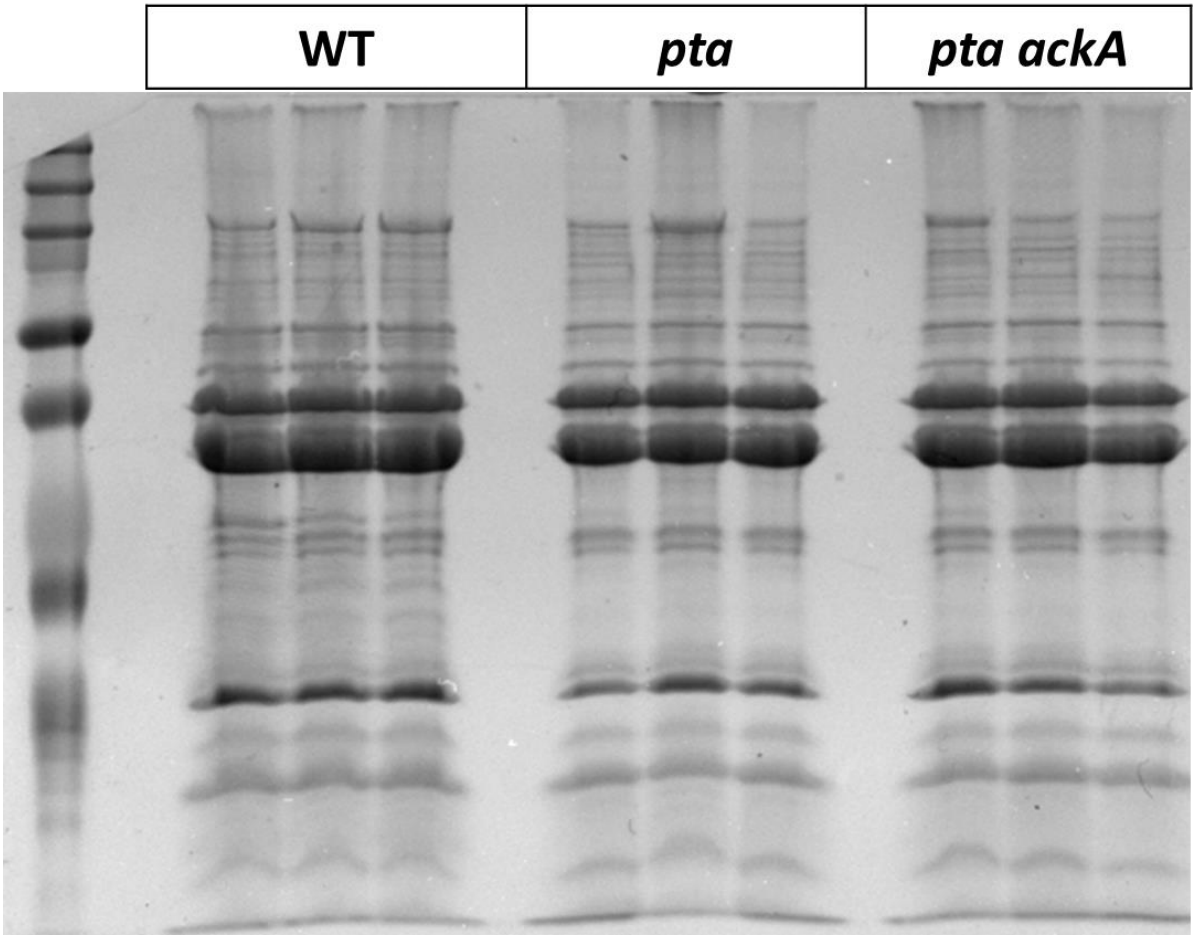

Figure 22. AcP-Dependent Acetylation Mutants Do Not Affect Protein Aggregation. Triplicate cultures of wild-type cells, Δ*pta* mutants, and Δ*pta ackA* mutants of *E. coli* (strain BW25113) were aerated at 37°C in TB7 supplemented with 0.4% glucose. After 10 hours, equivalent numbers of cells were harvested, and protein aggregates were isolated. Aggregated proteins were separated by 1D-SDS PAGE and stained by Coomassie Brilliant Blue to visualize.

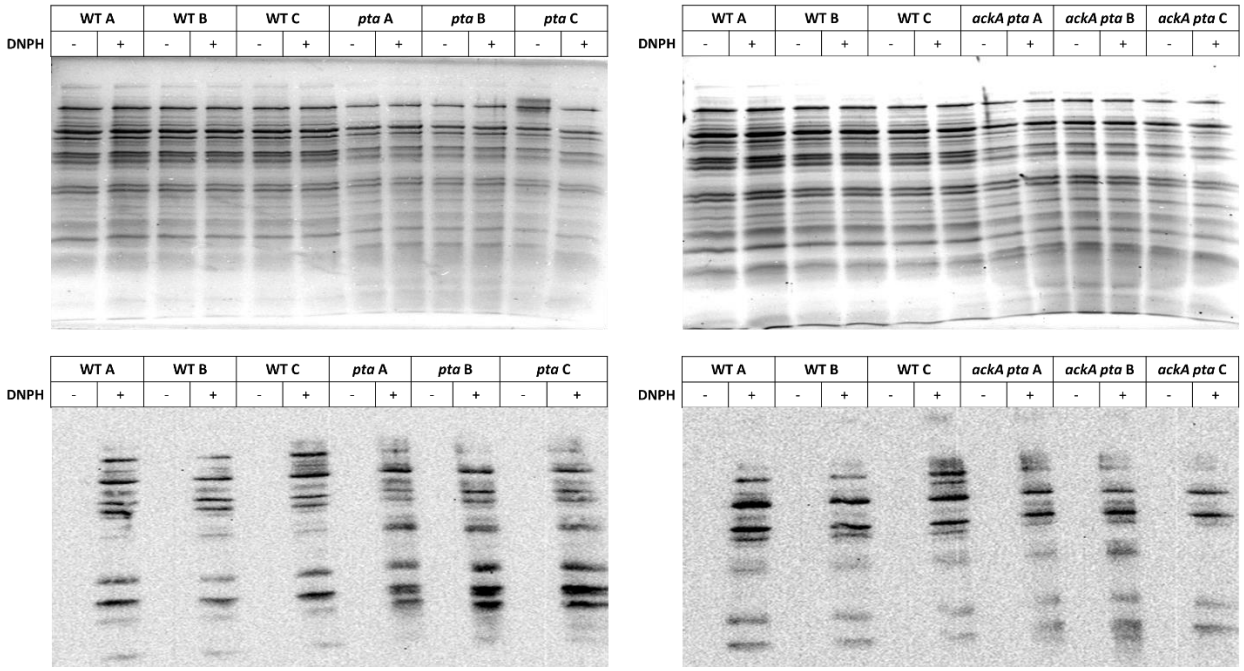

Figure 23. Loss of AcP Does Not Alter Carbonylation. Triplicate cultures (A-C) of wild-type cells, Δ*pta* mutants (Left panels), and Δ*pta ackA* mutants (Right panels) of *E. coli* (strain BW25113) were aerated at 37°C in TB7 supplemented with 0.4% glucose. Cells were harvested after 10 hours. Protein lysates were normalized to protein concentration and treated with or without DNPH to detect carbonylated proteins. The lysates were separated by 1D-SDS PAGE (Top panels) and assessed for protein acetylation by anti-DNP western immunoblot analysis (Bottom panels).

Acetylation Does Not Promote Survival under Starvation Conditions

To determine whether acetylation could serve as a carbon source, I began by asking whether carbon from acetylation was sufficient to promote colony formation in the absence of a carbon source. To do this, I grew WT cells in TB7 (low acetylation) or TB7/gl (high acetylation) overnight. I made serial dilutions and spread an aliquot of cells onto M9 minimal medium plates without a carbon source, such that the cells could only grow based on their carbon stores. However, no colonies developed indicating that the amount of carbon from glycogen and acetylation is insufficient to promote colony formation.

To further test this hypothesis, I performed competition experiments of Δ*pta* (low acetylation) and Δ*ackA* (high acetylation) mutants in liquid media without a carbon source. Each mutant contained a marker that permitted utilization of either arabinose (Ara+) or lactose (Lac+). Thus, I paired Δ*pta* Ara+ with Δ*ackA* Lac+ and vice versa. The mutants were initially cultured in M9 minimal medium supplemented with 0.4%glucose for 9 hours to ensure the cells had entered stationary phase and fully consumed all of the glucose. Then, equivalent cell numbers of each culture were pelleted in duplicate, one pellet for a monoculture control and one pellet for the competition assay. The pellets were resuspended in M9 minimal medium without a carbon source. Then, the resuspended pellets of the complementary Δ*pta* and Δ*ackA* mutants were combined. The colony forming units (CFUs) from the monocultures and competitions were measured over the course of approximately two weeks (a representative graph is shown in **Fig. 24**). No difference was detected in the monocultures of the Δ*pta* and Δ*ackA* mutants with either marker. While slight variations could be detected between the mutants in competition, the differences were not significant.

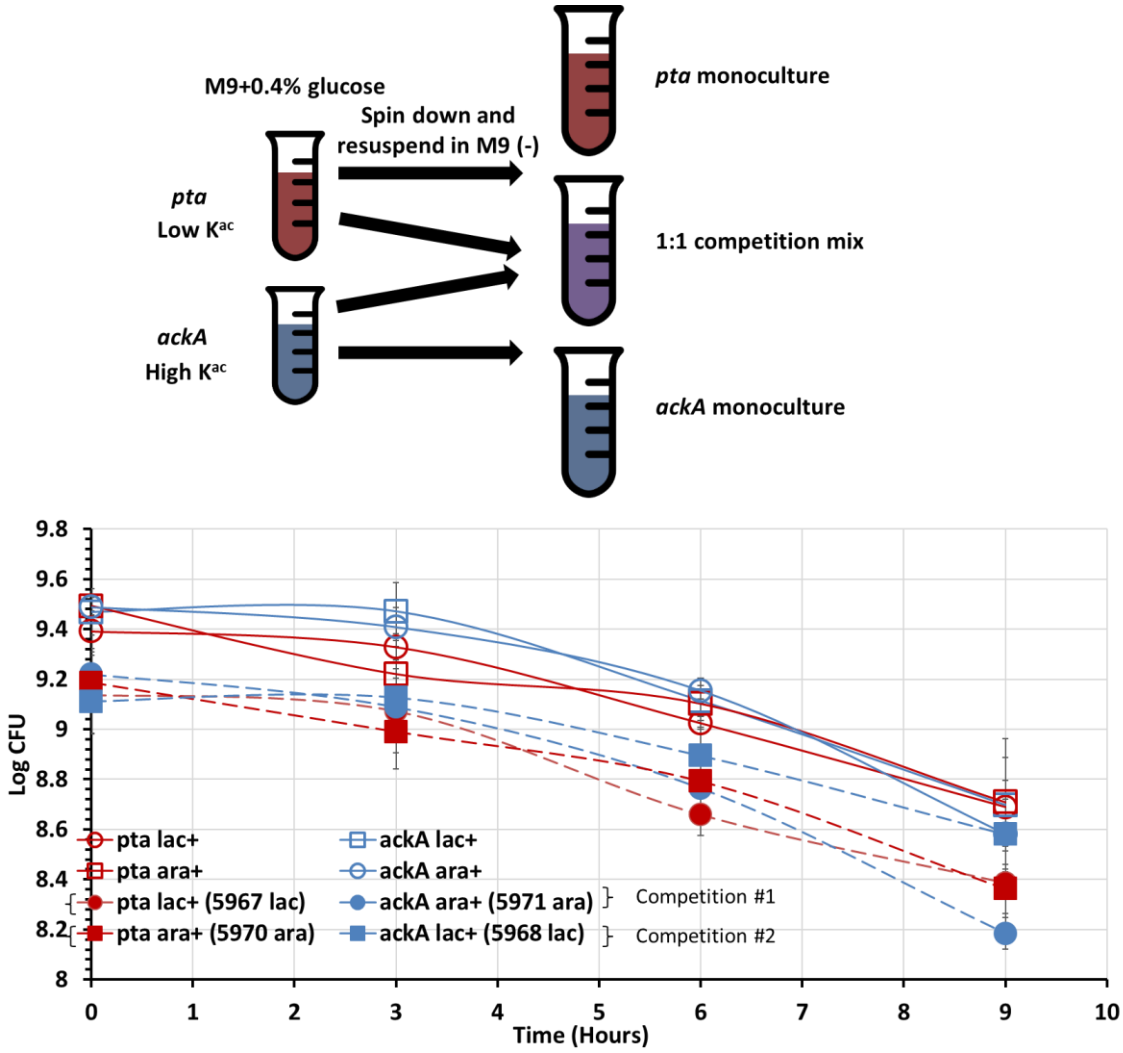

Figure 24. Carbon from Acetylation Does Not Promote Starvation Survival. Δ*pta* (Red lines) and Δ*ackA* (Blue lines) mutants of *E. coli* (strain BW25113) able to grow on either lactose (lac+) or arabinose (ara+) were aerated at 37°C in M9 minimal medium supplemented with 0.4% glucose for 9 hours. Equivalent cell numbers were spun down and resuspended in M9 minimal medium without carbon. To perform the competitions, Δ*pta* and Δ*ackA* mutants with opposing markers were cultured together. Survival was measured by plating for CFUs every three days for nine days.

Summary

In summary, I was unable to find a phenotype for AcP-dependent acetylation. The hypothesis that acetylation could serve as a protective modification is still sound. I only tested AcP-dependent as a protection against endogenous carbonylation, but it is possible that a

phenotype for acetylation may arise after treatment of cells with hydrogen peroxide to cause further oxidative stress. Furthermore, carbonylation can occur on other amino acids beyond lysine, so it is possible that a western blot would not be sensitive enough to determine the contribution of carbonylated lysines to the total carbonylation of proteins.

Acetylation was unable to sustain survival in starvation conditions. This could be because the hypothesis is incorrect, and acetylation is insufficient to provide carbon for starving cells. Alternatively, it could be that the contribution of glycogen to survival under starvation conditions obscures any contribution by acetylation. Thus, the exact phenotype for global, AcP-dependent acetylation remains elusive. However, recent reports studying the effect of AcP-dependent acetylation on specific lysines have found that acetylation may play a role in the function of certain proteins, including some proteins found in central metabolism (**Table 2**).

These studies lay the groundwork for future researchers to further investigate these hypotheses but under different conditions. I only assessed carbonylation under a single condition, but many chemicals can promote oxidative damage, which may exacerbate protein damage in the absence of acetylation. Importantly, I have generated differentially marked Δ*ackA* and Δ*pta* mutants. These stains can be used to perform competition experiments to assess how AcP-dependent acetylation affects a given phenotype with the caveat that the markers promote growth on either arabinose or lactose.

CHAPTER FOUR

EXPERIMENTAL RESULTS

Identification of GNATs in *E. coli* That Have KAT Activity and Their Targets

Introduction

Prior to this work, two mechanisms were known to acetylate proteins in *E. coli*. As described in **Chapters One and Three**, AcP is produced as an intermediate of the Pta-AckA acetate fermentation pathway and readily acetylates proteins non-enzymatically. The other mechanism is the canonical enzymatic mechanism where a KAT, YfiQ, catalyzes the transfer of the acetyl group of AcCoA onto the target lysine side chain. Data obtained by Alaa AbouElfetouh suggested that these may not be the only means of acetylating proteins in *E. coli*. She showed that a strain lacking AcP and YfiQ (Δ*pta ackA yfiQ*) could still produce acetylation detected by anti-acetyllysine western blot (**Fig. 25**).

I hypothesized that this acetylation could result from at least one of three possible sources. First, acetylation could be catalyzed by an uncharacterized KAT. Second, AcCoA could serve as a non-enzymatic acetyl donor, like AcP. Finally, there could be another non-AcP, non-AcCoA compound that could serve as an acetyl donor. I chose to focus on the first two hypotheses. In the following chapter, I assess the KAT activity of proteins encoded by *E. coli* predicted to be members of the Gcn5-related N-acetyltransferase (GNAT) family, of which YfiQ is a member, identifying four of these GNATs as KATs. We then identified the proteins that were acetylated in a KAT-dependent manner.

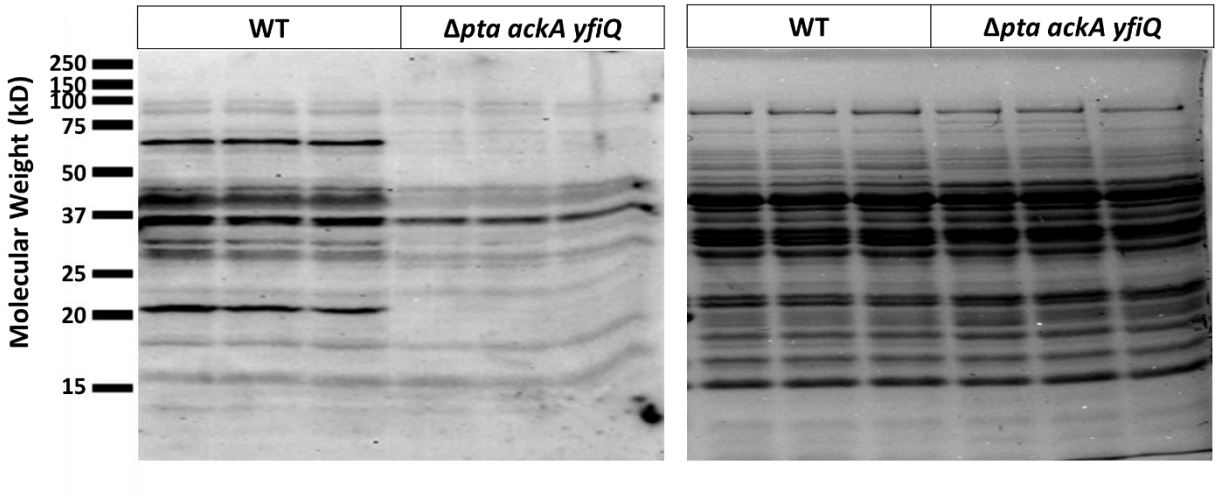

Figure 25. A Strain Lacking Known Mechanisms of Acetylation Contains Residual Lysine Acetylation. Triplicate cultures of wild-type cells and Δ*pta ackA yfiQ* mutants of *E. coli* (strain AJW678) were aerated at 37°C in TB7 supplemented with 0.4% glucose. After 8.5 hours, cells were harvested. Protein lysates were normalized to protein concentration, separated by 1D-SDS PAGE, and assessed for protein acetylation by anti-acetyllysine (α-acK) western immunoblot analysis (Left panel). Coomassie-stained SDS-PAGE gel (Right panel) to confirm protein normalization is shown.

PhnO, RimI, YiaC, YjaB, and YjgM Enhance Acetylation of One or More Proteins

Within the *E. coli* genome, 26 genes are annotated as GNATs, one of which is YfiQ (113, 126, 162). This family of enzymes catalyzes the donation of an acetyl group from AcCoA onto a molecule. When the molecule acetylated is a lysine on a protein, these enzymes are called KATs. The existence of these other GNATs may explain YfiQ-independent, AcP-independent acetylation. Thus, I wanted to determine whether, in addition to YfiQ, any of the gene products annotated as GNATs have KAT activity.

To determine whether these GNATs have KAT activity, I compared acetylation profiles of strains overexpressing each of the GNATs via anti-acetyllysine western blotting. I used a Δ*pta yfiQ acs cobB* background to enhance the signal-to-noise ratio, which I refer to as the acetylation "gutted" strain. This strain reduces background acetylation levels from AcP and YfiQ (Δ*pta*

yfiQ), while ensuring that the residual acetylation that occurs is not reversed by the CobB deacetylase (Δ*cobB*). Acs was also deleted, as it has been reported to acetylate the chemotaxis response regulator CheY (339). Furthermore, YfiQ regulates Acs activity and loss of that control can have a detrimental effect on growth due to energy depletion (383). As with a Δ*pta ackA yfiQ* mutant, the gutted strain (Δ*pta yfiQ acs cobB*) exhibited only limited acetylation (**Fig. 26**). To validate that this strain behaved as expected and hyperacetylated specific lysine sites with the known KAT YfiQ, I first compared YfiQ overexpression in a gutted strain that expresses the known YfiQ substrate Acs (Δ*pta yfiQ cobB,* Acs+) to that in a gutted strain that does not express Acs (Δ*pta yfiQ cobB,* Acs-). Indeed, by anti-acetyllysine western blot analysis, I observed an acetylated band in the gutted Acs+ strain that was absent in the gutted Acs- strain (**Fig. 27**, **denoted by an asterisk**). Upon induction of each of the 25 GNAT family members in the gutted strain, I found that overexpression of four GNATs (Aat, ElaA, YiiD, and YafP) inhibited growth. For the 21 strains that did grow, only 8 of the putative GNATs - plus YfiQ - resulted in the appearance of one or more acetylated protein band(s) (**Fig. 28**). Induction of YncA (17 kDa) and AstA (38.5 kDa) each produced a single acetylated band that migrated consistent with its expected molecular mass, suggesting acetylation of the proteins themselves. Induction of RimI, YiaC, YjaB, YjgM, and PhnO expression reproducibly produced acetylated protein band(s) across multiple replicates; in contrast, induction of RimJ did not (data not shown). Thus, I selected RimI, YiaC, YjaB, YjgM, and PhnO for further assessment of their ability to function as KATs. However, the subsequent mass spectrometry studies described below were unable to identify any targets of YjgM, so it will not be discussed further.

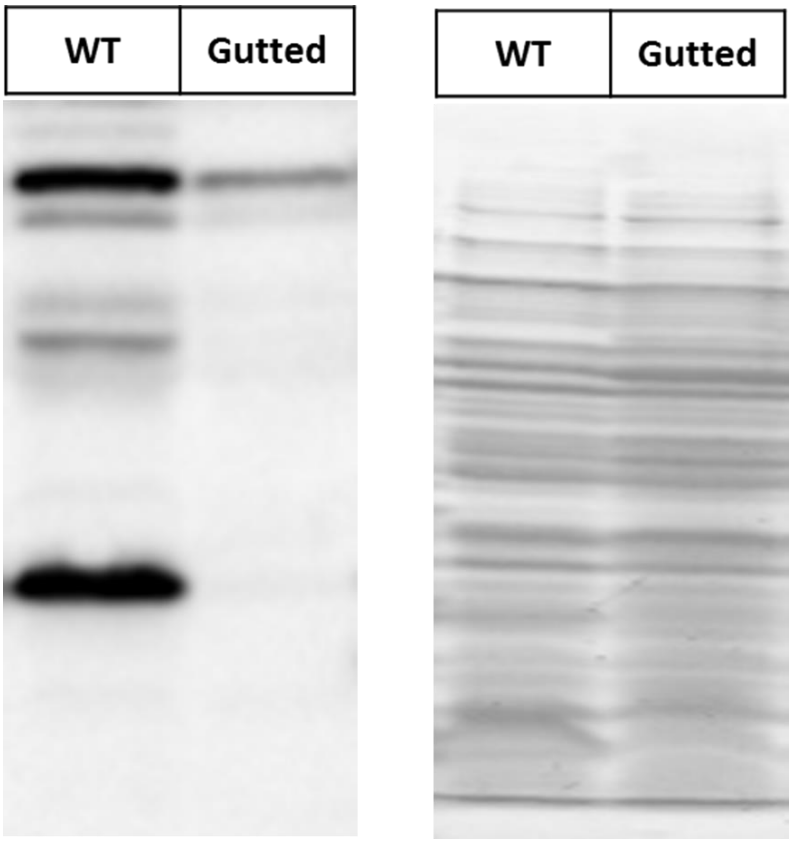

Figure 26. Gutted Strain of *E. coli* Has Low Background Acetylation. Wild-type cells and Δ*pta yfiQ cobB acs* (Gutted) mutant of *E. coli* (strain BW25113) were aerated at 37°C in TB7 supplemented with 0.4% glucose. After 10 hours, cells were harvested. Protein lysates were normalized to protein concentration, separated by 1D-SDS PAGE, and assessed for protein acetylation by anti-acetyllysine (α-acK) western immunoblot analysis (Left panel). Coomassie-stained SDS-PAGE gel (Right panel) to confirm protein normalization is shown.

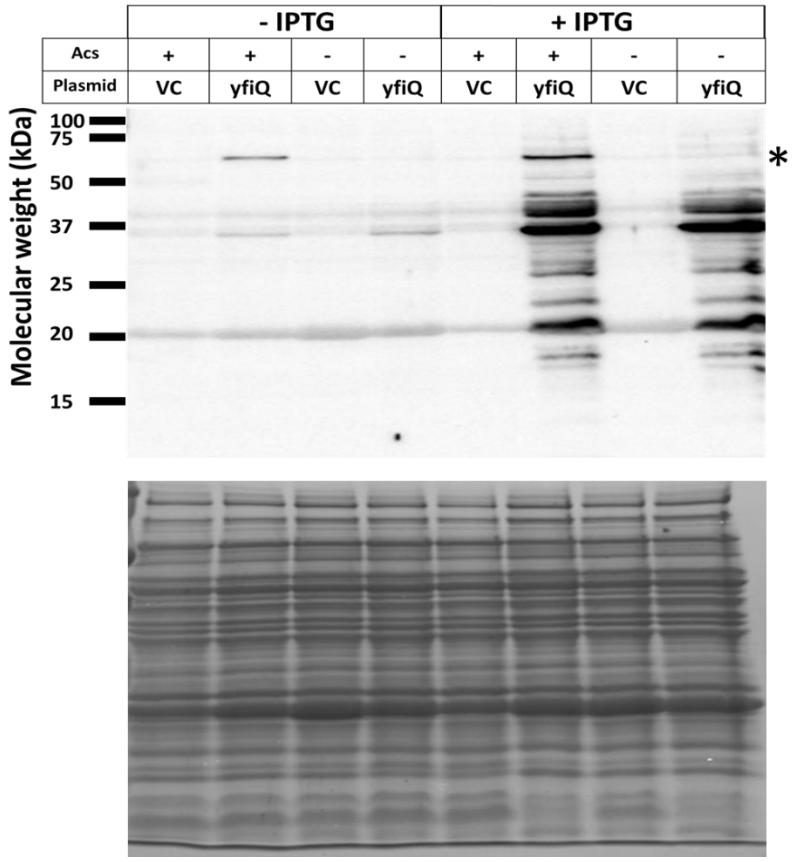

Figure 27. Overexpressing YfiQ Results in Increased Acetylation. BW25113 Δ*pta yfiQ cobB* cells (Acs+) or Δ*pta yfiQ acs cobB* (Acs-) were transformed with pCA24n-YfiQ or the empty vector (VC). The resultant strains were aerated in TB7 supplemented with 0.4% glucose and 25 μg/ml chloramphenicol for 10 hours. IPTG was added to a final concentration of 50 μM where indicated. Whole cell lysates were analyzed by Coomassie blue-stained SDS-PAGE gel (Bottom panel) to ensure equivalent loading and by anti-acetyllysine (α-acK) western blot (Top panel). The acetylated Acs band is indicated by an asterisk (*). Note, leaky expression of YfiQ results in acetylation of Acs in the absence of IPTG.

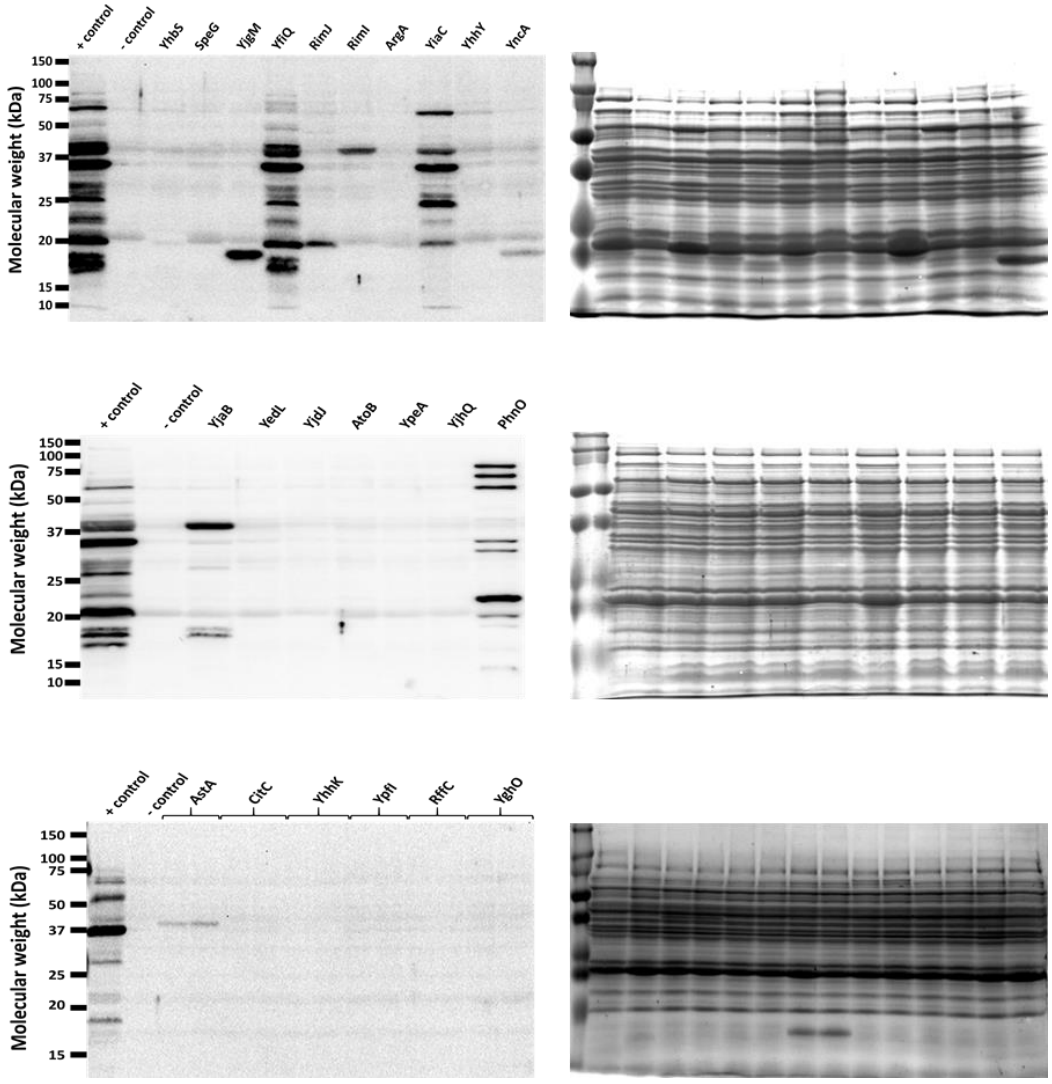

Figure 28. Overexpression of Five GNAT Family Members Results in Altered Lysine Acetylation Patterns by Anti-Acetyllysine Western Blot. The gutted strain (BW25113 Δ*pta yfiQ acs cobB*) was transformed with the pCA24n vector control (negative (-) control) or pCA24n containing the indicated genes under an IPTG inducible promoter (69). As a positive (+) control, an isogenic strain that retained the WT allele of *acs* (Δ*pta yfiQ cobB*) was transformed with pCA24n containing YfiQ. The resulting strains were aerated in TB7 supplemented with 0.4% glucose, 50 μM IPTG, and 25 μg/mL chloramphenicol for 10 hours. Whole cell lysates were analyzed by Coomassie blue-stained SDS-PAGE gel (Right panels) to ensure equivalent loading and by anti-acetyllysine western blot (Left panels). Note that the band in RimJ was not reproducible. The positive control contains one additional YfiQ-dependent band around 72 kDa, which corresponds to Acs. YncA and AstA each produce an acetylated band that can be observed in the Coomassie stained gel at the expected molecular weight of these proteins.

Mutation of Conserved Catalytic Residues Inactivates PhnO, RimI, YiaC, and YjaB

The enzymatic acetylation mechanism is catalyzed in three steps 1) deprotonation of the target lysine via a general base like glutamate or via a "proton wire"-type mechanism, 2) nucleophilic attack of the lysine on the carbonyl carbon of the acetyl group of AcCoA, and 3) protonation of CoA via a general acid like tyrosine. Thus, I hypothesized that if I could identify and mutate these residues in the putative KATs, I could prevent acetylation by them *in vivo*. I compared their sequences and utilized the protein structure prediction tool Phyre2 to identify residues that would be required for catalysis. I was able to identify the catalytic tyrosine that should protonate CoA for each of the four putative KATs (PhnO Y128, RimI Y115, YiaC Y115, and Yjab Y117). I was only able to identify a catalytic glutamate in PhnO (E78), suggesting these other three enzymes may use a "proton wire"-type mechanism (131). Additionally, Phyre2 suggested that a phenylalanine (F70) of YiaC could affect activity.

I made alanine substitutions at each of these residues and repeated the western blot with these variant proteins (**Fig. 29**). Each of the variants lost all acetylation detected in the WT isoforms, except YiaC F70A. The YiaC F70A variant produced the same pattern as WT YiaC but at a reduced intensity. This is not surprising since this residue was predicted to be important for function, but not necessarily catalysis. Because these plasmids encoded proteins carrying an N-terminal His-tag, I could ensure that the loss of acetylation in these variant proteins was due to a loss of activity rather than unstable proteins. Thus, I performed an anti-His-tag western blot, and found that protein levels of the variant proteins were equivalent to the WT protein in every case, except YjaB Y117A. I hypothesized that this may be due to the tyrosine having a role in the structure of YjaB, and mutation of that tyrosine destabilized the protein. However, since the role of tyrosine in catalysis is hypothesized to be for the donation of the proton from the hydroxyl

group to CoA, I expected that if I mutated tyrosine to phenylalanine, the protein should be structurally identical but lack the hydroxyl group needed for catalysis. As I predicted, the YjaB Y117F mutant produced a stabilized protein that could not produce the YjaB-dependent band on an anti-acetyllysine western blot (**Fig. 30**).

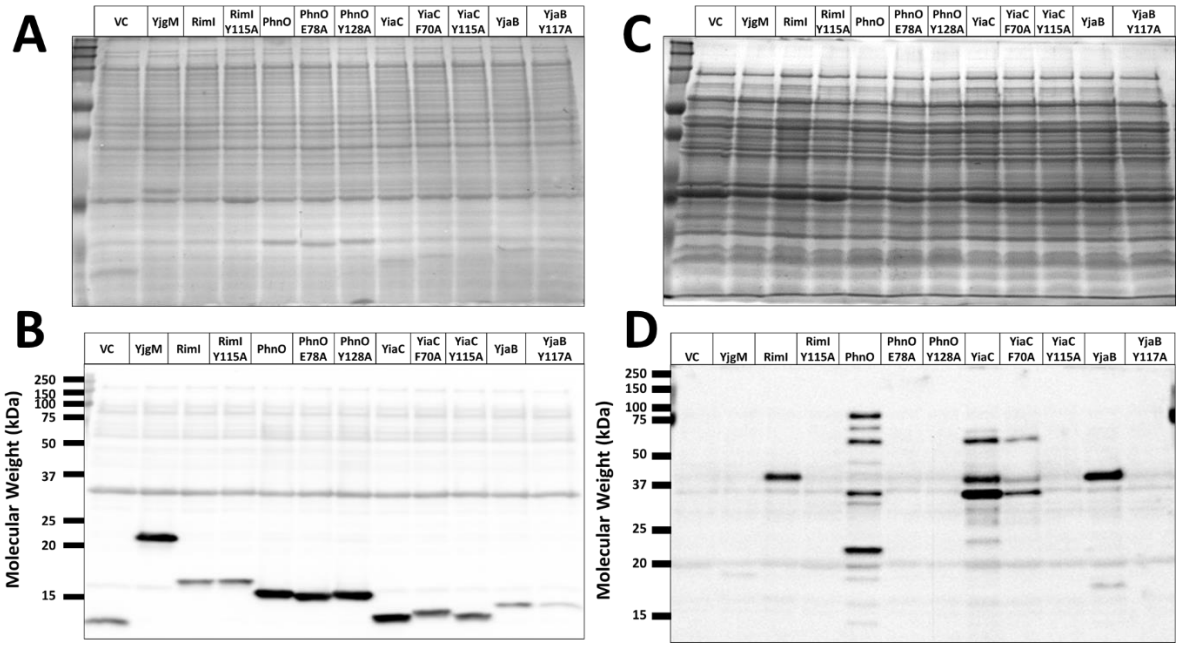

Figure 29. Mutation of Conserved Catalytic Amino Acids Prevents RimI, PhnO, YjaB, and YiaC-Dependent Acetylation. The gutted strain (BW25113 Δ*pta yfiQ acs cobB*) was transformed with the pCA24n vector control, pCA24n carrying the wild-type allele for each putative KAT, or mutant alleles for each putative KAT with alanine substitutions of the indicated residues. The resulting strains were grown in TB7 supplemented with 0.4% glucose, 100 μM IPTG, and 25 μg/mL chloramphenicol for 8 hours. Crude lysates harvested after 4 hours were analyzed for expression of the KAT proteins. Whole cell lysates harvested after 8 hours were analyzed for acetylation. Coomassie stained SDS-PAGE gels (A, C) served as loading controls for anti-His (B) and an anti-acetyllysine (D) western blots.

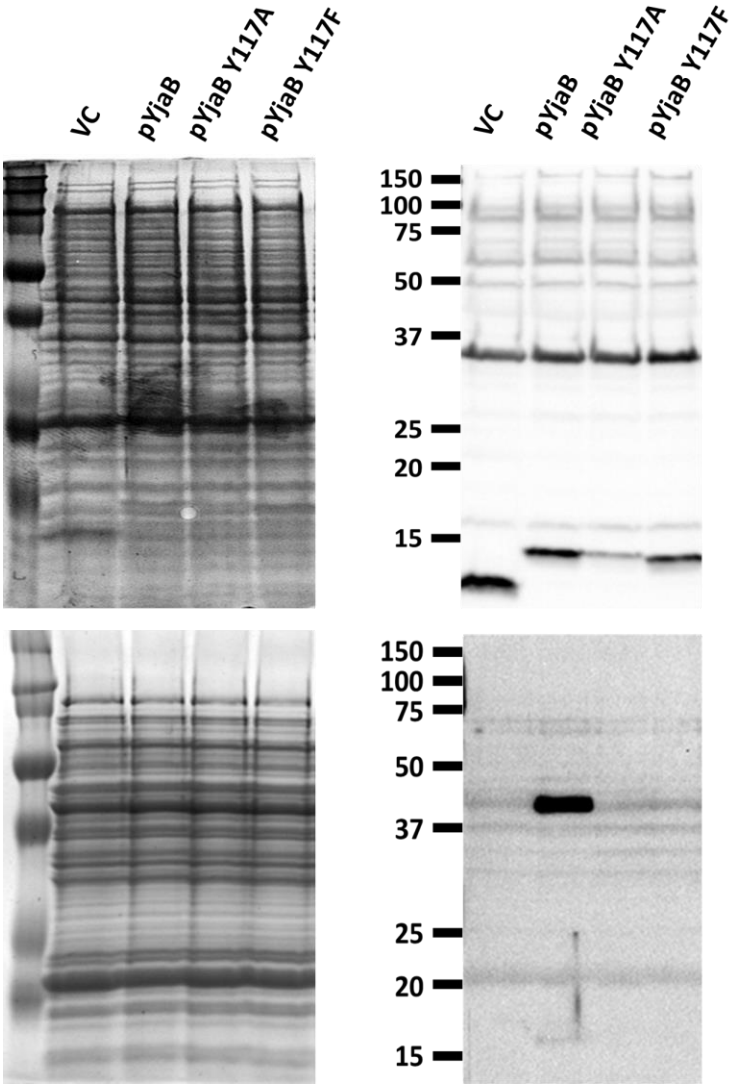

Figure 30. The Hydroxyl Group of Tyrosine 117 Is Required for the KAT Activity of YjaB. The gutted strain (BW25113 Δ*pta yfiQ acs cobB*) was transformed with the pCA24n vector control, pCA24n carrying the wild-type YjaB or the indicated YjaB mutants. The resultant strains were grown in TB7 supplemented with 0.4% glucose, 100 μM IPTG, and 25 μg/mL chloramphenicol for 8 hours. Crude lysates harvested after 4 hours were analyzed for expression of the KAT proteins. Whole cell lysates harvested after 8 hours were analyzed for acetylation. Coomassie stained SDS-PAGE gels (left) served as loading controls for anti-His (top right) and an anti-acetyllysine (bottom right) western blots.

We next confirmed that the amino acids I chose to mutate were active site residues. The sequence identity between these KATs is low (<30%), but since GNATs share a common structural fold, our collaborator at San Francisco State University, Misty Kuhn, performed a structural comparison of these KATs. The goal was to confirm that the chosen residues were in the correct location within the 3D structure (**Fig. 31**). An *E. coli* crystal structure of RimI (5isv) and an NMR structure of YjaB (2kcw) have been deposited into the Protein Data Bank (PDB); however, PhnO, YfiQ, and YiaC lack crystal structures. Thus, Dr. Kuhn built homology models for these three KATs. All of their active sites, with the exception of YfiQ, contained a conserved tyrosine known to act as a general acid in other GNAT homologs (384, 385), which were the same tyrosines that I mutated. However, as Phyre2 indicated, the identity/presence of the general base that deprotonates the lysine shows lower conservation than the general acid. RimI E103 acts as the general base in *S. enterica* serovar Typhimurium (386) and is conserved in the *E. coli* RimI and YiaC. In contrast, YjaB and PhnO have N105 and S116 in this position, respectively. Since I found PhnO E78 was required for acetylation dependent upon PhnO, E78 may be required for catalysis, which may suggest the general base may be found in a different 3D location for the different KATs.

The requirement for conserved catalytic amino acids for production of the PhnO-, RimI-, YiaC-, and YjaB-dependent bands suggests that these putative GNATs have KAT activity. However, the best evidence that an enzyme is a KAT would be demonstration that the enzyme can acetylate a target *in vitro*. Therefore, we needed to determine what proteins are acetylated by these putative KATs.

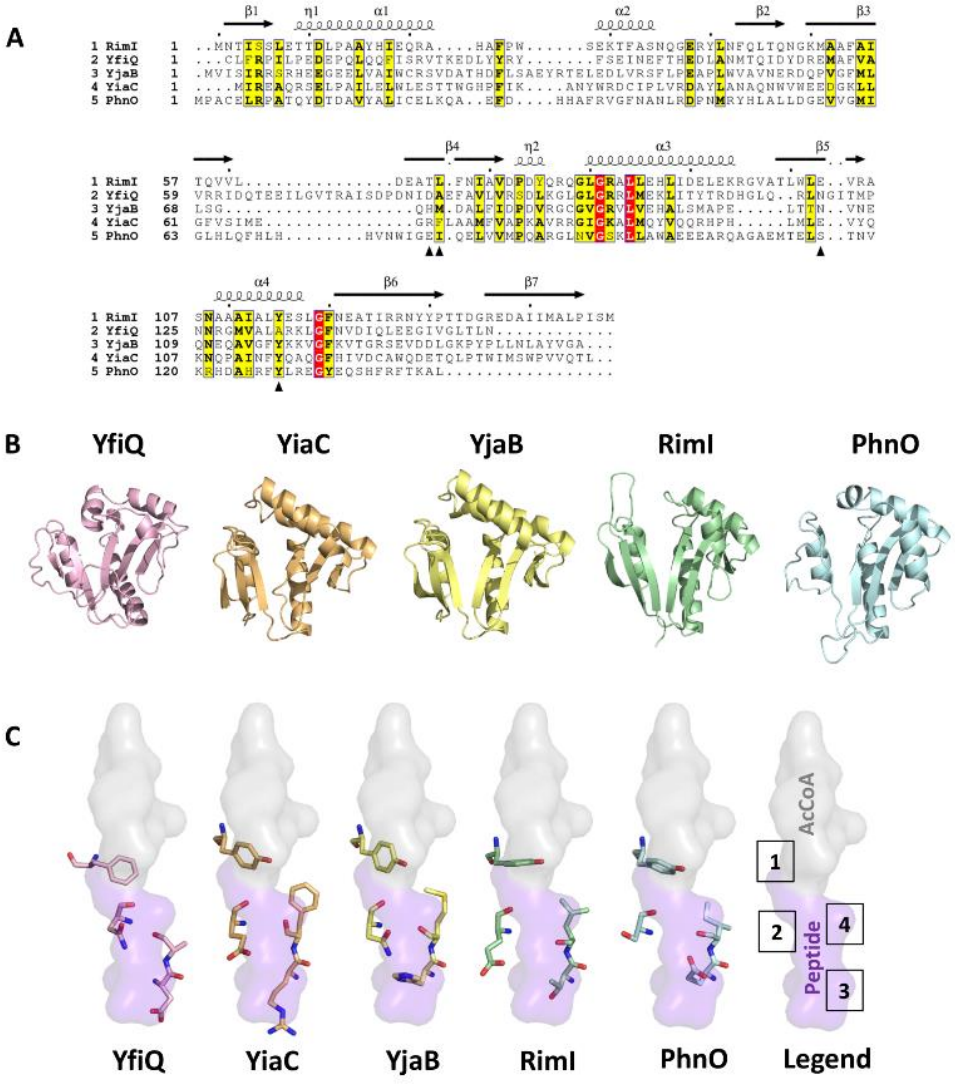

F138	Y115	Y117	Y115	Y128	1
N119	E103	N105	E103	S116	2
D82	R69	H72	T65	E78	3
A83	F70	M73	L66	I79	4

Figure 31. Sequence and Structural Comparison of KAT Proteins and Their Key Catalytic Residues. (A) Sequence alignment of all five *E. coli* KATs. Only the GNAT portion of the sequence for YfiQ is shown. The structural elements above the sequences are based on the 5isv RimI structure. Red highlighting represents 100% identity, whereas yellow highlighting shows a global score of 70% identity based on ESPript 3.0 parameters. Black arrows beneath the sequences indicate the residues selected for structural comparison in panel C. (B) Comparison of overall structures and homology models of *E. coli* YfiQ (pink), YiaC (orange), YjaB (yellow),

RimI (green; full C-terminus not shown in the figure), and PhnO (blue) proteins in a ribbon representation. 3D structures of YjaB and RimI were determined previously (PDB IDs 2kcw and 5isv, respectively). We built homology models of the remaining KATs using the following structures as templates: 4nxy for YfiQ, 2kcw for YiaC, and 1z4e for PhnO. Only the GNAT portion of the YfiQ protein sequence was used for the homology model. Further details regarding parameters for building and selecting representative homology models for these proteins are described in Materials and Methods. (C) Comparison of select active site residues potentially important for substrate recognition and catalysis in GNATs. The crystal structure of RimI (5isv) has the C-terminus of one monomer bound in the active site of the second monomer. A surface representation of this portion of the protein that encompasses the AcCoA donor (gray) and peptide acceptor (purple) site are shown. Each of the KAT homology models and structures were aligned using TopMatch and Pymol. Four active site residues are shown. A table beneath the structures shows the specific residue numbers for each KAT. Residues that were mutated are shown in red. This figure was generated by Dr. Misty Kuhn (SFSU) and published in (153).

Identification and Gene Ontologies of Proteins Acetylated by the KATs

To identify proteins whose acetylation depended on these putative KATs, I grew the "gutted" *E. coli* strains overexpressing RimI, YiaC, YjaB, and PhnO, as well as the known acetyltransferase YfiQ as a positive control and the empty vector as a negative control. I harvested pellets and submitted them to our collaborator Birgit Schilling for mass spectrometric analysis. We identified a total of 1539 unique acetylation sites on 668 unique proteins across all samples (see (153) for the published data). To determine the set of acetylation sites regulated by these novel KATs and YfiQ, we applied stringent filters to the quantitative comparisons between the overexpression samples and control (q-value < 0.01 and log2 [FC] ≥ 2, which is a ≥4-fold increase over vector control), resulting in a total of 818 acetylation sites on 434 proteins whose acetylation increased with overexpression of at least one KAT. YfiQ, acetylated the most lysines, with a total of 649 sites with significantly enhanced acetylation on 364 proteins. YiaC and YjaB overexpression resulted in lower, yet substantial, numbers of significantly increased acetylation of sites/proteins (391/251 and 171/128, respectively). Overexpression of RimI and PhnO elicited the fewest changes, each acetylating fewer than 20 sites. It should be noted that we observed

many more acetylated proteins by mass spectrometry than the number of bands we obtained via Western blot analysis. Mass spectrometry will detect site-specific acetylated peptides with greater sensitivity than western blotting, as previously shown (57, 78). Additionally, different acetylated proteins may migrate together on a gel and result in the appearance of only one band on a western blot.

To further explore the specificity of these KATs, we compared the sites acetylated by KAT overexpression with sites that we previously found to be sensitive to deletion of *ackA*, which causes accumulation of the highly reactive acetyl donor AcP and therefore results in non-enzymatic protein acetylation (57). Remarkably, of the 592 AckA-regulated sites, only 29 overlapped the 818 sites acetylated by PhnO, RimI, YiaC, YjaB, or YfiQ, further reinforcing their specificity and thus likely distinct functions. We also analyzed the primary amino acid sequences surrounding lysines that were acetylated by these novel KATs and found no specific neighboring residue preference. This suggests that substrate specificity cannot be determined by primary sequence alone and that three-dimensional analysis of protein structures should be considered.

To determine what pathways or functions these novel KATs may regulate, we assessed the gene ontologies of the KAT-regulated targets. Translation proteins and central metabolic enzymes were the most heavily acetylated cellular function. Almost all ribosomal protein subunits were acetylated (51 of 55 proteins); some were acetylated by AcP only (8/55) and some were acetylated by one or more KATs but not AcP (11/55), but most were acetylated by at least one KAT and AcP (32/55). Of the lysines on those ribosomal proteins, one-quarter (46/184) of them were targeted by more than one KAT, with as many as 3 KATs acetylating the same lysine. Acetylation by a KAT and AcP only occurred in 9/184 lysines. In addition to the ribosome itself,

amino acid tRNA ligases (16/23 proteins) were acetylated; some were acetylated by AcP only (6/23), some by KATs only (5/23), and some by both (5/23). Three of the 7 elongation factors were acetylated; these acetylations were largely dependent on AcP (13/15). All of the initiation factors were acetylated, and these acetylations were almost entirely KAT dependent (7/8). These data support a hypothesis where acetylation by AcP and by KATs have distinct roles.

Twenty-seven proteins comprise the three glycolytic pathways in *E. coli* (Embden-Meyerhof-Parnas [EMP], Entner-Doudoroff [ED],and pentose phosphate [PP]). Of these 27 proteins, 20 were detected as acetylated: 2 strictly by KAT(s), 7 by KAT(s) and AcP, and 11 by AcP alone (**Fig. 32**). A total of 97 lysines were acetylated: 9 by KAT(s) alone, 86 by AcP alone, and only 2 by both AcP and a KAT. Intriguingly, the majority of KAT-dependent acetylations (7/11) were found on proteins responsible for either the early or late steps of glycolysis, i.e., prior to the formation ofglyceraldehyde 3-phosphate (GAP) or on enzymes responsible for aerobic AcCoA synthesis. In contrast, the majority of AcP-dependent acetylations (66/88) were found on proteins that all glycolytic pathways share. In support of the concept that KAT-dependent acetylation helps direct flux, 3 other proteins relevant to glycolysis are exclusively acetylated by KAT(s). YfiQ and YiaC acetylated the transcription factor GntR,which controls expression of the enzymes (Eda [2-keto-4-hydroxyglutarate aldolase]and Edd [phosphogluconate dehydratase]) that comprise the ED pathway. LipA synthesizes lipoate, whereas LipB transfers a lipoyl group onto a lysine in the E2 subunit (AceF) of the pyruvate dehydrogenase complex (PDHC). The 3 subunits of PDHC, whose activity requires lipoylation, are highly acetylated, but almost entirely by AcP. Incontrast, LipA and LipB are entirely acetylated by KATs (7 lysines on LipA by YfiQ, YiaC,and YjaB and 1 lysine on LipB by YfiQ). These observations are consistent with the hypothesis that KAT-dependent acetylation helps direct flux through the 3 different glycolytic

pathways and regulates the transition from glycolysis to AcCoA-dependent pathways, such as the TCA cycle, fatty acid biosynthesis, and different forms of fermentation.

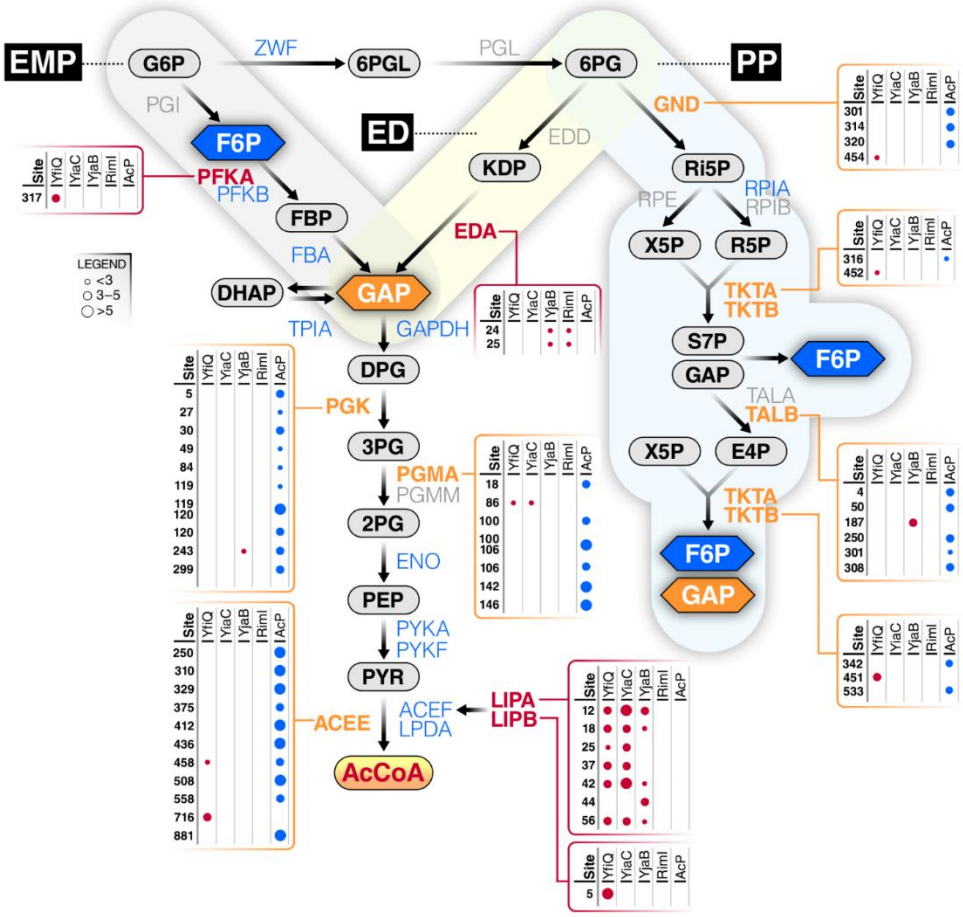

Figure 32. Most of Central Metabolism Is Differentially Acetylated by AcP and/or KATs. The three glycolytic pathways, Embden-Parnas-Meyerhof (EMP), Entner-Dourdoroff (ED), and Pentose Phosphate (PP) are shown with metabolites and enzymes indicated. Some enzymes are not acetylated (gray), while others are acetylated by acetyl-P alone (blue), KATs alone (red), or both (orange). Enzymes with boxes were modified by at least one KAT (as indicated); some were also acetylated by acetyl-P (AcP). The size of the dot indicates the fold upregulation for each lysine by either a KAT or AcP.

In Vitro Acetylation with YiaC

To determine whether these KATs truly have lysine acetyltransferase activity, I sought to demonstrate that incubation of a KAT with a target protein in the presence of AcCoA would yield an acetylated target protein. I chose a representative target protein that met the following criteria of having i) a high chance of being purified, ii) a lysine in a provocative location, and iii) an established assay to assess the effect of acetylation. I found that the YiaC target, cysteine synthase A (CysK), met my criteria. CysK catalyzes the second step in cysteine biosynthesis. CysK activity can be assessed *in vitro*, and a Δ*cysK* mutant is a cysteine auxotroph. Furthermore, I found that CysK was acetylated on a critical lysine that normally is covalently bound to the catalytic cofactor pyridoxal-5'-phosphate (PLP). Therefore, I hypothesized that acetylation of CysK would inactive the enzyme by preventing PLP from binding, which could be assessed by *in vitro* or *in vivo* assays.

To begin, I obtained purified YiaC from our collaborator Ekaterina Filippova, then at Northwestern Unviersity. I then purified His-tagged CysK encoded on a plasmid from the ASKA collection, an overexpression library containing most *E. coli* genes. I incubated CysK in the presence of YiaC, AcCoA, or both with the expectation that I should only see acetylation catalyzed in the presence of both YiaC and AcCoA. However, I consistently found that CysK was acetylated by AcCoA in the absence of YiaC, indicating that AcCoA non-enzymatic acetylation can occur *in vitro* (**Fig. 33**). This is consistent with other findings that histones (387), mitochondrial proteins (288), and bacterial proteins (232, 339, 388) can be acetylated by AcCoA non-enzymatically *in vitro*.

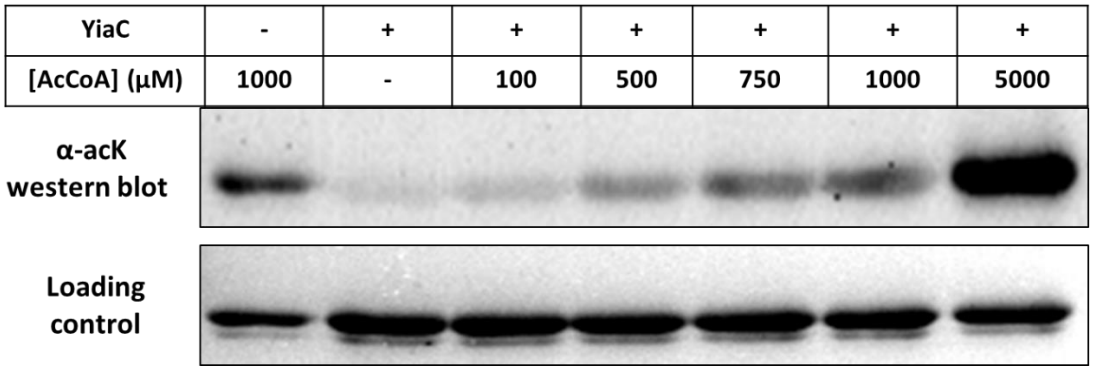

Figure 33. Non-Enzymatic AcCoA-Dependent Acetylation. Purified His-tagged CysK protein (0.6 μg) was incubated with YiaC (0.26 μg) and/or the indicated concentrations of AcCoA for 1 hour at 37°C. Reaction was stopped by heating at 100°C for 5 minutes. Proteins were resolved by SDS-PAGE and assessed for protein acetylation by anti-acetyllysine (α-acK) western immunoblot analysis.

I attempted to disfavor non-enzymatic acetylation by manipulating the reaction conditions. First, I boiled the samples prior to loading onto the SDS-PAGE gel for Coomassie staining and anti-acetyllysine western blotting. However, this might have enhanced hydrolysis of AcCoA and perhaps drive acetylation. Thus, I compared acetylation between samples that had and had not been boiled (**Fig. 34A**). Boiling resulted in more acetylation than the samples that were not boiled. However, this modification to the procedure still did not demonstrate any effect of YiaC on CysK acetylation.

To further modify the reaction conditions to disfavor non-enzymatic acetylation, I did not boil my samples and reduced the pH from 8 to 7 with the hypothesis that a less basic pH would result in fewer lysines becoming becoming spontaneously deprotonated. As expected, pH 8 promoted increased acetylation intensity more than pH 7 (**Fig. 34B**). Unfortunately, there was no visible effect of YiaC beyond that of AcCoA alone. Misty Kuhn is continuing to optimize conditions so that she can test the other KATs and targets for *in vitro* acetylation. Reasons for the

prevalence of non-enzymatic acetylation and caveats of this approach will be covered in the **Discussion** section.

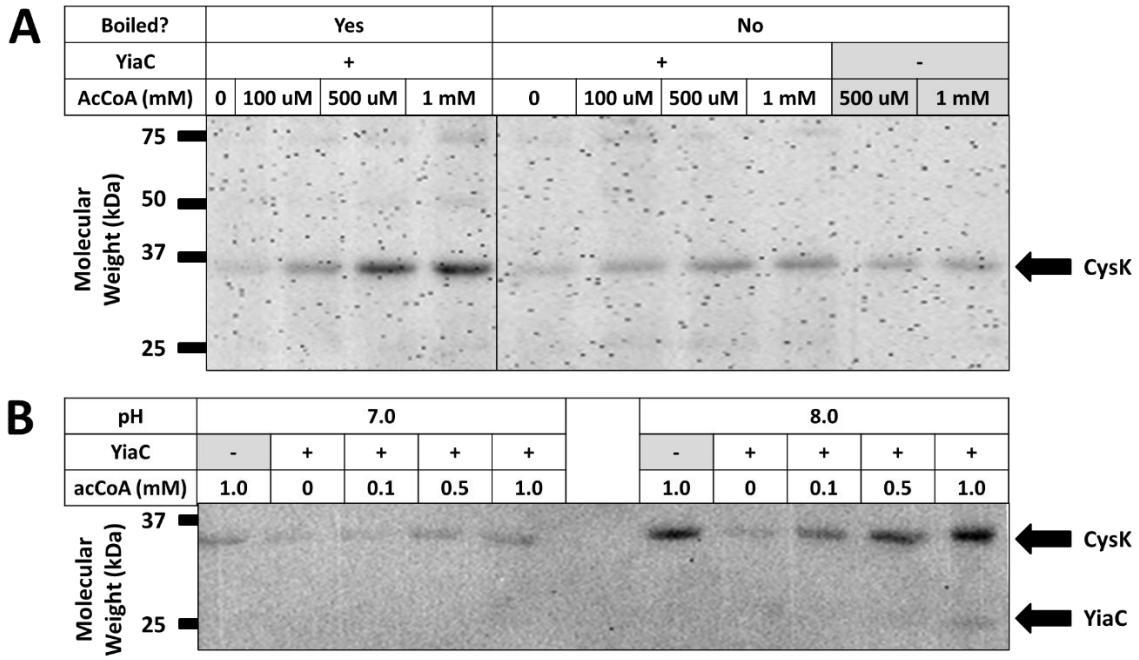

Figure 34. Non-Enzymatic AcCoA-Dependent Acetylation Is Enhanced by Boiling, High pH. (A) Purified His-tagged CysK protein (0.37 μg) was incubated with YiaC (0.26 μg) and/or the indicated concentrations of AcCoA for 1 hour at 37°C. (A) Reactions were either stopped by boiling at 100°C for 5 minutes or by adding loading buffer. Proteins were resolved by SDS-PAGE and assessed for protein acetylation by anti-acetyllysine (α-acK) western immunoblot analysis. (B) Reactions were buffered to pH 7 or pH 8 and carried out as described in A. Reactions were stopped by adding loading buffer and not boiling.

Conservation of the KATs across Bacteria Phylogeny

I wondered whether these novel KATs are present in other bacteria, and thus whether anything we learn about these KATs in *E. coli* may apply to other organisms. Unfortunately, these KATs are generally small (~145 amino acids / 16-17 kD) and tend to have low sequence homology. This proved to be troublesome for BLAST analysis. Thus, we reached out to our collaborators William Nelson and Samuel Payne. To find orthologs of these KATs, William

Nelson generated Hidden Markov Models for each KAT gene and searched against 5,589 genomes from Refseq (389, 390). To ensure we were looking at orthologs and not paralogs, strict cutoffs were used to ensure each genome contained at most only one match. As a highly conserved gene, *rimI* was identified in 4,459 genomes. The *yiaC* and *yjaB* genes were all broadly distributed across bacterial taxa and found in 421 and 692 genomes, respectively. However, *phnO* was found to have a very limited distribution, identified in only 22 genomes, and appears to belong exclusively to the gammaproteobacteria.

The Gutted Strain as a Tool

The "gutted strain" used to identify these *E. coli* KATs could be utilized as a tool to identify KATs from other bacteria. The low signal-to-noise ratio and knowledge about how to manipulate *E. coli* to favor and disfavor acetylation could allow for relatively high-throughput analysis of many genes for KAT activity. This also bypasses the requirement to purify the enzyme and know a target. A downside, however, is that there must be a protein encoded by *E. coli* that can be acetylated by the heterologously expressed KAT. Additionally, if a target is detected as acetylated in *E. coli*, it may not be the same protein acetylated in the native host. Thus, this should be used as an exploratory system and followed up with further study in the organism of interest.

To test this concept, I received 12 plasmids from John Kirby and David Payne that encoded GNAT family members from two strains of *Neisseria gonorrhoeae* and transformed them into the gutted strain. Of these 12 genes, 7 GNATs proteins were represented with two of their sequences identical between the two strains and the other five with divergent sequences between the two strains. Using the same protocol that I used to identify the novel KATs of *E. coli*, I observed that the RimI homolog of each *Neisseria* strain was capable of acetylating a band

around 40 kD (**Fig. 35, lanes FA-2 and 1291-2**), which appeared to be the same band acetylated by *E. coli* RimI (**Fig. 28**). These data confirm that the system can work. However, for the heterologously expressed proteins for which I was unable to detect acetyltransferase activity, these results suggest that they are either not KATs or that their native targets are distinct from the proteins present in *E. coli*.

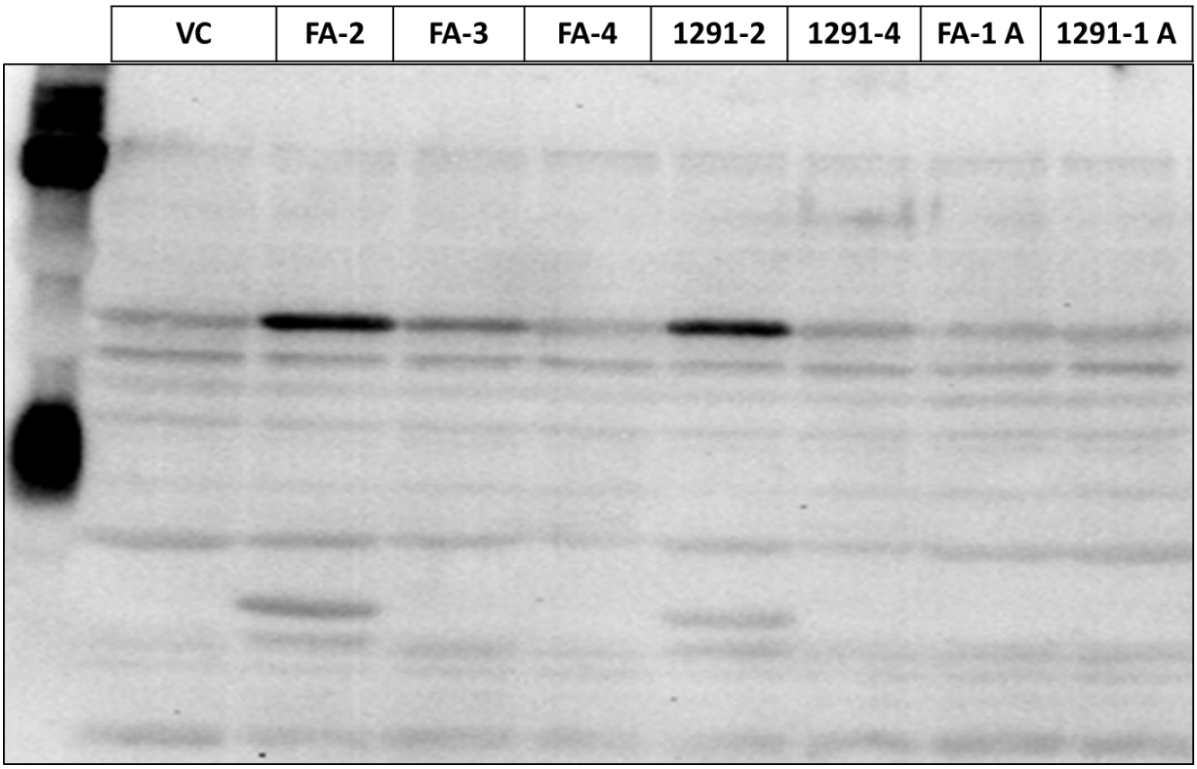

Figure 35. RimI Homologs FA-2 and 1291-2 from *Neisseria gonorrhoeae* Acetylate a Protein in *E. coli*. The gutted strain (BW25113 Δ*pta yfiQ acs cobB*) was transformed with the pCA24n vector control (VC) or pCA24n containing the indicated genes under an IPTG inducible promoter. The genes come from either the FA 1090 strain or 1291 strain of *Neisseria gonorrhoeae*. Each strain was aerated at 37°C for 10 hours in TB7 supplemented with 0.4% glucose, 50μM IPTG, and 25 μg/mL chloramphenicol. The whole cell protein lysate was normalized to protein concentration, separated by 1D-SDS PAGE and assessed for protein acetylation by anti-acetyllysine (α-acK) western immunoblot analysis.

Summary

In this section, I have demonstrated that *E. coli* appears to have at least four KATs in addition to the one known KAT, YfiQ. These KATs are single domain proteins that share a common GNAT fold and correspond to Class II (Type IV) GNAT classification. The proteins acetylated by the KATs were distinct from those proteins acetylated by AcP, suggesting that KATs have evolved distinct regulatory roles from AcP.

While I was unable to show that one of these KATs, YiaC, could acetylate CysK *in vitro*, mutation of residues suspected to be catalytic based on structural predictions inactived each enzyme. Based on prior structures and modelling, each KAT has a catalytic tyrosine that acts as a general acid to protonate CoA to regenerate the enzyme. The KATs appear to be highly conserved across bacterial phylogeny, which may suggest that what we learn in *E. coli* also can be applied to other bacteria. Indeed, I was able to identify a homolog of RimI from *Neisseria gonorrhoeae* that was capable of acetylating a protein at a molecular weight comparable to the band acetylated by *E. coli* RimI.

Phenotypic Assessment of the Novel KATs

Introduction

In the above section, I described the discovery of four *E. coli* proteins that appear to have KAT activity. Of these, non-KAT activities of RimI and PhnO have already been described. RimI from both *E. coli* and *Salmonella* Typhimurium is known to function as an N-terminal alanine acetyltransferase that has but one known target, the ribosomal protein S18 (32, 384, 391). PhnO is an aminoalkylphosphonate acetyltransferase in both *E. coli* and *S. enterica* (392, 393). PhnO is part of a gene cluster involved in the utilization of phosphonate under inorganic phosphate starvation conditions. While PhnO is not absolutely required for phosphonic acid

utilization, it does acetylate (*S*)-1-aminoethylphosphonate and aminomethylphosphonate (393, 394). In all cases, however, a role for KAT activity is unknown.

To find a role for acetylation, I utilized the *E. coli* gene expression database (https://genexpdb.okstate.edu/databases/genexpdb/) to find conditions under which these KATs may be expressed and, thus, when they may be relevant. I also searched for genomic context for nearby genes that may suggest a role for these KATs. Finally, I analyzed the targets of each KAT to determine whether there were any clear phenotypes that acetylation by a KAT would affect. In the following section, I will describe my attempts at uncovering a phenotype for deletion or overexpression of these KATs.

Assessing Growth and Survival of KAT Mutants and Overexpression strains in Various Stresses

To begin, I searched the genomic neighborhood in which these KATs are located and found RimI, YiaC, and PhnO are encoded in polycistronic operons, while YjgM and YjaB are monocistronic. The *yiaC* gene is directly downstream and overlaps four nucleotides of the *tag* gene that encodes 3-methyl-adenine DNA glycosylase I. The product of the *tag* gene is important for removing potentially mutagenic alkylation damage from DNA, but it is not induced through the adaptive response. As mentioned previously, the *phnO* gene is located with the other genes necessary for phosphonate utilization. RimI overlaps with DNA polymerase III subunit ψ, which is known to form a dimer with subunit χ to enhance affinity of DNA polymerase III preinitiation complex for DNA to stabilize the complex (395, 396). Since RimI is known to acetylate the ribosome, perhaps linking these genes coordinates replication and translation in some way.

The simplest hypothesis from the above information was that YiaC may help cells respond to DNA damage. Thus, I hypothesized that deletion of *yiaC* could reduce or enhance

cellular survival against a mutagenic chemical, N-methyl-N'-nitro-N-nitrosoguanidine (MNNG), an alkylating agent that methylates DNA. The cell encodes DNA glycosylase I (encoded by the *tag* gene) and DNA glycosylase II (encoded by the *alkA* gene) to remove the mutagenic lesion. Deletion of *tag* results in impaired survival to MNNG, while deletion of *tag* and *alkA* results in extreme sensitivity to MNNG (397). Thus, I performed an epistasis analysis between *tag*, *alkA*, and *yiaC* to determine whether YiaC contributes to survival against alkylating agents. I began by optimizing the protocol to determine killing of the Δ*alkA tag* mutant compared to WT, and I found that treatment with 50 μg/mL MNNG for 20 minutes showed the greatest difference in survival between WT and the Δ*alkA tag* mutant. With the established protocol, I tested the single mutants Δ*tag*, Δ*alkA*, and Δ*yiaC*, the double mutants Δ*alkA yiaC* and Δ*tag yiaC*, Δ*alkA tag*, and the triple mutant Δ*alkA tag yiaC* for survival in MNNG. Consistent with the literature, Δ*tag* mutants were more sensitive to MNNG compared to WT, while the Δ*alkA* mutant was more sensitive than the Δ*tag* mutant, and Δ*alkA tag* mutant was the most sensitive (**Fig. 36**). However, deletion of *yiaC* alone or in combination with any other deletion survived as well as the respective parent strain. Thus, under these conditions, YiaC does not appear to play a role in survival against MNNG.

Next, I analyzed microarray data that has been collected on the *E. coli* gene expression database to get a sense for conditions under which these KATs are expressed. The microarray datasets suggest that conditions that might upregulate KAT expression include heat shock and cold shock. To test this hypothesis, I performed growth curves at different temperatures, choosing a low temperature (24°C) and a high temperature (46°C) to compare to the standard temperature of 37°C. However, neither overexpression nor deletion of any of the KATs affected

growth at any temperature in LB (**Fig. 37**). Thus, while these KATs may affect growth at these temperatures, they do not under the conditions tested here.

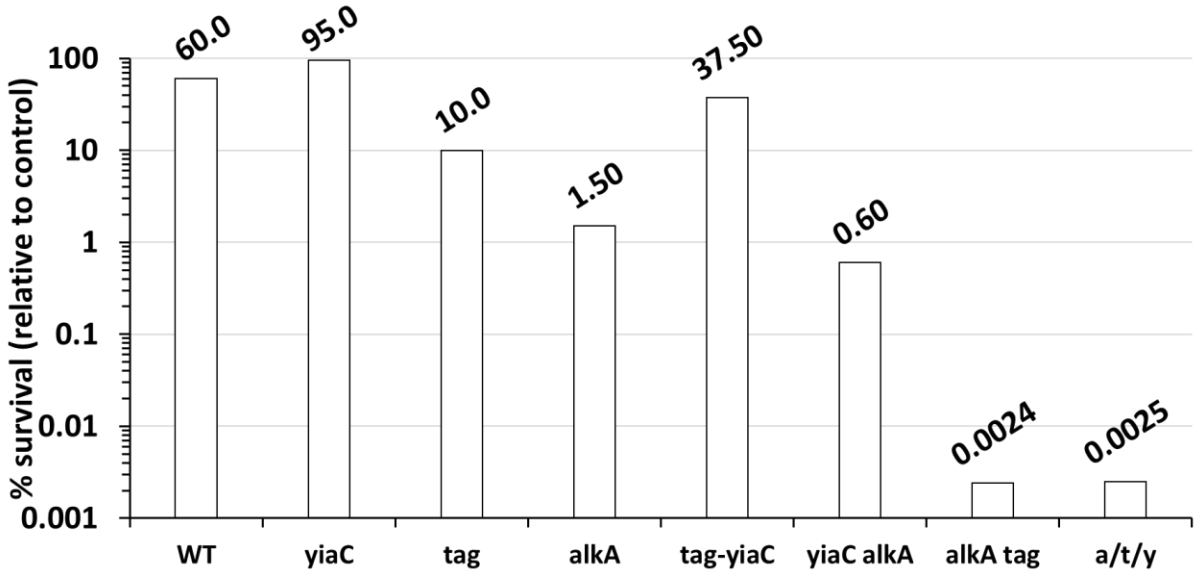

Figure 36. YiaC Does Not Play a Role in Survival Against MNNG. Mutants of *E. coli* (strain BW25113) or the WT strain were aerated at 37°C to 0.5 OD600. Each strain was treated with 50 µg/mL N-methyl-N'-nitro-N-nitrosoguanidine (MNNG) or left untreated (control). Cultures were incubated for 20 minutes at 37°C. Treatment was stopped by adding 2 volumes of PBS, and serial dilutions were plated to enumerate CFUs. Percent survival of the MNNG treated CFUs relative to the control CFUs are shown above the bars.

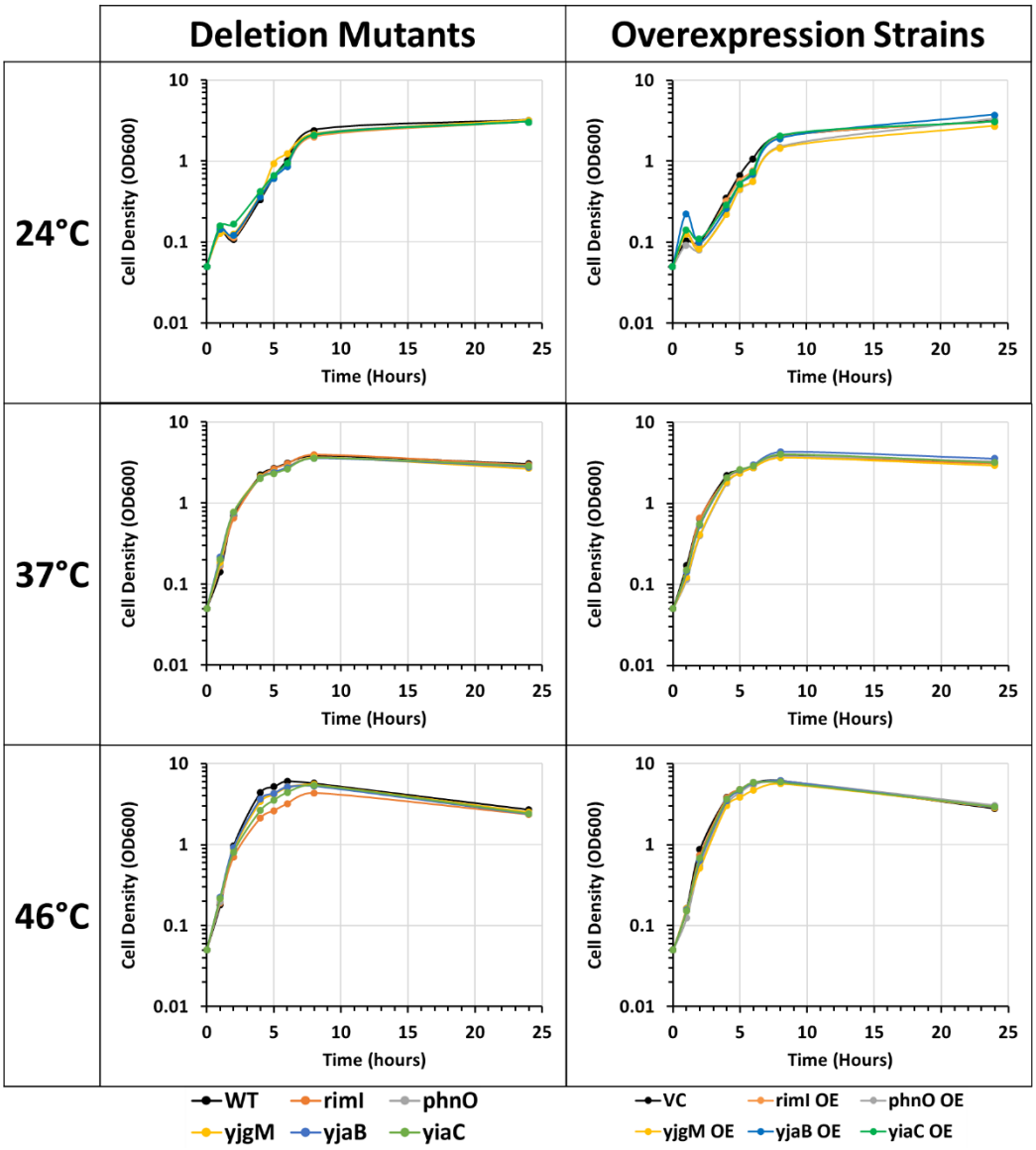

Figure 37. KAT Deletion or Overexpression Does Not Affect Growth at Different Temperatures. WT cells, KAT deletion mutants, and KAT overexpression (OE) strains of *E. coli* (strain BW25113) were aerated in LB at 24°C, 37°C, and 46°C in LB or LB supplemented with 50μM IPTG and 25 μg/mL chloramphenicol for the overexpression strains and vector control (VC).

Overexpression of YiaC and YfiQ Inhibits Migration

Additional conditions under which all of these KATs were found expressed were stationary phase and biofilm. Thus, I tested overexpression constructs of the four novel KATs

and YfiQ in a mucoidy assay as a readout of capsule formation, which is a characteristic of biofilm formation in *E. coli* (398). but we did not observe any difference relative to wild-type cells. The multicellular lifestyle of the biofilm is often contrasted by the planktonic lifestyle where the cells are free swimming and migrate towards various chemoattractants or away from repellants. Therefore, KAT-dependent acetylation may be a way *E. coli* shuts down planktonic phenotypes like motility to prepare for biofilm formation. I asked whether overexpressing the KATs would affect the swimming motility of *E. coli* in a soft-agar motility assay. We found that overexpression of YiaC and YfiQ consistently reduced migration in a soft agar motility assay (**Fig. 38A** and **B**). The inhibition of migration was not due to a reduction in growth rate as the overexpression strains grew as well as their vector controls (Data not shown).

To determine whether this reduction required the acetyltransferase activity of YiaC, we tested overexpression of YiaC F70A, which had reduced acetyltransferase activity, and YiaC Y115A, which lost activity as shown in **Fig. 29**. Overexpression of YiaC YF70A inhibited migration similarly to overexpression of wild-type YiaC (**Fig. 38C**). In contrast, YiaC Y115A was unable to inhibit migration. This suggests that acetyltransferase activity is required for the YiaC phenotype. To ensure this was not a strain-specific phenomenon, I recapitulated these data for YiaC in another *E. coli* strain background, MG1655 (Data not shown). While, the YiaC data were reproducible, overexpression of YfiQ caused a growth defect in MG1655, which confounded any effect of YfiQ on motility. Finally, since YiaC and YfiQ overexpression reduced migration, I hypothesized that deleting *yiaC* or *yfiQ* would enhance migration. However, neither a Δ*yiaC* nor a Δ*yfiQ* mutant showed the expected enhancement of migration (**Fig. 38D**). The reasons for this lack will be covered in the **Discussion**.

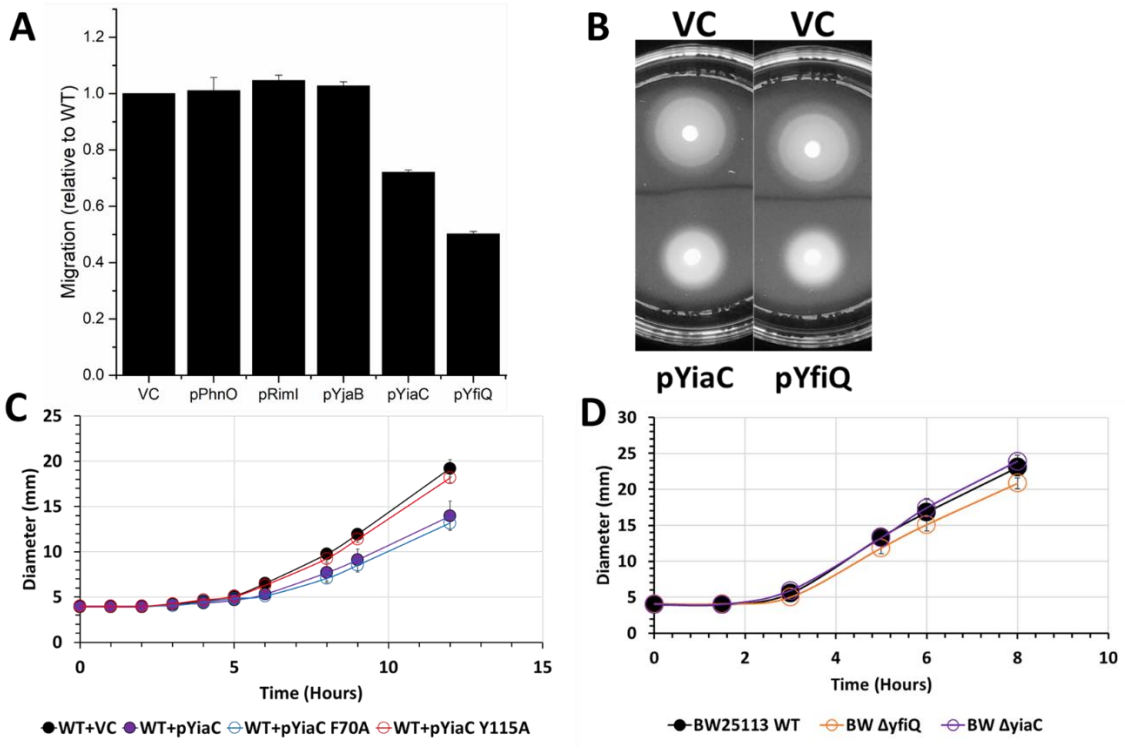

Figure 38. YiaC and YfiQ Inhibit Migration. Cultures of *E. coli* (strain BW25113) were grown overnight in TB medium supplemented with chloramphenicol and 50 μM IPTG. 5 μL of each normalized culture was spotted on low percentage TB plates supplemented with chloramphenicol and 50 μM IPTG. The diameter of the cell spot was measured hourly. (A) Final diameter relative to vector control (VC) after 12 hours is shown for WT strains carrying the indicated plasmids. (B) Representative motility plates of WT strains carrying VC, pYiaC, or pYfiQ. (C) Hourly migration of WT strains carrying pCA24n encoding YiaC, YiaC mutants, or vector control (VC). (D) Hourly migration of WT strain or isogenic deletion mutants on low percentage TB plates without supplement.

Summary

While I have identified four new KATs in *E. coli*, the phenotypes associated with their acetyltransferase activity are still unknown. Those who wish to take up this project in the future have many tools at their disposal. I have generated an isogenic set of deletion mutants of these KATs and the corresponding complementation constructs for some of them. Furthermore, I produced a set of overexpression constructs of WT and catalytically inactive isoforms of the

KATs that can be used to determine whether a KAT phenotype truly depends on the acetyltransferase activity.

I was successful in showing that overexpression of either YfiQ or YiaC inhibits migration of *E. coli*, and that phenotype this required the acetyltransferase activity of YiaC. However, I was unable to show a phenotype for deletion mutants of these KATs. This may suggest that they are not expressed under these conditions or the overexpression phenotype is artifactual. Another student in the lab, Sarah Feid, has generated fusions of the KAT promoters to beta-galactosidase. With these promoter constructs, we will be able to definitively say whether the KATs are expressed and under what conditions. Indeed, Sarah has recently found that *yiaC* is not transcribed under the conditions tested above. In the future, this knowledge will be able to better inform phenotypic assays to test these KAT mutants.

CHAPTER FIVE

DISCUSSION

Overall Summary: Chapter Three

The evidence presented in Chapter Three, in combination with previously published data, supports a model in which non-enzymatic, AcP-dependent acetylation is an unavoidable consequence of fermentation that accumulates on an aging proteome. Since AcP is made as an intermediate of fermentation, the only means of regulating acetylation would be by regulating fermentation, deacetylating acetyllysines with a KDAC, and/or evolving protein structures to optimally favor/disfavor acetylation of specific lysines. Because acetate fermentation has evolved as a key mechanism that allows many bacteria to regenerate the limiting pool of CoA, this would suggest that *E. coli* has evolved to cope with or utilize this global modification over millions of years. What is this global, unavoidable modification doing to the cell? Multiple studies have shown that acetylation by AcP can modulate protein activity (**Table 2**); but often, these studies fall short of physiological relevance due to the assumption that 100% of the enzyme being studied is acetylated or unacetylated at a given lysine, which is rarely if ever the case (77, 81). Therefore, I sought to find physiologically relevant phenotypes that would explain how *E. coli* has evolved to utilize acetylation, i.e., as a carbon source or protection against oxidative damage. Though I was unsuccessful in identifying an effect of acetylation on these phenotypes, perhaps other conditions or experimental designs are necessary to test these hypotheses.

Carbon Overflow Induces AcP-Dependent Acetylation

When glucose consumption rate depletes free CoA faster than it can be recycled, *E. coli* will ferment acetate from AcCoA via the Pta-AckA pathway in a process called overflow metabolism to regenerate the limiting pools of CoA (296, 297). However, the production of AcP by Pta is faster than the conversion of AcP to acetate by AckA, leaving a pool of the intermediate AcP (284, 399). AcP stores carbon and phosphate, as well as energy via its anhydride bond. This high energy bond makes it a very reactive molecule. Initially, this property prompted studies that identified AcP as a non-enzymatic phosphoryl donor and subsequently encouraged studies that explored the physiological consequences of AcP-dependent phosphorylation (291).

Later, AcP was shown to be the predominant acetyl donor in *E. coli*, and mass spectrometry confirmed the existence of thousands of lysines on hundreds of proteins that are sensitive to AcP metabolism (56, 57). For most acetylated lysines, the increase in acetylation was uniformly low, yet certain hotspots were identified whereby a lysine was more frequently acetylated by AcP. Anti-acetyllysine western blot analysis confirmed the correlation between AcP and excess carbon by showing that glucose-induced acetylation depended on the ability of cells to synthesize AcP (56, 57). In addition to glucose, I demonstrated that global acetylation could be induced by two other fermentable sugars, fructose (**Fig. 14B**) and xylose (**Fig. 20**), as well as the organic acid, lactate (**Fig. 5**), Thus, I hypothesized that AcP-dependent acetylation was primarily the result of overflow metabolism. If this hypothesis were correct, a few predictions could be made. I would expect the same lysines should be susceptible to both glucose-induced acetylation and AcP-dependent acetylation. Similarly, acetylation of these lysines should not depend on the source of carbon, but simply the capacity of the carbon to enter

the Pta-AckA pathway. Finally, by preventing overflow metabolism, acetylation should be reduced.

In my work, I showed that glucose-induced acetylation modified ~30% of the lysines and ~45% of the proteins sensitive to AcP (**Fig. 11**), especially in central metabolism (**Fig. 12**) (57, 78). Though the overlap was not 100%, this discrepancy could be explained by the fact that these two experiments were carried out in two different strain backgrounds, which could express different proteins under the same conditions. Also, AcP-dependent acetylation was determined by studying a Δ*ackA* mutant, while glucose-dependent acetylation was determined with a WT strain. Deletion of *ackA* could lead to a metabolic imbalance that might alter gene expression, which could directly or indirectly affect which acetylated targets we would detect. The metabolic imbalance in a Δ*ackA* mutant is exemplified by the 3- to 5-fold increase in AcP levels compared to WT cells (56, 284, 399), and an *ackA* mutation is known to cause phenotypic differences from WT cells that, in some cases, can be attributed to altered expression (221, 223, 398, 400). For the mass spectrometric studies, a lysine was determined to be sensitive to glucose or AcP based on a threshold value of >2-fold increase relative to a control. Since the AcP levels are higher than physiologically relevant in a Δ*ackA* mutant, it is possible that the increased concentration of AcP permitted the fold increase of certain lysines to exceed the threshold value, which was not possible in WT cells. Additionally, improvements in workflow and software in the time between these two studies also may have contributed to these differences. I conclude that, while the mass spectrometry data do not perfectly correlate glucose-induced acetylation with AcP-sensitive acetylation, these data along with western blot data strongly imply that most glucose-induced acetylation is AcP-dependent and vice versa.

Though the work above was performed with glucose, I suspected that the AcP-dependent acetylation would overlap with acetylation induced by other fermentable carbon sources. Indeed, I have shown that cells grown on lactate, fructose, and xylose promote acetylation in a similar manner to glucose. Additionally, I tested whether acetylated lysines that were induced by glucose were the same acetylated lysines induced by xylose. Indeed, mass spectrometry showed that most lysines that were acetylated in response to glucose were also acetylated in response to xylose. Additionally, western blot analysis showed that glucose and xylose induced very comparable acetylation profiles (**Fig. 20**). Indeed, the only protein whose acetylation was sensitive to the choice of growth sugar was xylose isomerase, the first enzyme in xylose catabolism. Since *xylA* requires active cAMP-CRP and xylose-XylR for transcriptional activation, it is surprising that it was detected in the glucose conditions at all. While acetylation was similar regardless of sugar identity, the variable that significantly altered acetylation was concentration of the sugar. High sugar (4%) produced more acetylation than low sugar (0.4%), but again, the acetylation differences between glucose and xylose at each concentration were small.

Finally, I provided evidence that supports the model that AcP-dependent acetylation is a response to overflow metabolism. I prevented rapid carbon flux both into the cell and through glycolysis by making targeted mutants at different stages of glucose metabolism. In each case, I observed a reduction in acetylation in these mutants compared to WT cells. I prevented rapid carbon flux into the cell by deleting the major glucose transporter EIICB^{glc}, which is known to reduce acetate excretion (371). I found that acetylation in the Δ*ptsG* mutant was comparable to that in cells grown in the absence of glucose (**Fig. 13 lane 1** and **16A**), but I could avoid the need

for EIICB^{glc} by supplementing the medium with lactate, a carbon source that does not require EIICB^{glc} for its uptake (**Fig. 13 lane 6**). Similarly, preventing rapid carbon flux through the glycolytic EMP pathway and forcing the cells to use alternative glycolytic pathways by deleting phosphoglucose isomerase has been shown to reduce acetate excretion (401-403). Though not as defective as the Δ*ptsG* mutant, I showed that a Δ*pgi* mutant had reduced acetylation compared to WT cells (**Fig. 14** and **15**). The defect could be suppressed by using fructose instead of glucose, which bypasses the need for phosphoglucose isomerase (**Fig. 15**). Interestingly, the Δ*pgi* mutant grown in fructose achieved stronger acetylation than WT cells in glucose. In part, this may be due to the ability of fructose, through fructose 1,6-bisphosphate, to activate pyruvate kinase, one of the three rate-limiting enzymes of glycolysis (404). Also, the Δ*pgi* mutant achieved stronger acetylation in fructose than WT cells grown in fructose. I suspect that this may be due to an inability of a Δ*pgi* mutant to convert fructose-6-phosphate into glucose-6-phosphate, which directs all carbon through glycolysis towards pyruvate by removing the final step of gluconeogenesis catalyzed by Pgi.

I predict that the reason a Δ*pgi* mutant has reduced acetylation is two-fold. First, by blocking the EMP pathway, *E. coli* is forced to use the less preferred PP and ED glycolytic pathways (**Fig. 3**) (405). Second, to enter the PP pathway, glucose-6-phosphate must be converted to 6-phosphogluconolactone via the rate-limiting enzyme glucose-6-phosphate dehydrogenase (406). Thus, a bottleneck formed at the entry into the PP pathway would slow further glucose consumption. Therefore, one might expect that carbon sources using the PP pathway would induce less acetylation compared to glucose. However, xylose is catabolized via the PP pathway, but readily promotes acetylation to levels comparable to glucose (**Fig. 20**). I

predict that acetylation is reduced in cells catabolizing glucose through the PP pathway (Δ*pgi* mutant) versus WT cells catabolizing xylose because the Δ*pgi* mutant requires 5 steps for glucose to enter the EMP pathway, one of which is rate-limiting, while xylose can enter the EMP in only 2 steps, neither of which are rate-limiting (406).

AcP-Dependent Acetylation Accumulates in Stationary Phase

Previously, our group had shown that acetylation increased in *E. coli* cells growing in TB7/glucose compared to those grown in TB7 alone when analyzed by anti-acetyllysine western blot (57). The most striking increase in this glucose-induced acetylation occurred in stationary phase cells, while only minor changes could be observed during exponential phase. Thus, one of the major questions prior to my work was understanding why acetylation occurred in stationary phase. By harvesting more samples over this time course, I showed more finely that acetylation noticeably increased after the cells transitioned from exponential phase to stationary phase and that acetylation continued to accumulate for hours after cessation of growth (**Fig. 4C**). Strikingly, the reason acetylation accumulated was because much of the glucose in the medium was not consumed until the cells entered stationary phase (**Fig. 4A**). Mass spectrometry data of select time points along this growth curve showed that many (~39%) of the lysines that we detect as acetylated in stationary phase (12 hours) are already acetylated when the bacteria are in exponential phase (2 hours). Additionally, the population of those lysines that were detected as acetylated at 2 hours became more acetylated over time. Thus, the increase in acetylation observed in stationary phase by western blot is a result of two major changes to the acetylome: unique lysines/proteins become acetylated and acetylation occurs on unacetylated isoforms.

Compared to exponential phase, two facets of stationary phase make it the perfect growth phase to promote acetylation when excess carbon is present: reduced protein synthesis and reduced respiration. In stationary phase, rates of growth cannot be sustained due to depletion of a limiting nutrient (315). Thus, cells reduce rates of transcription and translation, which greatly reduces the generation of new proteins (312). Since the rate of protein biosynthesis is reduced, fewer TCA cycle intermediates are used to make new biomass. This will cause a bottleneck at the TCA cycle, and carbon must enter other pathways. In conjunction with reduced translation, total cellular protein becomes further reduced due to increased protein turnover. When *E. coli* enters stationary phase, aerobic metabolism is repressed (312, 314). As such, the carbon flux is driven towards fermentation. The combination of a reduced proteome in stationary phase and the continued metabolism of a fermentable carbon source increases the probability that any susceptible lysine will become acetylated.

My data appears to support this model. Continual exposure to carbon was required for *E. coli* cells to accumulate acetylation because removal of glucose prior to complete depletion (**Fig. 4A**) prevented further acetylation (**Fig. 7**). Supplementing TB7/glucose with magnesium extended exponential growth and increased the biomass of the cultures (**Fig. 18**). This magnesium addition permitted complete glucose consumption prior to entry into stationary phase (**Fig. 18)** and reduced acetylation (**Fig. 19**). I hypothesize that magnesium reduces acetylation through two mechanisms. Magnesium makes more carbon available for biomass, which results in less carbon available for fermentation. Additionally, any proteins that become acetylated in magnesium-supplemented cultures would be diluted into nascent proteins during the extended

exponential phase. However, once the culture enters stationary phase, there is no glucose remaining in the medium that can be fermented and therefore acetylation does not accumulate.

Acetylation Does Not Always Increase on Individual Lysines

While acetylation accumulates globally over time in stationary phase, the same is not necessarily true for individual lysines on proteins. In our time course experiment, we determined that the dynamics of acetylation varied across different lysines (78). Acetylation of some lysines increased over time, others diminished over time, and yet others had a constant basal level of acetylation. Intriguingly, many acetylations that diminished only did so between 8 and 12 hours (**Fig. 10**). This is a period well after the culture has transitioned into stationary phase. For certain proteins, perhaps acetylation reveals degradation signals or perhaps acetylation itself is a degradation signal. Thus, the isoforms carrying these acetylated lysines in the population would diminish. For CRP, the opposite appears to be true; CRP is stabilized by the loss of the K100 positive charge by substituting a glutamine residue mimicking acetylation (218). Additionally, acetylation has been linked to protein aggregation, but whether this leads to increased degradation of acetylated proteins remains to be tested (407-409).

Nutrient Limitation Promotes Acetylation When Carbon Is in Excess

As described in the previous section, magnesium limitation in the TB7/glucose medium commonly used in our experiments promotes acetylation. However, this phenomenon is not exclusive to magnesium. In most cases, a nutrient that becomes limiting while carbon remains abundant would be expected to promote acetylation. In each case, nutrient limitation would favor fermentation and/or cause the culture to enter stationary phase. In the case of the facultative anaerobe *E. coli*, oxygen is a nutrient that, when limiting, would favor fermentation, and

therefore promote synthesis of AcP, but would not cause the culture to enter stationary phase. As described above, stationary phase is a time when the proteome becomes relatively stagnant due to increased proteolysis and reduced translation. Therefore, continued carbon metabolism would cause acetylation to accumulate on this stagnant proteome. Below, I will discuss how certain nutrient limitations would promote acetylation.

In the case of magnesium, the cation is found throughout the cell, often as a counterion to stabilize membrane phospholipids, lipopolysaccharide, polyphosphate compounds like DNA and RNA, and the ribosome (410-412). Magnesium is also required to make ATP biologically active. If cells continue to divide without consideration of available magnesium, cellular activity would cease to function. One mechanism that cells appear to use to sense this magnesium depletion is through ribosomes. Without sufficient magnesium, translation will nearly cease due to dissociation of ribosomes (413). Thus, when magnesium concentration is insufficient for proliferation, carbon flux would be directed away from generating biomass like amino acids or lipids, and instead would be directed towards acetate fermentation.

In addition to magnesium, nitrogen limitation has also been shown to promote acetylation (56). Weinert *et al.* found that acetylation increased when cells were artificially forced into stationary phase by transferring exponential phase cells into glucose replete minimal medium lacking nitrogen. In contrast, nitrogen replete minimal medium lacking carbon did not promote acetylation. In *E. coli*, ammonia is the preferred nitrogen source, but nitrogen also can come from amino acids (379, 414). Ammonia assimilation primarily produces glutamate and glutamine, two of the major sources of cellular nitrogen used to synthesize purines, pyrimidines, and many amino acids (379). If cells deplete nitrogen, glutamine and glutamate would diminish,

which would cause the precursor molecule α-ketoglutarate to accumulate. Since α-ketoglutarate is an intermediate of the TCA cycle, accumulation of α-ketoglutarate would slow flux of carbon from AcCoA into the TCA cycle, drive carbon flux into fermentation, and thus promote acetylation.

I highly expect that oxygen limitation will promote acetylation. Though the effect of oxygen on acetylation has not been shown directly, low oxygen increases acetate production (415, 416). While magnesium and nitrogen are required to make new cells, oxygen is not required. Oxygen allows *E. coli* to use the electron transport chain with oxygen as the terminal electron acceptor, which increases growth rate and biomass yield (415). In anaerobic conditions, the TCA cycle becomes a branched pathway rather than a cyclic pathway and flux through these branches is reduced due to anaerobic repression (417). In this branched form, these pathways satisfy the biosynthetic requirements for proliferation, while fermentative pathways generate cellular energy. In anaerobic conditions like during overflow metabolism, *E. coli* will produce acetate, ethanol, and formate as well as some lactate and succinate in order to maintain redox balance (418, 419). Thus, I would expect that anaerobiosis would increase acetylation because of increased acetate production. However, the amount of carbon converted into the other non-acetate fermentation products may siphon carbon away from acetate fermentation, and thus the acetylation of anaerobic cells may be comparable to aerobically grown *E. coli*. In either case, I would predict that anaerobically grown *E. coli* would have stronger acetylation in stationary phase compared to exponential phase due to the reasons outlined in the previous section.

Production of AcP via Pta depends on both carbon and free inorganic phosphate. Also, the glycolytic enzyme glyceraldehyde-3-phosphate dehydrogenase requires inorganic phosphate

to convert glyceraldehyde-3-phosphate into 1,3-bisphosphoglycerate. Thus, phosphate starvation may be one of the starvation conditions besides carbon limitation that would reduce rather than enhance acetylation. Phosphorous compounds are the major building blocks of various molecules and are critical for many signal transduction pathways (420). Due to the importance of phosphate, *E. coli* has evolved a regulon designed to sense and respond to low phosphate conditions (421). One of the mediators of the response to phosphate limitation is ppGpp, the alarmone responsible for the stringent response to amino acid starvation that slows transcription, translation, and replication (422, 423). This suggests that when cells starve for phosphate, they behave like they are starving for amino acids. However, recent data suggests that ppGpp levels are directly correlated to AcP levels (424). Furthermore, in *Pseudovibrio*, phosphate limitation decreased citrate synthase gene expression and increased Pta-AckA gene expression (425). Therefore, the hypothesis that phosphate starvation would reduce acetylation could be incorrect and, instead, it may promote acetylation. Determining which hypothesis is correct could provide insight into how *E. coli* senses and responds to phosphate starvation.

Early Glucose Exposure Is Required for AcP-Dependent Acetylation

While most of my data support the model that carbon-induced, AcP-dependent acetylation is a consequence of acetate fermentation, there are a few pieces of data that do not fit this model. Because I hypothesized that acetylation accumulates on a relatively unchanging proteome during stationary phase, I thought that adding glucose later in growth, and thus having more carbon to ferment, would result in stronger acetylation than when glucose is used for biomass during growth. However, this was not the case (**Fig. 8A and 8C**). If I supplemented cultures with glucose at 0, 1, or 2 hours after inoculation, then acetylation was strong. However,

adding glucose after 2 hours resulted in a significantly weaker pattern, comparable to cells that had never been exposed to glucose. I suspected that perhaps these stationary phase cells were not consuming glucose; however, these cultures readily consumed glucose (**Fig. 9A**). I confirmed that lactate-induced acetylation also requires the carbon source to be added early, although the timing was slightly different (**Fig. 8B**). Thus, something was different between these exponentially growing cells and their stationary phase counterparts.

The most plausible explanation for the lack of acetylation when carbon is supplemented during stationary phase growth is pyruvate oxidase (PoxB). PoxB directly oxidizes pyruvate into acetate, bypassing the Pta-AckA pathway and therefore avoiding generation of AcP. PoxB is the major acetate production pathway during stationary phase (362), in part because its transcription depends on σ^S, the stationary phase sigma factor (426). Thus, when glucose is added to a stationary phase culture, the carbon passes through glycolysis to pyruvate where it is converted to acetate by PoxB. Similarly, lactate dehydrogenase directly converts lactate to pyruvate, which subsequently can be converted to acetate by PoxB.

If PoxB expression prevents acetylation when glucose is added in stationary phase, why does acetylation still accumulate when glucose is added in the first two hours of growth? This suggests that glucose exerts a regulatory effect in exponential growth that restricts PoxB expression. While this could be directly determined by measuring *poxB* transcript levels, the literature offers some suggestions as to a mechanism by which glucose would prevent PoxB expression. PoxB transcription is reduced in the presence of glucose (427). Biochemical experimentation and *in silico* inference have proposed that transcription of *poxB* can be activated by Cra (428), MarA (429), OxyR (430), and SoxS (429); repressed by NsrR (431); and may be

regulated by Fnr (432), NarL (433), and NarP (433). Of relevance here is Cra, the catabolite repressor/activator protein that exerts a catabolite repressing effect independent of the cAMP-CRP complex (434). Cra is inactive in the presence of glucose; specifically, *in vitro* evidence suggests sugar catabolites like fructose-1-phosphate bind to Cra and prevent Cra from interacting with operator sites, such as the one found upstream of *poxB* (435, 436). Indeed, this mechanism fits the data. When cells are exposed to glucose during exponential growth, there would be sufficient glucose metabolism to produce sugar catabolites that prevent Cra from functioning even once the cells enter stationary phase. Without active Cra, PoxB would not be expressed and instead acetate fermentation would proceed through Pta-AckA, generating AcP to acetylate proteins. In contrast, cells that have begun to express σ^S in the absence of glucose would activate *poxB* transcription with Cra. Once the glucose was added to these cells, PoxB would already be synthesized, preventing AcP generation and acetylation.

While Cra provides the most obvious explanation, this does not preclude other mechanisms from mediating the different cellular responses to glucose addition at exponential phase and stationary phase. When cells consume glucose, acetate is formed, which can freely diffuse into the cell as acetic acid. Acetic acid can then dissociate in the cytoplasm, leaving a proton that reduces the intracellular pH and decreases the proton gradient, which may interfere with energy metabolism. Since PoxB is linked to the electron transport chain via ubiquinone, perhaps acetate production through PoxB is disadvantageous when acetate levels are already rising. However, a transcriptional, translational, or post-translational means of regulating PoxB through acetate or pH has not been reported.

CRP Is Required for Glucose-Induced Acetylation

One of the most perplexing questions about acetylation was why CRP, a transcription factor best known for being active in the absence of glucose, was required for glucose-induced acetylation. CRP binds cAMP to generate a cAMP-CRP complex that can activate transcription of certain genes via interactions with RNA polymerase; these interactions are mediated by activating regions found on CRP. Since glucose import shuts down production of cAMP, I hypothesized that CRP could control acetylation through a function beyond activating transcription. However, this was not the case. I was able to phenocopy the loss of acetylation observed in the Δ*crp* mutant by either deleting adenylate cyclase (**Fig. 16B**) or mutating both activating regions of CRP (**Fig. 17A**). These data suggest that transcriptional activation by CRP is required for glucose-induced acetylation.

I propose that CRP is required to activate transcription of the genes encoding enzymes in the Embden-Meyerhof-Parnas (EMP) glycolytic pathway and the genes encoding the PTS system, including the major glucose transporter $EIICB^{glc}$. Overexpressing $EIICB^{glc}$ in a Δ*crp* mutant partially restored acetylation in the presence of glucose (**Fig. 13, lane 9**). It is possible that overexpressing all of the CRP-regulated genes encoding PTS system enzymes (*ptsG*, *ptsH*, *ptsI*, and *crr*) could more completely restore wild-type levels of acetylation. While I did not test the exact target(s) of CRP in the EMP pathway, it has been shown that CRP enhances flux through the EMP pathway while diminishing flux through the pentose phosphate pathway (374). Indeed, CRP activates transcription of glycolytic enzyme encoding genes *fbaA*, *gapA*, *pgk*, as well as the genes of pyruvate dehydrogenase *aceE*, *aceF*, and *lpdA* (437).

Unexpectedly, a Δ*crp* mutant also lost lactate-induced acetylation (**Fig. 13**). *E. coli* encodes three lactate dehydrogenases that interconvert pyruvate and lactate: Dld, LdhA, and LldD. LdhA is an NAD^+-dependent D-lactate dehydrogenase (438). Dld is quinone-dependent D-lactate hydrogenase (439, 440). LldD is a quinone-dependent L-lactate dehydrogenase (441, 442). Therefore, CRP may regulate one or more of these lactate oxidation genes. In the closely related organism, *Shewanella oneidensis* MR-1, CRP is required for transcription of the genes that encode Dld and LldP, the outer membrane permease for lactate (443). Indeed, a Δ*crp* mutant of *Shewanella* cannot grow on D-lactate but can grow on L-lactate. In my experiment, the cells were grown on a racemic mixture of D- and L-lactate and, as such, I cannot pinpoint whether a single enantiomer or both enantiomers are responsible for lactate-dependent acetylation. While a connection between CRP and lactate assimilation has not been established in *E. coli*, my data suggest that a regulatory mechanism comparable to that in *Shewanella* may exist. Thus, this remains an active hypothesis to be tested.

Acetylated Acs: A Marker for Catabolite Repression

After growth on glucose and excretion of acetate, *E. coli* can convert acetate back into AcCoA via Acs, a high affinity enzyme utilized by many bacteria to assimilate acetate for use in biosynthesis or generation of energy. Acetylation of a single conserved lysine (K609 in *E. coli*) inactivates Acs, which prevents growth on low concentrations of acetate (135). The acetylation is YfiQ-dependent and can be removed by CobB. Thus, the cells can reversibly and rapidly regulate Acs activity.

Both the *acs* and *yfiQ* genes are transcriptionally activated by CRP. Thus, these genes are catabolite repressed and are strongly upregulated in the absence of glucose. Transcriptionally

regulating both the target and KAT with the same transcription factor ensures that YfiQ will be available to quickly shut down Acs when necessary. In a coordinated system, Acs produces AcCoA, which can then be utilized by YfiQ to acetylate and inactivate Acs.

In my work, I consistently detected a 72 kD protein band on western blot in TB7 cultures. This band was also found in TB7/glucose cultures, but only once the glucose had been fully consumed. This band was also CRP-dependent, specifically in a class I-dependent manner (**Fig. 17A**). As shown in **Appendix A**, I determined that this band was Acs. Knowing the identity of this band permitted me to perform a control experiment when determining whether my YfiQ construct was behaving appropriately (**Fig. 27**). For experiments carried out in glucose, future studies can use the Acs band as a sensor of whether glucose or any other catabolite-repressing carbon source has been depleted from the medium. Furthermore, it can act as a diagnostic marker for whether mutant strains are experiencing catabolite repression or not. For example, a Δ*ptsG* mutant expressed Acs even though glucose was abundant in the medium. In summary, I hope that researchers can avoid pitfalls in data interpretation by recognizing this acetylated band is Acs and that its acetylation depends on YfiQ but not AcP.

Acylation as a Selective Pressure of Protein Structure

One of the conclusions from my work is that acetylation is an inevitable consequence of metabolism. Because nearly all life has evolved to utilize activated acetate as a key molecule in metabolism, all organisms must inevitably cope with the potential for protein acetylation. Recent literature suggests that this is probably not exclusive to acetylation. Succinylation (8), butyrylation (5), malonylation (9, 10), crotonylation (6, 7), and propionylation (5) are all acylations that arise from addition of metabolites onto a lysine side chain. Acylation of a

catalytic lysine can be extremely detrimental to protein function, and inability to remove these acetylations can result in a "dead" enzyme. Similarly, acylation of lysines that make salt bridges between proteins, DNA, or small molecules can completely prevent a protein from performing its activity. Thus far, only acetylation has been shown to promote certain proteins to associate with aggregates of misfolded proteins, which would presumably negatively impact their function (409). Whether these acylations are due to non-enzymatic mechanisms or catalyzed enzymatically, life must have balanced the possibility of detrimental acylation with benign or beneficial acylations. The best ways to ensure that only the optimal lysines are being acetylated in a given condition is to either 1) evolve a lysine deacylase to remove deleterious modifications or 2) evolve proteins such that they do not have lysines susceptible to acylation.

Deacylation is a mechanism to ensure that a given lysine will be unmodified despite the presence of reactive metabolites that are endogenously produced. Almost all acetylated linear peptides are susceptible to CobB (205), but not all acetylated *E. coli* proteins are CobB-sensitive *in vivo* (57). The CobB-sensitive lysines tend to be surface exposed (205). Indeed, for a lysine to be deacylated, it almost certainly cannot be buried within the protein structure unless the acylated residue becomes accessible through protein breathing, large scale conformational changes of the protein structure (444). However, the extent of breathing *in vivo* is probably restricted due to molecular crowding in the cytoplasm (445). Thus, the protein must be structured in such a way to favor deacylation of the target lysine without disrupting the activity of the protein.

If an acylated lysine blocks protein function and is not accessible to CobB or another deacylase, the cell must replace that protein by degrading it and synthesizing an entirely new

protein. Not all lysines can be acetylated, but those that do become modified can be acetylated at different rates (78, 287) (**Fig. 10**). As buried lysines would be refractory to CobB, I would also expect that acetylation of these lysines is rarely enzymatic due to the inability for an enzyme to access the lysine. I hypothesize that evolution may have selected for molecular environments that disfavor acetylation of these buried and other critical lysines. For acetylation by AcP, we know that a lysine requires two molecular determinants (57). First, the lysine must be deprotonated by either an adjacent residue or by a water molecule. Second, the protein must be able to bind and coordinate the phosphate moiety, such that the carbonyl carbon of the acetyl group is susceptible to a nucleophilic attack by a deprotonated lysine. However, any changes made over evolution that would disfavor acetylation had to be balanced with a protein sequence that permits proper folding and activity.

Finally, we detect acetylation of many lysines that would have no obvious effect on protein function. While this gives support to the hypothesis that acetylation is simply unavoidable, I hypothesize that these lysines could serve as a sink for acetyl groups that would otherwise acetylate lysines with critical functions. Indeed, comparing the stoichiometry of acetylation on these seemingly unimportant residues versus those that occur on critical residues may shed some light on whether this hypothesis is valid. In addition to their possible role as a sink for acetyl groups, these residues may have an as of yet undetermined physiological consequence.

In conclusion, it could be possible that acetylation has prevented certain protein structures from forming, and thus limited the potential configurations a protein can obtain. As research continues to identify the molecular determinants that facilitate acylation of lysines with

the other acyl donors, this may further shed light on restrictions that protein structures can make. It would be very interesting to determine what degree of control acylations like acetylation have exerted over shaping the proteome along evolution.

Physiological Consequences of Global AcP-Dependent Acetylation

Even though many AcP-dependent acetylations appear to be unavoidable, I propose that this global modification has physiological consequences. It seems likely that cells would have evolved to utilize such a prevalent PTM. Of the possibilities, I hypothesized that acetylation could be a carbon source, a metabolic feedback mechanism, and/or a preventative measure taken against oxidative damage of lysines.

To test whether acetylation was a carbon source, I competed cells with high acetylation (Δ*ackA* mutants) against cells with very low acetylation (Δ*pta* mutants) in medium without a carbon source (**Fig. 24**). These two extremes should have showed whether acetylation sustains survival of *E. coli* or whether it is irrelevant. In my experiment, there was no survival difference between the mutants, suggesting acetylation could not promote survival in carbon starvation. Perhaps acetylated proteins and their degradation products become common goods, which could explain why the Δ*ackA* mutant did not outcompete the Δ*pta* mutant (446). In eukaryotic cells, the product of the sirtuin reaction, *O*-acetyl-ADP-ribose can be degraded into acetate and ADP-ribose. While the outcome of *O*-acetyl-ADP-ribose metabolism in bacteria has not been deeply studied, *E. coli* encodes at least one protein, YmdB, that has *O*-acetyl-ADP-ribose deacetylase activity and produces free acetate (447, 448). Thus, as cells die in the competition culture, the acetylated proteins and any free acetate originating from Δ*ackA* mutants could be taken up and

consumed by either Δ*pta* or Δ*ackA* mutants. In future experiments, the contribution of reassimilation of acetate by Acs should be considered.

To determine whether acetylation could be a protective modification against oxidative damage, I qualitatively measured the differences in carbonylation between WT cells and Δ*pta* mutants with the hypothesis that the acetylation in WT cells would be a preventative modification against carbonylation. Production of reactive oxygen species is an inherent downside of aerobic respiration that can generate oxidative damage to macromolecules. These reactive oxygen species can react with amino acids in a variety of ways, one of which is carbonylation. Carbonylation is the conversion of lysine, arginine, threonine, and proline side chains into carbonyls (277, 449, 450). These carbonyl groups are very reactive and promote misfolding and aggregation. However, I was unable to find any increase in carbonylation between WT and Δ*pta* cells (**Fig. 23**). This could mean that the amount of acetylation achieved in WT cells in insufficient to protect against carbonylation. However, it is possible that acetylation does protect against carbonylation, but the assay was not sensitive enough to detect the effect. Since multiple different types of residues can be carbonylated, and the experiment I performed measures total carbonylation, carbonylation of non-lysine residues may have obscured the protective effect of lysine acetylation.

In an effort to determine whether acetylation promoted or protected against protein aggregation, I repeated the carbonylation experiment and purified protein aggregates and qualitatively assessed the amounts of aggregated proteins (**Fig. 22**). I was unable to determine any significant differences between WT, a Δ*pta* mutant, or a Δ*pta ackA* mutant. However, the literature provides two contrasting examples. First, Mizrahi *et al*. showed that exponential phase

MG1655 cells exposed to heat shock at 46°C increased their protein aggregation (407, 408). This heat-induced protein aggregation was further exacerbated in an isogenic Δ*pta ackA* mutant. These data are in direct conflict, however, with the data presented by Kuczyńska-Wiśnik *et al.*, who found that acetylation tended to disfavor protein aggregation (409). In contrast to Mizrahi *et al.*, this study used a different strain background, BW25113, and did not subject the cells to heat stress. The latter study also used stationary phase cells grown in LB with glucose instead of exponential phase cells in LB alone. As we now know from my work, the cells in stationary phase would have strong acetylation, while those in exponential phase would have weak acetylation. As Kuczyńska-Wiśnik *et al.* suggest, this discrepancy might be attributed to AcP-dependent phosphorylation in exponential phase versus AcP-dependent acetylation in stationary phase. However, my data do not fit either of these datasets. I suspect my data differs from Mizrahi *et al.* for the same reasons that Kuczyńska-Wiśnik *et al.* differed. I used different strain backgrounds, different growth phase, and different media. My experiment was much closer to that of Kuczyńska-Wiśnik *et al*. with two exceptions. First, their experiment used LB supplemented with glucose, while I used TB7/glucose. Addition of glucose to LB without buffering acidifies the media through production of acetic acid, while my conditions were buffered against pH changes. No attention was paid to whether acidification played any role in the study by Kuczyńska-Wiśnik and coworkers. Second, the purification of aggregated proteins was carried out in an almost identical manner, except I used 2% NP40 to separate my proteins from the membranes, while the other study used 2% Triton X-100. Both of these detergents should behave similarly, but until these are tested and shown to behave the same, the choice of detergent may partially explain the discrepancies. In conclusion, there appears to be a

contribution of acetylation to protein aggregation, but further work must be done to disentangle the current conflicting reports.

Specific Examples of AcP-Dependent Acetylation

AcP-dependent acetylation has been shown to modify approximately 750 proteins on almost 2500 lysines (57). Though the stoichiometry of AcP-dependent acetylation is not known, the techniques capable of determining acetylation stoichiometry are becoming more tractable (77, 81, 451-455). Until that work is performed, we must rely on relative increases of acetylation to inform our hypotheses about AcP-dependent acetylation. As stated above, these fold changes can be a source of misleading data due to a fold change from 9% to 90% acetylated peptides yielding the same change as 0.1% to 1% acetylated peptides. With this caveat in mind, I will describe some of the proteins that have been shown to be regulated by AcP-dependent acetylation in other studies, and how that matches to our data acquired here.

Acetylation of all aminoacyl-tRNA ligases of *E. coli* has been detected in our studies that determined glucose- or AcP-regulated acetylation (57, 78, 231). These enzymes catalyze the charging of tRNA molecules with the appropriate amino acids. The effect of acetylation has been assessed for four of these amino acyl tRNA ligases, AlaRS, ArgRS, LeuRS, and TyrRS (217, 231). These enzymes are responsible with charging tRNA molecules with alanine, arginine, leucine, or tyrosine, respectively. In the presence of glucose and/or AcP, we detected acetylation on 17 lysines on AlaRS, nine lysines on ArgRS, seven lysines on LeuRS, and eight lysines on TyrRS. AlaRS contained two lysines regulated by AcP and glucose (K592 and K731), and six upregulated by glucose (K74, K279, K536, K605, K750, and K784). LeuRS contained three lysines regulated by glucose (K21, K598, and K619), but none were considered regulated by

AcP with our thresholds. TyrRS had two lysines sensitive to glucose and AcP (K8 and K85) and two lysines regulated by glucose (K144 and K235). In contrast, no lysines on ArgRS achieved fold changes consistent or significant enough to be considered regulated by either glucose or AcP.

In work performed by Umehara *et al.*, non-canonical amino acid substitution was used to generate an AlaRS variant that contained an acetyllysine in place of K74, a residue known to interact with the 3' end of the $tRNA^{Ala}$ (231, 456). Acetylation of this residue reduced alanylation activity of the enzyme, but treatment with CobB restored the activity closer to the WT protein. While K74 did not achieve our threshold to be considered acetylated by AcP, it is glucose-regulated and does not appear to depend on YfiQ or any of the novel KATs. Therefore, K74 is most likely acetylated by AcCoA or AcP and reversed by CobB to regulate the activity of AlaRS. Interestingly, acetylation of K74 has been found in *Vibrio parahaemolyticus*, mice, and humans, which may imply a conserved mechanism of regulation (110, 457). However, the effect and interplay of the other acetylations on AlaRS activity remain to be tested. Ye *et al*. investigated the role of acetylation on LeuRS and ArgRS (217). Three lysine residues of LeuRS were chosen due to their conservation from bacteria to humans. Of these, only K619 was detected in our studies. A LeuRS variant with acetylation mimic K619Q exhibited decreased enzymatic activity, while non-canonical amino acid substitution of K619 with acetyllysine abolished enzymatic activity. Similarly, they determined that ArgRS variants with either glutamine or acetyllysine incorporation at K126 and K408 reduced enzymatic activity. Both lysines were sensitive to AcP and CobB *in vitro*, and deacetylation restored activity to the acetyllysine variants. However, it is uncertain whether acetylation of ArgRS would be relevant *in*

vivo since we did not determine ArgRS to be regulated by AcP or glucose. Venkat *et al.* examined how acetylation of multiple lysines on TyrRS would influence aminoacylation activity (222). Replacing either K85, K235, or K238 with acetyllysine abolished activity of TyrRS. While we detected each of these lysines as acetylated, only K85 was sensitive to AcP and induced by glucose. Though it may be tempting to make strong conclusions based on *in vitro* data, one should consider the native stoichiometry and whether the lysine residues are detected as acetylated *in vivo*. With this in mind, these data support AlaRS K74 and TyrRS K85 as the best candidates for biologically important acetylated lysines that are regulated *in vivo* with effects on enzymatic activity *in vitro*.

AcP heavily acetylates central metabolism both by fold-change and by number of lysines acetylated on proteins (**Fig. 32**). However, the effect of acetylation, and more specifically AcP-dependent acetylation, on these pathways and enzymes has only begun to be explored. In *Borrelia burgdorferi*, GAPDH is acetylated by AcP, which reduces activity (458). While the residue(s) that mediate this effect are unknown, *E. coli* GAPDH is acetylated on 15 lysines, of which seven are regulated by AcP and glucose. In *E. coli*, malate dehydrogenase (Mdh), an enzyme of the TCA cycle, is acetylated on 13 lysines. Four of these lysines are sensitive to AcP and glucose, while six are sensitive to glucose alone. Interestingly, Venkat *et al.* used non-canonical amino acid substitution to demonstrate that acetylation of two AcP-sensitive lysines, K99 and K140, cooperatively enhanced Mdh activity. In contrast, acetylation of K162, a lysine that was not regulated by AcP or glucose, had no effect (219, 220). K140 could be deacetylated by CobB, while K99 was insensitive. Thus, Mdh activity can be regulated by acetylation, but the effect of the other eight regulated lysine residues remains to be determined. Finally, Nakayasu *et*

al. determined the effect of acetylation on enolase (55). Enolase generates phosphoenolpyruvate during the penultimate step of glycolysis and utilizes two substrate-binding lysine residues (K342 and K393) to perform this activity. We have detected 24 lysines acetylated on enolase, making it one of the most heavily acetylated proteins in *E. coli*. Of these lysines, six are sensitive to both AcP and glucose, while nine are sensitive to glucose alone. One of the lysine residues sensitive to glucose was K342, one of the substrate-binding residues. Nakayasu *et al*. generated two enolase variants with either K342 or K393 changed to glutamine to mimic an acetylated lysine and found that these variants lost catalytic activity. While we did not detect K393 as acetylated, Nakayasu *et al.* assessed proteomes of 48 species of bacteria and found the lysine equivalent to K393 in enolase orthologs could be acetylated in at least eight of them. Comparing the structures of the *E. coli* enolase to these other enolases could provide interesting insight into what makes the *E. coli* enolase refractory to AcP-dependent acetylation on K393, while enolase enzymes from other bacteria are sensitive to AcP.

Multiple studies have shown that acetylation of multiple transcriptional regulators and the transcriptional machinery itself is AcP-dependent, and that acetylation has diverse effects on the function of these proteins. In *Rhodobacter sphaeroides*, FnrL is a transcriptional activator in response to a switch from aerobic to anaerobic growth; it is homologous to *E. coli* Fnr. In *Rhodobacter*, acetylation of three lysine residues (K175, K213, and K223) reduced the association of FnrL with DNA (250). Interestingly, the homolog from *E. coli* only encodes K229, the equivalent lysine to K223, while K213 is a glutamine, and K175 is missing entirely. As we utilize K→Q variants to mimic acetyllysines, it appears that *E. coli* may have evolved to permanently lose the positive charge at K213 in the same way. Study of these two orthologs may

reveal how these bacteria have evolved to utilize acetylation of certain lysine residues for regulation, while other lysines are entirely dispensable. The *E. coli* transcription factor RcsB is response regulator that that positively regulates transcription of capsule biosynthesis genes for biofilm formation, while reducing transcription of flagellar genes. Hu *et al.* found that RcsB can be acetylated by AcP on a lysine (K154) that is found in the helix-turn-helix DNA binding motif (223, 459). Acetylation of K154 is both glucose- and AcP-dependent. Similarly to Fnr, this acetylation reduces DNA binding, which enhances migration of the bacteria and sensitizes the bacteria to acid (82). However, regulation of RcsB is rather complex. In addition to K154, RcsB can be acetylated on K180 *in vitro* with YfiQ, though we have yet to detect this modification *in vivo* using mass spectrometry (173). Furthermore, RcsB only activates transcription when it is phosphorylated. RcsB can be phosphorylated on D56 by either AcP or through its cognate sensor kinase RcsC (223, 460). Thus, the interplay between acetylation and phosphorylation on RcsB suggests *E. coli* regulates RcsB activity through an intricate balance that takes into account AcP levels, RcsC activity, and deacetylation by CobB. Besides directly influencing DNA binding, acetylation can modulate transcriptional activation through other mechanisms. CRP activates transcription of genes that mediate utilization of carbon sources by interacting with RNA polymerase at Class I or Class II sites on DNA. Using variant proteins encoding the acetylation mimic glutamine, Davis *et al.* inferred that acetylation of CRP on K100 had two effects (218). First, acetylation of K100 directly reduced Class II promoter activation by preventing interactions between CRP and RNA polymerase, while having no effect or mixed effects at Class I promoters. Acetylation of K100 also enhanced CRP stability, which may explain some of the mixed results from Class I-dependent promoters. Thus, acetylation of CRP at K100 may be a

way for the cell to specifically activate Class I sites and prevent activation of Class II sites. Finally, transcriptional activation can be prevented by modifying RNA polymerase rather than the transcription factors themselves. The α-subunit of the RNA polymerase core enzyme was found to be acetylated in an AcP-dependent manner in the C-terminal domain (CTD), which is confirmed from our mass spectrometry data (221). K291 on the α-CTD mediates interactions with the transcription factor CpxR, and acetylation of this lysine prevented transcription from the CpxR-dependent promoter *cpxP*. In contrast, Lima *et al.* inferred that acetylation of a different lysine, K298, depended on YfiQ and activated transcription from the *cpxP* promoter (201). This is one of the few examples identified thus far where acetylation of two lysines on the same protein have opposing effects on protein activity. Since RpoA is part of the core RNA polymerase complex, the effect of these acetylations on global transcription may be substantial but has yet to be explored.

Another critical cellular process that AcP-dependent acetylation may regulate is maintenance and replication of the genome. Two groups have probed how acetylation impacts topoisomerase I and replication initiator protein DnaA activities. Topoisomerase I relaxes negatively supercoiled DNA that would otherwise destabilize the genome. We detected topoisomerase I as acetylated on eight lysines, of which three were both glucose-sensitive and AcP-sensitive. Zhou *et al.* found that *in vitro* acetylation of topoisomerase I with AcP yielded four lysines (K13, K45, K346, and K488) (224, 225). While we never detected acetylation of K13, K45, or K488, we did detect K346 and K484. Since K484 and K488 can be found on the same peptide, these may actually be the same acetylated residue that were called out differently because different algorithms were utilized: Skyline by our group and MaxQuant by Zhou *et al.*

Acetylation of topoisomerase I inhibited relaxation activity due to reduced DNA binding and reduced cleavage activity; however, the exact acetylated residue(s) that mediated this effect were not identified. Two of these acetylated lysines, K346 and K484/8, were glucose- and AcP-dependent. Thus, future studies could determine whether K346 and/or K484/8 contribute to the reduction in topoisomerase activity. DnaA is the initiator of DNA replication that binds to *oriC* and opens the origin to generate replication forks. We have only detected DnaA acetylated on one residue, K455. However, two reports found 13 lysine residues were acetylated on DnaA, of which two had effects on DnaA activity (226, 227). K178 could be acetylated by YfiQ and AcP *in vitro* and deacetylated by CobB. This acetylation prevents interaction of DnaA with *oriC*. Similarly, K243 is acetylated by YfiQ and AcP, which can be reversed by CobB. DnaA acetylated on K243 cannot bind ATP. In both instances, acetylation would reduce the ability of DnaA to initiate replication, but through different mechanisms. Whether these acetylations work in concert or independently remains to be determined.

AcP-dependent acetylation has the potential to exert wide-spread regulatory effects due to the vast amount of targets that are acetylated. Indeed, AcP-dependent acetylation appears to modify multiple enzymes in essential pathways like translation, transcription, and DNA replication on lysines that one would expect to affect protein function. In most cases, assays have been performed *in vitro* to test these hypotheses, yet the *in vivo* significance has not been determined for many of these acetylated lysines. Indeed, the *in vivo* stoichiometry of these lysines is unknown in most cases. Therefore, while acetylation may occur *in vivo*, it may not occur at a stoichiometry that exerts a physiological effect. Future studies should be aware of this and confirm the findings *in vivo* through phenotypic analysis when possible. By focusing on

those lysines that appear to be regulated by AcP or glucose, one may identify conditions under which acetylation by AcP is relevant.

Overall Summary: Chapter Four

In Chapter Four, I discovered that *E. coli* encodes four KATs (PhnO, RimI, YiaC, and YjaB) in addition to YfiQ (**Fig. 28**). These proteins are conserved across phylogeny, and in one example, I successfully confirmed that a RimI homolog from *Neisseria gonorrhoeae* also has KAT activity like the *E. coli* RimI (**Fig. 35**). Unfortunately, I was unable to demonstrate KAT activity for any of these novel KATs *in vitro*. Instead, protein variants, in which predicted catalytic residues were replaced by alanine, were found to lose function *in vivo*, supporting their roles as KATs (**Fig. 29**).

We identified proteins that were acetylated by each of the KATs, and from this information, I was able to generate hypotheses for the roles of these proteins. I attempted to determine the physiological relevance of each of these novel *E. coli* KATs and YfiQ in multiple assays. Of these KATs, I found that overexpression of YiaC and YfiQ was able to reduce *E. coli* migration in soft agar plates, and this inhibition of migration depended on their KAT activities. However, deletion mutants had little effect on this phenotype. Thus, the KATs remain a source of new research. When are they expressed? What are the physiological consequences of acetylation by these KATs? Do the orthologs in other bacteria have the same functions as those in *E. coli* and, if they do, is the function mediated through acetylation of the same targets? For example, the activity of YfiQ on Acs is highly conserved from bacteria to humans (266). Perhaps acetylations by these other KATs have also maintained their functions across phylogeny. Some of these questions are being followed up by Sarah Feid.

The Gutted Strain: A Tool and a Lesson

To identify KATs in *E. coli*, I generated the gutted strain that lacked both known mechanisms of acetylation (Δ*pta yfiQ*) and the deacetylase CobB (Δ*cobB*) (**Fig. 26**). The gutted strain was successfully built to increase the signal-to-noise ratio of the putative KATs over the background acetylation. To ensure there was enough substrate for the KATs (i.e., AcCoA), I wanted to grow the cells in glucose. However, if I grew WT cells overexpressing these KATs in glucose, I knew that there would be a strong background of AcP-dependent acetylation, hence I deleted *pta*. While YfiQ should not be expressed in the presence of glucose since it is transcribed in a CRP-dependent manner (135), I wanted to minimize any possible contribution of YfiQ-dependent acetylation to that of the KATs, especially when performing mass spectrometry to determine the targets of each KAT. Thus, I chose to delete YfiQ. Finally, CobB was deleted to ensure that any acetylation that occurred would not be reversed.

While I was able to successfully identify that four of the 26 putative GNATs in *E. coli* exhibited increased acetylation of certain proteins by using this gutted strain, I only determined this under one condition, TB7/glucose. However, we do not know under what conditions these KATs are expressed. Since we used overexpression constructs, I did not have to worry about ensuring that the enzymes were expressed under our conditions. However, the targets that we determined in TB7/glucose may not necessarily be bona fide targets under physiological conditions. For example, if I had grown the cells in a non-catabolite repressing condition like TB7, the expression pattern of *E. coli* would shift because of CRP-dependent transcriptional activation (169). Thus, the proteins acetylated due to overexpression of these KATs may also have shifted. Therefore, in addition to the caveats inherent in using overexpression constructs,

one should temper conclusions made when using the gutted strain to identify acetylated targets unless a condition that is known to natively express the KAT is used. Indeed, it would be useful to determine what proteins are acetylated by these KATs under different conditions.

I hope that the gutted strain can be used as an example for future researchers looking to identify mechanisms of acetylation in other bacteria. By knowing the possible sources of acetylation in a bacterium, both enzymatic and non-enzymatic, a bacterium can be genetically modified to eliminate those mechanisms. Then, by searching the genome for GNAT family members, these genes can be cloned and overexpressed as I have done. Perhaps a whole library of ORFs from the bacterium of interest could be screened initially in a dot blot assay, permitting that the background acetylation is low enough, and signal from the gene product is sufficiently high. This would also bypass one of the major caveats of using the *E. coli* gutted strain to assess heterologously expressed acetyltransferases, which is that, in many cases, *E. coli* may not encode the native targets of KATs from other bacteria. Indeed, while I was able to find that RimI from *Neisseria* acetylated a protein in *E. coli*, the PhnO and YfiQ homologs did not acetylate any proteins. Similarly, a KAT from *Borrelia burgdorferi* that I overexpressed in the gutted strain showed no effect. Therefore, if possible, the native host should be used.

Novel KATs of *E. coli*

Using the gutted strain, I identified one or more acetylated bands when PhnO, RimI, YiaC, and YjaB were overexpressed (**Fig. 28**). Each of these enzymes is a member of the GNAT family of enzymes, a broadly conserved enzyme family that extends from bacteria to eukaryotes. These enzymes are characterized by their ability to bind AcCoA and transfer acetyl groups onto molecules. In this case, PhnO, RimI, YiaC, and YjaB appear to acetylate proteins, indicating that

these GNATs are KATs. Further confirming this hypothesis are the data in **Fig. 29**, where the acetylated bands were absent upon mutation of conserved catalytic glutamine or tyrosine amino acids that have been shown to be required for activity in other KATs.

To better understand the physiological role of these KATs, I submitted pellets of cells overexpressing these novel KATs for mass spectrometry to identify proteins that these KATs may acetylate. This analysis showed that each KAT acetylated multiple proteins, including RimI and YjaB, which only showed one acetylated band via western blot. Proteins separated via SDS-PAGE migrate by size, and thus proteins that are approximately the same size migrate together. Alternatively, this discrepancy could be due to detection limitations of western blots compared to mass spectrometry. Specifically, our threshold for a lysine to be considered regulated by a KAT was a >4-fold increase in the KAT overexpression strain over the vector control strain. This 4-fold increase could mean that a given lysine goes from 20% to 80% acetylation across the population of that lysine, or it could mean acetylation increases from 0.1% to 0.4% on that lysine, which likely would not be detected by western blot. Thus, future work should seek to determine the stoichiometry of acetylation upon overexpression of these KATs to better understand their physiological targets. Below, I will describe what is known about each KAT and what I currently hypothesize acetylation by these KATs may do.

RimI

RimI was initially described as one of three N-terminal acetyltransferases (NATs) of *E. coli* in addition to RimJ and RimL. RimI acetylates the N-terminal alanine of the 30S subunit protein S18 (32, 391). We detected 11 proteins that were acetylated in a RimI-dependent manner. Interestingly, none of these proteins were an exact match for the band that was found around 40

kD. The closest match was the protein RarA (49.6 kD), which RimI acetylated ~6-fold above the vector control. RarA is a recombination factor that is suspected to be associated with DNA replication. Specifically, RarA is proposed to facilitate repair of stalled replication forks (461). The site of acetylation, K378, does not have a clear role in protein function. A similarly sized band as one detected in RimI is also observed in YiaC and YjaB but not PhnO, and RarA is detected as acetylated in both YiaC and YjaB but not PhnO. Whether this is actually RarA or another protein remains to be determined. The highest acetylation fold change upon RimI overexpression was RimI itself (~60-fold). Since the fold changes are normalized to protein levels, this suggests that RimI may autoacetylate or acetylate other RimI proteins.

RimI is part of a polycistronic operon downstream of DNA polymerase III subunit ψ and upstream of YjjG, a pyrimidine 5'-nucleotidase. DNA polymerase III subunit ψ forms a dimer with subunit χ to stabilize the DNA polymerase III preinitiation complex (395, 396). YjjG is a monophosphatase towards UMP, dUMP, and dTMP (462), and its nucleosidase activity also protects cells against mutagenic noncanonical pyrimidine nucleotides (463). If RimI truly regulates RarA, a DNA repair enzyme, it makes some sense that RimI is encoded near other DNA replication and protection enzymes. Perhaps RimI inactivates RarA when it is not needed during regular replication or RimI might enhance RarA activity during replication repair. No transcriptional regulation has been described for this operon yet. However, microarray data suggest that RimI expression can be activated by the cationic biocide polyhexamethylene biguanide (PHMB) (464), which has been shown to condense bacterial chromosomes (465).

RimI, RimJ, and RimL N-terminally acetylate alanine of S18, alanine of S5, and serine of L12, respectively. While RimI shows KAT activity, it is interesting that RimJ does not. RimL

was not assessed for KAT activity in this study because it was not found in the ASKA collection, so whether this protein does or does not have KAT activity is still an open line to test. All three proteins share a very low sequence identity, with RimL and RimJ having the highest identity at 23%. All three proteins share some overlap in residues near the catalytic tyrosine Y115 of RimI (Y109 of RimJ, Y98 of RimL). Thus, it would be useful to identify the structural determinants that render RimI a KAT and NAT but RimJ only a NAT. Any insights learned from this analysis may inform what interfaces these KATs/NATs use to specifically acetylate their targets. Structures have been solved for RimI from *Salmonella typhimurium* (386) and *E. coli* (**5isv**), RimJ from *Vibrio fischeri* (**3IGR**), and RimL from *Salmonella typhimurium* (466). While the sequences of these orthologs are not identical to those of *E. coli*, the structures may assist in dissecting what differentiates these enzymes.

RimI was found to be the most conserved of the KATs, identified in over 4,400 bacterial genomes (55). Presumably this conservation is linked to its ability to acetylate the highly conserved ribosomal subunit. However, whether NAT and/or KAT activity of RimI has been conserved across phylogeny should be considered. If the RimI orthologs do acetylate lysines, it would be interesting to determine whether these lysines are the same as those acetylated in *E. coli*.

PhnO

PhnO was initially described as an aminoalkylphosphonate acetyltransferase (392, 393). PhnO exists in an operon dedicated to utilization of phosphonate during phosphate starvation. PhnO is not absolutely required for phosphonate utilization, but it does acetylate (*S*)-1-aminoethylphosphonate and aminomethylphosphonate for their utilization (393, 394).

Transcription of *phnO* can be driven from two promoters, of which one is controlled by PhoB, which responds to phosphate limitation. In addition, microarray studies have found PhnO upregulated in biofilms (467, 468) and heat shock, but downregulated in cold shock (469).

By mass spectrometry, we identified 10 proteins acetylated when PhnO is overexpressed. Nine bands can be observed in the PhnO overexpression strain. Like RimI, PhnO itself was highly acetylated upon overexpression (~700-fold). GlyQ was the next most highly acetylated protein, achieving ~22-fold acetylation. A band close to 75 kD may correspond to ribonuclease II (78 kD), an exoribonuclease required for processing tRNAs (470) and mRNAs (471). Another band at about 55 kD may be another RNase, ribonuclease G (51 kD), that matures the 16S rRNA (472, 473) and participates in RNA turnover (474, 475). A weakly acetylated band can be seen just below 50 kD that may be YgiF (48.4 kD), an inorganic triphosphatase (476), of which little is known. Just below 37 kD, a band that might be GlyQ (35 kD) can be observed. GlyQ is subunit α of the glycine–tRNA ligase (477). A strong band between 20 and 25 kD may match to YrbL (24.3 kD), an uncharacterized protein that is part of the PhoP regulon (478). There remain two acetylated bands that do not have a corresponding protein, one at ~70 kD and one at 32 kD, which may suggest that PhnO overexpression increases the absolute amount of these proteins, and not the acetylation itself. Therefore, after normalization, the mass spectrometry analysis shows an insignificant fold-change. The above targets paint a picture where PhnO may regulate ribonuclease activity, perhaps in response to phosphate starvation conditions, when the cell needs to conserve phosphate for energy. Alternatively, it may simply free building blocks for synthesis of new mRNA to translate proteins necessary for responding to starvation stress. Perhaps YgiF

has a role in abstracting phosphate from certain molecules, and acetylation may enhance or reduce this activity.

PhnO was mostly conserved in the γ-proteobacteria (22 genomes). Thus, it would be interesting to perform a focused study to determine whether the same proteins are acetylated by PhnO homologs of these other γ-proteobacteria or whether the PhnO homologs can acetylate the same proteins when expressed in *E. coli*. If acetylation of GlyQ or another target regulates its activity, it would be interesting to determine how other organisms outside of γ-proteobacteria may regulate the orthologs of these targets.

YjaB

The mRNA encoding YjaB is monocistronic and expressed from a divergent promoter that drives transcription of homoserine O-succinyltransferase, which catalyzes the first step of *de novo* methionine biosynthesis (479). While there are no known activators of YjaB, microarray data suggests YjaB is downregulated upon exposure to PHMB (464) but upregulated in heat stress (469) and in stationary phase dependent on the stationary phase sigma factor, σ^S (480-482).

YjaB overexpression resulted in 128 proteins acetylated at a level above vector control. Like RimI and PhnO, it appears to be highly acetylated when overexpressed. By western blot, there appear to be four acetylated bands sensitive to YjaB with the most robust and reproducible signal coming from around 40 kD and around 17 kD. The proteins within the 40 kD band may correspond to one of the following: YcbX (40 kD), FtsZ (40 kD), or YfiF (38 kD). YfiF is annotated as a putative methyltransferase; but, as of yet, no work on YfiF has been reported. If it is a methyltransferase and regulated by YjaB, it would be interesting to determine how this cascade of modification would affect physiology. YcbX has detoxification activity toward toxic

N-hydroxylated base analogs (483). FtsZ assembles to form the Z-ring structure at the future cell division site. It is essential and highly conserved in bacteria, archaea, some chloroplasts, and some mitochondria (484). FtsZ is acetylated by YjaB on K380, a residue that is present in the C-terminal variable (CTV) region of the protein. This CTV and K380, specifically, are important for interaction with ZapD, a protein that facilitates FtsZ polymerization. Additionally, we detected that acetylation of FtsA, FtsE, and FtsK was regulated by YjaB. Each of these participate in formation of the septal ring and cell division (485). Thus, YjaB-dependent acetylation may be important for regulating cell division.

The band corresponding to 17 kD may be comprised of one or more of the following proteins that approximately fit that molecular weight: YjgM (18.6 kD), SmpB (18.3 kD), Bcp (18 kD), RpsE (17.6 kD), GreA (17.6 kD), IscU (17 kD), or YjaB itself (16.5 kD). However, the anti-His western blot suggests that YjaB runs below 15 kD (**Fig. 29B**). YjgM was one of the putative GNATs studied here, but nothing is known about its function. SmpB with tmRNA (*ssrA*) work together in the process called trans-translation that releases stalled ribosomes and tags partially synthesized proteins for degradation (486). Being a small (160 AA) protein, acetylation of a single residue by YjaB may critically affect SmpB activity. Bcp is a thiol peroxidase that can assist in detoxifying hydrogen peroxide (487), though the effect of acetylation by YjaB is not apparent. RpsE is one of about twenty ribosomal proteins that YjaB acetylates, but the only one that fits the molecular weight observed by western blot. Interestingly, this is protein S5 of the 30S ribosomal subunit, the same protein N-terminally acetylated by RimJ (32). Future studies could determine whether these acetylations undergo any cross-talk to regulate translation or assembly of the ribosome. GreA is a transcription elongation factor that

helps to release a stalled polymerase complex (488). The acetylated lysine, K43, is found on an exposed hairpin between two helices, and is sensitive to CobB (205). However, what acetylation of K43 does to the protein function is unclear. Finally, IscU is a scaffold protein for iron-sulfur cluster assembly (489). Since IscU must serve as a docking site for multiple proteins of this assembly system, acetylation might disrupt or enhance these interactions. Though not apparent on western blot, three more groups of proteins acetylated by YjaB may be physiologically interesting: cysteine biosynthesis enzymes, translation initiation enzymes, and trehalose metabolism enzymes.

CysB, a transcriptional regulator of sulfur utilization genes and cysteine biosynthetic genes (490), is acetylated by YjaB on K54, which is near the helix-turn-helix DNA binding motif. Three members of the CysB regulon are also acetylated by YjaB: CysC, CysI, and CysK. CysC and CysI are required for two of the steps that assimilate sulfate for subsequent utilization in cysteine biosynthesis. Interestingly, CysI is a protein that contains an iron sulfur cluster, which may suggest YjaB acetylates IscU concomitantly with cysteine biosynthetic enzymes. CysK generates cysteine by condensing *O*-acetyl-L-serine with the output of the sulfate assimilation pathway, hydrogen sulfide. Thus, acetylation by YjaB may be a means for the cell to regulate cysteine biosynthesis.

E. coli encodes three translation initiation factors: IF-1, IF-2, and IF-3. Each of them is acetylated in a YjaB-dependent manner. IF-1 is the smallest initiation factor and its function is not fully established, but with IF-2, it is proposed to ensure correct binding of fMet-tRNA^{fMet} in the ribosomal P-site (491). The sites acetylated on IF-1 and IF-2 do not present any obvious interpretation of their function. IF-3 appears to stimulate dissociation of the deacylated tRNA

from a post-termination ribosome and may assist in recycling stalled ribosomes (492, 493). Excitingly, the YjaB-acetylated lysine of IF-3, K110, is important for interaction with the 30S subunit, and mutation of this residue reduces affinity (494). Thus, YjaB may be important for regulating translation.

Finally, YjaB acetylated three enzymes required for metabolism of trehalose. Trehalose is a glucose disaccharide that can serve as carbon storage, osmoprotectant, cryoprotectant, and a chemical chaperone of protein folding (495, 496). TreR is a repressor of trehalose import (TreB) and catabolism (TreC) genes. TreR is acetylated in the helix-turn-helix motif, which may prevent repression of its regulon. TreC allowed *E. coli* to utilize trehalose as the sole carbon source and breaks trehalose into glucose and glucose-6-phosphate (497). However, the acetylated lysine K144, does not appear to be in a provocative location. Finally, trehalose-6-phosphate synthase (*otsA*) catalyzes the first step in trehalose biosynthesis, which essentially catalyzes the reverse reaction of TreC by condensing glucose-6-phosphate and UDP-glucose to trehalose-6-phosphate (498). Extensive characterization of OtsA has found many residues required for substrate binding, but none of them correspond to the acetylated lysine, K244 (499). Since YjaB acetylates proteins with opposing functions, perhaps these acetylations can direct the flux of carbon to or from trehalose.

YiaC

YiaC is encoded in a polycistronic mRNA downstream of and overlapping with Tag, which encodes DNA glycosylase I, one of two DNA glycosylases that protect *E. coli* against potentially mutagenic lesions. This mRNA is not known to be activated by any factors, and as such, this is thought to be a constitutive operon, which would imply *yiaC* is constitutively made.

However, microarray data indicate that YiaC transcription is reduced when σ^{32}, the heat shock sigma factor, is overexpressed (500). YiaC transcription is also reduced by PHMB treatment (464). However, YiaC transcription is upregulated in stationary phase (480, 482) and when cells are challenged by oxidative stress (469).

While YiaC overexpression produces eight acetylated bands reproducibly, mass spectrometry revealed 251 proteins acetylated in a YiaC-dependent manner. The most intense bands were found at about 70, 40, 35, 25, and 20 kD. Of the proteins detected by mass spectrometry, six to eleven proteins could comprise each of these bands. Not only does YiaC produce the most acetylated proteins of any of the novel KATs, but it also exhibited some of the highest fold changes of any of the KATs. Indeed, 26 proteins exhibited ≥100-fold increases in acetylation. Ten of these proteins are ribosomal proteins, and the most highly acetylated protein was the 50S ribosomal subunit protein L15. In addition to the ribosomal subunits, YiaC acetylates the three translation initiation factors that are acetylated by YjaB. It also acetylates the ribosome assembly factor, BipA. This may suggest that YiaC could be a regulator of translation, and perhaps may have an overlapping role with YjaB. Alternatively, this could suggest that there are comparable determinants that dictate whether a protein is acetylated YiaC and YjaB.

Due to the great amount of proteins acetylated by YiaC, the role of YiaC could be truly extensive or simply obscured. Like YjaB, cysteine biosynthesis genes are highly acetylated by YiaC. YiaC may prevent glycine tRNA charging as both subunits of glycine-tRNA ligase are acetylated. YiaC may also regulate nucleotide biosynthesis. Pyrimidine biosynthetic gene PyrH and purine biosynthetic genes PurC and PurH are all acetylated, but the effect of acetylation of

these lysines is not clear. Finally, consistent with each other KAT, YiaC itself was acetylated, which implies that it can either auto-acetylate or acetylate another YiaC protein.

Phenotypic Analysis of KATs

If a bacterium encodes a protein, it suggests that that protein has biological importance; otherwise the gene would be lost to optimize fitness (501). Thus, these KATs and presumably their acetyltransferase activities are important for *E. coli* under some condition. So, when are these KATs important? Hypotheses can be formed by determining when the KATs are expressed, the genomic neighborhood of the KATs, and the proteins acetylated by KATs. I searched the *E. coli* gene expression database for conditions when the KATs were upregulated or downregulated. Based on these data, I hypothesized that low temperature (24°C) or high temperature (42°C) may affect the growth of KAT mutant strains or KAT overexpression strains. At each temperature, every strain behaved like the WT reference strain (**Fig. 37**). Future studies attempting to perform a similar experiment should begin by determining whether the KATs are expressed under these conditions. Perhaps these KATs were not expressed in this medium and, thus, KAT mutants would not have any effect. Similarly, perhaps in this medium, the target of these KATs that is relevant is not expressed. More extreme temperatures may also be used to investigate the requirement for these KATs. These KATs may also have some redundant functions, and therefore a single deletion may not show a phenotype.

In the *E. coli* genome, *yiaC* is encoded downstream and overlaps four nucleotides of *tag*. Since *tag* encodes one of the two DNA glycosylase repair enzymes involved in base excision repair, I hypothesized that YiaC may regulate DNA repair. Of the YiaC targets, three are related to DNA repair, RarA, RuvC, and Ssb. However, these enzymes act in a separate pathway than

the Tag or the other DNA glycosylase, AlkA. I tested the survival of *E. coli* mutants deleted for *yiaC* in WT, Δ*tag*, Δ*alkA*, and Δ*alkA tag* backgrounds against the chemical mutagen MNNG (**Fig. 36**). However, deletion of *yiaC* did not cause any difference compared to the parent strains. This suggests that YiaC does not play a role in DNA repair that Tag protects against. Perhaps YiaC can regulate enzymes required for other types of DNA damage, and thus Δ*yiaC* mutants should be tested in mutagens that promote other DNA lesions like single strand breaks, double strand breaks, or thymine dimers.

AcCoA-Dependent Acetylation

I showed that residual acetylation in the gutted strain could partially be explained by the presence of GNATs that exhibit KAT activity. In the gutted strain that lacks YfiQ and AcP, there remains a low level of acetylation on many proteins (**Fig. 26**). While some of these proteins may be KAT-dependent, there are some that do not respond to KAT overexpression (**Fig. 28**). This suggests that there are either proteins with KAT activity yet to be discovered, or AcCoA could non-enzymatically acetylate proteins like AcP.

Wagner *et al.* used *in vitro* acetylation assays that mimicked the mitochondrial microenvironment to make the claim that non-enzymatic AcCoA-dependent acetylation could occur within the mitochondrion (288). Since AcCoA is a highly reactive molecule like AcP, it is highly probable that this chemical reaction can happen (291). The difficulty arises in trying to demonstrate that this mechanism of acetylation occurs *in vivo*. For AcP, there are no known enzymes that have been shown to catalyze AcP-dependent acetylation. Furthermore, by deleting the Pta-AckA pathway that synthesizes AcP, AcP-dependent acetylation was undetectable. The same cannot be said for AcCoA. KATs utilize AcCoA to catalyze acetylation. Therefore, to

determine whether non-enzymatic AcCoA-dependent acetylation occurs, one would first need to remove all KATs of the organism such that the only means of acetylating is directly by AcCoA. Furthermore, there is no way to completely eliminate AcCoA. AcCoA is an essential node of central metabolism in almost all organisms and, thus, mutations to prevent synthesis of AcCoA would be inviable. One possible organism that could be used is *Borrelia burgdorferi*, which only synthesizes AcCoA to make mevalonate, a precursor to cell wall lipid biosynthesis (502). By supplementing mevalonate, this bacterium can survive without AcCoA, Indeed, only two proteins were detected as acetylated by mass spectrometry analysis of a *B. burgdorferi* mutant that cannot synthesize AcCoA or AcP. Unfortunately, this study did not determine acetylated proteins of a strain that could synthesize AcCoA alone to determine its contribution compared to that of AcP.

In my work, I found that I could acetylate CysK *in vitro* with AcCoA in the absence of an acetyltransferase (**Fig. 33**). Since I was trying to demonstrate that YiaC had KAT activity *in vitro*, I manipulated the conditions in an attempt to promote enzymatic acetylation and disfavor non-enzymatic acetylation. I first realized that boiling my samples to stop the reaction simply enhanced non-enzymatic acetylation of CysK, but non-enzymatic acetylation occurred even without boiling (**Fig. 34A**). Boiling may enhance acetylation by promoting dissociation of AcCoA and increasing reactivity of AcCoA with protein substrates. Lysines must be deprotonated before becoming acetylated. In the context of a KAT, this can occur via a glutamate residue. In a non-enzymatic acetylation reaction, either a glutamate residue near the lysine can deprotonate the lysine, or the proton can be abstracted by a basic molecule from the medium if the pH is sufficiently high. Thus, I lowered the buffer pH from 8.0 to 7.0. Again, this

disfavored non-enzymatic acetylation, but was insufficient to demonstrate any KAT activity for YiaC. Therefore, I conclude that at least one *E. coli* protein can be readily non-enzymatically acetylated *in vitro*, and the conditions to promote this acetylation are high temperature and high pH.

While AcCoA cannot be eliminated from *E. coli*, the concentration of AcCoA within the cell can be modulated. AcCoA concentrations are limited by production of CoA. Pantothenate kinase is the first enzyme in the biosynthesis pathway for CoA, and it is highly regulated (503). Pantothenate kinase is sensitive to feedback regulation by CoA, and therefore limits the amount of CoA made (504, 505). By overexpressing pantothenate kinase and supplementing the culture with extra pantothenate, *E. coli* increases the amount of free CoA about 3-fold and AcCoA almost 10-fold (506, 507). Similarly, acetyl groups can be drained from AcCoA by overexpressing machinery required for making the bioplastic monomer polyhydroxybutyrate (PHB) (508). Three enzymes compose the PHB synthesis pathway, and the first enzyme performs a condensation reaction of two AcCoA molecules to generate acetoacetyl-CoA.

I did not test whether PHB synthesis affected acetylation, but I did test whether overexpressing pantothenate kinase could increase AcP- and YfiQ-independent acetylation in the gutted strain. Indeed, adding 100 μM and 1 mM pantothenic acid showed a dose-dependent increase in acetylation, while no change was observed between 1 mM and 5 mM. These data suggest that AcCoA can increase global acetylation. However, this experiment was performed prior to identification of the KATs. Thus, the gutted strain still contained the KATs, which could explain any increases in acetylation. A future study could delete all of the KATs from the gutted

strain and repeat this experiment to determine whether non-enzymatic AcCoA-dependent acetylation occurs.

Future Directions

These results open many paths for future work. The most efficient path would be to study the novel KATs. Since *E. coli* has maintained these enzymes over evolutionary time to acetylate proteins, it is reasonable to hypothesize that the catalyzed acetylations are important for *E. coli*. While we have identified four novel KATs, we still do not know when they are physiologically relevant. Monitoring the expression of the KATs via a transcriptional reporter or by monitoring production of His-tagged variants of the KATs at the native sites in the chromosome would allow one to rapidly test under what conditions these KATs are made. Another way to determine the relevance of the KATs is to perform a Tn-seq experiment in strains deleted for each of the novel KATs. By identifying genes that produce a synthetic lethal phenotype, one could cross-reference these genes with the acetylated target list to identify true substrates of the KATs. Because we know what residues are required for the acetyltransferase activity of each KAT, if one would combine the inactive variant KAT with the gene that produces the synthetic phenotype, one could ensure that acetylation by the KAT is responsible.

Alternatively, we have identified hundreds of targets acetylated by these KATs. It would be relatively simple to make variant proteins encoding genetic mimics of a handful of these protein targets. Plenty of enzymes, like CysK, are acetylated in provocative locations that would be detrimental for the enzymatic activity. Transcription factors, like ArcA, are similarly tempting targets because of how acetylation could clearly block the DNA binding activity. Similarly, other groups have shown that HU of *M. tuberculosis* can alter the nucleoid compaction in the

bacterium. As we detect HU of *E. coli* as acetylated, the KATs may influence *E. coli* nucleoid compaction and transcription.

AcP-dependent acetylation is directly tied to metabolism. It is distinctly possible that the inevitability of acetylation on certain lysines has little to no effect on certain proteins, which makes determination of which acetylations are physiologically relevant difficult. With the recent discovery that enolase activity can be regulated by AcP-dependent acetylation, one should consider testing the other central metabolic enzymes to determine whether AcP-dependent acetylation could be a feedback mechanism to sense glycolytic flux. Finally, we detected much of the translational machinery including most of the ribosomal subunits acetylated in an AcP-dependent manner. Since ribosomes are a complex of proteins and must associate with various protein factors as well as RNA, each acetylation has the potential to disrupt salt bridges and/or sterically hinder proper interactions. To determine whether acetylation affects translation rate, one could perform an *in vitro* translation assay using highly acetylated ribosomes (from a Δ*ackA* mutant) or weakly acetylated ribosomes (from a Δ*pta* mutant) added to the PURExpress® ΔRibosome Kit. Similarly, translational assays could be performed using individual elongation or initiation factors that are highly acetylated or weakly acetylated to determine whether acetylated isoforms inhibit translation rate.

Concluding Remarks

Metabolism is an essential process that permits generation of both biomass and energy in every living organism. While these metabolic processes have been honed over evolution to suit the needs of a particular organism, there are inevitable “extra-metabolic” reactions that may occur. One of these “extra-metabolic” reactions appears to be non-enzymatic AcP-dependent

acetylation of lysines. Indeed, the work presented here suggests that AcP-dependent acetylation is simply a consequence of acetate fermentation, and acetylation will accumulate during periods of stagnant growth when the proteome is relatively unchanging, such as stationary phase, for as long as a fermentable carbon source is available. This inevitability suggests that other bacteria that produce AcP via fermentation would experience global acetylation like *E. coli*. Indeed, other works have shown that *B. subtilis* and *N. gonorrhoeae* exhibit AcP-dependent acetylation on a scale comparable to *E. coli*. Specificity of this non-enzymatic acetylation is dictated by the three-dimensional protein structures, which causes some lysines to be more sensitive to AcP than others. While I hypothesized that this global, non-enzymatic, AcP-dependent acetylation might protect against oxidative damage or serve as a carbon source during starvation, I was unable to generate data to support these ideas. Thus, whether *E. coli* has evolved to cope with or utilize non-enzymatic acetylation is an open question.

Due to the prevalence and essentiality of AcCoA in almost all organisms, sensing these levels and ensuring that carbon flux to and from the AcCoA node is critical. Thus, the evolution of enzymes that tie their activity to AcCoA is not a surprise. I found that *E. coli* encodes four KATs in addition to the known KAT, YfiQ. Each of these KATs acetylates a distinct set of targets that differ not only from each other but from AcP as well. While the biological importance of acetylation by these KATs is not clear, deciphering when these KATs are expressed and which proteins are bona fide targets will help to determine how *E. coli* has evolved to utilize acetylation.

Due to conservation of both enzymatic and non-enzymatic acetylation, some of what is learned in *E. coli* may be applied to other organisms. Therefore, using *E. coli*, we can get closer to establishing a more complete picture of the inner workings of the cell.

APPENDIX A

ACETYLATED Acs CAN BE IDENTIFIED VIA WESTERN BLOT

Introduction

The best-known and most extensively studied acetylated protein in bacteria is AcCoA synthetase (Acs), an enzyme conserved from bacteria to humans (266). Acs activates acetate to generate AcCoA via a two-step process (290). First, Acs uses ATP to adenylate acetate, which yields an enzyme-bound acetyl-AMP intermediate and releases pyrophosphate. Second, Acs uses its CoA-ligase activity to generate AcCoA and release AMP. While the enzyme is reversible, the reaction is essentially irreversible *in vivo* due to pyrophosphatases that break down pyrophosphate generated in the first reaction (343). Acs has high affinity for acetate and thus it is primarily used to scavenge low concentration of this carbon source (172, 265, 290). As such, Δ*acs* mutants or cells with reduced Acs activity grow poorly or not at all in media with low levels of acetate (< 10 mM) as the sole carbon source.

In *E. coli*, Acs can be regulated at two levels, transcriptionally and post-translationally. Fis, a small nucleoid associated protein and transcriptional regulator, inhibits transcription of *acs* during exponential growth. In contrast, CRP activates transcription of the *acs* gene; thus, Acs will not be synthesized in the presence of a catabolite repressing sugar like glucose (343). Regulation by CRP is complex, as *acs* is positively regulated in an AR1-dependent manner, but negatively regulated in an AR2-dependent manner. Binding to the AR1-dependent site is higher affinity than binding to the AR2-dependent site; thus, *acs* is activated at lower CRP concentrations, but repressed at higher ones.

Acetylation of a single lysine on Acs inactivates the protein. Strikingly, this method of regulation is conserved across phylogeny (134, 139, 142, 144, 146-148, 164, 199, 241, 260, 262, 266), and extends to other Acs-like enzymes (134, 159, 164, 509). In each case, acetylation of this lysine blocks the first half-reaction of Acs by preventing the formation of acetyl-AMP (199).

In *E. coli*, the acetylated lysine is K609. Acetylation of this lysine is catalyzed by YfiQ, and deacetylation is catalyzed by CobB. In *B. subtilis*, Acs was found to be propionylated at this site, which also resulted in inactivation (388). However, this has not yet been tested in *E. coli*.

In my studies, I consistently detected an acetylated band by anti-acetyllysine western blot that mimicked properties of Acs (**Fig. 5, TB7 lane**). This band was around 72 kD, the molecular weight of Acs. The band was present throughout growth in TB7, but it was absent in the presence of glucose or excess carbon source. However, once glucose or the other carbon source was depleted, the band appeared (**Fig. 5, 24 hour lane**). The band depended on CRP, specifically AR1. Interestingly, even in the presence of glucose, I was able to detect this band in a Δ*ptsG* mutant. Since a Δ*ptsG* mutant does not catabolite repress lactose consumption even in the presence of glucose, this suggests that CRP is active in a Δ*ptsG* mutant (510). Thus, I wanted to confirm whether this band was truly Acs, which could then be used as a diagnostic marker for the presence or absence of glucose in the medium.

Results

I decided to genetically determine whether the 72 kD band I observed corresponded to Acs. Specifically, I used a Δ*ptsG* mutant background, which produces this band, and made one of two additional mutations. I either deleted *yfiQ* or *acs*. If the acetylated band is Acs, then deletion of *yfiQ* would prevent acetylation and thus detection of the band. Similarly, deleting the *acs* gene will prevent the expression of the protein, such that it can neither be acetylated nor detected. Thus, I grew the Δ*ptsG yfiQ* mutant, Δ*ptsG acs* mutant, and parent strain in TB7/glucose for 10 hours and performed an anti-acetyllysine western blot. There was no difference in protein loading or pattern as determined by Coomassie-stained SDS-PAGE gel analysis. As expected, while the Δ*ptsG* single mutant produced the acetylated band, neither the

Δ*ptsG yfiQ* nor Δ*ptsG acs* mutant produced that band (**Fig. 39**). Taken together with my previous results, I conclude that this 72 kD band is Acs.

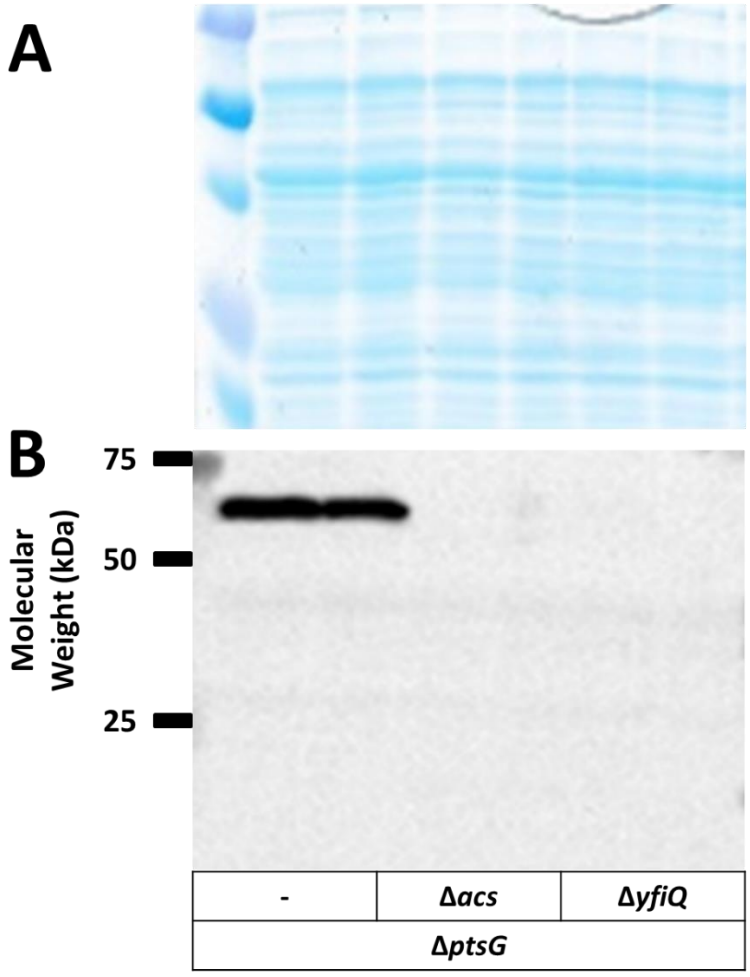

Figure 39. A 72 kD Acetylated Band Corresponds to Acs. Duplicate cultures of mutant strains of *E. coli* (strain BW25113) with the indicated deletions were aerated at 37°C in TB7 supplemented with 0.4% (w/v) glucose. After 10 hours, cells were harvested. The whole cell protein lysate was normalized to protein concentration, separated by 1D-SDS PAGE and stained with Coomassie blue stain (A) and assessed for protein acetylation by anti-acetyllysine (α-acK) Western immunoblot analysis (B).

Discussion

While the data I generated and data from other papers (57) heavily suggested that the 72 kD band could be Acs, the experiment described above fully supports that conclusion. This band

is catabolite-repressed, YfiQ-dependent, CRP-dependent, and Acs-dependent. In my experiments, I used this Acs band as a diagnostic marker to tell me when cells had completely consumed the glucose from their medium. Identifying that this band is Acs told me that the Δ*ptsG* mutant did not appear to be experiencing catabolite repression. Also, I was able to confirm that the CRP variants were behaving as expected using this band (**Fig. 17A**). Furthermore, this band was used as a marker to show that a YfiQ-overexpression was working correctly (**Fig. 27**). When possible, future studies can now confidently utilize Acs as a diagnostic marker without the explicit need for additional experiments.

APPENDIX B

MAGNESIUM LIMITATION IN PEPTIDE-BASED MEDIA

Introduction

Bacteria are routinely grown in complex media containing a rich assortment of nutrients. For example, lysogeny broth (LB) contains tryptone and yeast exact. Together, these components provide a rich mixture of nutrients that supports growth of numerous bacteria. However, the complexity of such media obscures factors governing cell behavior, especially those that limit cell growth.

While studying glucose-induced protein acetylation, I found that *E. coli* continues to consume the glucose in TB7/glucose even after the cultures reach stationary phase. In fact, most of the glucose was consumed after the cultures ceased exponential growth. This behavior was contrary to my initial expectations, which were based upon the behavior of *E. coli* cultures in minimal medium containing glucose as the sole carbon source (361). Under these conditions, the cultures enter stationary phase when glucose is depleted. I sought to explain this confounding phenomenon. In doing so, I found that TB7 as well as many other peptide-based media are balanced between carbon and magnesium as the growth limiting nutrients. However, supplementation with carbon on top of these complex media, such as TB7/glucose or LB, renders the bacteria limited for magnesium. These data and thoughts are mostly published in (341).

A Component of Buffered Tryptone Broth Limits Growth.

While growing *E. coli* in TB7/glucose, I noticed that the cells continued to consume glucose even after the culture reached stationary phase (**Fig. 4A**). In fact, the majority of glucose was consumed during stationary phase. Because glucose is consumed during exponential growth in minimal media (e.g., M9) with glucose as the sole carbon source (361), I wondered whether tryptone might somehow inhibit glucose consumption by *E. coli*.

To test whether tryptone inhibited glucose consumption, I grew *E. coli* in M9/glucose and varying concentrations of tryptone. Instead of inhibiting glucose consumption as initially hypothesized, tryptone increased glucose consumption in a dose-dependent manner (**Fig. 40**). Tryptone also increased the growth rate and growth yield (i.e., final cell density). This suggests that tryptone does not inhibit glucose uptake per se but rather that some compound present in M9 minimal medium, but not in TB7, enables better cell growth.

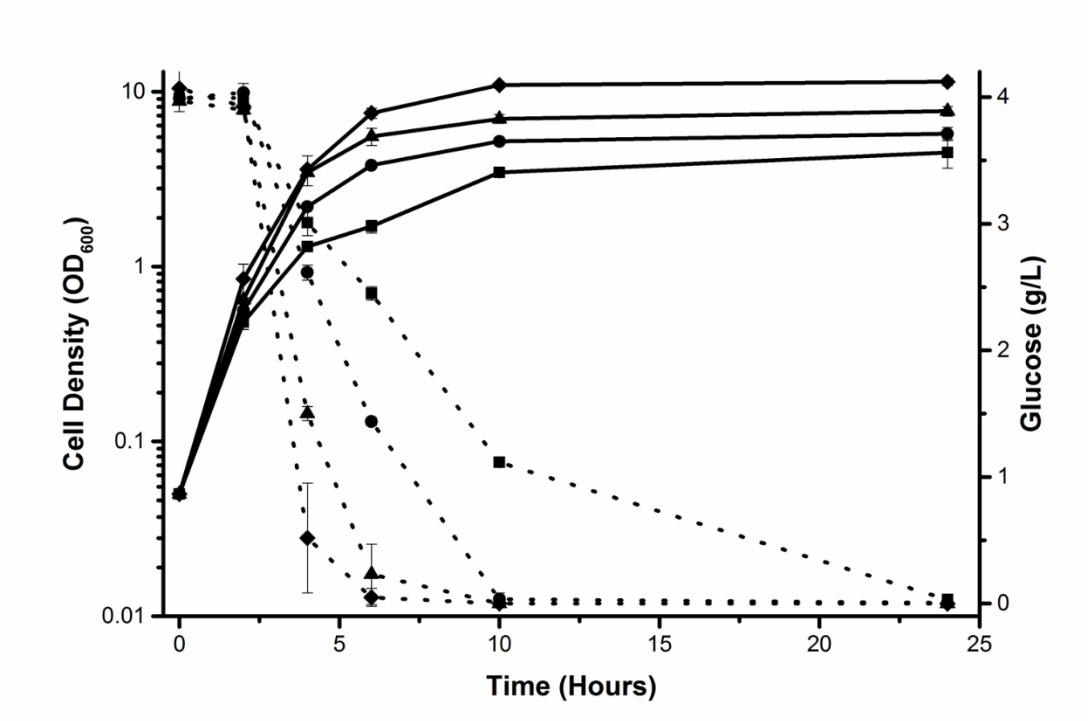

Figure 40. Addition of Tryptone to M9 Increases Growth Rate and Glucose Consumption. Wild-type *E. coli* cells (strain BW25113) were aerated in M9 minimal medium supplemented with 4 g/liter glucose and increasing concentrations of tryptone: 0.1% (squares), 0.2% (circles), 0.5% (triangles), and 1% (diamonds). Growth was measured at OD600 (solid lines) and the filtered culture medium assessed for glucose (dotted lines).

Magnesium Increases Cell Growth in Buffered Tryptone Broth

M9 minimal medium contains five compounds not present in TB7 medium: ferric citrate, calcium chloride, magnesium sulfate, thiamine, and ammonia. To determine whether the addition

of these compounds would increase cell growth in TB7/glucose, I first grew the cells in TB7/glucose supplemented with four of the five compounds. I expected that if a single compound were responsible for the growth yield increase, then removing it would cause the cells to grow as if they were in TB7/glucose alone. Indeed, I found that when magnesium sulfate was not added to TB7/glucose, the cells grew as if they were in TB7/glucose alone (**Fig. 41**). Based on these results, I conclude that magnesium is the limiting compound.

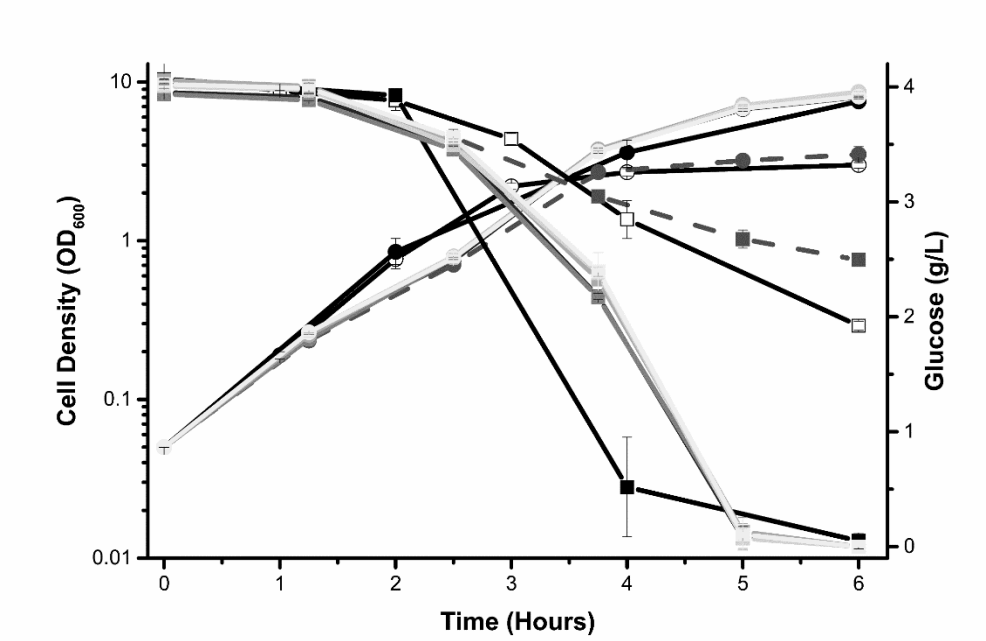

Figure 41. Magnesium Is Necessary for Robust Growth in Buffered Tryptone Broth. Cell density (circles) and glucose concentration in the medium (squares) were measured hourly for wild-type *E. coli* cells (strain BW25113) aerated in TB7 supplemented with 4 g/liter glucose alone (open symbols), with addition of 5 M9 compounds (ferric citrate, calcium chloride, magnesium sulfate, thiamine, and ammonium chloride), or with 4 out of 5 M9 supplements (shades of gray). This was compared to cells of the same strain aerated in M9 supplemented with 4 g/liter glucose and 1% tryptone (black symbols). Only medium supplemented without magnesium sulfate (dashed lines) behaved like TB7-glucose.

While these results demonstrate that magnesium is necessary for robust growth in TB7/glucose, they do not establish that it alone is sufficient. Therefore, I tested cell growth in TB7/glucose supplemented with 1 mM magnesium sulfate. As shown in **Fig. 42A**, the addition

of magnesium sulfate to TB7/glucose increased the growth yield. I further found that increased growth yield was, in fact, due to magnesium and not to sulfate, as supplementation with magnesium chloride increased the growth yield, whereas potassium sulfate had no effect (**Fig. 42A**). The magnesium effect was dose-dependent, where magnesium sulfate increased the growth yield in a dose-dependent manner up to a concentration of 1 mM (**Fig. 42B**). I also found that supplementation with magnesium or glucose alone could exert a minor enhancement on the growth yield in TB7, but the growth yield was greatly increased in the presence of both (**Fig. 43**). Buffering was not required to achieve an increased growth yield in the presence of both glucose and magnesium; however, magnesium exerted a greater effect when the medium was buffered with either phosphate or MOPS buffer (**Fig. 43**).

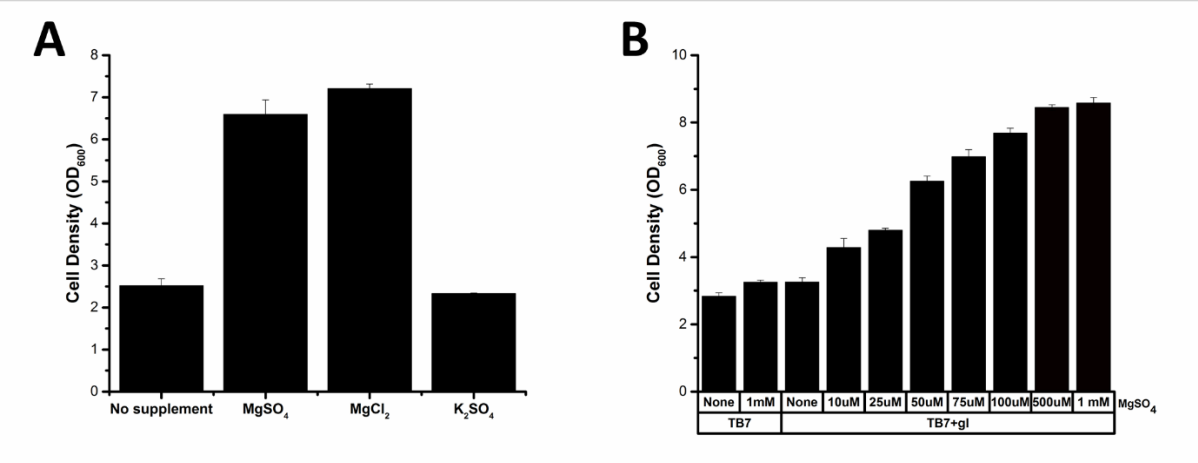

Figure 42. Magnesium Is Sufficient for Increased Cell Growth Only When Glucose Is Present. (A) Wild type *E. coli* cells (strain BW25113) were aerated for 10 hours in TB7 supplemented with 4 g/L glucose alone or with the addition of 1 mM MgSO4, 1 mM MgCl2, or 1mM K2SO4. The final optical density is shown. (B) Cells were grown in TB7 supplemented with 4 g/L glucose and/or the indicated concentrations of MgSO4 for 10 hours. The final optical density is shown.

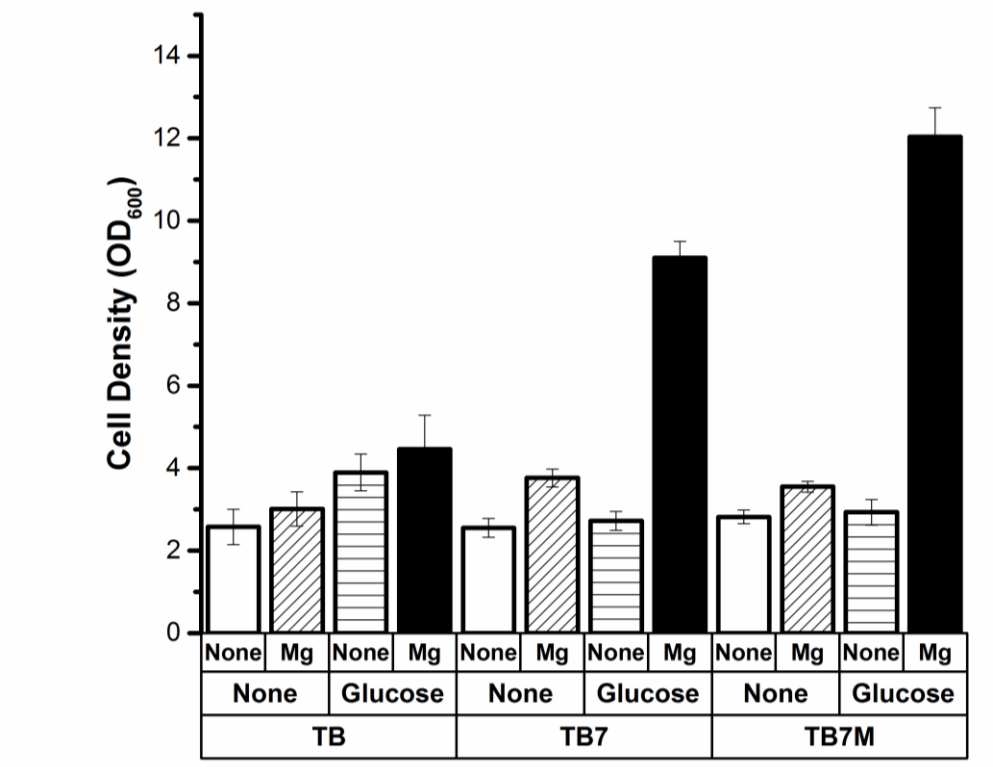

Figure 43. Buffering Enhances Magnesium-Dependent Growth Increase. Wild type *E. coli* cells (strain BW25113) were aerated in unbuffered tryptone broth (TB), phosphate buffered TB (TB7), or MOPS buffered TB (TB7M) (open bars). Cultures were supplemented with 4 g/L glucose (diagonal stripes), 1mM MgSO4 (horizontal stripes), or both (black bars). The final optical density is shown.

To determine whether the effect was unique to magnesium, our collaborator James Orr (University of Illinois Urbana-Champaign) also tested other divalent cations. No increases in cell growth were observed when TB7/glucose was supplemented with calcium chloride, cobalt chloride, cobalt sulfate, nickel chloride, or manganese sulfate (**Fig. 44A**). James and I tested whether magnesium increased growth yield in TB7 containing seven other carbon sources (lactate, succinate, fructose, lactose, arabinose, pyruvate, and acetate). In all cases, magnesium increased the growth yield in a manner similar to glucose (**Fig. 44B**). Thus, this magnesium effect is not specific to glucose.

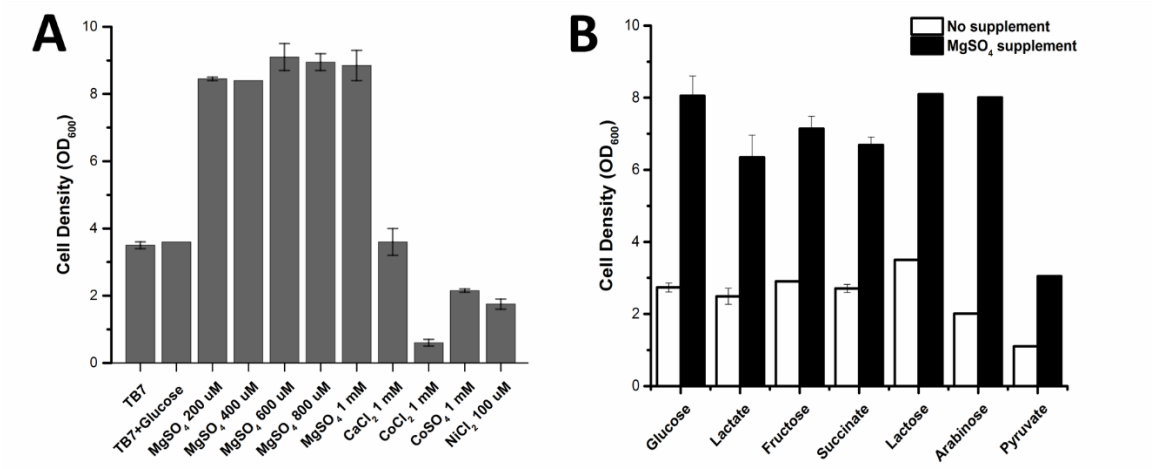

Figure 44. Magnesium Is the Only Divalent Cation That Supports Increased Growth in TB7 Supplemented with Various Carbon Sources. (A) Wild type *E. coli* cells (strain BW25113) were aerated in the indicated media for 10 hours. In addition to magnesium supplementation, other metal compounds including calcium chloride, cobalt chloride, cobalt sulfate, and nickel chloride were added at the indicated concentrations. The final optical density is shown. (B) Wild type *E. coli* cells (strain BW25113) were aerated in buffered TB7/glucose or a concentration of the indicated carbon source to provide equimolar carbon. These cultures were either supplemented with 1 mM MgSO4 (black bars) or left untreated (white bars).

Magnesium Increases the Growth Yield in Other Peptide-Based Media

To determine whether magnesium increases the growth yield in other peptide-based media, we tested growth in phosphate-buffered peptone (P7) and casamino acids (CA7), both supplemented with 4 g/L glucose. The cells grew best in TB7/glucose medium, slightly worse in CA7/glucose medium, and very poorly in P7/glucose medium (**Fig. 45A**). The final cell densities achieved in these media were directly related to the magnesium content per dry weight of these peptide-based media: tryptone, 195 μg/g; casamino acids, 48 μg/g; and peptone, 17 μg/g (511). In all three cases, the addition of 1 mM magnesium sulfate increased growth yield. These results indicate that the lack of magnesium limits the growth yield in these complex, buffered peptide-based media when carbon is in excess.

I also tested whether the addition of magnesium to the commonly used medium, lysogeny broth (LB), could increase the cell yield. The use of unbuffered LB supplemented with both 4 g/L glucose and 1 mM magnesium resulted in a minor growth yield increase that was comparable to adding 1 mM magnesium alone (**Fig. 45B**). However, buffering LB with either phosphate or MOPS resulted in a greater growth yield when both glucose and magnesium were added, and again, magnesium alone resulted in a partial growth yield increase (**Fig. 45A and B**).

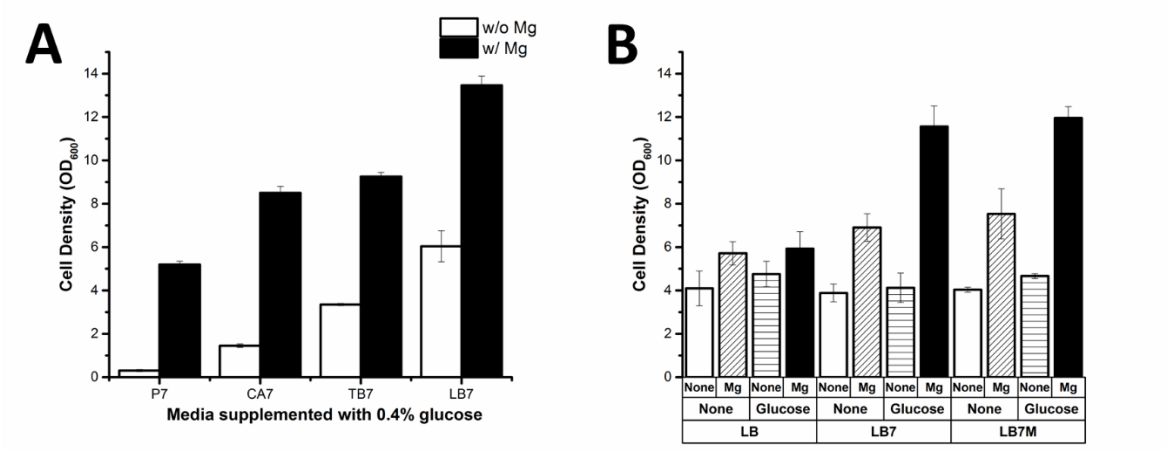

Figure 45. *E. coli* Grown in Other Carbon Sources or Peptide-Based Media also Benefit from Magnesium Supplementation. (A) Wild type *E. coli* cells (strain BW25113) were inoculated into the indicated media supplemented with 4 g/L glucose and buffered to pH 7 with (black bars) or without (white bars) 1 mM MgSO4 (Mg). The base media tested here are peptone (P7), casamino acids (CA7), tryptone (TB7), and lysogeny broth (LB7). (B) Cells were grown in unbuffered LB, phosphate buffered LB (TB7), or MOPS buffered LB (LB7M) (open bars). Cultures were supplemented with 4 g/L glucose (diagonal stripes), 1mM MgSO4 (horizontal stripes), or both (black bars). The final optical density is shown.

Buffering Permits Increased Growth Yield by Preventing Growth Inhibition by Metabolism Byproducts, Acetate and Ammonium

I observed that buffering my media increased the growth yield upon magnesium supplementation to TB/glucose, LB/glucose or LB alone (**Fig. 43 and Fig. 45B**). Acetate produced from glucose consumption is known to acidify media and inhibit growth of *E. coli*.

Thus, I predicted that the differences between buffered and unbuffered media supplemented with magnesium resulted from inhibitory pH levels. The pH of unbuffered LB/glucose and TB/glucose supplemented with magnesium dropped to about 5 compared to about 7 for the buffered media. However, buffering also exerted a positive effect on growth in LB when supplemented with magnesium alone. Ammonium produced from amino acid consumption results in alkalization of the medium. Indeed, unbuffered LB supplemented with magnesium reached pH 8.7, while the buffered medium reached pH 7.5. These results indicate that magnesium is limiting in LB, but the effect is more pronounced when the LB is buffered and contains glucose.

Magnesium Increases Cell Growth in Multiple Strains of *E. coli* and Species of Bacteria

The experimental results described above were obtained using *E. coli* BW25113. To ensure the magnesium effect was not limited to this particular strain, I tested the growth of the *E. coli* strains MC4100, MG1655, and AJW678 in TB7/glucose and found that magnesium increased the growth yield for all three strains (**Fig. 46A**). I also tested whether magnesium increased the growth yield of *B. subtilis* (strain PY79) and *V. fischeri* (strain ES114) grown in TB7/glucose and TB7/glucose supplemented with 2% sodium chloride, respectively. *V. fischeri* is a marine bacterium that must be grown in higher salt conditions that mimic its natural seawater environment. For these bacterial species, magnesium increased growth yield, albeit to a lesser extent than *E. coli* (**Fig. 46B**). Even in the absence of glucose, *V. fischeri* achieved higher biomass with magnesium. The results indicate that magnesium supplementation increases the growth of diverse bacteria in complex peptide-based media.

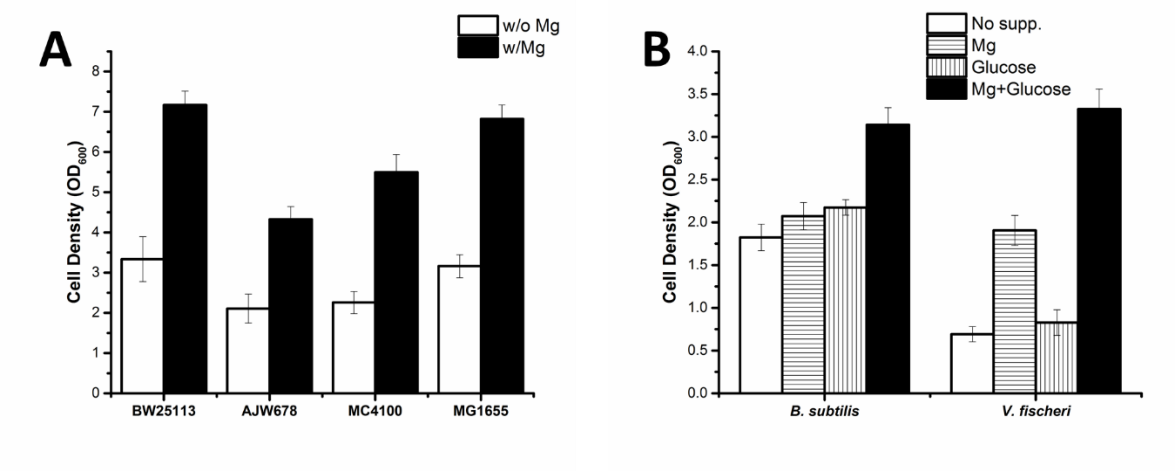

Figure 46. Magnesium Increases Cell Growth in Multiple Strains of *E. coli* and Species of Bacteria. (A) Three strains of *E. coli* (MG1655, MC4100, and AJW678) were aerated in TB7/glucose alone (open bars) or supplemented with 1 mM MgSO4 (closed bars). (B) *Bacillus subtilis* PY79 and *Vibrio fischeri* ES114 were aerated for 24 hours in TB7 or TBS7, respectively. The media were left untreated (white bars) or supplemented with 1 mM MgSO4 (horizontal stripes), 4 g/L glucose (vertical stripes), or both (black bars).

Magnesium Directs Glucose to Biomass Formation

I noted that the addition of magnesium to peptide-based media supplemented with glucose did not alter the growth rate, but rather extended the duration of exponential growth. Based on this observation, I hypothesized that magnesium depletion causes cell division to cease, thus preventing the remaining carbon from being used for cell biomass. Whereas a TB7/glucose culture supplemented with magnesium increased in optical density while consuming glucose, a TB7/glucose culture (without added magnesium) did not increase cell growth even though it consumed glucose during stationary phase (**Fig. 47**). The cell density of the magnesium-supplemented culture continued to increase, even after glucose was fully consumed. This appears to be due to consumption of excreted acetate (**Fig. 18**)**.** James further established that the magnesium-dependent increase in optical density resulted from both increased cell number and increased biomass (**Fig. 48**).

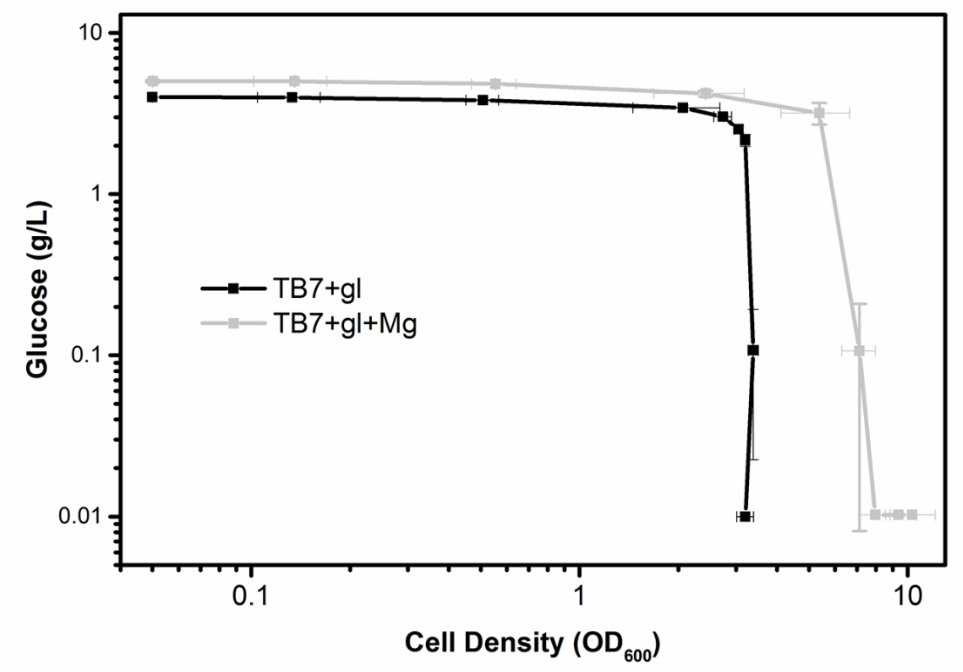

Figure 47. Magnesium Diverts Carbon from Glucose into Biomass. Wild-type *E. coli* cells (strain BW25113) were aerated in TB7-glucose (black line) or TB7-glucose supplemented with MgSO4 (gray line) for 9 h. Optical density and glucose concentration measurements were taken hourly and plotted on a log-log scale.

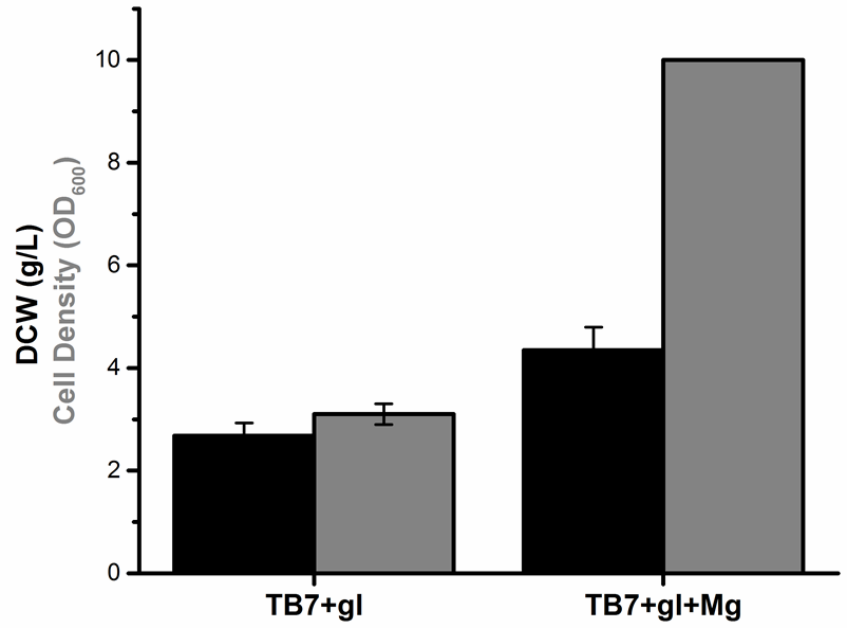

Figure 48. Magnesium Diverts Carbon into Biomass. Dry cell weight (black bars) and optical densities (gray bars) from the 24h time point are shown from the indicated condition.

Magnesium-Dependent Cell Growth Is Lost in a Δ*glnA* Mutant

I next tested whether the loss of any genes would eliminate the magnesium effect. If magnesium-dependent cell growth simply depended on magnesium as a nutrient, then only a mutation that reduced maximum cell density would lose the effect. I tested various mutants of carbon regulation, amino acid biosynthesis, central metabolism and TCA cycle, magnesium transporters/sensors, and phosphate transporters/regulators. Of the mutants tested, only a Δ*glnA* mutant lost the magnesium-dependent growth yield increase (**Table 6**). The *glnA* gene encodes glutamine synthetase, and thus the Δ*glnA* mutant is a glutamine auxotroph (512). I hypothesized that these cells could not respond to magnesium because glutamine now was limiting. Indeed, supplementation with glutamine restored the magnesium-dependent biomass increase to Δ*glnA* mutants (**Fig. 49**). I further investigated the reason why the Δ*glnA* mutant does not respond to magnesium by testing mutants in glutamine-dependent pathways downstream of *glnA*. I found that three nucleotide biosynthesis mutants, Δ*guaA,* Δ*purF,* and Δ*carA,* also did not respond to magnesium (**Table 7**). I suspect that the Δ*glnA* mutant lacks sufficient glutamine for both amino acid and nucleotide biosynthesis and is thus limited for glutamine rather than magnesium in TB7/glucose.

Table 6. Mutants Tested for Loss of Mg^{2+}-Dependent Biomass Increase [a]

Carbon regulators	Amino acid biosynthesis	Central metabolism/ TCA cycle	Magnesium transport related	GlnA regulators/ related	Phosphate related
fnr	*aspA*	*gltA*	*corA*	*glnB*	*phoB*
crp	*aspC*	*ackA*	*mgtA*	*gltB*	*phnA*
cra	*glnA*	*pta-ackA*	*phoP*	*glnG*	*phnC*
arcA	*gdhA*	*pgi*		*glnL*	
		sucA		*glnD*	
				glnE	
				glnK	

[a] Mutants were grown in buffered tryptone broth supplemented with 0.4% glucose alone or with 1 mM $MgSO_4$ for 10 h. Biomass increase was determined by OD600 measurements. Cells were considered limited for magnesium if they had increased biomass with $MgSO_4$ supplementation relative to no supplementation. The Δ*glnA* mutant, highlighted in bold, did not respond. Growth defects and magnitudes of the effects are not reflected here.

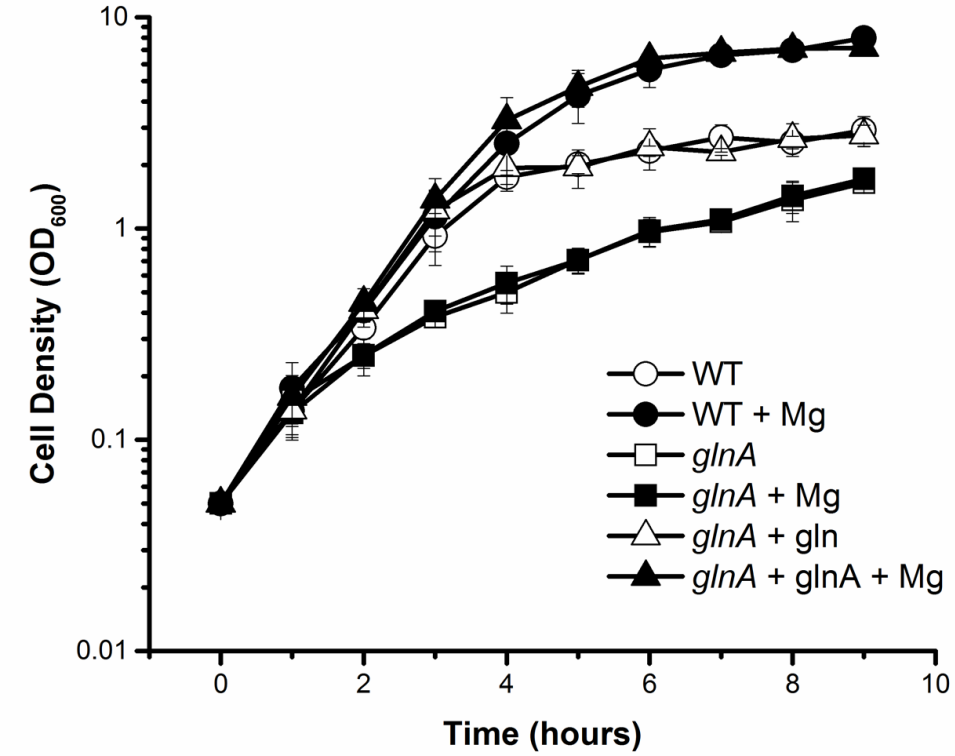

Figure 49. A Δ*glnA* Mutant Does Not Respond to Magnesium Unless Supplemented with Glutamine. Wild-type (WT) *E. coli* cells (strain BW25113) (circles) or an isogenic *glnA* mutant (triangles or squares [see below]) were aerated in TB7-glucose alone (open symbols) or with 1 mM MgSO4 (closed symbols). The *glnA* mutant cells were supplemented with 1.4 g/liter glutamine (triangles) or left untreated (squares).

Table 7. Mutants Related to *glnA* That Lose the Magnesium Effect [a]

Responded to magnesium [b]	No Response [c]
ybaS	*guaA*
yneH	*purF*
asnB	*purl*
hisH	*carB*
trpE	*carA*
crr	*ptsH*
ptsG	*ptsI*

[a] Mutants were grown in buffered tryptone broth supplemented with 0.4% glucose alone or with 1 mM $MgSO_4$ for 24 h. Biomass was determined by OD600 measurements.
[b] By 9 h of growth, mutants that had increased biomass with magnesium supplementation were considered responders.
[c] Mutants in bold did not respond even after 24 h; other mutants responded between 9 and 24 h.

Discussion

During growth on buffered, peptide-based media (e.g., TB7) supplemented with a sugar (e.g., glucose), cultures of *E. coli* entered stationary phase prior to complete consumption of the sugar. The majority of the sugar was consumed after the culture stopped growing. This behavior provides a simple explanation for why protein acetylation occurs primarily during stationary phase, because that is when AcP, the major acetyl donor in *E. coli* (56, 57), is produced as an intermediate of the acetate fermentation pathway (513). When I supplemented TB7/glucose with magnesium, exponential growth was extended, resulting in consumption of glucose prior to entry into stationary phase, increased biomass, and decreased protein acetylation. I observed the same general behavior in other peptide-based media containing glucose and in two other bacterial species, *Vibrio fischeri* and *Bacillus subtilis*. Collectively, these results further our understanding of bacterial growth in complex media and enable us to control global acetylation levels in *E. coli*.

In Gram-negative bacteria such as *E. coli*, magnesium is involved in stabilization of membrane phospholipids, lipopolysaccharide, polyphosphate compounds like DNA and RNA,

and the ribosome (410-412). Magnesium is also required to make ATP biologically active and participates in catalysis of certain enzymatic reactions through either direct or indirect mechanisms (514, 515). Almost half of total magnesium is found associated with NTPs (primarily ATP) (410), approximately one third is associated with the cell wall (412), and the remaining bound to various molecules or free in the cytoplasm. Almost a quarter of this cytoplasmic magnesium is thought to stabilize ribosomes (413). As such, magnesium deprivation can result in cessation of translation due to dissociation of ribosomes (413). In the magnesium-starved conditions found in complex peptide-based media, it would not be surprising for ribosome control to be a mechanism by which cells cease growth and division.

Hiroshi Nikaido proposed that the amount of magnesium in LB medium is not sufficient to achieve the maximum possible cell growth (516). LB contains between 30-200 μM magnesium. In contrast, the magnesium concentration is 528 μM in MOPS medium, a defined minimal medium that avoids the excess of any one ionic species (517). Our data suggests that magnesium is limiting in LB. A minor increase in growth yield was achieved in unbuffered LB supplemented with magnesium, while buffered LB produced a much more pronounced effect. The results were similar for TB, where the addition of magnesium produced a minor effect that was enhanced upon buffering. Likely, yeast extract provides LB with extra carbon, which allows for increased growth upon magnesium supplementation. However, when both carbon and magnesium were added together to buffered or unbuffered TB or LB, we observed a substantial increase in the cell yield, which then becomes limited due to some other factor(s).

LB medium has been reported to be limited for carbon by Sezonov and coworkers (518). In that study, glucose supplementation of cell-free, spent LB medium was shown to support further cell growth upon re-inoculation with *E. coli*. I observed that magnesium supplementation to LB

or LB7 was able to permit additional growth, while glucose addition did not. The differences between this study and that of Sezonov and coworkers may be due to possible variation in different preparations of LB. LB can vary between different tryptone and yeast extract preparations from different companies. Thus, our LB medium may have contained a higher amount of carbon, creating a more balanced carbon/magnesium ratio, whereas their LB medium may have been relatively more magnesium-rich.

In an attempt to find genes that may mediate the magnesium-dependent growth yield increase, I sought mutants that did not respond to added magnesium. I identified that a Δ*glnA* mutant did not respond to magnesium and determined the mutant did not respond because it is a glutamine auxotroph (512). Glutamine is the scarcest amino acid in tryptone at 0.1% (511); supplementation of TB7 with glutamine permitted the Δ*glnA* mutant to respond to magnesium. Glutamine is a required precursor for both protein biosynthesis and nucleotide biosynthesis. Presumably, TB7/glucose does not contain sufficient glutamine in the Δ*glnA* mutant for both needs, and thus its growth was limited by glutamine rather than by magnesium. Supporting this contention, I found that genes required for nucleotide biosynthesis downstream of glutamine also could not respond to magnesium. Would this have been true for other amino acid auxotrophs? Presumably not, because the other amino acids are present in much higher concentrations than glutamine in tryptone.

The magnesium-dependent biomass increase was not exclusive to *E. coli* but also found to occur in *Bacillus subtilis*, a Gram-positive bacterium, and *Vibrio fischeri*, another Gram-negative bacterium. Both achieved higher optical density when magnesium was supplemented to TB7/glucose. I predict that magnesium limits growth for multiple bacteria in peptide-based media. Interestingly, *V. fischeri* achieved increased optical density from magnesium

supplementation even without the additional glucose. This suggests the possibility that *V. fischeri* may be able to more efficiently utilize amino acids for growth compared to *E. coli* or *B. subtilis,* or that *V. fischeri* simply requires more magnesium for growth. O'Shea and coworkers reported that *V. fischeri* grown in TBS (1% tryptone with 342 mM NaCl) did not benefit from addition of $MgSO_4$, but did benefit from KCl (519). As I utilized TBS7, which is the same medium but buffered with potassium phosphate, our results suggest that *V. fischeri* may experience potassium limitation, then magnesium limitation, and finally carbon limitation in TBS. This need for high magnesium may reflect the naturally high magnesium concentration (~50 mM) of seawater in which *V. fischeri* lives (519).

I conclude with the following two observations. First, there is hidden potential in peptide-based media. The addition of excess carbon and magnesium can increase the final cell density anywhere from 2-fold to 17-fold. The addition of magnesium alone could also increase the final cell densities. Buffering the culture is important to ensure the medium does not become overly acidic or alkaline due to the consumption of glucose and amino acids, respectively. Second, we can now tune the level of acetylation in cultures without using genetic manipulation. Those who use *E. coli* for recombinant protein production may benefit most from this work. Each acetylated isoform of a recombinant protein has the potential to have different biological implications. To reduce the number of acetylated isoforms, excess carbon should be avoided (520), and the growth medium should be buffered and supplemented with magnesium.

REFERENCE LIST

1. Peregrín-Alvarez JM, Sanford C, Parkinson J. 2009. The conservation and evolutionary modularity of metabolism. Genome Biol 10:R63.

2. Dickinson BC, Chang CJ. 2011. Chemistry and biology of reactive oxygen species in signaling or stress responses. Nat Chem Biol 7:504-11.

3. Golubev A, Hanson AD, Gladyshev VN. 2017. Non-enzymatic molecular damage as a prototypic driver of aging. J Biol Chem 292:6029-6038.

4. Hood MI, Skaar EP. 2012. Nutritional immunity: transition metals at the pathogen-host interface. Nat Rev Microbiol 10:525-37.

5. Chen Y, Sprung R, Tang Y, Ball H, Sangras B, Kim SC, Falck JR, Peng J, Gu W, Zhao Y. 2007. Lysine propionylation and butyrylation are novel post-translational modifications in histones. Mol Cell Proteomics 6:812-9.

6. Tan M, Luo H, Lee S, Jin F, Yang JS, Montellier E, Buchou T, Cheng Z, Rousseaux S, Rajagopal N, Lu Z, Ye Z, Zhu Q, Wysocka J, Ye Y, Khochbin S, Ren B, Zhao Y. 2011. Identification of 67 histone marks and histone lysine crotonylation as a new type of histone modification. Cell 146:1016-28.

7. Sabari BR, Tang Z, Huang H, Yong-Gonzalez V, Molina H, Kong HE, Dai L, Shimada M, Cross JR, Zhao Y, Roeder RG, Allis CD. 2015. Intracellular crotonyl-CoA stimulates transcription through p300-catalyzed histone crotonylation. Mol Cell 58:203-15.

8. Zhang Z, Tan M, Xie Z, Dai L, Chen Y, Zhao Y. 2011. Identification of lysine succinylation as a new post-translational modification. Nat Chem Biol 7:58-63.

9. Peng C, Lu Z, Xie Z, Cheng Z, Chen Y, Tan M, Luo H, Zhang Y, He W, Yang K, Zwaans BM, Tishkoff D, Ho L, Lombard D, He TC, Dai J, Verdin E, Ye Y, Zhao Y. 2011. The first identification of lysine malonylation substrates and its regulatory enzyme. Mol Cell Proteomics 10:M111.012658.

10. Du J, Zhou Y, Su X, Yu JJ, Khan S, Jiang H, Kim J, Woo J, Kim JH, Choi BH, He B, Chen W, Zhang S, Cerione RA, Auwerx J, Hao Q, Lin H. 2011. Sirt5 is a NAD-dependent protein lysine demalonylase and desuccinylase. Science 334:806-9.

11. Tan M, Peng C, Anderson KA, Chhoy P, Xie Z, Dai L, Park J, Chen Y, Huang H, Zhang Y, Ro J, Wagner GR, Green MF, Madsen AS, Schmiesing J, Peterson BS, Xu G, Ilkayeva OR, Muehlbauer MJ, Braulke T, Mühlhausen C, Backos DS, Olsen CA, McGuire PJ, Pletcher SD, Lombard DB, Hirschey MD, Zhao Y. 2014. Lysine glutarylation is a protein posttranslational modification regulated by SIRT5. Cell Metab 19:605-17.

12. Dai L, Peng C, Montellier E, Lu Z, Chen Y, Ishii H, Debernardi A, Buchou T, Rousseaux S, Jin F, Sabari BR, Deng Z, Allis CD, Ren B, Khochbin S, Zhao Y. 2014. Lysine 2-hydroxyisobutyrylation is a widely distributed active histone mark. Nat Chem Biol 10:365-70.

13. Xie Z, Zhang D, Chung D, Tang Z, Huang H, Dai L, Qi S, Li J, Colak G, Chen Y, Xia C, Peng C, Ruan H, Kirkey M, Wang D, Jensen LM, Kwon OK, Lee S, Pletcher SD, Tan M, Lombard DB, White KP, Zhao H, Roeder RG, Yang X, Zhao Y. 2016. Metabolic Regulation of Gene Expression by Histone Lysine β-Hydroxybutyrylation. Mol Cell 62:194-206.

14. Choudhary C, Kumar C, Gnad F, Nielsen ML, Rehman M, Walther TC, Olsen JV, Mann M. 2009. Lysine acetylation targets protein complexes and co-regulates major cellular functions. Science 325:834-40.

15. Kim SC, Sprung R, Chen Y, Xu Y, Ball H, Pei J, Cheng T, Kho Y, Xiao H, Xiao L, Grishin NV, White M, Yang XJ, Zhao Y. 2006. Substrate and functional diversity of lysine acetylation revealed by a proteomics survey. Mol Cell 23:607-18.

16. Hebbes TR, Thorne AW, Crane-Robinson C. 1988. A direct link between core histone acetylation and transcriptionally active chromatin. EMBO J 7:1395-402.

17. Cunin R, Glansdorff N, Piérard A, Stalon V. 1986. Biosynthesis and metabolism of arginine in bacteria. Microbiol Rev 50:314-52.

18. Kawabe H, Kondo S, Umezawa H, Mitsuhashi S. 1975. R factor-mediated aminoglycoside antibiotic resistance in Pseudomonas aeruginosa: a new aminoglycoside 6'-N-acetyltransferase. Antimicrob Agents Chemother 7:494-9.

19. Shaw WV, Hopwood DA. 1976. Chloramphenicol acetylation in Streptomyces. J Gen Microbiol 94:159-66.

20. Garneau-Tsodikova S, Labby KJ. 2016. Mechanisms of Resistance to Aminoglycoside Antibiotics: Overview and Perspectives. Medchemcomm 7:11-27.

21. Bulkley D, Innis CA, Blaha G, Steitz TA. 2010. Revisiting the structures of several antibiotics bound to the bacterial ribosome. Proc Natl Acad Sci U S A 107:17158-63.

22. Bernard E, Rolain T, Courtin P, Guillot A, Langella P, Hols P, Chapot-Chartier MP. 2011. Characterization of O-acetylation of N-acetylglucosamine: a novel structural variation of bacterial peptidoglycan. J Biol Chem 286:23950-8.

23. Lee J, Manning AJ, Wolfgeher D, Jelenska J, Cavanaugh KA, Xu H, Fernandez SM, Michelmore RW, Kron SJ, Greenberg JT. 2015. Acetylation of an NB-LRR Plant Immune-Effector Complex Suppresses Immunity. Cell Rep 13:1670-82.

24. Mukherjee S, Hao YH, Orth K. 2007. A newly discovered post-translational modification--the acetylation of serine and threonine residues. Trends Biochem Sci 32:210-6.

25. Mukherjee S, Keitany G, Li Y, Wang Y, Ball HL, Goldsmith EJ, Orth K. 2006. Yersinia YopJ acetylates and inhibits kinase activation by blocking phosphorylation. Science 312:1211-4.

26. Paquette N, Conlon J, Sweet C, Rus F, Wilson L, Pereira A, Rosadini CV, Goutagny N, Weber AN, Lane WS, Shaffer SA, Maniatis S, Fitzgerald KA, Stuart L, Silverman N. 2012. Serine/threonine acetylation of TGFβ-activated kinase (TAK1) by Yersinia pestis YopJ inhibits innate immune signaling. Proc Natl Acad Sci U S A 109:12710-5.

27. Ouidir T, Jarnier F, Cosette P, Jouenne T, Hardouin J. 2015. Characterization of N-terminal protein modifications in Pseudomonas aeruginosa PA14. J Proteomics 114:214-25.

28. Brown CW, Sridhara V, Boutz DR, Person MD, Marcotte EM, Barrick JE, Wilke CO. 2017. Large-scale analysis of post-translational modifications in E. coli under glucose-limiting conditions. BMC Genomics 18:301.

29. Polevoda B, Sherman F. 2003. N-terminal acetyltransferases and sequence requirements for N-terminal acetylation of eukaryotic proteins. J Mol Biol 325:595-622.

30. Helbig AO, Gauci S, Raijmakers R, van Breukelen B, Slijper M, Mohammed S, Heck AJ. 2010. Profiling of N-acetylated protein termini provides in-depth insights into the N-terminal nature of the proteome. Mol Cell Proteomics 9:928-39.

31. Helsens K, Van Damme P, Degroeve S, Martens L, Arnesen T, Vandekerckhove J, Gevaert K. 2011. Bioinformatics analysis of a Saccharomyces cerevisiae N-terminal proteome provides evidence of alternative translation initiation and post-translational N-terminal acetylation. J Proteome Res 10:3578-89.

32. Yoshikawa A, Isono S, Sheback A, Isono K. 1987. Cloning and nucleotide sequencing of the genes rimI and rimJ which encode enzymes acetylating ribosomal proteins S18 and S5 of *Escherichia coli* K12. Mol Gen Genet 209:481-8.

33. Tanaka S, Matsushita Y, Yoshikawa A, Isono K. 1989. Cloning and molecular characterization of the gene rimL which encodes an enzyme acetylating ribosomal protein L12 of *Escherichia coli* K12. Mol Gen Genet 217:289-93.

34. Roy-Chaudhuri B, Kirthi N, Kelley T, Culver GM. 2008. Suppression of a cold-sensitive mutation in ribosomal protein S5 reveals a role for RimJ in ribosome biogenesis. Mol Microbiol 68:1547-59.

35. White-Ziegler CA, Low DA. 1992. Thermoregulation of the pap operon: evidence for the involvement of RimJ, the N-terminal acetylase of ribosomal protein S5. J Bacteriol 174:7003-12.

36. White-Ziegler CA, Black AM, Eliades SH, Young S, Porter K. 2002. The N-acetyltransferase RimJ responds to environmental stimuli to repress pap fimbrial transcription in *Escherichia coli*. J Bacteriol 184:4334-42.

37. Lange S, Rosenkrands I, Stein R, Andersen P, Kaufmann SH, Jungblut PR. 2014. Analysis of protein species differentiation among mycobacterial low-Mr-secreted proteins by narrow pH range Immobiline gel 2-DE-MALDI-MS. J Proteomics 97:235-44.

38. Okkels LM, Müller EC, Schmid M, Rosenkrands I, Kaufmann SH, Andersen P, Jungblut PR. 2004. CFP10 discriminates between nonacetylated and acetylated ESAT-6 of Mycobacterium tuberculosis by differential interaction. Proteomics 4:2954-60.

39. Mba Medie F, Champion MM, Williams EA, Champion PA. 2014. Homeostasis of N-α-terminal acetylation of EsxA correlates with virulence in Mycobacterium marinum. Infect Immun 82:4572-86.

40. Mittal R, Peak-Chew SY, Sade RS, Vallis Y, McMahon HT. 2010. The acetyltransferase activity of the bacterial toxin YopJ of Yersinia is activated by eukaryotic host cell inositol hexakisphosphate. J Biol Chem 285:19927-34.

41. Birhanu AG, Yimer SA, Holm-Hansen C, Norheim G, Aseffa A, Abebe M, Tønjum T. 2017. N ε- and O-Acetylation in Mycobacterium tuberculosis Lineage 7 and Lineage 4 strains: Proteins Involved in Bioenergetics, Virulence and Antimicrobial Resistance are Acetylated. J Proteome Res 16:4045-4059.

42. VanDrisse CM, Escalante-Semerena JC. 2018. In Streptomyces lividans, acetyl-CoA synthetase activity is controlled by O-serine and N. Mol Microbiol 107:577-594.

43. Yang XJ, Seto E. 2008. Lysine acetylation: codified crosstalk with other posttranslational modifications. Mol Cell 31:449-61.

44. Xiong Y, Guan KL. 2012. Mechanistic insights into the regulation of metabolic enzymes by acetylation. J Cell Biol 198:155-64.

45. Glozak MA, Sengupta N, Zhang X, Seto E. 2005. Acetylation and deacetylation of non-histone proteins. Gene 363:15-23.

46. PHILLIPS DM. 1963. The presence of acetyl groups of histones. Biochem J 87:258-63.

47. ALLFREY VG, FAULKNER R, MIRSKY AE. 1964. ACETYLATION AND METHYLATION OF HISTONES AND THEIR POSSIBLE ROLE IN THE REGULATION OF RNA SYNTHESIS. Proc Natl Acad Sci U S A 51:786-94.

48. Gershey EL, Vidali G, Allfrey VG. 1968. Chemical studies of histone acetylation. The occurrence of epsilon-N-acetyllysine in the f2a1 histone. J Biol Chem 243:5018-22.

49. Vidali G, Gershey EL, Allfrey VG. 1968. Chemical studies of histone acetylation. The distribution of epsilon-N-acetyllysine in calf thymus histones. J Biol Chem 243:6361-6.

50. Zhang J, Sprung R, Pei J, Tan X, Kim S, Zhu H, Liu CF, Grishin NV, Zhao Y. 2009. Lysine acetylation is a highly abundant and evolutionarily conserved modification in *Escherichia coli*. Mol Cell Proteomics 8:215-25.

51. Marsh VL, Peak-Chew SY, Bell SD. 2005. Sir2 and the acetyltransferase, Pat, regulate the archaeal chromatin protein, Alba. J Biol Chem 280:21122-8.

52. Spange S, Wagner T, Heinzel T, Krämer OH. 2009. Acetylation of non-histone proteins modulates cellular signalling at multiple levels. Int J Biochem Cell Biol 41:185-98.

53. Zhao K, Chai X, Marmorstein R. 2003. Structure of a Sir2 substrate, Alba, reveals a mechanism for deacetylation-induced enhancement of DNA binding. J Biol Chem 278:26071-7.

54. Yu BJ, Kim JA, Moon JH, Ryu SE, Pan JG. 2008. The diversity of lysine-acetylated proteins in *Escherichia coli*. J Microbiol Biotechnol 18:1529-36.

55. Nakayasu ES, Burnet MC, Walukiewicz HE, Wilkins CS, Shukla AK, Brooks S, Plutz MJ, Lee BD, Schilling B, Wolfe AJ, Müller S, Kirby JR, Rao CV, Cort JR, Payne SH. 2017. Ancient Regulatory Role of Lysine Acetylation in Central Metabolism. MBio 8.

56. Weinert BT, Iesmantavicius V, Wagner SA, Schölz C, Gummesson B, Beli P, Nyström T, Choudhary C. 2013. Acetyl-phosphate is a critical determinant of lysine acetylation in E. coli. Mol Cell 51:265-72.

57. Kuhn ML, Zemaitaitis B, Hu LI, Sahu A, Sorensen D, Minasov G, Lima BP, Scholle M, Mrksich M, Anderson WF, Gibson BW, Schilling B, Wolfe AJ. 2014. Structural, kinetic and proteomic characterization of acetyl phosphate-dependent bacterial protein acetylation. PLoS One 9:e94816.

58. Kosono S, Tamura M, Suzuki S, Kawamura Y, Yoshida A, Nishiyama M, Yoshida M. 2015. Changes in the Acetylome and Succinylome of Bacillus subtilis in Response to Carbon Source. PLoS One 10:e0131169.

59. Post DMB, Schilling B, Reinders LM, D'Souza AK, Ketterer MR, Kiel SJ, Chande AT, Apicella MA, Gibson BW. 2017. Identification and characterization of AckA-dependent protein acetylation in Neisseria gonorrhoeae. PLoS One 12:e0179621.

60. Thao S, Escalante-Semerena JC. 2011. Control of protein function by reversible Nε-lysine acetylation in bacteria. Curr Opin Microbiol 14:200-4.

61. Latrasse D, Benhamed M, Henry Y, Domenichini S, Kim W, Zhou DX, Delarue M. 2008. The MYST histone acetyltransferases are essential for gametophyte development in Arabidopsis. BMC Plant Biol 8:121.

62. Dancy BM, Cole PA. 2015. Protein lysine acetylation by p300/CBP. Chem Rev 115:2419-52.

63. Wang Q, Zhang Y, Yang C, Xiong H, Lin Y, Yao J, Li H, Xie L, Zhao W, Yao Y, Ning ZB, Zeng R, Xiong Y, Guan KL, Zhao S, Zhao GP. 2010. Acetylation of metabolic enzymes coordinates carbon source utilization and metabolic flux. Science 327:1004-7.

64. Kentache T, Jouenne T, Dé E, Hardouin J. 2016. Proteomic characterization of Nα- and Nε-acetylation in Acinetobacter baumannii. J Proteomics 144:148-58.

65. Lv Y. 2017. Proteome-wide profiling of protein lysine acetylation in Aspergillus flavus. PLoS One 12:e0178603.

66. Liu L, Wang G, Song L, Lv B, Liang W. 2016. Acetylome analysis reveals the involvement of lysine acetylation in biosynthesis of antibiotics in Bacillus amyloliquefaciens. Sci Rep 6:20108.

67. Sun XL, Yang YH, Zhu L, Liu FY, Xu JP, Huang XW, Mo MH, Liu T, Zhang KQ. 2018. The lysine acetylome of the nematocidal bacterium Bacillus nematocida and impact of nematode on the acetylome. J Proteomics 177:31-39.

68. Kim D, Yu BJ, Kim JA, Lee YJ, Choi SG, Kang S, Pan JG. 2013. The acetylproteome of Gram-positive model bacterium Bacillus subtilis. Proteomics 13:1726-36.

69. Ravikumar V, Nalpas NC, Anselm V, Krug K, Lenuzzi M, Šestak MS, Domazet-Lošo T, Mijakovic I, Macek B. 2018. In-depth analysis of Bacillus subtilis proteome identifies new ORFs and traces the evolutionary history of modified proteins. Sci Rep 8:17246.

70. Reverdy A, Chen Y, Hunter E, Gozzi K, Chai Y. 2018. Protein lysine acetylation plays a regulatory role in Bacillus subtilis multicellularity. PLoS One 13:e0204687.

71. Carabetta VJ, Greco TM, Tanner AW, Cristea IM, Dubnau D. 2016. Temporal Regulation of the Bacillus subtilis Acetylome and Evidence for a Role of MreB Acetylation in Cell Wall Growth. mSystems 1:e00005-16.

72. Bontemps-Gallo S, Gaviard C, Richards CL, Kentache T, Raffel SJ, Lawrence KA, Schindler JC, Lovelace J, Dulebohn DP, Cluss RG, Hardouin J, Gherardini FC. 2018. Global Profiling of Lysine Acetylation in *Borrelia burgdorferi* B31 Reveals Its Role in Central Metabolism. Front Microbiol 9:2036.

73. Xu JY, Xu Z, Liu X, Tan M, Ye BC. 2018. Protein Acetylation and Butyrylation Regulate the Phenotype and Metabolic Shifts of the Endospore-forming *Clostridium acetobutylicum*. Mol Cell Proteomics 17:1156-1169.

74. Mizuno Y, Nagano-Shoji M, Kubo S, Kawamura Y, Yoshida A, Kawasaki H, Nishiyama M, Yoshida M, Kosono S. 2016. Altered acetylation and succinylation profiles in Corynebacterium glutamicum in response to conditions inducing glutamate overproduction. Microbiologyopen 5:152-73.

75. Chen Z, Zhang G, Yang M, Li T, Ge F, Zhao J. 2017. Lysine Acetylome Analysis Reveals Photosystem II Manganese-stabilizing Protein Acetylation is Involved in Negative Regulation of Oxygen Evolution in Model Cyanobacterium. Mol Cell Proteomics 16:1297-1311.

76. Wu X, Vellaichamy A, Wang D, Zamdborg L, Kelleher NL, Huber SC, Zhao Y. 2013. Differential lysine acetylation profiles of Erwinia amylovora strains revealed by proteomics. J Proteomics 79:60-71.

77. Baeza J, Dowell JA, Smallegan MJ, Fan J, Amador-Noguez D, Khan Z, Denu JM. 2014. Stoichiometry of site-specific lysine acetylation in an entire proteome. J Biol Chem 289:21326-38.

78. Schilling B, Christensen D, Davis R, Sahu AK, Hu LI, Walker-Peddakotla A, Sorensen DJ, Zemaitaitis B, Gibson BW, Wolfe AJ. 2015. Protein acetylation dynamics in response to carbon overflow in *Escherichia coli*. Mol Microbiol 98:847-63.

79. Zhang K, Zheng S, Yang JS, Chen Y, Cheng Z. 2013. Comprehensive profiling of protein lysine acetylation in *Escherichia coli*. J Proteome Res 12:844-51.

80. Colak G, Xie Z, Zhu AY, Dai L, Lu Z, Zhang Y, Wan X, Chen Y, Cha YH, Lin H, Zhao Y, Tan M. 2013. Identification of lysine succinylation substrates and the succinylation regulatory enzyme CobB in *Escherichia coli*. Mol Cell Proteomics 12:3509-20.

81. Weinert BT, Satpathy S, Hansen BK, Lyon D, Jensen LJ, Choudhary C. 2017. Accurate Quantification of Site-specific Acetylation Stoichiometry Reveals the Impact of Sirtuin Deacetylase CobB on the. Mol Cell Proteomics 16:759-769.

82. Castaño-Cerezo S, Bernal V, Post H, Fuhrer T, Cappadona S, Sánchez-Díaz NC, Sauer U, Heck AJ, Altelaar AF, Cánovas M. 2014. Protein acetylation affects acetate metabolism, motility and acid stress response in *Escherichia coli*. Mol Syst Biol 10:762.

83. Lee DW, Kim D, Lee YJ, Kim JA, Choi JY, Kang S, Pan JG. 2013. Proteomic analysis of acetylation in thermophilic Geobacillus kaustophilus. Proteomics 13:2278-82.

84. Liu J, Wang Q, Jiang X, Yang H, Zhao D, Han J, Luo Y, Xiang H. 2017. Systematic Analysis of Lysine Acetylation in the Halophilic Archaeon Haloferax mediterranei. J Proteome Res 16:3229-3241.

85. Guo J, Wang C, Han Y, Liu Z, Wu T, Liu Y, Tan Y, Cai X, Cao Y, Wang B, Zhang B, Liu C, Tan S, Zhang T. 2016. Identification of Lysine Acetylation in Mycobacterium abscessus Using LC-MS/MS after Immunoprecipitation. J Proteome Res 15:2567-78.

86. Xu JY, Zhao L, Liu X, Hu H, Liu P, Tan M, Ye BC. 2018. Characterization of the Lysine Acylomes and the Substrates Regulated by Protein Acyltransferase in Mycobacterium smegmatis. ACS Chem Biol 13:1588-1597.

87. Liu F, Yang M, Wang X, Yang S, Gu J, Zhou J, Zhang XE, Deng J, Ge F. 2014. Acetylome analysis reveals diverse functions of lysine acetylation in Mycobacterium tuberculosis. Mol Cell Proteomics 13:3352-66.

88. Bi J, Wang Y, Yu H, Qian X, Wang H, Liu J, Zhang X. 2017. Modulation of Central Carbon Metabolism by Acetylation of Isocitrate Lyase in Mycobacterium tuberculosis. Sci Rep 7:44826.

89. Xie L, Wang X, Zeng J, Zhou M, Duan X, Li Q, Zhang Z, Luo H, Pang L, Li W, Liao G, Yu X, Li Y, Huang H, Xie J. 2015. Proteome-wide lysine acetylation profiling of the human pathogen Mycobacterium tuberculosis. Int J Biochem Cell Biol 59:193-202.

90. Yang H, Sha W, Liu Z, Tang T, Liu H, Qin L, Cui Z, Chen J, Liu F, Zheng R, Huang X, Wang J, Feng Y, Ge B. 2018. Lysine acetylation of DosR regulates the hypoxia response of Mycobacterium tuberculosis. Emerg Microbes Infect 7:34.

91. van Noort V, Seebacher J, Bader S, Mohammed S, Vonkova I, Betts MJ, Kühner S, Kumar R, Maier T, O'Flaherty M, Rybin V, Schmeisky A, Yus E, Stülke J, Serrano L, Russell RB, Heck AJ, Bork P, Gavin AC. 2012. Cross-talk between phosphorylation and lysine acetylation in a genome-reduced bacterium. Mol Syst Biol 8:571.

92. Butler CA, Veith PD, Nieto MF, Dashper SG, Reynolds EC. 2015. Lysine acetylation is a common post-translational modification of key metabolic pathway enzymes of the anaerobe Porphyromonas gingivalis. J Proteomics 128:352-64.

93. Gaviard C, Broutin I, Cosette P, Dé E, Jouenne T, Hardouin J. 2018. Lysine Succinylation and Acetylation in Pseudomonas aeruginosa. J Proteome Res 17:2449-2459.

94. Crosby HA, Pelletier DA, Hurst GB, Escalante-Semerena JC. 2012. System-wide studies of N-lysine acetylation in Rhodopseudomonas palustris reveal substrate specificity of protein acetyltransferases. J Biol Chem 287:15590-601.

95. Henriksen P, Wagner SA, Weinert BT, Sharma S, Bacinskaja G, Rehman M, Juffer AH, Walther TC, Lisby M, Choudhary C. 2012. Proteome-wide analysis of lysine acetylation suggests its broad regulatory scope in Saccharomyces cerevisiae. Mol Cell Proteomics 11:1510-22.

96. Huang D, Li ZH, You D, Zhou Y, Ye BC. 2015. Lysine acetylproteome analysis suggests its roles in primary and secondary metabolism in Saccharopolyspora erythraea. Appl Microbiol Biotechnol 99:1399-413.

97. Li L, Wang W, Zhang R, Xu J, Wang R, Wang L, Zhao X, Li J. 2018. First acetyl-proteome profiling of Salmonella Typhimurium revealed involvement of lysine acetylation in drug resistance. Vet Microbiol 226:1-8.

98. Meng Q, Liu P, Wang J, Wang Y, Hou L, Gu W, Wang W. 2016. Systematic analysis of the lysine acetylome of the pathogenic bacterium Spiroplasma eriocheiris reveals acetylated proteins related to metabolism and helical structure. J Proteomics 148:159-69.

99. Zhang Y, Wu Z, Wan X, Liu P, Zhang J, Ye Y, Zhao Y, Tan M. 2014. Comprehensive profiling of lysine acetylome in S*taphylococcus aureus*. Science China Chemistry 57:732-738.

100. Liu YT, Pan Y, Lai F, Yin XF, Ge R, He QY, Sun X. 2018. Comprehensive analysis of the lysine acetylome and its potential regulatory roles in the virulence of Streptococcus pneumoniae. J Proteomics 176:46-55.

101. Ishigaki Y, Akanuma G, Yoshida M, Horinouchi S, Kosono S, Ohnishi Y. 2017. Protein acetylation involved in streptomycin biosynthesis in Streptomyces griseus. J Proteomics 155:63-72.

102. Liao G, Xie L, Li X, Cheng Z, Xie J. 2014. Unexpected extensive lysine acetylation in the trump-card antibiotic producer Streptomyces roseosporus revealed by proteome-wide profiling. J Proteomics 106:260-9.

103. Türkowsky D, Esken J, Goris T, Schubert T, Diekert G, Jehmlich N, von Bergen M. 2018. A Retentive Memory of Tetrachloroethene Respiration in Sulfurospirillum halorespirans - involved Proteins and a possible link to Acetylation of a Two-Component Regulatory System. J Proteomics 181:36-46.

104. Mo R, Yang M, Chen Z, Cheng Z, Yi X, Li C, He C, Xiong Q, Chen H, Wang Q, Ge F. 2015. Acetylome analysis reveals the involvement of lysine acetylation in photosynthesis and carbon metabolism in the model cyanobacterium Synechocystis sp. PCC 6803. J Proteome Res 14:1275-86.

105. Okanishi H, Kim K, Masui R, Kuramitsu S. 2013. Acetylome with structural mapping reveals the significance of lysine acetylation in Thermus thermophilus. J Proteome Res 12:3952-68.

106. Jeffers V, Sullivan WJ. 2012. Lysine acetylation is widespread on proteins of diverse function and localization in the protozoan parasite Toxoplasma gondii. Eukaryot Cell 11:735-42.

107. Xue B, Jeffers V, Sullivan WJ, Uversky VN. 2013. Protein intrinsic disorder in the acetylome of intracellular and extracellular Toxoplasma gondii. Mol Biosyst 9:645-57.

108. Xu X, Liu T, Yang J, Chen L, Liu B, Wang L, Jin Q. 2018. The First Whole-Cell Proteome- and Lysine-Acetylome-Based Comparison between Trichophyton rubrum Conidial and Mycelial Stages. J Proteome Res 17:1436-1451.

109. Jers C, Ravikumar V, Lezyk M, Sultan A, Sjöling Å, Wai SN, Mijakovic I. 2017. The Global Acetylome of the Human Pathogen. Front Cell Infect Microbiol 7:537.

110. Pan J, Ye Z, Cheng Z, Peng X, Wen L, Zhao F. 2014. Systematic analysis of the lysine acetylome in Vibrio parahemolyticus. J Proteome Res 13:3294-302.

111. Ramirez MS, Tolmasky ME. 2010. Aminoglycoside modifying enzymes. Drug Resist Updat 13:151-71.

112. Yang XJ, Ogryzko VV, Nishikawa J, Howard BH, Nakatani Y. 1996. A p300/CBP-associated factor that competes with the adenoviral oncoprotein E1A. Nature 382:319-24.

113. Vetting MW, S de Carvalho LP, Yu M, Hegde SS, Magnet S, Roderick SL, Blanchard JS. 2005. Structure and functions of the GNAT superfamily of acetyltransferases. Arch Biochem Biophys 433:212-26.

114. Spencer TE, Jenster G, Burcin MM, Allis CD, Zhou J, Mizzen CA, McKenna NJ, Onate SA, Tsai SY, Tsai MJ, O'Malley BW. 1997. Steroid receptor coactivator-1 is a histone acetyltransferase. Nature 389:194-8.

115. Bannister AJ, Kouzarides T. 1996. The CBP co-activator is a histone acetyltransferase. Nature 384:641-3.

116. Marmorstein R, Roth SY. 2001. Histone acetyltransferases: function, structure, and catalysis. Curr Opin Genet Dev 11:155-61.

117. Mizzen CA, Yang XJ, Kokubo T, Brownell JE, Bannister AJ, Owen-Hughes T, Workman J, Wang L, Berger SL, Kouzarides T, Nakatani Y, Allis CD. 1996. The TAF(II)250 subunit of TFIID has histone acetyltransferase activity. Cell 87:1261-70.

118. Yan Y, Harper S, Speicher DW, Marmorstein R. 2002. The catalytic mechanism of the ESA1 histone acetyltransferase involves a self-acetylated intermediate. Nat Struct Biol 9:862-9.

119. Liu X, Wang L, Zhao K, Thompson PR, Hwang Y, Marmorstein R, Cole PA. 2008. The structural basis of protein acetylation by the p300/CBP transcriptional coactivator. Nature 451:846-50.

120. Wolf E, Vassilev A, Makino Y, Sali A, Nakatani Y, Burley SK. 1998. Crystal structure of a GCN5-related N-acetyltransferase: Serratia marcescens aminoglycoside 3-N-acetyltransferase. Cell 94:439-49.

121. Wright GD, Ladak P. 1997. Overexpression and characterization of the chromosomal aminoglycoside 6'-N-acetyltransferase from Enterococcus faecium. Antimicrob Agents Chemother 41:956-60.

122. Neuwald AF, Landsman D. 1997. GCN5-related histone N-acetyltransferases belong to a diverse superfamily that includes the yeast SPT10 protein. Trends Biochem Sci 22:154-5.

123. Shaw KJ, Rather PN, Hare RS, Miller GH. 1993. Molecular genetics of aminoglycoside resistance genes and familial relationships of the aminoglycoside-modifying enzymes. Microbiol Rev 57:138-63.

124. Davies J, Wright GD. 1997. Bacterial resistance to aminoglycoside antibiotics. Trends Microbiol 5:234-40.

125. Favrot L, Blanchard JS, Vergnolle O. 2016. Bacterial GCN5-Related N-Acetyltransferases: From Resistance to Regulation. Biochemistry 55:989-1002.

126. Hentchel KL, Escalante-Semerena JC. 2015. Acylation of Biomolecules in Prokaryotes: a Widespread Strategy for the Control of Biological Function and Metabolic Stress. Microbiol Mol Biol Rev 79:321-46.

127. Liszczak G, Arnesen T, Marmorstein R. 2011. Structure of a ternary Naa50p (NAT5/SAN) N-terminal acetyltransferase complex reveals the molecular basis for substrate-specific acetylation. J Biol Chem 286:37002-10.

128. Tanner KG, Trievel RC, Kuo MH, Howard RM, Berger SL, Allis CD, Marmorstein R, Denu JM. 1999. Catalytic mechanism and function of invariant glutamic acid 173 from the histone acetyltransferase GCN5 transcriptional coactivator. J Biol Chem 274:18157-60.

129. Trievel RC, Rojas JR, Sterner DE, Venkataramani RN, Wang L, Zhou J, Allis CD, Berger SL, Marmorstein R. 1999. Crystal structure and mechanism of histone acetylation of the yeast GCN5 transcriptional coactivator. Proc Natl Acad Sci U S A 96:8931-6.

130. Berndsen CE, Albaugh BN, Tan S, Denu JM. 2007. Catalytic mechanism of a MYST family histone acetyltransferase. Biochemistry 46:623-9.

131. Dyda F, Klein DC, Hickman AB. 2000. GCN5-related N-acetyltransferases: a structural overview. Annu Rev Biophys Biomol Struct 29:81-103.

132. Dutnall RN, Tafrov ST, Sternglanz R, Ramakrishnan V. 1998. Structure of the yeast histone acetyltransferase Hat1: insights into substrate specificity and implications for the Gcn5-related N-acetyltransferase superfamily. Cold Spring Harb Symp Quant Biol 63:501-7.

133. Lin Y, Fletcher CM, Zhou J, Allis CD, Wagner G. 1999. Solution structure of the catalytic domain of GCN5 histone acetyltransferase bound to coenzyme A. Nature 400:86-9.

134. Tucker AC, Escalante-Semerena JC. 2013. Acetoacetyl-CoA synthetase activity is controlled by a protein acetyltransferase with unique domain organization in Streptomyces lividans. Mol Microbiol 87:152-67.

135. Castaño-Cerezo S, Bernal V, Blanco-Catalá J, Iborra JL, Cánovas M. 2011. cAMP-CRP co-ordinates the expression of the protein acetylation pathway with central metabolism in *Escherichia coli*. Mol Microbiol 82:1110-28.

136. Tucker AC, Taylor KC, Rank KC, Rayment I, Escalante-Semerena JC. 2014. Insights into the specificity of lysine acetyltransferases. J Biol Chem 289:36249-62.

137. Mackay DT, Botting CH, Taylor GL, White MF. 2007. An acetylase with relaxed specificity catalyses protein N-terminal acetylation in Sulfolobus solfataricus. Mol Microbiol 64:1540-8.

138. Bernal V, Castaño-Cerezo S, Gallego-Jara J, Écija-Conesa A, de Diego T, Iborra JL, Cánovas M. 2014. Regulation of bacterial physiology by lysine acetylation of proteins. N Biotechnol 31:586-95.

139. Lu YX, Liu XX, Liu WB, Ye BC. 2017. Identification and characterization of two types of amino acid-regulated acetyltransferases in actinobacteria. Biosci Rep 37.

140. Xu H, Hegde SS, Blanchard JS. 2011. Reversible acetylation and inactivation of Mycobacterium tuberculosis acetyl-CoA synthetase is dependent on cAMP. Biochemistry 50:5883-92.

141. Nambi S, Basu N, Visweswariah SS. 2010. cAMP-regulated protein lysine acetylases in mycobacteria. J Biol Chem 285:24313-23.

142. Liu XX, Liu WB, Ye BC. 2015. Regulation of a Protein Acetyltransferase in Myxococcus xanthus by the Coenzyme NADP. J Bacteriol 198:623-32.

143. Nambi S, Badireddy S, Visweswariah SS, Anand GS. 2012. Cyclic AMP-induced conformational changes in mycobacterial protein acetyltransferases. J Biol Chem 287:18115-29.

144. Nambi S, Gupta K, Bhattacharyya M, Ramakrishnan P, Ravikumar V, Siddiqui N, Thomas AT, Visweswariah SS. 2013. Cyclic AMP-dependent protein lysine acylation in mycobacteria regulates fatty acid and propionate metabolism. J Biol Chem 288:14114-24.

145. Lee HJ, Lang PT, Fortune SM, Sassetti CM, Alber T. 2012. Cyclic AMP regulation of protein lysine acetylation in Mycobacterium tuberculosis. Nat Struct Mol Biol 19:811-8.

146. Xu JY, You D, Leng PQ, Ye BC. 2014. Allosteric regulation of a protein acetyltransferase in Micromonospora aurantiaca by the amino acids cysteine and arginine. J Biol Chem 289:27034-45.

147. Gardner JG, Grundy FJ, Henkin TM, Escalante-Semerena JC. 2006. Control of acetyl-coenzyme A synthetase (AcsA) activity by acetylation/deacetylation without NAD(+) involvement in Bacillus subtilis. J Bacteriol 188:5460-8.

148. You D, Yao LL, Huang D, Escalante-Semerena JC, Ye BC. 2014. Acetyl coenzyme A synthetase is acetylated on multiple lysine residues by a protein acetyltransferase with a single Gcn5-type N-acetyltransferase (GNAT) domain in Saccharopolyspora erythraea. J Bacteriol 196:3169-78.

149. Brent MM, Iwata A, Carten J, Zhao K, Marmorstein R. 2009. Structure and biochemical characterization of protein acetyltransferase from Sulfolobus solfataricus. J Biol Chem 284:19412-9.

150. VanDrisse CM, Parks AR, Escalante-Semerena JC. 2017. A Toxin Involved in. MBio 8.

151. Lee W, VanderVen BC, Walker S, Russell DG. 2017. Novel protein acetyltransferase, Rv2170, modulates carbon and energy metabolism in Mycobacterium tuberculosis. Sci Rep 7:72.

152. Cheverton AM, Gollan B, Przydacz M, Wong CT, Mylona A, Hare SA, Helaine S. 2016. A Salmonella Toxin Promotes Persister Formation through Acetylation of tRNA. Mol Cell 63:86-96.

153. Christensen DG, Meyer JG, Baumgartner JT, D'Souza AK, Nelson WC, Payne SH, Kuhn ML, Schilling B, Wolfe AJ. 2018. Identification of Novel Protein Lysine Acetyltransferases in *Escherichia coli*. MBio 9.

154. Ghosh S, Padmanabhan B, Anand C, Nagaraja V. 2016. Lysine acetylation of the Mycobacterium tuberculosis HU protein modulates its DNA binding and genome organization. Mol Microbiol 100:577-88.

155. Green KD, Biswas T, Pang AH, Willby MJ, Reed MS, Stuchlik O, Pohl J, Posey JE, Tsodikov OV, Garneau-Tsodikova S. 2018. Acetylation by Eis and Deacetylation by Rv1151c of Mycobacterium tuberculosis HupB: Biochemical and Structural Insight. Biochemistry 57:781-790.

156. Kim KH, An DR, Song J, Yoon JY, Kim HS, Yoon HJ, Im HN, Kim J, Kim DJ, Lee SJ, Lee HM, Kim HJ, Jo EK, Lee JY, Suh SW. 2012. Mycobacterium tuberculosis Eis protein initiates suppression of host immune responses by acetylation of DUSP16/MKP-7. Proc Natl Acad Sci U S A 109:7729-34.

157. Zaunbrecher MA, Sikes RD, Metchock B, Shinnick TM, Posey JE. 2009. Overexpression of the chromosomally encoded aminoglycoside acetyltransferase eis confers kanamycin resistance in Mycobacterium tuberculosis. Proc Natl Acad Sci U S A 106:20004-9.

158. Chen W, Biswas T, Porter VR, Tsodikov OV, Garneau-Tsodikova S. 2011. Unusual regioversatility of acetyltransferase Eis, a cause of drug resistance in XDR-TB. Proc Natl Acad Sci U S A 108:9804-8.

159. Garrity J, Gardner JG, Hawse W, Wolberger C, Escalante-Semerena JC. 2007. N-lysine propionylation controls the activity of propionyl-CoA synthetase. J Biol Chem 282:30239-45.

160. Sun M, Xu J, Wu Z, Zhai L, Liu C, Cheng Z, Xu G, Tao S, Ye BC, Zhao Y, Tan M. 2016. Characterization of Protein Lysine Propionylation in *Escherichia coli*: Global Profiling, Dynamic Change, and Enzymatic Regulation. J Proteome Res 15:4696-4708.

161. Hodawadekar SC, Marmorstein R. 2007. Chemistry of acetyl transfer by histone modifying enzymes: structure, mechanism and implications for effector design. Oncogene 26:5528-40.

162. Escalante-Semerena JC. 2010. Nε-Lysine Acetylation Control Conserved in All Three Life Domains. Microbe Magazine 5:340-344.

163. Starai VJ, Escalante-Semerena JC. 2004. Identification of the protein acetyltransferase (Pat) enzyme that acetylates acetyl-CoA synthetase in Salmonella enterica. J Mol Biol 340:1005-12.

164. Crosby HA, Heiniger EK, Harwood CS, Escalante-Semerena JC. 2010. Reversible N epsilon-lysine acetylation regulates the activity of acyl-CoA synthetases involved in anaerobic benzoate catabolism in Rhodopseudomonas palustris. Mol Microbiol 76:874-88.

165. Thao S, Escalante-Semerena JC. 2012. A positive selection approach identifies residues important for folding of Salmonella enterica Pat, an N(ε)-lysine acetyltransferase that regulates central metabolism enzymes. Res Microbiol 163:427-35.

166. Thao S, Escalante-Semerena JC. 2011. Biochemical and thermodynamic analyses of Salmonella enterica Pat, a multidomain, multimeric N(ε)-lysine acetyltransferase involved in carbon and energy metabolism. MBio 2.

167. de Diego Puente T, Gallego-Jara J, Castaño-Cerezo S, Bernal Sánchez V, Fernández Espín V, García de la Torre J, Manjón Rubio A, Cánovas Díaz M. 2015. The Protein Acetyltransferase PatZ from *Escherichia coli* Is Regulated by Autoacetylation-induced Oligomerization. J Biol Chem 290:23077-93.

168. Hentchel KL, Thao S, Intile PJ, Escalante-Semerena JC. 2015. Deciphering the Regulatory Circuitry That Controls Reversible Lysine Acetylation in Salmonella enterica. MBio 6:e00891.

169. Busby S, Ebright RH. 1999. Transcription activation by catabolite activator protein (CAP). J Mol Biol 293:199-213.

170. Walker-Peddakotla A. 2012. Understanding the Regulation of Metabolic Enzyme Acetylation in E. Coli. Master of Science. Loyola University Chicago.

171. Liu W, Tan Y, Cao S, Zhao H, Fang H, Yang X, Wang T, Zhou Y, Yan Y, Han Y, Song Y, Bi Y, Wang X, Yang R, Du Z. 2018. Protein Acetylation Mediated by YfiQ and CobB Is Involved in the Virulence and Stress Response of Yersinia pestis. Infect Immun 86.

172. Kumari S, Tishel R, Eisenbach M, Wolfe AJ. 1995. Cloning, characterization, and functional expression of acs, the gene which encodes acetyl coenzyme A synthetase in *Escherichia coli*. J Bacteriol 177:2878-86.

173. Thao S, Chen CS, Zhu H, Escalante-Semerena JC. 2010. Nε-lysine acetylation of a bacterial transcription factor inhibits Its DNA-binding activity. PLoS One 5:e15123.

174. Crosby HA, Rank KC, Rayment I, Escalante-Semerena JC. 2012. Structure-guided expansion of the substrate range of methylmalonyl coenzyme A synthetase (MatB) of Rhodopseudomonas palustris. Appl Environ Microbiol 78:6619-29.

175. Blander G, Guarente L. 2004. The Sir2 family of protein deacetylases. Annu Rev Biochem 73:417-35.

176. Yang XJ, Seto E. 2008. The Rpd3/Hda1 family of lysine deacetylases: from bacteria and yeast to mice and men. Nat Rev Mol Cell Biol 9:206-18.

177. Gregoretti IV, Lee YM, Goodson HV. 2004. Molecular evolution of the histone deacetylase family: functional implications of phylogenetic analysis. J Mol Biol 338:17-31.

178. Marmorstein R. 2001. Structure of histone deacetylases: insights into substrate recognition and catalysis. Structure 9:1127-33.

179. Lombardi PM, Cole KE, Dowling DP, Christianson DW. 2011. Structure, mechanism, and inhibition of histone deacetylases and related metalloenzymes. Curr Opin Struct Biol 21:735-43.

180. Hildmann C, Riester D, Schwienhorst A. 2007. Histone deacetylases--an important class of cellular regulators with a variety of functions. Appl Microbiol Biotechnol 75:487-97.

181. Davie JR. 2003. Inhibition of histone deacetylase activity by butyrate. J Nutr 133:2485S-2493S.

182. Sanders BD, Jackson B, Marmorstein R. 2010. Structural basis for sirtuin function: what we know and what we don't. Biochim Biophys Acta 1804:1604-16.

183. Frye RA. 2000. Phylogenetic classification of prokaryotic and eukaryotic Sir2-like proteins. Biochem Biophys Res Commun 273:793-8.

184. Denu JM. 2003. Linking chromatin function with metabolic networks: Sir2 family of NAD(+)-dependent deacetylases. Trends Biochem Sci 28:41-8.

185. Zhao K, Harshaw R, Chai X, Marmorstein R. 2004. Structural basis for nicotinamide cleavage and ADP-ribose transfer by NAD(+)-dependent Sir2 histone/protein deacetylases. Proc Natl Acad Sci U S A 101:8563-8.

186. Bitterman KJ, Anderson RM, Cohen HY, Latorre-Esteves M, Sinclair DA. 2002. Inhibition of silencing and accelerated aging by nicotinamide, a putative negative regulator of yeast sir2 and human SIRT1. J Biol Chem 277:45099-107.

187. Avalos JL, Bever KM, Wolberger C. 2005. Mechanism of sirtuin inhibition by nicotinamide: altering the NAD(+) cosubstrate specificity of a Sir2 enzyme. Mol Cell 17:855-68.

188. Sauve AA, Schramm VL. 2003. Sir2 regulation by nicotinamide results from switching between base exchange and deacetylation chemistry. Biochemistry 42:9249-56.

189. Jackson MD, Schmidt MT, Oppenheimer NJ, Denu JM. 2003. Mechanism of nicotinamide inhibition and transglycosidation by Sir2 histone/protein deacetylases. J Biol Chem 278:50985-98.

190. Wimpenny JW, Firth A. 1972. Levels of nicotinamide adenine dinucleotide and reduced nicotinamide adenine dinucleotide in facultative bacteria and the effect of oxygen. J Bacteriol 111:24-32.

191. Schmidt MT, Smith BC, Jackson MD, Denu JM. 2004. Coenzyme specificity of Sir2 protein deacetylases: implications for physiological regulation. J Biol Chem 279:40122-9.

192. Guarente L. 2005. Calorie restriction and SIR2 genes--towards a mechanism. Mech Ageing Dev 126:923-8.

193. Porcu M, Chiarugi A. 2005. The emerging therapeutic potential of sirtuin-interacting drugs: from cell death to lifespan extension. Trends Pharmacol Sci 26:94-103.

194. Park J, Chen Y, Tishkoff DX, Peng C, Tan M, Dai L, Xie Z, Zhang Y, Zwaans BM, Skinner ME, Lombard DB, Zhao Y. 2013. SIRT5-mediated lysine desuccinylation impacts diverse metabolic pathways. Mol Cell 50:919-30.

195. Smith BC, Denu JM. 2007. Acetyl-lysine analog peptides as mechanistic probes of protein deacetylases. J Biol Chem 282:37256-65.

196. Bao X, Wang Y, Li X, Li XM, Liu Z, Yang T, Wong CF, Zhang J, Hao Q, Li XD. 2014. Identification of 'erasers' for lysine crotonylated histone marks using a chemical proteomics approach. Elife 3.

197. Xu JY, Xu Z, Liu X, Tan M, Ye BC. 2018. Protein Acetylation and Butyrylation Regulate the Phenotype and Metabolic Shifts of the Endospore-forming. Mol Cell Proteomics 17:1156-1169.

198. Frye RA. 1999. Characterization of five human cDNAs with homology to the yeast SIR2 gene: Sir2-like proteins (sirtuins) metabolize NAD and may have protein ADP-ribosyltransferase activity. Biochem Biophys Res Commun 260:273-9.

199. Starai VJ, Celic I, Cole RN, Boeke JD, Escalante-Semerena JC. 2002. Sir2-dependent activation of acetyl-CoA synthetase by deacetylation of active lysine. Science 298:2390-2.

200. Starai VJ, Takahashi H, Boeke JD, Escalante-Semerena JC. 2003. Short-chain fatty acid activation by acyl-coenzyme A synthetases requires SIR2 protein function in Salmonella enterica and Saccharomyces cerevisiae. Genetics 163:545-55.

201. Lima BP, Antelmann H, Gronau K, Chi BK, Becher D, Brinsmade SR, Wolfe AJ. 2011. Involvement of protein acetylation in glucose-induced transcription of a stress-responsive promoter. Mol Microbiol 81:1190-204.

202. Yang M, Wang Y, Chen Y, Cheng Z, Gu J, Deng J, Bi L, Chen C, Mo R, Wang X, Ge F. 2015. Succinylome analysis reveals the involvement of lysine succinylation in metabolism in pathogenic Mycobacterium tuberculosis. Mol Cell Proteomics 14:796-811.

203. Olesen SV, Rajabi N, Svensson B, Olsen CA, Madsen AS. 2018. An NAD. Biochemistry 57:3903-3915.

204. Rowland EA, Greco TM, Snowden CK, McCabe AL, Silhavy TJ, Cristea IM. 2017. Sirtuin Lipoamidase Activity Is Conserved in Bacteria as a Regulator of Metabolic Enzyme Complexes. MBio 8.

205. AbouElfetouh A, Kuhn ML, Hu LI, Scholle MD, Sorensen DJ, Sahu AK, Becher D, Antelmann H, Mrksich M, Anderson WF, Gibson BW, Schilling B, Wolfe AJ. 2015. The E. coli sirtuin CobB shows no preference for enzymatic and nonenzymatic lysine acetylation substrate sites. Microbiologyopen 4:66-83.

206. Tu S, Guo SJ, Chen CS, Liu CX, Jiang HW, Ge F, Deng JY, Zhou YM, Czajkowsky DM, Li Y, Qi BR, Ahn YH, Cole PA, Zhu H, Tao SC. 2015. YcgC represents a new protein deacetylase family in prokaryotes. Elife 4.

207. Kremer M, Kuhlmann N, Lechner M, Baldus L, Lammers M. 2018. Comment on 'YcgC represents a new protein deacetylase family in prokaryotes'. Elife 7.

208. Khan AN, Lewis PN. 2005. Unstructured conformations are a substrate requirement for the Sir2 family of NAD-dependent protein deacetylases. J Biol Chem 280:36073-8.

209. Wolfe AJ, Chang DE, Walker JD, Seitz-Partridge JE, Vidaurri MD, Lange CF, Prüss BM, Henk MC, Larkin JC, Conway T. 2003. Evidence that acetyl phosphate functions as a global signal during biofilm development. Mol Microbiol 48:977-88.

210. Gurard-Levin ZA, Mrksich M. 2008. Combining self-assembled monolayers and mass spectrometry for applications in biochips. Annu Rev Anal Chem (Palo Alto Calif) 1:767-800.

211. Gurard-Levin ZA, Kim J, Mrksich M. 2009. Combining mass spectrometry and peptide arrays to profile the specificities of histone deacetylases. Chembiochem 10:2159-61.

212. Gardner JG, Escalante-Semerena JC. 2008. Biochemical and mutational analyses of AcuA, the acetyltransferase enzyme that controls the activity of the acetyl coenzyme a synthetase (AcsA) in Bacillus subtilis. J Bacteriol 190:5132-6.

213. Gardner JG, Escalante-Semerena JC. 2009. In Bacillus subtilis, the sirtuin protein deacetylase, encoded by the srtN gene (formerly yhdZ), and functions encoded by the acuABC genes control the activity of acetyl coenzyme A synthetase. J Bacteriol 191:1749-55.

214. Suzuki S, Kondo N, Yoshida M, Nishiyama M, Kosono S. 2019. Dynamic changes in lysine acetylation and succinylation of the elongation factor Tu in Bacillus subtilis. Microbiology 165:65-77.

215. Ogura M, Asai K. 2016. Glucose Induces ECF Sigma Factor Genes, s*igX* and s*igM*, Independent of Cognate Anti-sigma Factors through Acetylation of CshA in B*acillus subtilis*. Front Microbiol 7:1918.

216. Ogura M, Kanesaki Y. 2018. Newly Identified Nucleoid-Associated-Like Protein YlxR Regulates Metabolic Gene Expression in Bacillus subtilis. mSphere 3.

217. Ye Q, Ji QQ, Yan W, Yang F, Wang ED. 2017. Acetylation of lysine ϵ-amino groups regulates aminoacyl-tRNA synthetase activity in *Escherichia coli*. J Biol Chem 292:10709-10722.

218. Davis R, Écija-Conesa A, Gallego-Jara J, de Diego T, Filippova EV, Kuffel G, Anderson WF, Gibson BW, Schilling B, Canovas M, Wolfe AJ. 2018. An acetylatable lysine controls CRP function in E. coli. Mol Microbiol 107:116-131.

219. Fan C, Xiong H, Reynolds NM, Söll D. 2015. Rationally evolving tRNAPyl for efficient incorporation of noncanonical amino acids. Nucleic Acids Res 43:e156.

220. Venkat S, Gregory C, Sturges J, Gan Q, Fan C. 2017. Studying the Lysine Acetylation of Malate Dehydrogenase. J Mol Biol 429:1396-1405.

221. Lima BP, Thanh Huyen TT, Bäsell K, Becher D, Antelmann H, Wolfe AJ. 2012. Inhibition of acetyl phosphate-dependent transcription by an acetylatable lysine on RNA polymerase. J Biol Chem 287:32147-60.

222. Venkat S, Gregory C, Gan Q, Fan C. 2017. Biochemical Characterization of the Lysine Acetylation of Tyrosyl-tRNA Synthetase in *Escherichia coli*. Chembiochem 18:1928-1934.

223. Hu LI, Chi BK, Kuhn ML, Filippova EV, Walker-Peddakotla AJ, Bäsell K, Becher D, Anderson WF, Antelmann H, Wolfe AJ. 2013. Acetylation of the response regulator RcsB controls transcription from a small RNA promoter. J Bacteriol 195:4174-86.

224. Zhou Q, Zhou YN, Jin DJ, Tse-Dinh YC. 2017. Deacetylation of topoisomerase I is an important physiological function of E. coli CobB. Nucleic Acids Res 45:5349-5358.

225. Zhou Q, Gomez Hernandez ME, Fernandez-Lima F, Tse-Dinh YC. 2018. Biochemical Basis of *E. coli* Topoisomerase I Relaxation Activity Reduction by Nonenzymatic Lysine Acetylation. Int J Mol Sci 19.

226. Zhang Q, Zhou A, Li S, Ni J, Tao J, Lu J, Wan B, Zhang J, Zhao S, Zhao GP, Shao F, Yao YF. 2016. Reversible lysine acetylation is involved in DNA replication initiation by regulating activities of initiator DnaA in *Escherichia coli*. Sci Rep 6:30837.

227. Li S, Zhang Q, Xu Z, Yao YF. 2017. Acetylation of Lysine 243 Inhibits the *oriC* Binding Ability of DnaA in *Escherichia coli*. Front Microbiol 8:699.

228. Barak R, Eisenbach M. 2001. Acetylation of the response regulator, CheY, is involved in bacterial chemotaxis. Mol Microbiol 40:731-43.

229. Liarzi O, Barak R, Bronner V, Dines M, Sagi Y, Shainskaya A, Eisenbach M. 2010. Acetylation represses the binding of CheY to its target proteins. Mol Microbiol 76:932-43.

230. Li R, Gu J, Chen YY, Xiao CL, Wang LW, Zhang ZP, Bi LJ, Wei HP, Wang XD, Deng JY, Zhang XE. 2010. CobB regulates *Escherichia coli* chemotaxis by deacetylating the response regulator CheY. Mol Microbiol 76:1162-74.

231. Umehara T, Kosono S, Söll D, Tamura K. 2018. Lysine Acetylation Regulates Alanyl-tRNA Synthetase Activity in *Escherichia coli*. Genes (Basel) 9.

232. Sun M, Guo H, Lu G, Gu J, Wang X, Zhang XE, Deng J. 2016. Lysine acetylation regulates the activity of *Escherichia coli* S-adenosylmethionine synthase. Acta Biochim Biophys Sin (Shanghai) 48:723-31.

233. Zhang QF, Zhang Q, Gu J, Gong P, Wang XD, Wang X, Tu S, Bi LJ, Bi L, Yu ZN, Yu Z, Zhang ZP, Zhang Z, Cui ZQ, Cui Z, Wei HP, Wei H, Tao SC, Tao S, Zhang XE, Zhang X, Deng JY. 2013. Reversibly acetylated lysine residues play important roles in the enzymatic activity of *Escherichia coli* N-hydroxyarylamine O-acetyltransferase. FEBS J 280:1966-79.

234. Song L, Wang G, Malhotra A, Deutscher MP, Liang W. 2016. Reversible acetylation on Lys501 regulates the activity of RNase II. Nucleic Acids Res 44:1979-88.

235. Liang W, Malhotra A, Deutscher MP. 2011. Acetylation regulates the stability of a bacterial protein: growth stage-dependent modification of RNase R. Mol Cell 44:160-6.

236. Liang W, Deutscher MP. 2012. Post-translational modification of RNase R is regulated by stress-dependent reduction in the acetylating enzyme Pka (YfiQ). RNA 18:37-41.

237. Vergnolle O, Xu H, Blanchard JS. 2013. Mechanism and regulation of mycobactin fatty acyl-AMP ligase FadD33. J Biol Chem 288:28116-25.

238. Vergnolle O, Xu H, Tufariello JM, Favrot L, Malek AA, Jacobs WR, Blanchard JS. 2016. Post-translational Acetylation of MbtA Modulates Mycobacterial Siderophore Biosynthesis. J Biol Chem 291:22315-22326.

239. Zhou Y, Chen T, Zhou L, Fleming J, Deng J, Wang X, Wang L, Wang Y, Zhang X, Wei W, Bi L. 2015. Discovery and characterization of Ku acetylation in Mycobacterium smegmatis. FEMS Microbiol Lett 362.

240. Sakatos A, Babunovic GH, Chase MR, Dills A, Leszyk J, Rosebrock T, Bryson B, Fortune SM. 2018. Posttranslational modification of a histone-like protein regulates phenotypic resistance to isoniazid in mycobacteria. Sci Adv 4:eaao1478.

241. Hayden JD, Brown LR, Gunawardena HP, Perkowski EF, Chen X, Braunstein M. 2013. Reversible acetylation regulates acetate and propionate metabolism in Mycobacterium smegmatis. Microbiology 159:1986-99.

242. Duan L, Yi M, Chen J, Li S, Chen W. 2016. Mycobacterium tuberculosis EIS gene inhibits macrophage autophagy through up-regulation of IL-10 by increasing the acetylation of histone H3. Biochem Biophys Res Commun 473:1229-1234.

243. Noy T, Xu H, Blanchard JS. 2014. Acetylation of acetyl-CoA synthetase from Mycobacterium tuberculosis leads to specific inactivation of the adenylation reaction. Arch Biochem Biophys 550-551:42-9.

244. Bi J, Gou Z, Zhou F, Chen Y, Gan J, Liu J, Wang H, Zhang X. 2018. Acetylation of lysine 182 inhibits the ability of Mycobacterium tuberculosis DosR to bind DNA and regulate gene expression during hypoxia. Emerg Microbes Infect 7:108.

245. Singhal A, Arora G, Virmani R, Kundu P, Khanna T, Sajid A, Misra R, Joshi J, Yadav V, Samanta S, Saini N, Pandey AK, Visweswariah SS, Hentschker C, Becher D, Gerth U, Singh Y. 2015. Systematic Analysis of Mycobacterial Acylation Reveals First Example of Acylation-mediated Regulation of Enzyme Activity of a Bacterial Phosphatase. J Biol Chem 290:26218-34.

246. Jose L, Ramachandran R, Bhagavat R, Gomez RL, Chandran A, Raghunandanan S, Omkumar RV, Chandra N, Mundayoor S, Kumar RA. 2016. Hypothetical protein Rv3423.1 of Mycobacterium tuberculosis is a histone acetyltransferase. FEBS J 283:265-81.

247. Hockenberry AM, Post DMB, Rhodes KA, Apicella M, So M. 2018. Perturbing the acetylation status of the Type IV pilus retraction motor, PilT, reduces Neisseria gonorrhoeae viability. Mol Microbiol 110:677-688.

248. Li Y, Krishnan K, Duncan MJ. 2018. Post-translational regulation of a *Porphyromonas gingivalis* regulator. J Oral Microbiol 10:1487743.

249. Mishra A, Roy F, Dou Y, Zhang K, Tang H, Fletcher HM. 2018. Role of Acetyltransferase PG1842 in Gingipain Biogenesis in Porphyromonas gingivalis. Journal of Bacteriology 200:e00385-18.

250. Wei W, Liu T, Li X, Wang R, Zhao W, Zhao G, Zhao S, Zhou Z. 2017. Lysine acetylation regulates the function of the global anaerobic transcription factor FnrL in Rhodobacter sphaeroides. Mol Microbiol 104:278-293.

251. Crosby HA, Escalante-Semerena JC. 2014. The acetylation motif in AMP-forming Acyl coenzyme A synthetases contains residues critical for acetylation and recognition by the protein acetyltransferase pat of Rhodopseudomonas palustris. J Bacteriol 196:1496-504.

252. You D, Wang MM, Ye BC. 2017. Acetyl-CoA synthetases of Saccharopolyspora erythraea are regulated by the nitrogen response regulator GlnR at both transcriptional and post-translational levels. Mol Microbiol 103:845-859.

253. You D, Yin BC, Li ZH, Zhou Y, Yu WB, Zuo P, Ye BC. 2016. Sirtuin-dependent reversible lysine acetylation of glutamine synthetases reveals an autofeedback loop in nitrogen metabolism. Proc Natl Acad Sci U S A 113:6653-8.

254. Sang Y, Ren J, Ni J, Tao J, Lu J, Yao YF. 2016. Protein Acetylation Is Involved in Salmonella enterica Serovar Typhimurium Virulence. J Infect Dis 213:1836-45.

255. Sang Y, Ren J, Qin R, Liu S, Cui Z, Cheng S, Liu X, Lu J, Tao J, Yao YF. 2017. Acetylation Regulating Protein Stability and DNA-Binding Ability of HilD, thus Modulating Salmonella Typhimurium Virulence. J Infect Dis 216:1018-1026.

256. Ren J, Sang Y, Tan Y, Tao J, Ni J, Liu S, Fan X, Zhao W, Lu J, Wu W, Yao YF. 2016. Acetylation of Lysine 201 Inhibits the DNA-Binding Ability of PhoP to Regulate Salmonella Virulence. PLoS Pathog 12:e1005458.

257. Qin R, Sang Y, Ren J, Zhang Q, Li S, Cui Z, Yao YF. 2016. The Bacterial Two-Hybrid System Uncovers the Involvement of Acetylation in Regulating of Lrp Activity in. Front Microbiol 7:1864.

258. Starai VJ, Garrity J, Escalante-Semerena JC. 2005. Acetate excretion during growth of Salmonella enterica on ethanolamine requires phosphotransacetylase (EutD) activity, and acetate recapture requires acetyl-CoA synthetase (Acs) and phosphotransacetylase (Pta) activities. Microbiology 151:3793-801.

259. VanDrisse CM, Parks AR, Escalante-Semerena JC. 2017. A Toxin Involved in *Salmonella* Persistence Regulates Its Activity by Acetylating Its Cognate Antitoxin, a Modification Reversed by CobB Sirtuin Deacetylase. MBio 8.

260. Mikulik K, Felsberg J, Kudrnáčová E, Bezoušková S, Setinová D, Stodůlková E, Zídková J, Zídek V. 2012. CobB1 deacetylase activity in Streptomyces coelicolor. Biochem Cell Biol 90:179-87.

261. Amin R, Franz-Wachtel M, Tiffert Y, Heberer M, Meky M, Ahmed Y, Matthews A, Krysenko S, Jakobi M, Hinder M, Moore J, Okoniewski N, Maček B, Wohlleben W, Bera A. 2016. Post-translational Serine/Threonine Phosphorylation and Lysine Acetylation: A Novel Regulatory Aspect of the Global Nitrogen Response Regulator GlnR in S. coelicolor M145. Front Mol Biosci 3:38.

262. Liimatta K, Flaherty E, Ro G, Nguyen DK, Prado C, Purdy AE. 2018. A Putative Acetylation System in Vibrio cholerae Modulates Virulence in Arthropod Hosts. Appl Environ Microbiol 84.

263. Tucker AC, Escalante-Semerena JC. 2010. Biologically active isoforms of CobB sirtuin deacetylase in Salmonella enterica and Erwinia amylovora. J Bacteriol 192:6200-8.

264. Umehara T, Kosono S, Söll D, Tamura K. 2018. Lysine Acetylation Regulates Alanyl-tRNA Synthetase Activity in. Genes (Basel) 9.

265. Starai VJ, Escalante-Semerena JC. 2004. Acetyl-coenzyme A synthetase (AMP forming). Cell Mol Life Sci 61:2020-30.

266. Kim GW, Yang XJ. 2011. Comprehensive lysine acetylomes emerging from bacteria to humans. Trends Biochem Sci 36:211-20.

267. Prüss BM, Besemann C, Denton A, Wolfe AJ. 2006. A complex transcription network controls the early stages of biofilm development by *Escherichia coli*. J Bacteriol 188:3731-9.

268. Wang Q, Zhao Y, McClelland M, Harshey RM. 2007. The RcsCDB signaling system and swarming motility in Salmonella enterica serovar typhimurium: dual regulation of flagellar and SPI-2 virulence genes. J Bacteriol 189:8447-57.

269. Gallego-Jara J, Écija Conesa A, de Diego Puente T, Lozano Terol G, Cánovas Díaz M. 2017. Characterization of CobB kinetics and inhibition by nicotinamide. PLoS One 12:e0189689.

270. Ren J, Sang Y, Ni J, Tao J, Lu J, Zhao M, Yao YF. 2015. Acetylation Regulates Survival of Salmonella enterica Serovar Typhimurium under Acid Stress. Appl Environ Microbiol 81:5675-82.

271. Martínez-Antonio A, Collado-Vides J. 2003. Identifying global regulators in transcriptional regulatory networks in bacteria. Curr Opin Microbiol 6:482-9.

272. Brinkman AB, Ettema TJ, de Vos WM, van der Oost J. 2003. The Lrp family of transcriptional regulators. Mol Microbiol 48:287-94.

273. Ma Q, Wood TK. 2011. Protein acetylation in prokaryotes increases stress resistance. Biochem Biophys Res Commun 410:846-51.

274. Deutscher J, Francke C, Postma PW. 2006. How phosphotransferase system-related protein phosphorylation regulates carbohydrate metabolism in bacteria. Microbiol Mol Biol Rev 70:939-1031.

275. Park YH, Lee BR, Seok YJ, Peterkofsky A. 2006. In vitro reconstitution of catabolite repression in *Escherichia coli*. J Biol Chem 281:6448-54.

276. Carabetta VJ, Cristea IM. 2017. Regulation, Function, and Detection of Protein Acetylation in Bacteria. J Bacteriol 199.

277. Madian AG, Regnier FE. 2010. Proteomic identification of carbonylated proteins and their oxidation sites. J Proteome Res 9:3766-80.

278. Brownlee M. 2005. The pathobiology of diabetic complications: a unifying mechanism. Diabetes 54:1615-25.

279. Di Sabato G, Jencks WP. 1961. Mechanism and Catalysis of Reactions of Acyl Phosphates. I. Nucleophilic Reactions. , vol 83, p 4393-4400, Journal of Biological Chemistry.

280. Jencks WP. 1969. Catalysis in Chemistry and Enzymology. McGraw-Hill Book Company, New York.

281. Ramponi G, Manao G, Camici G. 1975. Nonenzymatic acetylation of histones with acetyl phosphate and acetyl adenylate. Biochemistry 14:2681-5.

282. Voet D, Voet JG. 1990. Biochemistry. John Wiley and Sons, Inc., New York.

283. J K, E D. 1952. Effect of Catalysts on the Hydrolysis of Acetyl Phosphate. Nucleophilic Displacement Mechanisms in Enzymatic Reactions. Journal of the American Chemical Society 74:2286-2292.

284. Klein AH, Shulla A, Reimann SA, Keating DH, Wolfe AJ. 2007. The intracellular concentration of acetyl phosphate in *Escherichia coli* is sufficient for direct phosphorylation of two-component response regulators. J Bacteriol 189:5574-81.

285. Ramos-Montañez S, Kazmierczak KM, Hentchel KL, Winkler ME. 2010. Instability of ackA (acetate kinase) mutations and their effects on acetyl phosphate and ATP amounts in Streptococcus pneumoniae D39. J Bacteriol 192:6390-400.

286. Vallari DS, Rock CO. 1985. Pantothenate transport in *Escherichia coli*. J Bacteriol 162:1156-61.

287. Baeza J, Smallegan MJ, Denu JM. 2015. Site-specific reactivity of nonenzymatic lysine acetylation. ACS Chem Biol 10:122-8.

288. Wagner GR, Payne RM. 2013. Widespread and enzyme-independent Nε-acetylation and Nε-succinylation of proteins in the chemical conditions of the mitochondrial matrix. J Biol Chem 288:29036-45.

289. ROSE IA, GRUNBERG-MANAGO M, KOREY SR, OCHOA S. 1954. Enzymatic phosphorylation of acetate. J Biol Chem 211:737-56.

290. Brown TD, Jones-Mortimer MC, Kornberg HL. 1977. The enzymic interconversion of acetate and acetyl-coenzyme A in *Escherichia coli*. J Gen Microbiol 102:327-36.

291. Wolfe AJ. 2010. Physiologically relevant small phosphodonors link metabolism to signal transduction. Curr Opin Microbiol 13:204-9.

292. MAGASANIK B. 1961. Catabolite repression. Cold Spring Harb Symp Quant Biol 26:249-56.

293. Moses V, Prevost C. 1966. Catabolite repression of beta-galactosidase synthesis in *Escherichia coli*. Biochem J 100:336-53.

294. COHN M, HORIBATA K. 1959. Inhibition by glucose of the induced synthesis of the beta-galactoside-enzyme system of *Escherichia coli*. Analysis of maintenance. J Bacteriol 78:601-12.

295. Postma PW, Lengeler JW, Jacobson GR. 1993. Phosphoenolpyruvate:carbohydrate phosphotransferase systems of bacteria. Microbiol Rev 57:543-94.

296. Andersen KB, von Meyenburg K. 1980. Are growth rates of *Escherichia coli* in batch cultures limited by respiration? J Bacteriol 144:114-23.

297. Hollywood N, Doelle HW. 1976. Effect of specific growth rate and glucose concentration on growth and glucose metabolism of *Escherichia coli* K-12. Microbios 17:23-33.

298. Crabtree HG. 1928. The carbohydrate metabolism of certain pathological overgrowths. Biochem J 22:1289-98.

299. Warburg O, Wind F, Negelein E. 1927. THE METABOLISM OF TUMORS IN THE BODY. J Gen Physiol 8:519-30.

300. De Deken RH. 1966. The Crabtree effect: a regulatory system in yeast. J Gen Microbiol 44:149-56.

301. Hagman A, Piškur J. 2015. A study on the fundamental mechanism and the evolutionary driving forces behind aerobic fermentation in yeast. PLoS One 10:e0116942.

302. Mustea I, Muresian T. 1967. Crabtree effect in some bacterial cultures. Cancer 20:1499-501.

303. Pronk JT, Yde Steensma H, Van Dijken JP. 1996. Pyruvate metabolism in Saccharomyces cerevisiae. Yeast 12:1607-33.

304. Postma E, Verduyn C, Scheffers WA, Van Dijken JP. 1989. Enzymic analysis of the crabtree effect in glucose-limited chemostat cultures of Saccharomyces cerevisiae. Appl Environ Microbiol 55:468-77.

305. Petrik M KO, Fiechter A. 1983. An Expanded Concept for the Glucose Effect in the Yeast*Saccharomyces-Uvarum* — Involvement of Short-Term and Long-Term Regulation. J Gen Microbiol 129:43-49

306. Majewski RA, Domach MM. 1990. Simple constrained-optimization view of acetate overflow in E. coli. Biotechnol Bioeng 35:732-8.

307. Holms H. 2001. Flux analysis: a basic tool of microbial physiology. Adv Microb Physiol 45:271-340.

308. el-Mansi EM, Holms WH. 1989. Control of carbon flux to acetate excretion during growth of *Escherichia coli* in batch and continuous cultures. J Gen Microbiol 135:2875-83.

309. Basan M, Hui S, Okano H, Zhang Z, Shen Y, Williamson JR, Hwa T. 2015. Overflow metabolism in *Escherichia coli* results from efficient proteome allocation. Nature 528:99-104.

310. Finkel SE. 2006. Long-term survival during stationary phase: evolution and the GASP phenotype. Nat Rev Microbiol 4:113-20.

311. Pin C, Baranyi J. 2008. Single-cell and population lag times as a function of cell age. Appl Environ Microbiol 74:2534-6.

312. Navarro Llorens JM, Tormo A, Martínez-García E. 2010. Stationary phase in gram-negative bacteria. FEMS Microbiol Rev 34:476-95.

313. Gray JV, Petsko GA, Johnston GC, Ringe D, Singer RA, Werner-Washburne M. 2004. "Sleeping beauty": quiescence in Saccharomyces cerevisiae. Microbiol Mol Biol Rev 68:187-206.

314. Nyström T. 2004. Stationary-phase physiology. Annu Rev Microbiol 58:161-81.

315. Reeve CA, Bockman AT, Matin A. 1984. Role of protein degradation in the survival of carbon-starved *Escherichia coli* and Salmonella typhimurium. J Bacteriol 157:758-63.

316. GW H, M S, M Z, R K. 1996. Morphological and Physiological Changes During Stationary Phase. American Society for Microbiology Press, Washington, DC.

317. Almirón M, Link AJ, Furlong D, Kolter R. 1992. A novel DNA-binding protein with regulatory and protective roles in starved *Escherichia coli*. Genes Dev 6:2646-54.

318. Nair S, Finkel SE. 2004. Dps protects cells against multiple stresses during stationary phase. J Bacteriol 186:4192-8.

319. Wendrich TM, Blaha G, Wilson DN, Marahiel MA, Nierhaus KH. 2002. Dissection of the mechanism for the stringent factor RelA. Mol Cell 10:779-88.

320. Barker MM, Gaal T, Josaitis CA, Gourse RL. 2001. Mechanism of regulation of transcription initiation by ppGpp. I. Effects of ppGpp on transcription initiation in vivo and in vitro. J Mol Biol 305:673-88.

321. Barker MM, Gaal T, Gourse RL. 2001. Mechanism of regulation of transcription initiation by ppGpp. II. Models for positive control based on properties of RNAP mutants and competition for RNAP. J Mol Biol 305:689-702.

322. Jishage M, Kvint K, Shingler V, Nyström T. 2002. Regulation of sigma factor competition by the alarmone ppGpp. Genes Dev 16:1260-70.

323. Lacour S, Landini P. 2004. SigmaS-dependent gene expression at the onset of stationary phase in *Escherichia coli*: function of sigmaS-dependent genes and identification of their promoter sequences. J Bacteriol 186:7186-95.

324. Weber H, Polen T, Heuveling J, Wendisch VF, Hengge R. 2005. Genome-wide analysis of the general stress response network in *Escherichia coli*: sigmaS-dependent genes, promoters, and sigma factor selectivity. J Bacteriol 187:1591-603.

325. Jenkins DE, Chaisson SA, Matin A. 1990. Starvation-induced cross protection against osmotic challenge in *Escherichia coli*. J Bacteriol 172:2779-81.

326. Givskov M, Eberl L, Molin S. 1994. Responses to nutrient starvation in Pseudomonas putida KT2442: two-dimensional electrophoretic analysis of starvation- and stress-induced proteins. J Bacteriol 176:4816-24.

327. Fredriksson A, Ballesteros M, Dukan S, Nyström T. 2005. Defense against protein carbonylation by DnaK/DnaJ and proteases of the heat shock regulon. J Bacteriol 187:4207-13.

328. Lange R, Hengge-Aronis R. 1994. The cellular concentration of the sigma S subunit of RNA polymerase in *Escherichia coli* is controlled at the levels of transcription, translation, and protein stability. Genes Dev 8:1600-12.

329. Hirsch M, Elliott T. 2005. Stationary-phase regulation of RpoS translation in *Escherichia coli*. J Bacteriol 187:7204-13.

330. Tani TH, Khodursky A, Blumenthal RM, Brown PO, Matthews RG. 2002. Adaptation to famine: a family of stationary-phase genes revealed by microarray analysis. Proc Natl Acad Sci U S A 99:13471-6.

331. Ditto MD, Roberts D, Weisberg RA. 1994. Growth phase variation of integration host factor level in *Escherichia coli*. J Bacteriol 176:3738-48.

332. Altuvia S, Almirón M, Huisman G, Kolter R, Storz G. 1994. The dps promoter is activated by OxyR during growth and by IHF and sigma S in stationary phase. Mol Microbiol 13:265-72.

333. Colland F, Barth M, Hengge-Aronis R, Kolb A. 2000. sigma factor selectivity of *Escherichia coli* RNA polymerase: role for CRP, IHF and lrp transcription factors. EMBO J 19:3028-37.

334. Zhou Y, Gottesman S. 1998. Regulation of proteolysis of the stationary-phase sigma factor RpoS. J Bacteriol 180:1154-8.

335. Groat RG, Schultz JE, Zychlinsky E, Bockman A, Matin A. 1986. Starvation proteins in *Escherichia coli*: kinetics of synthesis and role in starvation survival. J Bacteriol 168:486-93.

336. Shaikh AS, Tang YJ, Mukhopadhyay A, Martín HG, Gin J, Benke PI, Keasling JD. 2010. Study of stationary phase metabolism via isotopomer analysis of amino acids from an isolated protein. Biotechnol Prog 26:52-6.

337. Yoshida H, Maki Y, Kato H, Fujisawa H, Izutsu K, Wada C, Wada A. 2002. The ribosome modulation factor (RMF) binding site on the 100S ribosome of *Escherichia coli*. J Biochem 132:983-9.

338. Yoshida H, Yamamoto H, Uchiumi T, Wada A. 2004. RMF inactivates ribosomes by covering the peptidyl transferase centre and entrance of peptide exit tunnel. Genes Cells 9:271-8.

339. Barak R, Welch M, Yanovsky A, Oosawa K, Eisenbach M. 1992. Acetyladenylate or its derivative acetylates the chemotaxis protein CheY in vitro and increases its activity at the flagellar switch. Biochemistry 31:10099-107.

340. Sclavi B, Beatty CM, Thach DS, Fredericks CE, Buckle M, Wolfe AJ. 2007. The multiple roles of CRP at the complex acs promoter depend on activation region 2 and IHF. Mol Microbiol 65:425-40.

341. Christensen DG, Orr JS, Rao CV, Wolfe AJ. 2017. Increasing Growth Yield and Decreasing Acetylation in *Escherichia coli* by Optimizing the Carbon-to-Magnesium Ratio in Peptide-Based Media. Applied and Environmental Microbiology 83:e03034-16.

342. Baba T, Ara T, Hasegawa M, Takai Y, Okumura Y, Baba M, Datsenko KA, Tomita M, Wanner BL, Mori H. 2006. Construction of *Escherichia coli* K-12 in-frame, single-gene knockout mutants: the Keio collection. Mol Syst Biol 2:2006.0008.

343. Kumari S, Beatty CM, Browning DF, Busby SJ, Simel EJ, Hovel-Miner G, Wolfe AJ. 2000. Regulation of acetyl coenzyme A synthetase in *Escherichia coli*. J Bacteriol 182:4173-9.

344. Datsenko KA, Wanner BL. 2000. One-step inactivation of chromosomal genes in *Escherichia coli* K-12 using PCR products. Proc Natl Acad Sci U S A 97:6640-5.

345. Zhou L, Lei XH, Bochner BR, Wanner BL. 2003. Phenotype microarray analysis of *Escherichia coli* K-12 mutants with deletions of all two-component systems. J Bacteriol 185:4956-72.

346. Boettcher KJ, Ruby EG. 1990. Depressed light emission by symbiotic Vibrio fischeri of the sepiolid squid Euprymna scolopes. J Bacteriol 172:3701-6.

347. DiGiuseppe PA, Silhavy TJ. 2003. Signal detection and target gene induction by the CpxRA two-component system. J Bacteriol 185:2432-40.

348. Guyer MS, Reed RR, Steitz JA, Low KB. 1981. Identification of a sex-factor-affinity site in E. coli as gamma delta. Cold Spring Harb Symp Quant Biol 45 Pt 1:135-40.

349. Youngman P, Perkins JB, Losick R. 1984. Construction of a cloning site near one end of Tn917 into which foreign DNA may be inserted without affecting transposition in Bacillus subtilis or expression of the transposon-borne erm gene. Plasmid 12:1-9.

350. Bell A, Gaston K, Williams R, Chapman K, Kolb A, Buc H, Minchin S, Williams J, Busby S. 1990. Mutations that alter the ability of the *Escherichia coli* cyclic AMP receptor protein to activate transcription. Nucleic Acids Res 18:7243-50.

351. Kitagawa M, Ara T, Arifuzzaman M, Ioka-Nakamichi T, Inamoto E, Toyonaga H, Mori H. 2005. Complete set of ORF clones of *Escherichia coli* ASKA library (a complete set of E. coli K-12 ORF archive): unique resources for biological research. DNA Res 12:291-9.

352. Cherepanov PP, Wackernagel W. 1995. Gene disruption in *Escherichia coli*: TcR and KmR cassettes with the option of Flp-catalyzed excision of the antibiotic-resistance determinant. Gene 158:9-14.

353. Stringer AM, Singh N, Yermakova A, Petrone BL, Amarasinghe JJ, Reyes-Diaz L, Mantis NJ, Wade JT. 2012. FRUIT, a scar-free system for targeted chromosomal mutagenesis, epitope tagging, and promoter replacement in *Escherichia coli* and Salmonella enterica. PLoS One 7:e44841.

354. Keshishian H, Addona T, Burgess M, Kuhn E, Carr SA. 2007. Quantitative, multiplexed assays for low abundance proteins in plasma by targeted mass spectrometry and stable isotope dilution. Mol Cell Proteomics 6:2212-29.

355. Schilling B, Rardin MJ, MacLean BX, Zawadzka AM, Frewen BE, Cusack MP, Sorensen DJ, Bereman MS, Jing E, Wu CC, Verdin E, Kahn CR, Maccoss MJ, Gibson BW. 2012. Platform-independent and label-free quantitation of proteomic data using MS1 extracted ion chromatograms in skyline: application to protein acetylation and phosphorylation. Mol Cell Proteomics 11:202-14.

356. Gillet LC, Navarro P, Tate S, Röst H, Selevsek N, Reiter L, Bonner R, Aebersold R. 2012. Targeted data extraction of the MS/MS spectra generated by data-independent

acquisition: a new concept for consistent and accurate proteome analysis. Mol Cell Proteomics 11:O111.016717.

357. Rardin MJ, Schilling B, Cheng LY, MacLean BX, Sorensen DJ, Sahu AK, MacCoss MJ, Vitek O, Gibson BW. 2015. MS1 Peptide Ion Intensity Chromatograms in MS2 (SWATH) Data Independent Acquisitions. Improving Post Acquisition Analysis of Proteomic Experiments. Mol Cell Proteomics 14:2405-19.

358. Schilling B, Gibson BW, Hunter CL. 2017. Generation of High-Quality SWATH. Methods Mol Biol 1550:223-233.

359. Hu LI, Lima BP, Wolfe AJ. 2010. Bacterial protein acetylation: the dawning of a new age. Mol Microbiol 77:15-21.

360. Choudhary C, Weinert BT, Nishida Y, Verdin E, Mann M. 2014. The growing landscape of lysine acetylation links metabolism and cell signalling. Nat Rev Mol Cell Biol 15:536-50.

361. Enjalbert B, Letisse F, Portais JC. 2013. Physiological and Molecular Timing of the Glucose to Acetate Transition in *Escherichia coli*. Metabolites 3:820-37.

362. Dittrich CR, Bennett GN, San KY. 2005. Characterization of the acetate-producing pathways in *Escherichia coli*. Biotechnol Prog 21:1062-7.

363. Irani MH, Maitra PK. 1977. Properties of *Escherichia coli* mutants deficient in enzymes of glycolysis. J Bacteriol 132:398-410.

364. Nikaido H. 1979. Permeability of the outer membrane of bacteria. Angew Chem Int Ed Engl 18:337-50.

365. Nikaido H, Nakae T. 1979. The outer membrane of Gram-negative bacteria. Adv Microb Physiol 20:163-250.

366. Ferenci T. 1996. Adaptation to life at micromolar nutrient levels: the regulation of *Escherichia coli* glucose transport by endoinduction and cAMP. FEMS Microbiol Rev 18:301-17.

367. Liu X, Ferenci T. 1998. Regulation of porin-mediated outer membrane permeability by nutrient limitation in *Escherichia coli*. J Bacteriol 180:3917-22.

368. Flores N, Xiao J, Berry A, Bolivar F, Valle F. 1996. Pathway engineering for the production of aromatic compounds in *Escherichia coli*. Nat Biotechnol 14:620-3.

369. Flores S, Gosset G, Flores N, de Graaf AA, Bolívar F. 2002. Analysis of carbon metabolism in *Escherichia coli* strains with an inactive phosphotransferase system by (13)C labeling and NMR spectroscopy. Metab Eng 4:124-37.

370. Hernández-Montalvo V, Martínez A, Hernández-Chavez G, Bolivar F, Valle F, Gosset G. 2003. Expression of galP and glk in a *Escherichia coli* PTS mutant restores glucose transport and increases glycolytic flux to fermentation products. Biotechnol Bioeng 83:687-94.

371. Steinsiek S, Bettenbrock K. 2012. Glucose transport in *Escherichia coli* mutant strains with defects in sugar transport systems. J Bacteriol 194:5897-908.

372. Hernández-Montalvo V, Valle F, Bolivar F, Gosset G. 2001. Characterization of sugar mixtures utilization by an *Escherichia coli* mutant devoid of the phosphotransferase system. Appl Microbiol Biotechnol 57:186-91.

373. Davis R. 2017. MUTUAL REGULATION OF CRP AND Ne-LYSINE ACETYLATION IN *ESCHERICHIA COLI*. DOCTOR OF PHILOSOPHY. Loyola University Chicago, Chicago, IL.

374. Perrenoud A, Sauer U. 2005. Impact of global transcriptional regulation by ArcA, ArcB, Cra, Crp, Cya, Fnr, and Mlc on glucose catabolism in *Escherichia coli*. J Bacteriol 187:3171-9.

375. Beatty CM, Browning DF, Busby SJ, Wolfe AJ. 2003. Cyclic AMP receptor protein-dependent activation of the *Escherichia coli* acsP2 promoter by a synergistic class III mechanism. J Bacteriol 185:5148-57.

376. Plumbridge J. 1998. Expression of ptsG, the gene for the major glucose PTS transporter in *Escherichia coli*, is repressed by Mlc and induced by growth on glucose. Mol Microbiol 29:1053-63.

377. Kimata K, Inada T, Tagami H, Aiba H. 1998. A global repressor (Mlc) is involved in glucose induction of the ptsG gene encoding major glucose transporter in *Escherichia coli*. Mol Microbiol 29:1509-19.

378. Lipmann F, Tuttle LC. 1944. Acetyl phosphate: chemistry, determination, and synthesis. Journal of Biological Chemistry 153:571-582.

379. Reitzer L. 2003. Nitrogen assimilation and global regulation in *Escherichia coli*. Annu Rev Microbiol 57:155-76.

380. Koirala S, Wang X, Rao CV. 2016. Reciprocal Regulation of l-Arabinose and d-Xylose Metabolism in *Escherichia coli*. J Bacteriol 198:386-93.

381. Rodriguez GM, Hussain MS, Gambill L, Gao D, Yaguchi A, Blenner M. 2016. Engineering xylose utilization in *Yarrowia lipolytica* by understanding its cryptic xylose pathway. Biotechnol Biofuels 9:149.

382. Dukan S, Nyström T. 1998. Bacterial senescence: stasis results in increased and differential oxidation of cytoplasmic proteins leading to developmental induction of the heat shock regulon. Genes Dev 12:3431-41.

383. Chan CH, Garrity J, Crosby HA, Escalante-Semerena JC. 2011. In *Salmonella enterica*, the sirtuin-dependent protein acylation/deacylation system (SDPADS) maintains energy homeostasis during growth on low concentrations of acetate. Mol Microbiol 80:168-83.

384. Vetting MW, Park CH, Hegde SS, Jacoby GA, Hooper DC, Blanchard JS. 2008. Mechanistic and structural analysis of aminoglycoside N-acetyltransferase AAC(6')-Ib and its bifunctional, fluoroquinolone-active AAC(6')-Ib-cr variant. Biochemistry 47:9825-35.

385. Majorek KA, Osinski T, Tran DT, Revilla A, Anderson WF, Minor W, Kuhn ML. 2017. Insight into the 3D structure and substrate specificity of previously uncharacterized GNAT superfamily acetyltransferases from pathogenic bacteria. Biochim Biophys Acta 1865:55-64.

386. Vetting MW, Bareich DC, Yu M, Blanchard JS. 2008. Crystal structure of RimI from Salmonella typhimurium LT2, the GNAT responsible for N(alpha)-acetylation of ribosomal protein S18. Protein Sci 17:1781-90.

387. Kuo YM, Andrews AJ. 2013. Quantitating the specificity and selectivity of Gcn5-mediated acetylation of histone H3. PLoS One 8:e54896.

388. Wang MM, You D, Ye BC. 2017. Site-specific and kinetic characterization of enzymatic and nonenzymatic protein acetylation in bacteria. Sci Rep 7:14790.

389. Eddy SR. 1998. Profile hidden Markov models. Bioinformatics 14:755-63.

390. Tatusova T, Ciufo S, Fedorov B, O'Neill K, Tolstoy I. 2015. RefSeq microbial genomes database: new representation and annotation strategy. Nucleic Acids Res 43:3872.

391. Isono K, Isono S. 1980. Ribosomal protein modification in *Escherichia coli*. II. Studies of a mutant lacking the N-terminal acetylation of protein S18. Mol Gen Genet 177:645-51.

392. Errey JC, Blanchard JS. 2006. Functional annotation and kinetic characterization of PhnO from Salmonella enterica. Biochemistry 45:3033-9.

393. Hove-Jensen B, McSorley FR, Zechel DL. 2012. Catabolism and detoxification of 1-aminoalkylphosphonic acids: N-acetylation by the phnO gene product. PLoS One 7:e46416.

394. Metcalf WW, Wanner BL. 1993. Mutational analysis of an *Escherichia coli* fourteen-gene operon for phosphonate degradation, using TnphoA' elements. J Bacteriol 175:3430-42.

395. Glover BP, McHenry CS. 1998. The chi psi subunits of DNA polymerase III holoenzyme bind to single-stranded DNA-binding protein (SSB) and facilitate replication of an SSB-coated template. J Biol Chem 273:23476-84.

396. Anderson SG, Williams CR, O'donnell M, Bloom LB. 2007. A function for the psi subunit in loading the *Escherichia coli* DNA polymerase sliding clamp. J Biol Chem 282:7035-45.

397. Boiteux S, Huisman O, Laval J. 1984. 3-Methyladenine residues in DNA induce the SOS function sfiA in *Escherichia coli*. EMBO J 3:2569-73.

398. Fredericks CE, Shibata S, Aizawa S, Reimann SA, Wolfe AJ. 2006. Acetyl phosphate-sensitive regulation of flagellar biogenesis and capsular biosynthesis depends on the Rcs phosphorelay. Mol Microbiol 61:734-47.

399. Keating DH, Shulla A, Klein AH, Wolfe AJ. 2008. Optimized two-dimensional thin layer chromatography to monitor the intracellular concentration of acetyl phosphate and other small phosphorylated molecules. Biol Proced Online 10:36-46.

400. Prüss BM, Wolfe AJ. 1994. Regulation of acetyl phosphate synthesis and degradation, and the control of flagellar expression in *Escherichia coli*. Mol Microbiol 12:973-84.

401. Haverkorn van Rijsewijk BR, Nanchen A, Nallet S, Kleijn RJ, Sauer U. 2011. Large-scale 13C-flux analysis reveals distinct transcriptional control of respiratory and fermentative metabolism in *Escherichia coli*. Mol Syst Biol 7:477.

402. Toya Y, Ishii N, Nakahigashi K, Hirasawa T, Soga T, Tomita M, Shimizu K. 2010. 13C-metabolic flux analysis for batch culture of *Escherichia coli* and its Pyk and Pgi gene knockout mutants based on mass isotopomer distribution of intracellular metabolites. Biotechnol Prog 26:975-92.

403. Charusanti P, Conrad TM, Knight EM, Venkataraman K, Fong NL, Xie B, Gao Y, Palsson B. 2010. Genetic basis of growth adaptation of *Escherichia coli* after deletion of pgi, a major metabolic gene. PLoS Genet 6:e1001186.

404. Iwami Y, Yamada T. 1980. Rate-limiting steps of the glycolytic pathway in the oral bacteria Streptococcus mutans and Streptococcus sanguis and the influence of acidic pH on the glucose metabolism. Arch Oral Biol 25:163-9.

405. Fischer E, Sauer U. 2003. Metabolic flux profiling of *Escherichia coli* mutants in central carbon metabolism using GC-MS. Eur J Biochem 270:880-91.

406. Tian WN, Braunstein LD, Pang J, Stuhlmeier KM, Xi QC, Tian X, Stanton RC. 1998. Importance of glucose-6-phosphate dehydrogenase activity for cell growth. J Biol Chem 273:10609-17.

407. Mizrahi I, Biran D, Ron EZ. 2006. Requirement for the acetyl phosphate pathway in *Escherichia coli* ATP-dependent proteolysis. Mol Microbiol 62:201-11.

408. Mizrahi I, Biran D, Ron EZ. 2009. Involvement of the Pta-AckA pathway in protein folding and aggregation. Res Microbiol 160:80-4.

409. Kuczyńska-Wiśnik D, Moruno-Algara M, Stojowska-Swędrzyńska K, Laskowska E. 2016. The effect of protein acetylation on the formation and processing of inclusion bodies and endogenous protein aggregates in *Escherichia coli* cells. Microb Cell Fact 15:189.

410. Laursen BS, Sørensen HP, Mortensen KK, Sperling-Petersen HU. 2005. Initiation of protein synthesis in bacteria. Microbiol Mol Biol Rev 69:101-23.

411. Coughlin RT, Tonsager S, McGroarty EJ. 1983. Quantitation of metal cations bound to membranes and extracted lipopolysaccharide of *Escherichia coli*. Biochemistry 22:2002-7.

412. Groisman EA, Kayser J, Soncini FC. 1997. Regulation of polymyxin resistance and adaptation to low-$Mg2^{+}$ environments. J Bacteriol 179:7040-5.

413. Pontes MH, Sevostyanova A, Groisman EA. 2015. When too much atp is bad for protein synthesis. J Mol Biol 427:2586-94.

414. Chubukov V, Gerosa L, Kochanowski K, Sauer U. 2014. Coordination of microbial metabolism. Nat Rev Microbiol 12:327-40.

415. O'Beirne D, Hamer G. 2000. Oxygen availability and the growth of *Escherichia coli* . Biotechnology and Bioprocess Engineering 23:487–494.

416. Phue JN, Shiloach J. 2005. Impact of dissolved oxygen concentration on acetate accumulation and physiology of *E. coli* BL21, evaluating transcription levels of key genes at different dissolved oxygen conditions. Metab Eng 7:353-63.

417. Guest JR. 1992. Oxygen-regulated gene expression in *Escherichia coli*. The 1992 Marjory Stephenson Prize Lecture. J Gen Microbiol 138:2253-63.

418. Vuoristo KS, Mars AE, Sangra JV, Springer J, Eggink G, Sanders JP, Weusthuis RA. 2015. Metabolic engineering of the mixed-acid fermentation pathway of *Escherichia coli* for anaerobic production of glutamate and itaconate. AMB Express 5:61.

419. Clark DP. 1989. The fermentation pathways of *Escherichia coli*. FEMS Microbiol Rev 5:223-34.

420. Wanner BL. 1996. Phosphorus assimilation and control of the phosphate regulon, p 1357–1381. *In* Neidhardt F, Curtiss III R, Ingraham J, Lin E, Low K, Magasanik B, Reznikoff W, Riley M, Schaechter M, Umbrager H (ed), *Escherichia coli* and Salmonella: Cellular and Molecular Biology. American Society for Microbiology, Washington DC.

421. Rao NN, Liu S, Kornberg A. 1998. Inorganic polyphosphate in *Escherichia coli*: the phosphate regulon and the stringent response. J Bacteriol 180:2186-93.

422. Spira B, Silberstein N, Yagil E. 1995. Guanosine 3',5'-bispyrophosphate (ppGpp) synthesis in cells of *Escherichia coli* starved for Pi. J Bacteriol 177:4053-8.

423. Liu K, Bittner AN, Wang JD. 2015. Diversity in (p)ppGpp metabolism and effectors. Curr Opin Microbiol 24:72-9.

424. Fernández-Coll L, Cashel M. 2018. Contributions of SpoT Hydrolase, SpoT Synthetase, and RelA Synthetase to Carbon Source Diauxic Growth Transitions in *Escherichia coli*. Front Microbiol 9:1802.

425. Romano S, Schulz-Vogt HN, González JM, Bondarev V. 2015. Phosphate Limitation Induces Drastic Physiological Changes, Virulence-Related Gene Expression, and Secondary Metabolite Production in Pseudovibrio sp. Strain FO-BEG1. Appl Environ Microbiol 81:3518-28.

426. Chang YY, Wang AY, Cronan JE. 1994. Expression of *Escherichia coli* pyruvate oxidase (PoxB) depends on the sigma factor encoded by the rpoS(katF) gene. Mol Microbiol 11:1019-28.

427. Gosset G, Zhang Z, Nayyar S, Cuevas WA, Saier MH. 2004. Transcriptome analysis of Crp-dependent catabolite control of gene expression in *Escherichia coli*. J Bacteriol 186:3516-24.

428. Cortay JC, Nègre D, Scarabel M, Ramseier TM, Vartak NB, Reizer J, Saier MH, Cozzone AJ. 1994. In vitro asymmetric binding of the pleiotropic regulatory protein, FruR, to the ace operator controlling glyoxylate shunt enzyme synthesis. J Biol Chem 269:14885-91.

429. Martin RG, Gillette WK, Rhee S, Rosner JL. 1999. Structural requirements for marbox function in transcriptional activation of mar/sox/rob regulon promoters in *Escherichia coli*: sequence, orientation and spatial relationship to the core promoter. Mol Microbiol 34:431-41.

430. Seth D, Hausladen A, Wang YJ, Stamler JS. 2012. Endogenous protein S-Nitrosylation in E. coli: regulation by OxyR. Science 336:470-3.

431. Chismon DL, Browning DF, Farrant GK, Busby SJ. 2010. Unusual organization, complexity and redundancy at the *Escherichia coli* hcp-hcr operon promoter. Biochem J 430:61-8.

432. Takahashi K, Hattori T, Nakanishi T, Nohno T, Fujita N, Ishihama A, Taniguchi S. 1994. Repression of in vitro transcription of the *Escherichia coli* fnr and nar X genes by FNR protein. FEBS Lett 340:59-64.

433. Filenko N, Spiro S, Browning DF, Squire D, Overton TW, Cole J, Constantinidou C. 2007. The NsrR regulon of *Escherichia coli* K-12 includes genes encoding the hybrid cluster protein and the periplasmic, respiratory nitrite reductase. J Bacteriol 189:4410-7.

434. Ramseier TM. 1996. Cra and the control of carbon flux via metabolic pathways. Res Microbiol 147:489-93.

435. Chavarría M, de Lorenzo V. 2018. The imbroglio of the physiological Cra effector clarified at last. Mol Microbiol 109:273-277.

436. Saier MH, Ramseier TM. 1996. The catabolite repressor/activator (Cra) protein of enteric bacteria. J Bacteriol 178:3411-7.

437. Zhang Z, Gosset G, Barabote R, Gonzalez CS, Cuevas WA, Saier MH. 2005. Functional interactions between the carbon and iron utilization regulators, Crp and Fur, in *Escherichia coli*. J Bacteriol 187:980-90.

438. Tarmy EM, Kaplan NO. 1968. Kinetics of *Escherichia coli* B D-lactate dehydrogenase and evidence for pyruvate-controlled change in conformation. J Biol Chem 243:2587-96.

439. Futai M. 1973. Membrane D-lactate dehydrogenase from *Escherichia coli*. Purification and properties. Biochemistry 12:2468-74.

440. Kohn LD, Kaback HR. 1973. Mechanisms of active transport in isolated bacterial membrane vesicles. XV. Purification and properties of the membrane-bound D-lactate dehydrogenase from *Escherichia coli*. J Biol Chem 248:7012-7.

441. Futai M, Kimura H. 1977. Inducible membrane-bound L-lactate dehydrogenase from *Escherichia coli*. Purification and properties. J Biol Chem 252:5820-7.

442. Kimura H, Futai M. 1978. Effects of phospholipids on L-lactate dehydrogenase from membranes of *Escherichia coli*. Activation and stabilization of the enzyme with phospholipids. J Biol Chem 253:1095-110.

443. Kasai T, Kouzuma A, Watanabe K. 2017. CRP Regulates D-Lactate Oxidation in *Shewanella oneidensis* MR-1. Front Microbiol 8:869.

444. Kossiakoff AA. 1986. Protein dynamics investigated by neutron diffraction. Methods Enzymol 131:433-47.

445. Makowski L, Rodi DJ, Mandava S, Minh DD, Gore DB, Fischetti RF. 2008. Molecular crowding inhibits intramolecular breathing motions in proteins. J Mol Biol 375:529-46.

446. Levin SA. 2014. Public goods in relation to competition, cooperation, and spite. Proc Natl Acad Sci U S A 111 Suppl 3:10838-45.

447. Zhang W, Wang C, Song Y, Shao C, Zhang X, Zang J. 2015. Structural insights into the mechanism of *Escherichia coli* YmdB: A 2'-O-acetyl-ADP-ribose deacetylase. J Struct Biol 192:478-486.

448. Chen D, Vollmar M, Rossi MN, Phillips C, Kraehenbuehl R, Slade D, Mehrotra PV, von Delft F, Crosthwaite SK, Gileadi O, Denu JM, Ahel I. 2011. Identification of macrodomain proteins as novel O-acetyl-ADP-ribose deacetylases. J Biol Chem 286:13261-71.

449. Dalle-Donne I, Rossi R, Giustarini D, Milzani A, Colombo R. 2003. Protein carbonyl groups as biomarkers of oxidative stress. Clin Chim Acta 329:23-38.

450. Dalle-Donne I, Giustarini D, Colombo R, Rossi R, Milzani A. 2003. Protein carbonylation in human diseases. Trends Mol Med 9:169-76.

451. Meyer JG, D'Souza AK, Sorensen DJ, Rardin MJ, Wolfe AJ, Gibson BW, Schilling B. 2016. Quantification of Lysine Acetylation and Succinylation Stoichiometry in Proteins Using Mass Spectrometric Data-Independent Acquisitions (SWATH). J Am Soc Mass Spectrom 27:1758-1771.

452. Miyagi M. 2017. Site-Specific Quantification of Lysine Acetylation Using Isotopic Labeling. Methods Enzymol 586:85-95.

453. Nakayasu ES, Wu S, Sydor MA, Shukla AK, Weitz KK, Moore RJ, Hixson KK, Kim JS, Petyuk VA, Monroe ME, Pasa-Tolic L, Qian WJ, Smith RD, Adkins JN, Ansong C. 2014. A method to determine lysine acetylation stoichiometries. Int J Proteomics 2014:730725.

454. Wei L, Meyer JG, Schilling B. 2018. Quantification of Site-specific Protein Lysine Acetylation and Succinylation Stoichiometry Using Data-independent Acquisition Mass Spectrometry. J Vis Exp.

455. Weinert BT, Iesmantavicius V, Moustafa T, Schölz C, Wagner SA, Magnes C, Zechner R, Choudhary C. 2015. Acetylation dynamics and stoichiometry in Saccharomyces cerevisiae. Mol Syst Biol 11:833.

456. Filley SJ, Hill KA. 1993. Amino acid substitutions at position 73 in motif 2 of *Escherichia coli* alanyl-tRNA synthetase. Arch Biochem Biophys 307:46-51.

457. Hornbeck PV, Kornhauser JM, Tkachev S, Zhang B, Skrzypek E, Murray B, Latham V, Sullivan M. 2012. PhosphoSitePlus: a comprehensive resource for investigating the structure and function of experimentally determined post-translational modifications in man and mouse. Nucleic Acids Res 40:D261-70.

458. Bontemps-Gallo S, Gaviard C, Richards CL, Kentache T, Raffel SJ, Lawrence KA, Schindler JC, Lovelace J, Dulebohn DP, Cluss RG, Hardouin J, Gherardini FC. 2018. Global Profiling of Lysine Acetylation in *Borrelia burgdorferi* B31 Reveals Its Role in Central Metabolism. Front Microbiol 9:2036.

459. Zhang RG, Pappas KM, Pappas T, Brace JL, Miller PC, Oulmassov T, Molyneaux JM, Anderson JC, Bashkin JK, Winans SC, Joachimiak A. 2002. Structure of a bacterial quorum-sensing transcription factor complexed with pheromone and DNA. Nature 417:971-4.

460. Majdalani N, Gottesman S. 2005. The Rcs phosphorelay: a complex signal transduction system. Annu Rev Microbiol 59:379-405.

461. Sherratt DJ, Søballe B, Barre FX, Filipe S, Lau I, Massey T, Yates J. 2004. Recombination and chromosome segregation. Philos Trans R Soc Lond B Biol Sci 359:61-9.

462. Proudfoot M, Kuznetsova E, Brown G, Rao NN, Kitagawa M, Mori H, Savchenko A, Yakunin AF. 2004. General enzymatic screens identify three new nucleotidases in *Escherichia coli*. Biochemical characterization of SurE, YfbR, and YjjG. J Biol Chem 279:54687-94.

463. Titz B, Häuser R, Engelbrecher A, Uetz P. 2007. The *Escherichia coli* protein YjjG is a house-cleaning nucleotidase in vivo. FEMS Microbiol Lett 270:49-57.

464. Allen MJ, White GF, Morby AP. 2006. The response of *Escherichia coli* to exposure to the biocide polyhexamethylene biguanide. Microbiology 152:989-1000.

465. Chindera K, Mahato M, Sharma AK, Horsley H, Kloc-Muniak K, Kamaruzzaman NF, Kumar S, McFarlane A, Stach J, Bentin T, Good L. 2016. The antimicrobial polymer PHMB enters cells and selectively condenses bacterial chromosomes. Sci Rep 6:23121.

466. Vetting MW, de Carvalho LP, Roderick SL, Blanchard JS. 2005. A novel dimeric structure of the RimL Nalpha-acetyltransferase from Salmonella typhimurium. J Biol Chem 280:22108-14.

467. Domka J, Lee J, Bansal T, Wood TK. 2007. Temporal gene-expression in *Escherichia coli* K-12 biofilms. Environ Microbiol 9:332-46.

468. Weber MM, French CL, Barnes MB, Siegele DA, McLean RJ. 2010. A previously uncharacterized gene, yjfO (bsmA), influences *Escherichia coli* biofilm formation and stress response. Microbiology 156:139-47.

469. Jozefczuk S, Klie S, Catchpole G, Szymanski J, Cuadros-Inostroza A, Steinhauser D, Selbig J, Willmitzer L. 2010. Metabolomic and transcriptomic stress response of *Escherichia coli*. Mol Syst Biol 6:364.

470. Kitamura N, Ikeda H, Yamada Y, Ishikura H. 1977. Processing by ribonuclease II of the tRNATyr precursor of *Escherichia coli* synthesized in vitro. Eur J Biochem 73:297-306.

471. Mott JE, Galloway JL, Platt T. 1985. Maturation of *Escherichia coli* tryptophan operon mRNA: evidence for 3' exonucleolytic processing after rho-dependent termination. EMBO J 4:1887-91.

472. Li Z, Pandit S, Deutscher MP. 1999. RNase G (CafA protein) and RNase E are both required for the 5' maturation of 16S ribosomal RNA. EMBO J 18:2878-85.

473. Wachi M, Umitsuki G, Shimizu M, Takada A, Nagai K. 1999. *Escherichia coli* cafA gene encodes a novel RNase, designated as RNase G, involved in processing of the 5' end of 16S rRNA. Biochem Biophys Res Commun 259:483-8.

474. Umitsuki G, Wachi M, Takada A, Hikichi T, Nagai K. 2001. Involvement of RNase G in in vivo mRNA metabolism in *Escherichia coli*. Genes Cells 6:403-10.

475. Clarke JE, Kime L, Romero A D, McDowall KJ. 2014. Direct entry by RNase E is a major pathway for the degradation and processing of RNA in *Escherichia coli*. Nucleic Acids Res 42:11733-51.

476. Kohn G, Delvaux D, Lakaye B, Servais AC, Scholer G, Fillet M, Elias B, Derochette JM, Crommen J, Wins P, Bettendorff L. 2012. High inorganic triphosphatase activities in bacteria and mammalian cells: identification of the enzymes involved. PLoS One 7:e43879.

477. Webster TA, Gibson BW, Keng T, Biemann K, Schimmel P. 1983. Primary structures of both subunits of *Escherichia coli* glycyl-tRNA synthetase. J Biol Chem 258:10637-41.

478. Minagawa S, Ogasawara H, Kato A, Yamamoto K, Eguchi Y, Oshima T, Mori H, Ishihama A, Utsumi R. 2003. Identification and molecular characterization of the Mg2+ stimulon of *Escherichia coli*. J Bacteriol 185:3696-702.

479. Born TL, Blanchard JS. 1999. Enzyme-catalyzed acylation of homoserine: mechanistic characterization of the *Escherichia coli* metA-encoded homoserine transsuccinylase. Biochemistry 38:14416-23.

480. Ito A, May T, Kawata K, Okabe S. 2008. Significance of rpoS during maturation of *Escherichia coli* biofilms. Biotechnol Bioeng 99:1462-71.

481. Ito A, Taniuchi A, May T, Kawata K, Okabe S. 2009. Increased antibiotic resistance of *Escherichia coli* in mature biofilms. Appl Environ Microbiol 75:4093-100.

482. Cho BK, Zengler K, Qiu Y, Park YS, Knight EM, Barrett CL, Gao Y, Palsson B. 2009. The transcription unit architecture of the *Escherichia coli* genome. Nat Biotechnol 27:1043-9.

483. Kozmin SG, Leroy P, Pavlov YI, Schaaper RM. 2008. YcbX and yiiM, two novel determinants for resistance of *Escherichia coli* to N-hydroxylated base analogues. Mol Microbiol 68:51-65.

484. Vaughan S, Wickstead B, Gull K, Addinall SG. 2004. Molecular evolution of FtsZ protein sequences encoded within the genomes of archaea, bacteria, and eukaryota. J Mol Evol 58:19-29.

485. Reyes-Lamothe R, Nicolas E, Sherratt DJ. 2012. Chromosome replication and segregation in bacteria. Annu Rev Genet 46:121-43.

486. Hanawa-Suetsugu K, Takagi M, Inokuchi H, Himeno H, Muto A. 2002. SmpB functions in various steps of trans-translation. Nucleic Acids Res 30:1620-9.

487. Reeves SA, Parsonage D, Nelson KJ, Poole LB. 2011. Kinetic and thermodynamic features reveal that *Escherichia coli* BCP is an unusually versatile peroxiredoxin. Biochemistry 50:8970-81.

488. Borukhov S, Polyakov A, Nikiforov V, Goldfarb A. 1992. GreA protein: a transcription elongation factor from *Escherichia coli*. Proc Natl Acad Sci U S A 89:8899-902.

489. Bonomi F, Iametti S, Morleo A, Ta D, Vickery LE. 2008. Studies on the mechanism of catalysis of iron-sulfur cluster transfer from IscU[2Fe2S] by HscA/HscB chaperones. Biochemistry 47:12795-801.

490. Bielińska A, Hulanicka D. 1986. Regulation of the cysB gene expression in *Escherichia coli*. Acta Biochim Pol 33:133-7.

491. Antoun A, Pavlov MY, Lovmar M, Ehrenberg M. 2006. How initiation factors maximize the accuracy of tRNA selection in initiation of bacterial protein synthesis. Mol Cell 23:183-93.

492. Hirokawa G, Nijman RM, Raj VS, Kaji H, Igarashi K, Kaji A. 2005. The role of ribosome recycling factor in dissociation of 70S ribosomes into subunits. RNA 11:1317-28.

493. Singh NS, Das G, Seshadri A, Sangeetha R, Varshney U. 2005. Evidence for a role of initiation factor 3 in recycling of ribosomal complexes stalled on mRNAs in *Escherichia coli*. Nucleic Acids Res 33:5591-601.

494. De Bellis D, Liveris D, Goss D, Ringquist S, Schwartz I. 1992. Structure-function analysis of *Escherichia coli* translation initiation factor IF3: tyrosine 107 and lysine 110 are required for ribosome binding. Biochemistry 31:11984-90.

495. Iturriaga G, Suárez R, Nova-Franco B. 2009. Trehalose metabolism: from osmoprotection to signaling. Int J Mol Sci 10:3793-810.

496. Ruhal R, Kataria R, Choudhury B. 2013. Trends in bacterial trehalose metabolism and significant nodes of metabolic pathway in the direction of trehalose accumulation. Microb Biotechnol 6:493-502.

497. Rimmele M, Boos W. 1994. Trehalose-6-phosphate hydrolase of *Escherichia coli*. J Bacteriol 176:5654-64.

498. Richards AB, Krakowka S, Dexter LB, Schmid H, Wolterbeek AP, Waalkens-Berendsen DH, Shigoyuki A, Kurimoto M. 2002. Trehalose: a review of properties, history of use and human tolerance, and results of multiple safety studies. Food Chem Toxicol 40:871-98.

499. Gibson RP, Turkenburg JP, Charnock SJ, Lloyd R, Davies GJ. 2002. Insights into trehalose synthesis provided by the structure of the retaining glucosyltransferase OtsA. Chem Biol 9:1337-46.

500. Arsène F, Tomoyasu T, Bukau B. 2000. The heat shock response of *Escherichia coli*. Int J Food Microbiol 55:3-9.

501. Borenstein E, Shlomi T, Ruppin E, Sharan R. 2007. Gene loss rate: a probabilistic measure for the conservation of eukaryotic genes. Nucleic Acids Res 35:e7.

502. Richards CL, Lawrence KA, Su H, Yang Y, Yang XF, Dulebohn DP, Gherardini FC. 2015. Acetyl-Phosphate Is Not a Global Regulatory Bridge between Virulence and Central Metabolism in Borrelia burgdorferi. PLoS One 10:e0144472.

503. Jackowski S, Rock CO. 1981. Regulation of coenzyme A biosynthesis. J Bacteriol 148:926-32.

504. Song WJ, Jackowski S. 1994. Kinetics and regulation of pantothenate kinase from *Escherichia coli*. J Biol Chem 269:27051-8.

505. Vallari DS, Jackowski S, Rock CO. 1987. Regulation of pantothenate kinase by coenzyme A and its thioesters. J Biol Chem 262:2468-71.

506. Vadali RV, Bennett GN, San KY. 2004. Applicability of CoA/acetyl-CoA manipulation system to enhance isoamyl acetate production in *Escherichia coli*. Metab Eng 6:294-9.

507. Vadali RV, Bennett GN, San KY. 2004. Cofactor engineering of intracellular CoA/acetyl-CoA and its effect on metabolic flux redistribution in *Escherichia coli*. Metab Eng 6:133-9.

508. Hankermeyer CR, Tjeerdema RS. 1999. Polyhydroxybutyrate: plastic made and degraded by microorganisms. Rev Environ Contam Toxicol 159:1-24.

509. Crosby HA, Rank KC, Rayment I, Escalante-Semerena JC. 2012. Structural insights into the substrate specificity of the Rhodopseudomonas palustris protein acetyltransferase RpPat: identification of a loop critical for recognition by RpPat. J Biol Chem 287:41392-404.

510. Kimata K, Takahashi H, Inada T, Postma P, Aiba H. 1997. cAMP receptor protein-cAMP plays a crucial role in glucose-lactose diauxie by activating the major glucose transporter gene in *Escherichia coli*. Proc Natl Acad Sci U S A 94:12914-9.

511. BD. 2006. BD Bionutrients™ Technical Manual. Advanced Bioprocessing., Revised 3rd ed. ed, p 1–68.

512. Backman K, Chen YM, Magasanik B. 1981. Physical and genetic characterization of the glnA--glnG region of the *Escherichia coli* chromosome. Proc Natl Acad Sci U S A 78:3743-7.

513. Wolfe AJ. 2005. The acetate switch. Microbiol Mol Biol Rev 69:12-50.

514. Cowan JA. 1998. Metal Activation of Enzymes in Nucleic Acid Biochemistry. Chem Rev 98:1067-1088.

515. Sreedhara A, Cowan JA. 2002. Structural and catalytic roles for divalent magnesium in nucleic acid biochemistry. Biometals 15:211-23.

516. Nikaido H. 2009. The Limitations of LB Medium. http://schaechter.asmblog.org/schaechter/2009/11/the-limitations-of-lb-medium.html. Accessed 9/28/16.

517. Neidhardt FC, Bloch PL, Smith DF. 1974. Culture medium for enterobacteria. J Bacteriol 119:736-47.

518. Sezonov G, Joseleau-Petit D, D'Ari R. 2007. *Escherichia coli* physiology in Luria-Bertani broth. J Bacteriol 189:8746-9.

519. O'Shea TM, Deloney-Marino CR, Shibata S, Aizawa S, Wolfe AJ, Visick KL. 2005. Magnesium promotes flagellation of Vibrio fischeri. J Bacteriol 187:2058-65.

520. Szewczak J, Bierczyńska-Krzysik A, Piejko M, Mak P, Stadnik D. 2015. Isolation and Characterization of Acetylated Derivative of Recombinant Insulin Lispro Produced in *Escherichia coli*. Pharm Res 32:2450-7.

VITA

The author, David Christensen, was born in Berwyn, Illinois to Lori and Eric Christensen. He attended the University of Illinois at Urbana-Champaign where he earned his Bachelor of Science degree in Biochemistry with a minor in Chemistry in May 2012. During his undergraduate career, he worked in the lab of Dr. Raven H. Huang studying the Hen1 RNA repair protein.

In August 2012, David matriculated the Integrated Program in Biomedical Sciences Ph.D. and entered the Department of Microbiology and Immunology in Loyola University Chicago Biomedical Sciences campus. He joined the laboratory of Dr. Alan J. Wolfe where his research focused on determining the regulation of non-enzymatic acetyl phosphate-dependent acetylation and identified four novel lysine acetyltransferases in *E. coli*. He presented his work at several conferences including an oral presentation at the Molecular Genetics of Bacteria and Phages meeting in 2017.

After receiving his Ph.D., David will enter a postdoctoral fellowship with Dr. Karen L. Visick in the Department of Microbiology and Immunology at Loyola.